Determination of activity coefficients at infinite dilution using the inert gas stripping technique

(IN TEN CHAPTERS)

THESIS DISSERTATION

SALVANNES GEORGE
200272501
University of Kwa-Zulu Natal
Durban, Republic of South Africa

Supervisors: **Professor D Ramjugernath, Doctor P Naidoo and Professor J D Raal**
University of Kwa-Zulu Natal, Faculty of Chemical Engineering, Durban

Internal Examiner: **Professor M Carsky**
University of Kwa-Zulu Natal, Howard College

External Examiner: **Professor D Richon**
ENSMP, France

RW Print & Bookbinding Solutions
Hatfield, Pretoria

DETERMINATION OF ACTIVITY COEFFICIENTS AT INFINITE DILUTION USING THE INERT GAS STRIPPING TECHNIQUE

S. George

[BSc. Eng]

UNIVERSITY OF KWA-ZULU NATAL

March, 2008

In Loving Memory of

Steven George

Determination of Activity Coefficients at Infinite Dilution using the Inert Gas Stripping Technique

Submitted in partial fulfilment of the requirements for the degree of
Master of Science in the Department of Chemical Engineering
University Kwa-Zulu Natal

by

Salvannes George
BSc. (Eng)

All work performed in the School of Chemical Engineering
University of Kwa-Zulu Natal, Durban
South Africa

March 2008

Declaration

I hereby certify that the work presented in this thesis is the result of my own investigation under the supervision of Professor D. Ramjugernath and co-supervisors Professor J. D. Raal and Doctor P. Naidoo and has never been submitted in candidature for a degree in any other University or Institution.

I hereby certify that the above statement is correct

Salvannes George (Candidate)

I hereby certify that I find this work to be suitable for submission for the degree of MSc. in Chemical Engineering

Prof. D. Ramjugernath (Supervisor)

As the candidates co-supervisor's we approve this dissertation for submission

Prof. J. D. Raal (Co-supervisor)

Dr. P. Naidoo (Co-supervisor)

Acknowledgements

I would like to thank the following individuals, without whose effort, this work would not have been possible:

I acknowledge my gratitude to **Prof. Deresh Ramjugernath** for allowing me the opportunity to undertake a Masters Degree, and for financial assistance and expert supervision.

I am very grateful to my sister **Selena George** for providing me with support, encouragement and for being so accommodating.

I would like to gratefully acknowledge **Stevie Moodley** and **Shamane Moodley** for their love and support through difficult times.

The Workshop staff for aiding in the building and setting up of the equipment used for the project especially **Kelly** for his insight and experience.

Minal Soni, for his help with writing this thesis, as well as helping me in understanding better, certain aspects of my project and the equipment used.

I would like to extend my heartfelt thanks to my **grandma** for being so supportive in my studies, for encouraging me and for financial assistance.

Special thanks to **Dudley**, **Preole**, and **Colin** for their technical and electrical assistance and for their aid with University resources and equipment.

Finally I would also like to thank **Dominique Richon** for his advice on making improvements to the equipment and for valuable information.

The financial assistance of the National Research Foundation (NRF) and Sasol towards this research is acknowledged. Opinions expressed and conclusions arrived at, are those of the author and not necessarily attributed to the NRF, Sasol or any of the above mentioned people.

Abstract

The determination of limiting activity coefficients in liquid mixtures has become an important tool in chemical engineering. It has been investigated intensively during the past in order to find new alternatives and improved methods for its accurate determination. The limiting activity coefficient is a fundamental thermodynamic quantity which measures the solution non-ideality and acts as a correction factor to deviations from Raoult's Law. This dissertation involves the determination of limiting activity coefficients using the inert gas stripping (IGS) technique only. It is considered to be the best method as it is a direct method involving exact concentrations of components in the mixtures encountered in industry.

A comprehensive study of activity coefficients at infinite dilution for various systems, using the inert gas stripping (IGS) method has been undertaken. Various other methods and their suitability have also been discussed but preference is given to the superior quality of measurements obtained using the inert gas stripping technique. Extensive research has been conducted into the background and origination of the technique. Various improvements of the equilibrium cell designed by various authors for different types of systems have been outlined along with the various equations derived by the authors.

The equipment was designed for use with the double-cell technique as well as the single-cell technique and in some cases both techniques were used. The techniques involve the use of a dilutor cell in which the highly diluted, volatile solute is stripped from a liquid solution using the inert gas nitrogen, introduced into the cell through capillaries and dispersed through the solution as small bubbles, at a constant flow rate. Analysis of the stripped solution is accomplished through the use of a gas chromatograph; the peak areas obtained from these analyses as well as the residence times and other system data such as temperature, pressure, mass and flow rate were used to compute the infinite dilution activity coefficient through the use of the various equations available in literature.

The original equipment was designed for the use of the single cell technique by Soni (2004). Various modifications have been made to the equipment in order to measure limiting activity coefficients of more diverse systems with high accuracy. A major change to the equipment was the introduction of a second saturation cell of similar design to the dilutor cell. This enabled the determination of activity coefficients at infinite dilution of difficult systems i.e. systems where the solvent volatility is high and for higher order systems. The equipment was redesigned and built

using ideas and improvements by previous researchers in the field and commissioned using test systems that have been classed as easy systems for this technique. The new equipment is now applicable to almost all systems, however good separation in the GC column could be a problem for complex systems.

The determination of infinite dilution activity coefficients for one-component solute + one-component solvent systems and multi-component solvent systems were accomplished. The systems that were investigated consisted of a mixture of components of alkanes, alkenes, phenols and ketones, mostly in binary mixtures. Multi-component mixtures have also been investigated in the form of ternary systems involving a binary solvent mixture at varying concentrations, and a solute in order to show the diversity, uniqueness and efficiency of the IGS technique. Major variables affecting the system (the dilutor cell), namely the stripping gas flow rate and the dilutor cell temperature, were also investigated for all systems.

Two test systems, cyclohexane in 1-methyl-2-pyrrolidone (NMP) and n-heptane in NMP were used to determine if the equipment is operating properly by comparing values obtained, to literature values where the inert gas stripping technique was used to determine the activity coefficients at infinite dilution. Another test system n-hexane in NMP was used to compare the two techniques, i.e. the results of the single cell technique with the results of the double cell technique. The experimental results were thereafter compared to published literature values. Systems where the inert gas stripping technique has not been used to determine activity coefficients at infinite dilution were also investigated. These systems include 1-hexene in o-cresol as well as the ternary systems 1-hexene in various concentrations of NMP + o-cresol.

A thorough literature survey has been completed and the relevant theory has been summarized. The validity of the equations proposed by Bao and Han (1995), Duhem and Vidal (1978), Leroi et al. (1977), Hovorka and Dohnal (1997) and Krummen et al. (2000) for the determination of activity coefficients at infinite dilution were investigated. The experimental values obtained were consistent with literature values, with percentage errors of less than 1 % where the same equation was used to determine the limiting activity coefficient. Comparing limiting activity coefficients with the values obtained from other equations proposed by other authors mentioned above resulted in deviations no greater than 2.5 %, and where possible limiting activity coefficients were compared to values obtained from the single-cell technique.

The theory section of this thesis covers all the various formulae (and where possible a summary of their derivation) used in the analysis of results. Some limiting activity coefficients for the systems involving n-heptane, n-hexane, n-hexene, cyclohexane, o-cresol and n-methyl-2-

pyrrolidone under various experimental conditions have been reported making it readily available for use in other works. The effect of two major variables temperature and inert gas flow rate on the limiting activity coefficients with regard to all the systems studied have also been investigated and reported. This was also done in order to check that the data was reproducible.

A sensitivity analysis was also performed in order to check the effect that certain measured variables would have on the limiting activity coefficient. These errors are estimated possible errors and may not exist at all, so not much consideration was given to this when reporting limiting activity coefficients for the various systems. The maximum error range for any given limiting activity coefficient as determined by the sensitivity analysis is ±11 %. The inert gas stripping technique is also extended to the determination of Hendry's constants. The actual values for the Hendry's constants were not determined but a comprehensive study of its determination was undertaken by Miyano et al. (2003) and summarized here.

In addition the suitability and diversity of the inert gas stripping technique has been outlined, along with the advantages and disadvantages of the technique. The various designs of equilibrium cells have been outlined taking into account mass transfer considerations as proposed by Richon et al. (1980). The assumptions and limits of the method have also been outlined and must be taken into consideration when using the technique. A detailed description of the equipment setup and experimental procedure has been provided. The purpose, suitability, operation and applicability, of the various pieces of equipment used to make up the final equipment have been discussed in detail. Details for consideration when designing the equilibrium cells have also been provided.

Contents

List of Figures

List of Tables

Nomenclature

Symbols

A - solute peak area detected by gas chromatography

a - slope (min^{-1})

B_{ij} - virial coefficient characterizing bimolecular interaction between molecules i and j

B_M - mixture second virial coefficient ($cm^3\ mol^{-1}$)

c - concentration ($mol\ cm^{-3}$)

C_i^L - solute concentration in the liquid ($mol\ cm^{-3}$)

$C_{i,s}^L$ - solute concentration in the liquid at interface ($mol\ cm^{-3}$)

$C_{i,s}^G$ - solute concentration in the bubble at interface ($mol\ cm^{-3}$)

C_i^G - solute concentration in the bubble ($mol\ cm^{-3}$)

$\overline{C}_i^G$ - average solute concentration in the bubble ($mol\ cm^{-3}$)

D - carrier gas flow (pressure P, temperature T) ($cm^3\ min^{-1}$)

D_1 - total gas flow rate into the still ($cm^3\ min^{-1}$)

D_2 - total gas flow at still exit (pressure P, temperature T) ($cm^3\ min^{-1}$)

D_s - solvent gas stream entering the still ($cm^3\ min^{-1}$)

D_{ij}^L - diffusion constant of solute i in solvent j ($m^2\ s^{-1}$)

D_b - diameter of bubbles (mm)

f_i^{OL*} - reference fugacity for ith component (liquid pure state, zero pressure)

f_{sol}^L - solute fugacity

G - Gibbs energy

g - gravity ($cm\ s^{-2}$)

H_{12} - Hendry's law constant

h - path length of bubbles in solution (mm)

I_s - Poynting correction: $\exp\left(V_j^{OL} P / RT\right)$

K_{aw} - air-water partitioning coefficient

k - capacity

k_i - correction factors

k_L - mass transfer coefficient in the liquid

M - molar mass (g mol^{-1})

m - mass (g)

m/m - mass basis (mass percentage)

$m(t)$ - mass of solute in the bubble at time t (g)

N - amount of solvent in the still (mol)

n - amount of solute in the still (mol)

$\overline{n}_{sol}$ - mean amount of solute in the cell (mol)

P - pressure (atm)

P_i^0 - vapour pressure (atm)

P_i - partial pressure (atm)

Poy - Poynting factor

P_C - critical pressure (bar)

Pe - Peclet's number

R - gas constant (cm^3 atm gmol^{-1} K^{-1})

R_b - radius of bubbles (mm)

Re - Reynold's number

r - distance from centre of bubble (mm)

S - selectivity

Sh - Sherwood's number

T - cell temperature (K)

T_b - boiling point temperature (K)

T_C - critical temperature (K)

t - time (min)

V_b - volume of bubbles (cm^3)

V_C - critical volume (cm^3 mol^{-1})

V_c - equilibrium cell volume (cm^3)

V_G - volume of the vapour space in the still (cm^3)

x - mole fraction in the liquid phase

y - mole fraction in the vapour phase

Z - compressibility factor

Z_C - critical compressibility factor

Greek Symbols

γ - activity coefficient

φ - fugacity coefficient

ρ - density (g cm^{-3})

α - separation factor

κ - calibration detector constant

τ - line temperature after the cell (K)

τ_L - ratio of mass transfer in the cell to mass transfer to reach equilibrium taking into account liquid phase resistance only

τ_G - same as τ_L taking into account gas phase diffusion only

υ_w^L - liquid molar volume of pure water (cm^3 mol^{-1})

υ^∞ - limiting speed of bubbles in solution (cm s^{-1})

$\gamma_{sol}^{\infty,II}$ - corrected activity coefficient at infinite dilution

ν_L - kinematic viscosity (cSt)

ω - acentric factor

Subscripts

sol - solute

s - solvent (unless otherwise stated)

CG - carrier gas

i, j - components

c - cell

L - liquid phase

o - initial value

f - final value

FM - flowmeter

N - nitrogen

G - gas phase

C - critical property

Superscripts

∞ - at infinite dilution

0 - initial value

sat - at saturation

E - excess energy

v - property in vapour phase

L - property in liquid phase

exp - experimentally determined

a - air

w - water

1 - solute

2 - solvent

3 - carrier gas

Abbreviations

IGS	– Inert Gas Stripping
GLC	– Gas-Liquid Chromatography Method
DEM	– Differential Ebulliometry Method
DSC	– Differential Static Cell Method
RDIST	– Rayleigh Distillation Method
HSA	– Headspace Analysis Method
IHSC	– Indirect Headspace Chromatography
TENS	– Comparative Tensimetry
CIRC	– Circulation Still Method
DPM	– Dew Point Method
SPACE	– Solvatochromic Parameters for Activity Coefficient Estimation
COSMO-RS	– Conductor-like Screening Model for Real Solvents
QSPR	– Quantitative Structure-Property Relationship
GCS	– Group Contribution Solvation Model
LSER	– Linear Solvation Relationships
SCT	– Single Cell Technique

DCT	– Double Cell Technique
GC	– Gas Chromatography
SCRF	– Self-Consistent Reaction Field
IEF-PCM	– Equation Formalism-Polarized Continuum Model
HBD	– Hydrogen Bond Donor
HBA	– Hydrogen Bond Acceptor
GLC	– Gas Liquid Chromatography
FID	– Flame-Ionization Detector
TCD	– Thermocouple Detector
VLE	– Vapour Liquid Equilibrium
SRK	– Soave/Redlich/Kwong
PR	– Peng/Robinson
MSDS	– Material Safety Data Sheet

Chapter 1: Introduction

Infinite dilution activity coefficients (γ^{∞}) are of great value in both chemical and environmental engineering. If both infinite dilution activity coefficients are known for a binary system, parameters in a two-parameter activity coefficient model can be determined and then predictions of vapour-liquid equilibria over the entire composition range can be made (Lin and Sandler (1999)).

Infinite dilution activity coefficients or sometimes called limiting activity coefficients characterize the behaviour of a solute molecule when it is completely surrounded by solvent. It is extremely valuable for both theoretical and practical purposes. Some examples of the importance of activity coefficients at infinite dilution include:

1. Characterizing the behaviour of liquid mixtures
2. Predicting the existence of azeotropes
3. Screening solvents for extraction and extractive distillation processes
4. The calculation of Henry's Law constants and partition coefficients
5. The prediction of selectivity and retention times in a gas chromatograph
6. Improves understanding in theories for liquid solutions

An accurate representation of the thermodynamics of fluids is essential for the rational design of separation systems. For theoreticians, limiting activity coefficients provide inclsive information regarding solute-solvent interactions. From a practical point of view, infinite dilution activity coefficient data allow for the prediction of retention and selectivity, provide essential data in the design of separation equipment (e.g. distillation columns, gas absorption towers, and stripping towers), and guide in the selection of solvents for chemical reactions in which kinetic solvent effects are important. In new plants in the chemical process industry, the capital costs for the separation steps are about 70 % of the total cost, and the energy costs for separation average 90 % (Eckert and Sherman (1996)). Many other examples of the utility of the infinite dilution activity coefficient exist. Knowledge of the phase behaviour of the materials involved, especially of liquid phases, can permit not only the design of less expensive processes, but also can reduce contingency costs.

Industries are forced to manufacture cleaner and more ecological friendly products in a greener way due to tightening demands in legislation together with environmental concerns. The production of high purity reagents and the separation of pollutants require the greatest separation effort to remove the last traces of impurities. The reduction of emissions from gasoline with oxygenated additives like ethers has been a trend in oil refining. The sulfur content of fuel must be reduced without decreasing octane and cetane numbers or reducing yield. New regulations determine sulfur content of fuel to have a maximum value of 30 ppm in USA. For reliable process design accurate physical properties are needed for proper sizing of the separation processes. The infinite dilution activity coefficient is an important parameter in designing the processes producing very pure substances and processes to remove pollutants (Haimi et al. (2006)).

The infinite dilution activity coefficient is a limiting measurement of the non-ideality of the solute in the mixture. The state of infinite dilution in a binary mixture can be described as the state where the solute concentration goes to zero, while the solvent concentration tends to one. Thus solute-solute interactions can be ignored. One of the major applications of the dilute region in industry is in the purification process. It is often desired to raise the purification of a chemical from approximately 92 % to 99 %. Other applications for the dilute region includes characterizing the behaviour of liquid mixtures; the calculation of Henry's Law constants and partition coefficients and development of theoretical modes for liquid solutions.

Activity coefficients at infinite dilution are important thermodynamic properties and reliable knowledge thereof, is of particular importance for the synthesis, design and optimization of separation processes. Furthermore activity coefficients at infinite dilution assist in specifying selective solvents (entrainers) for separation processes such as extractive distillation and extraction. Perhaps the most important need for activity coefficients at infinite dilution is to identify separation problems such as azeotropic points and miscibility gaps.

Various methods, either experimental or predictive, can be used to determine limiting activity coefficients. Predictive methods are very tedious, especially for complex systems involving a mixture of components and they are not always accurate and have to be verified by experimental methods. Most predictive methods are group contribution based and are based on experimental data that are usually stored in data bases and which were used to predict limiting activity coefficient at different conditions; there will therefore always be a need for experimental analysis. Experimental methods do not always result in limiting activity coefficients that are reliable as well, but when the two agree its always good news for any researcher. The inert gas stripping technique is by far the simplest and most accurate technique for determining limiting

activity coefficients provided that all the experimental conditions are met and the assumptions are valid.

The concern of this study is with the inert gas stripping (IGS) technique as described by Leroi et al. (1977). This technique is finding more application for industrial systems especially with the development of new equilibrium cells. The development of new cells for a specific group of systems allows for more accurate determination of the limiting activity coefficient since the cells are designed to improve on certain non-idealities that may arise with these systems. The equations used to calculate limiting activity coefficients for the inert gas stripping technique were derived with certain simplifying assumptions and sometimes these assumptions are not valid for systems studied and therefore new cells are designed and equations derived to account for this.

The equations derived by Leroi et al. (1977), are simple equations for determining limiting activity coefficients and are not applicable to most systems because of the many simplifying assumptions. Equations proposed by other researchers have accounted for some of the simplifying assumptions in the derivation of their equations which are all primarily based on the equations proposed by Leroi et al. (1977). These equations are more complex and require more effort to evaluate. However all the equations are valid for the systems studied in this thesis and can be used to determine limiting activity coefficients where the simplifying assumptions are applicable. The types of systems studied here are ideal systems for the IGS technique; however data for new systems have also been obtained for industrial use, specifically for Sasol.

For all the systems studied there was no need for highly specialized equilibrium cells. Simple cells were used which provided a less expensive but efficient way to achieve equilibrium. The systems studied are non-foaming and very ideal in terms of use for this technique. The equipment was put together in the Thermodynamics Research Unit laboratory at the University of Kwa-Zulu Natal. It now serves as an additional means of determining limiting activity coefficients for comparison purposes with other techniques. These techniques may be either experimental or predictive. There are some flaws in the design of the equipment which can be improved in order to make experimental analysis easier. This can result in procuring data that is more accurate. Due to financial constraints it was not possible to make these changes and cheaper alternatives which do not compromise the accuracy of the results were used.

When using the inert gas stripping technique the equilibrium cells must be designed for the systems under investigation. The maximum bubble rise height through the solution in order to ensure equilibrium conditions in the cells must be determined. The cells need to be designed for the system that requires the greatest path for the bubbles. This allows for equilibrium conditions

for all the systems and avoids having different equilibrium cells for the different systems. The test systems used should also closely resemble the systems under inquest in order to ensure that the method will work for those systems. There are various improvements that can be made to the equipment used in this study and it is recommended that instruments with high precision and accuracy be used for the measurement variables (temperature, pressure, mass and flow rate). The limiting activity coefficients are very sensitive to pressure and flow rate, when using the IGS method.

The inert gas stripping technique can also be used to determine Henry's law constants. Henry's law constants are strongly related to limiting activity coefficients. They have particular importance in waste water treatment, which is a research area where these constants are needed since solubility affects volatilization of toxic compounds into the air. Determining the fate and distribution of polluting chemical compounds in different environmental compartments is an area of tremendous importance for the development of successful strategies for the solution of the problem of environmental contamination.

Chapter 2: Review of Experimental and Predictive Techniques

2.1 Experimental Methods

In the past forty years, numerous methods for the direct measurement of infinite dilution activity coefficients have been developed. These methods are always preferable to the extrapolation of classical VLE data from finite concentrations. Often a given method is applicable to one end of the concentration regime of a binary system, but not to the other. Some of the more important and widely used methods are discussed below.

2.1.1 Gas-Liquid Chromatography Method (GLC)

In this method, a solvent is firstly coated on an inert support as a stationary phase for a gas-liquid chromatograph. A small amount (usually only about several micro litres) of a solute is injected to detect the retention time of the solute in the solvent surroundings. The limiting activity coefficient can be measured by using other properties, such as the column temperature and pressure, the solvent amount in the column and the flow rate of the carrier gas. GLC is especially suitable for the limiting values of volatile solutes in non-volatile or low-volatile solvents because the solvents can be coated easily and steadily. For the same reason, however, it is often unsuitable for the measurement of values at the other end of the concentration regime, i.e. the limiting activity coefficients for the solvents in the solutes. This means that for a binary system, it is very difficult to obtain both ends of the limiting values (Dallinga et al. (1993)). Nevertheless, possible solute-support interactions or solvent-support interactions instead of solute-solvent interactions would have an effect on the accuracy of these measurements. It is also unsuitable for the measurement of limiting activity coefficients in solvent mixtures because the more volatile component is removed faster during gas liquid chromatography. This results in the composition of the solvent mixture altering with time, due to the unavoidable pressure drop across the column (Krummen et al. (2000)).

2.1.2 Differential Ebulliometry Method (DEM)

The limiting values can be obtained by measurements of the limiting slope of boiling temperature with respect to the solute concentration (Gautreaux and Coates (1955)). DEM has been successful in obtaining limiting values for many binary systems. Unfortunately, this technique is

not advised for highly non-ideal systems due to difficulties in operations. It works best when the relative volatilities are not very different, i.e. between 0.1 and 10.

2.1.3 Differential Static Cell Method (DSC)

A differential static cell method for limiting activity coefficients was developed by Sandler and co-workers (Pivedal, et al. (1992)), in which the pressure difference is measured quite accurately between a pure solvent and a very dilute solution that is mutually thermo-statted. Addition of successive, small samples of solute leads readily to good limiting activity coefficient data. Like ebulliometry, this has the advantage of being a difference technique. A limitation for this method however is the need to degas the liquids rigorously.

2.1.4 Rayleigh Distillation Method (RDIST)

In the RDIST method, which has been used for many systems, a known mass of a highly dilute solution ($x_1 < 10^{-3}$) is subjected to a one-stage distillation. This is accomplished by passing an inert gas through the thermo-statted solution in the form of bubbles. Having distilled off a suitable amount of the original solution, the remainder is weighed. Using gas chromatography, the ratio of the concentrations in the original solution and in the remaining solution is determined. From these values, one can readily calculate the limiting activity coefficients (Vrbka et al. (2005) and Dohnal and Horakova (1991)).

2.1.5 Headspace Analysis Method (HSA)

The HSA method for the determination of limiting activity coefficients consists of gas chromatographic measurements of the equilibrium solute partial pressure above the liquid solution of known composition. The HSA method is usually employed for solutes when the RDIST method can not be applied due to irreproducibility in the gas chromatographic analyses of the aqueous solutions. It is fairly difficult to do, and requires modifying the chromatographic columns and detectors for various solvent/solute combinations (Eckert and Sherman (1996) and Asprion et al. (1998)).

2.1.5.1 Indirect Headspace Chromatography (IHSC)

A variation on headspace chromatography that minimizes the difficulties of calibration is indirect headspace chromatography. In this method the liquid space consists of two (virtually immiscible) solvents, A and B. Small amounts of solute are first added to one of the solvents, and then increments of the second solvent are added, along with continual sampling and analysis of the

equilibrium vapour space. The changes in solute concentration in the vapour can be related to an A/B partition coefficient, which in turn can be related to an infinite dilution activity coefficient. This indirect headspace chromatography is especially applicable to systems of higher relative volatility (Eckert and Sherman (1996)).

2.1.6 Comparative Tensimetry (TENS)

This method for determining limiting activity coefficients consists of measuring (under isothermal conditions) the difference between the equilibrium pressures, above a dilute solution and the pure solvent, as a function of gravimetrically or volumetrically determined compositions of the synthetically prepared dilute solutions (Vrbka and Dohnal (2004) and Vrbka et al. (2005)).

2.1.7 Circulation Still Method (CIRC)

In this method, a VLE circulation still operated at constant pressure is employed to provide samples of corresponding vapour and liquid compositions in the region of high dilution. No measurement of temperature is required as the boiling temperature of the solution is indistinguishable from that of the pure solvent.

2.1.8 Dew Point Method (DPM)

A solvent, or solution of known composition is vapourised and thermo-statted, then allowed to impinge on a thermostatically controlled optical dew point sensor. This device employs a thermoelectric cooler to cool a small metal mirror until a thin film of condensation on the mirror is detected by laser light scattering. To date this method has been applied only to aqueous systems in the temperature range of 10 to 75 °C (Eckert and Sherman (1996)).

2.1.9 Inert Gas Stripping Method (IGS)

With the use of the inert gas stripping method, a dilute solution in an equilibrium cell is kept at a temperature of interest usually below the boiling point of the components. A constant inert gas flow is heated to the cell temperature and introduced into the solution contained in a dilutor cell and the components investigated are stripped into the vapour phase. The gas may be saturated with the solvent in a pre-saturation cell before entering the dilutor cell if the solvent volatility is high. If vapour-liquid equilibrium is established, the limiting activity coefficient can be calculated from the rate of variation of the solute vapour concentration versus the stripping time.

An ideal condition for the gas-stripping method, as a conclusion of previous studies is that the solute in the dilute solution, usually mole fraction $x_{sol} < 10^{-3}$, has appropriately high volatility so as to obtain an accurate measurement of the desorption of the solute from the solution as a function of time. The solvent, by contrast is best to be of low volatility so as to maintain the amount of the solution in the equilibrium cell and to hold equilibrium efficiency high. This would be the ideal case where the solute volatility is high while the solvent volatility is low (typically less than 1 mmHg is considered as low volatility here). Equations and corrections have been derived (Leroi et al. (1977), and Hovorka and Dohnal (1997)) in order to account for higher solvent volatilities, but for strongly non-ideal mixtures such as the ones studied in this project where the solute volatility is usually high but the solvent's volatility is relatively low, the method is superior to others. The dilutor technique combines inert gas stripping and gas-liquid chromatography. The dilutor technique has various potential advantages because this technique is capable of measuring small and large values of activity coefficients in pure or mixed solvents with good reproducibility (Atik et al. (2004)). An in-depth review of the inert gas stripping technique is given in Chapter 3.

2.2 Predictive Methods for Determination of Limiting Activity Coefficients

Thermodynamic models are used to predict infinite dilution activity coefficients where experimental data can be difficult and costly to obtain as well as for chemicals that are hazardous.

2.2.1 Group Contribution Methods (UNIFAC and ASOG)

UNIFAC (Universal Quasichemical Functional Group Activity Coefficients), (UNIQUAC functional group activity coefficients) and ASOG (analytical solution of groups) are the most commonly used prediction methods for liquid phase activity coefficients. These group-contribution methods are based on the fact that organic molecules belong to a given homologous series which contain varying numbers of the same kind of segments or groups. If it is assumed that the interaction energy between molecules really depends upon the interactions between individual groups that compose the molecules then configuration energy between molecules is given by the sum of all of the group interaction energies. Despite wide use, these methods have several disadvantages. Since the molecule is viewed as a collection of individual groups, the differences between isomers as well as group proximity effects cannot be determined. In addition, the models can give poor results for activity coefficients at infinite dilution and for systems whose components differ greatly in size. Also the models make no explicit accounting for hydrogen bonding behaviour (Eckert and Sherman (1996)).

2.2.2. Solvatochromic Parameters for Activity Coefficient Estimation (SPACE)

A new and superior predictive method for limiting activity coefficients in non-aqueous systems which incorporates the solvatochromic scales of Li and Carr (1994), which is now available to characterize solutes and solvents (Abraham (1993)). The SPACE equation is a modified form of the MOSCED (modified separation of cohesive energy density) models (Thomas and Eckert (1984) and Howell et al. (1989)). The advantage of this method over the group-addition methods is that it treats strong interactions like hydrogen bonding specifically, and thus is much more realistic for highly non-ideal systems. The SPACE equation however currently has no temperature dependence but relies on limiting activity coefficients evaluated at different temperatures by using the partial molar excess enthalpy.

2.2.3 Conductor-like Screening Model for Real Solvents (COSMO-RS)

COSMO-RS is an alternative predictive method from group contribution methods and can be used for a wide variety of systems that requires a limited minimum number of input parameters. A significant difference between group contribution methods and COSMO-RS is that a given group contribution methods' predictive ability is dependent on the availability of group interaction parameters, whereas COSMO-RS is only limited by the availability of individual component parameters.

COSMO-RS26 is an example of a simulation-based model that is quite close to reaching the point of becoming a practical chemical engineering utility. COSMO-RS is based solely upon uni-molecular quantum chemical calculations of the individual species in the system (i.e. not of the mixture itself). The COSMO-RS approach starts from a very different point of view, namely, from the complete molecule or, to be more precise, from the molecular surface as computed by quantum chemical methods. COSMO-RS combines an electrostatic theory of locally interacting molecular surface descriptors (which are available from quantum chemical method calculations), with an exact statistical thermodynamic methodology. In practice, each molecule that is involved in a mixture has to be computed by the quantum chemical conductor-like screening model.

COSMO-RS depends on a small number of 16 adjustable parameters, some of which are physically predetermined. COSMO-RS parameters are not specific regarding functional groups or molecule types. The parameters have to be optimized only for the method that is to be used as a basis for the COSMO-RS calculations. Thus, the resulting parameterisation is completely general and can be used to predict the properties of almost any imaginable compound mixture or system (Putnam et al. (2003)).

There is also a variation of this model known as segment activity coefficient (COSMO-SAC) model.

2.2.4 Quantitative Structure-Property Relationship (QSPR)

This involves the development of models that relate the structures of a heterogeneous group of organic compounds to their infinite dilution activity coefficients. The molecular structures are represented by calculated descriptors that encode their topological, electronic, and geometric features. The descriptors are used to develop multiple linear regression and computational neural network models to predict the limiting activity coefficient. Genetic algorithm and simulated annealing routines are used to select subsets of descriptors that form the best models. The models that are developed have predictive ability in the range of the experimental error of infinite dilution activity coefficient measurements (Mitchell and Jurs (1998)).

2.2.5 Group Contribution Solvation Model (GCS)

The GCS model was especially developed for prediction of infinite dilution activity coefficients. It is based on the idea of describing liquid phase non-idealities by solvation thermodynamics. In fact, the GCS model was derived by relating the interaction parameters in the UNIQUAC model to the solvation free energy. It involves quantum chemistry to calculate the so-called "charging" part of the solvation free energy, and the combinatorial term of the UNIQUAC model is used for the cavity formation contribution to the solvation free energy. Various different so-called self-consistent reaction field (SCRF) approaches have been formulated and are nowadays available to be used for calculating salvation energies and other properties in solution e.g. Integral Equation Formalism-Polarized Continuum Model (IEF-PCM). Modern computational chemistry is used to determine the energies of solvation of molecules in various solvents. From this and information about the size and shape of the molecule, we can then predict the infinite dilution activity coefficient directly.[1]

2.2.6 Linear Solvation Relationships (LSER)

The LSER is a generalized treatment of solvation which assumes that solute-solvent interactions are generally due to non-specific dipolarity/polarizability effects and specific hydrogen bonding interactions. The latter is subdivided into solute hydrogen bond donor (HBD)-solvent hydrogen bond acceptor (HBA) complexing and the converse, solute HBA-solvent HBD complexing. It is further assumed that these effects are independent and additive. The ability of a molecule to participate in these types of interactions is quantified by the assignment of solvatochromic

[1] www.wag.caltech.edu/home/stlin/research

parameters. The dipolarity/polarizability, hydrogen-bonding donation and acceptance tendencies of a molecule are represented parameters. The solvatochromic parameters for most molecules are scaled to lie mostly between 0 and 1 and are determined by spectroscopic or chromatographic means. There are several alternate solvatochromic scales, one for molecules as solvents and, unfortunately due to the rapid rate of development in this field, several different scales for molecules as infinitely dilute solutes (Sherman et al. (1996)).

Chapter 3 - The Inert Gas Stripping Method

3.1 Background

The inert gas stripping (IGS) method often referred to as the exponential dilutor method allows for quick and accurate determination of infinite dilution activity coefficients. The forerunners of this method were Fowlis and Scott (1963) who used this technique to calibrate chromatographic detectors, as well as Ritter and Adams (1976) who gave particular attention to the design of the equilibrium cell taking into account the essential role of mixing. Burnett (1963) applied this dilution method to determine partition coefficients for vapour-liquid equilibrium and Leroi et al. (1977) developed it to measure limiting activity coefficients.

Since then, the IGS technique has been extended to different systems. Richon et al. (1985) modified the apparatus in order to study viscous and foaming mixtures. Hradetzky et al. (1990), Oveckova et al. (1991) and Wobst et al. (1992) combined the analysis of the vapour with the analysis of the remaining liquid mixture and this allowed for measurements of the whole concentration range. Legret et al. (1981) developed a cell for high pressure measurements, while Boa and Han (1995) extended the method to various systems containing multi-component solutes or multi-component solvents.

Since the method was established by Leroi et al. (1977), a lot of progress has been made to ensure better results:

a) The Duhem and Vidal (1978) correction for the liquid concentration of the solute for partition between the vapour phase and the liquid phase in the equilibrium cell.
b) Modifications of the structure of the equilibrium cell (Richon et al. (1980) and Richon and Renon (1980)).
c) The pre-saturation technique (Dolezal et al. (1981) and Dolezal and Holub (1985)) which was proposed for the determination of limiting activity coefficients for highly volatile solvent systems
d) Fast expansion of the studying scope, such as for viscous and foaming systems (Richon et al. (1985)), and for mixtures containing food or oil (Lebert and Richon (1984)).
e) A liquid-conducted-tube was added between stainless steel capillaries and the cell body to generate a counter current of circulating solution to the stripping bubbles. This

improved mass transfer and made the process of stripping more efficient (Bao et al. (1990) and Bao et al. (1994)).

f) New cell design consisting of an inner glass tube for the determination of Henry's constants (Miyano et al. (2003))

IGS (or dilutor method) dates back to 1975 when it was first proposed by Anand et al. (1975). It originated from a technique used by Fowlis and Scott (1963) to calibrate chromatographic detectors (exponential dilution method). Leroi et al. (1977) showed that infinite dilution activity coefficients could be obtained by measuring the decrease in the gas-phase solute concentration as a function of time when the solute is stripped from the solvent due to an inert gas passing through the solution. A gas chromatograph is used only as a tool for quantifying the relative vapour phase concentration of the solute as a function of time. When a constant flow of inert gas is passed through a dilute solution to remove the solute, the vapour phase solute concentration, as measured by the gas chromatograph, will decrease in an approximately exponential fashion with time. This decay rate allows for direct calculation of the infinite dilution activity coefficient of the solute in the solvent. Since a decay rate is measured, there is no need to know the initial concentration of the solute. There is also no need to calibrate the detector, as long as a constant response factor is assumed. These are the two major advantages of this technique.

Since the success of Leroi et al (1977) with the IGS technique, only the dilutor cells have been changed or modified for different systems. Whilst other equipment used in conjunction with the cells may vary, the IGS technique itself has not changed. On the other hand researchers have improved on the equations used to determine limiting activity coefficients which now provide better results for certain types of systems. Gruber et al. (1999) derived an equation for the determination of limiting activity coefficients for various systems. They also designed a special cell for the systems they were investigating, as the original cell proposed by Leroi et al. (1977) had limitations and the validity of the method was being compromised.

The IGS method has also been extended to the determination of Henry's constants by Richon and Rennon (1980) and most recently by Miyano et al. (2003) and Miyano (2004). Using the IGS technique, as the basis of the analysis, they have derived equations for the determination of Henry's constants. The work by Miyano et al. (2005) is the most recent known advancement concerning the inert gas stripping technique. The IGS technique can now be used to determine limiting activity coefficients, as well as Henry's constants, thus making it more versatile. The same experimental setup can be used with only the data being analysed differently depending on the output required.

Over a number of years various equilibrium cells have been designed by various researchers to analyse different solutions based on properties of the solutions under investigation.

3.2 The Single Cell Technique and the Double Cell Technique

There are two types of techniques to consider when using the inert gas stripping technique as a means to determine limiting activity coefficients. The single cell technique and the double cell technique are the two variations of the method. The double cell technique can be used for any system and should be used if one is unsure of which technique to use. The single cell technique is more economically viable especially if the solvent used is expensive and in short supply but is only limited to certain types of systems.

3.2.1 Single Cell Technique (SCT)

In this technique, only one cell, the dilutor cell is used, just as in the original method proposed by Leroi et al. (1977). The SCT works well for systems where the solvent volatility is low and the solute (or solutes) volatility is relatively high. Some systems that have been successfully investigated include, alcohols in n-alkanes (Con and Delogu (1986)) and n-hexanes and benzene in binary mixtures with n-methylpyrolidone, dimethylsulfoxide, aniline, nitrobenzene and decalin (Leroi et al. (1977)). Henry's constants of light hydrocarbons in n-hexadecane and n-octadecane have also been investigated by Richon and Renon (1980).

If one is unable to categorize the volatility of any chemical component then it is best that the SCT be avoided and the more reliable double cell technique must be used for experimental analysis. Also, the SCT must not be used for systems containing more than one solvent. The SCT is unable to maintain a constant concentration and amount of solvent in the dilutor cell for multi-component solvent systems where there may be varying volatilities. The components with the higher volatilities in the solvent mixture will be stripped faster thus changing the concentration of the solvent mixture. This will thus result in errors in the obtained values of the limiting activity coefficients for the solvent/s.

3.2.2 Double Cell Technique (DCT)

Two equilibrium cells, a pre-saturation cell and a dilutor cell, must be used for the measurement of limiting activity coefficients in this technique. In the pre-saturation cell, a solvent which has the same composition as that in the main dilutor cell is always added. When an inert stripping gas is introduced, a saturated vapour flow of the solvent is generated and is used to maintain the

composition and the amount of solvent in the dilutor cell. This is particularly useful for systems of high solvent volatility, in maintaining the amount of solvent in the dilutor cell.

The DCT is the preferred method to use as it can handle many more systems than the SCT. The downfall of the DCT is that it requires the use of additional solvent. In some cases the solvent may be very expensive or available in small quantities. However, the solvent can be reused if its composition has not changed. This can be verified by injecting a small sample of the solvent from the cell into a GC with a suitable temperature program. One can also check for impurities in this manner. Impurities can accumulate from the inert gas entering the cell or the solvent may become contaminated by the seals or other materials used. It is best that the solvent be analysed after each run to check for the existence of foreign substances as this would affect the value of the activity coefficient at infinite dilution.

Systems that have been investigated previously for which good results have been obtained are alcohols in hydrocarbon mixtures (Vrbka et al. (2002)), hydrocarbons (n-hexane, cyclohexane, 1-hexene and benzene) in n-methyl-2-pyrrolidone/water mixtures (Krummen et al. (2000)) and n-formylmorpholine/water mixtures (Krummen et al. (2004)). Also alkenes and alkanes in ionic liquids such as 1-methyl-3-methylimidazolium bis(trifluoromethylsulphonyl)imide have been successfully investigated by Krummen et al. (2002).

3.3 Types of Systems that can be analysed using the Inert Gas Stripping Technique

There are various different categories of systems that can be analysed using the inert gas stripping technique. However all systems fall into four categories as far as the inert gas stripping technique is concerned. The technique can be used to analyse all types of systems as long as good separation can be achieved in the GC column and the simplifying assumptions from which the equations were derived are satisfied.

3.3.1 Type 1: One-Component Solute + One-Component Solvent Systems

For these types of systems (binary systems), use of the SCT or DCT depends mainly on the volatility of the solvent. If it is a non-volatile or low volatile substance, it is more convenient to use the SCT. For example, when alcohol + n-alkane systems were studied by the gas stripping method by Coni and Delogu (1986) and Bao et al. (1990), it was found that the solutes are always preferentially volatized, either an alcohol in an alkane or an alkane in an alcohol. Only one cell was necessary for the measurements.

When the limiting activity coefficient for solutes in acetone, which is obviously a high-volatile solvent, were measured by Bao et al. (1993a) and Bao et al. (1994), a pre-saturator, that means DCT was employed, to maintain the amount of solution in the dilutor cell and to keep the equilibrium efficiency high. For systems whose solvents have volatility that are neither very high nor very low compared with that of the solutes, such as benzene in acetonitrile, and n-heptane in benzene, either the SCT or the DCT can be used for the determination of infinite dilution activity coefficients.

3.3.2 Type 2: One-Component Solute + Multi-Component Solvent Systems

A multi-component solvent means that the solvent is composed of two or more substances. For such a system, the measurement will have no physical meaning if the SCT is used because the surroundings of the solute, i.e. the solvent, will be changed while stripping. For instance, consider the measurement of the limiting activity coefficient for solute chemical A in a solvent mixture of chemicals B and C with different volatilities. The concentration of the B in solution will be increased if C has higher volatility than B during the stripping process and vice versa. The solvent concentration will be changing with time during the experiment and as a result the limiting activity coefficient of chemical A will vary during the experiment. The SCT must not be used for such systems.

The DCT can eliminate this problem by introducing the solvent mixture, with the same concentration as in the dilutor cell (before addition of solute) into a pre-saturation cell. When this is done, the gas flowing out of the pre-saturator cell and into the main dilutor cell is saturated with the multi-component solvent vapour. The solvent concentration in the dilutor cell will now remain constant throughout the experiment. The concentration of solvent in the pre-saturation cell will change slightly, as the volume of the pre-saturator used is usually finite, while that in the dilutor cell will be constant within the whole experimental period. This is true as long as the stripping period is not too long and the gas leaving the pre-saturator is always saturated with solvent. The IGS technique can be used successfully to determine limiting activity coefficients for multi-component solvent systems provided the DCT is used.

3.3.3 Type 3: Multi-Component Solute + One-Component Solvent Systems

All the conditions for Type 1 apply to these types of systems. The only difficulty here is obtaining a perfect separation in the gas chromatograph column for all the components. The component peaks can be identified by their residence times obtained by injecting pure samples of each component into the gas chromatograph before performing the actual experiment. The more

components the solute consists of, the more difficult the analysis becomes especially when the residence times are very close.

3.3.4 Type 4: Multi-Component Solute + Solvent Systems

If a solute is multi-component, the system will have more than one limiting value. As mentioned previously, we can measure these values separately as long as perfect separation between the components can be achieved during gas chromatography. If the properties of the components making up the solute have volatilities that are close, and the detector (usually a gas chromatograph) can detect their vapour phases accurately, then the limiting values can be determined simultaneously if there are no experimental errors. The efficiency of determining limiting activity coefficients is enhanced for these types of systems when using the IGS technique (Bao and Han (1992)).

3.4 An Overall Scheme

Now that the different techniques (SCT or DCT) and types of systems (Types 1, 2, 3 and 4) are fully understood, an attempt has been made to illustrate which technique is most appropriate for a particular system. The illustration (Figure 3-1) serves as a quick reference and summarizes the different possible paths for the measurements.

Bao and Han (1995) found that the use of the SCT or DCT depends mainly on the volatility and nature of the solvent or solvents making up the solution. If the solvent is a non-volatile or low-volatile substance, SCT can usually be employed, but if it is a highly volatile substance or composed of two or more substances, DCT must be applied for a reasonable and accurate measurement.

For the solute, however, its volatility is not concerned directly with the use of SCT or DCT, but with the method employed. The solute should have certain volatility in the dilute solution (despite its pure properties) if the gas stripping method is applied for the determination of limiting coefficients (Richon et al. (1980)). However, if the dilute solute is highly volatile, the method is not accurate enough unless some modifications on the sampling technique or detecting equipment are made (Boa et al. (1993b)). Further, the nature of the solute/solutes can only tell us how many limiting activity coefficients the system has i.e. if the solute is made up of more than one component (multi-component), then one can expect the number of limiting activity coefficients to equal the number of solutes. It also tells us whether these limiting values can be determined simultaneously or not based on the solute/solutes relative volatility.

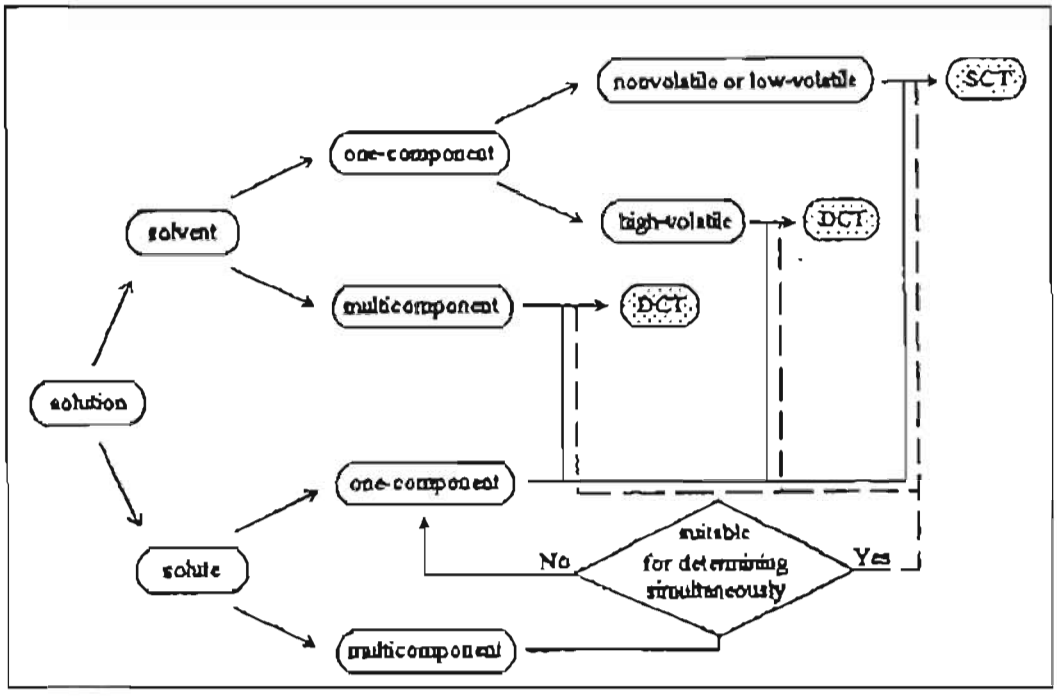

Figure 3-1: Overall scheme given by Bao and Han (1995) for choosing the SCT or DCT for the inert gas stripping technique, as used to measure infinite dilution activity coefficients.

3.5 Major Advances in Experimental Determination of Activity Coefficients and the IGS Method

There have been various improvements to the way limiting activity coefficients are obtained using the IGS technique over the passed few decades. These improvements include modifications to the equipments as well as improvements in the analysis of the experimental data. The inert gas stripping method was first introduced by Leroi et al. (1977); since then, various improvements and modifications were made, including

- The introduction of the Duhem and Vidal (1978) correction factor
- Modification of the structure of the dilutor cell
- The introduction of the double cell technique for highly volatile solvent systems
- Advanced cells for further research regarding viscous or foaming mixtures
- Improved experimental set-ups to ensure isothermal conditions
- Application of the technique to determine Henry's constants

There are two important assumptions to consider when using the inert gas stripping method. When determining infinite dilution activity coefficients using the IGS method, the following assumptions are made:

- The vapour phase is ideal.
- There is negligible solubility of the inert gas in the liquid

The inert gas stripping method is based on the principle of exponential dilution as discussed below.

3.5.1 Exponential Dilution

The inert gas stripping method was originally used for gas chromatograph detector calibration. An inert gas is allowed to flow through a flask that contains the calibration fluid. The fluid concentration in the exit stream will be observed to decrease exponentially as the solute is desorbed into the gas bubbles from the liquid. If the total area under the peaks in the graph on the left in Figure 3-2 is plotted against time then the exponential decay can be clearly seen.

A dilute solution in a cell is initially maintained at a specified temperature. The highly diluted component (solute) is stripped from a liquid solution (solvent and solute) by a constant inert gas flow. The solute concentration in the gaseous phase is monitored and measured using a gas chromatograph. A typical concentration profile can be seen in Figure 3-2 (left). The figure on the left is the solute peak areas only. The solvent peak areas have been omitted for clarity of the exponential decay. The figure on the right is a result of plotting the logarithmic ratio of peak areas to the first solute peak area (A_i / A_0), against time to form a straight line with slope *a*.

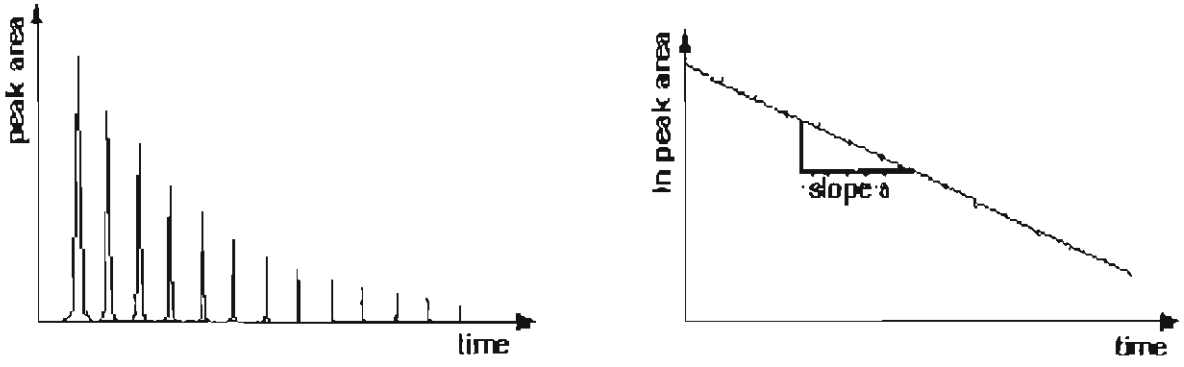

Figure 3-2: The figure on the left shows the typical solute peak profile formed as a result of 13 injections and the figure on the right is a plot of represented solute peak areas against time to give slope *a* (Gruber et al. (1999)).

3.5.2 Factors Affecting the Performance of the Equilibrium Cells

An illustration of the dilutor cell used in this study is shown in Figure 3-3. A cell of similar design was used as the pre-saturation cell. A number of factors affect the performance of the cells and is outlined below.

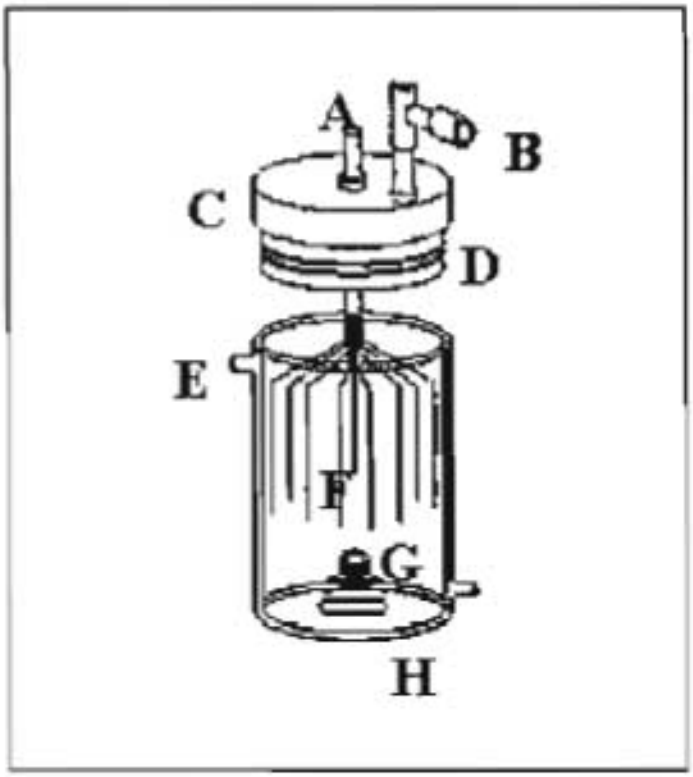

Figure 3-3: Dilutor cell used in this study

A – Stripping gas inlet; B – Stripping gas outlet; C – Teflon plug; D – O-ring seals; E – Circulating water inlet; F – Capillaries; G – Thermowell; H – Magnetic stirrer

3.5.2.1 Bubble Rise Height

The bubble rise height required for the gas phase to be in equilibrium with the liquid in the cell is most important and can be calculated using a procedure demonstrated by Richon et al. (1980). Both the mass transfer of solute to the bubble as well as diffusion of solute into the bubble must be considered. The bubble rise height is related to the cell height and bubble diameter. The greater the height of the cell, the longer the path for the bubbles in the solution and thus more time is allowed for equilibrium conditions. Also larger bubble diameters mean greater cell heights will be required in order to obtain equilibrium. The procedure for determining the bubble rise height is summarized in Chapter 5.

3.5.2.2 Double or Single Cell Technique

Of the two techniques the choice of which technique to use depends on the nature (one or multi-component) and the volatility of the solvent in the solution. For a non-volatile or low-volatile solvent, SCT is usually used, but for a highly volatile solvent or a multi-component solvent system, the DCT must be used for sufficiently accurate results. For the solute, however, the volatility is concerned with the method employed. If the gas stripping method is employed, the solute should have certain volatility in the dilute solution despite its pure properties. The effects of the two techniques on certain systems are observed in later chapters.

3.5.2.3 Type of Gas Dispersion Device

The type and effectiveness of the gas dispersion device determines the accuracy of the results. There is an optimum and often desired minimum bubble size to ensure good mass transfer in the cells. Further, it is undesirable for the bubbles to be allowed to coalesce. Initially the use of a sintered disk as a gas dispersion device was proposed. It was observed that the sintered disk often gave rise to bubble coalescence and Jourdain (2000) suggested that the magnetic stirrer was responsible for the coalescence and recommended modifications that avoid bubbles being introduced into the vortex created by the stirrer. Thus for experiments undertaken in this study, the use of evenly spaced capillaries were used as the dispersion medium (see Figure 3-3). Ten lengths of $^{1}/_{32}$ inch narrow bore stainless steel tubes were used to introduce the gas. This ensured optimal bubble size, and the absence of coalescence.

3.5.2.4 Flow Rate of Stripping Gas

The flow rate of the stripping gas determines the contact time of the bubbles with the solution. It is important that sufficient contact time be allowed for the bubbles with the liquid. The value of the ideal flow rate will be system dependant, but experiments indicate that a low gas flow rate is most appropriate. The flow rate also affects the size of the bubbles. The higher the inert gas flow rate the larger the bubble diameters. This is another reason for keeping the gas flow rate as low as possible to ensure equilibrium conditions are met within the cells.

3.5.2.5 Liquid Viscosity

Richon et al. (1985) found that the influence of viscosity is two-fold. The mass transfer is compromised when the viscosity is high. This is however, compensated for by the bubble rise velocity increasing and the contact time is therefore decreased. In fact Richon et al. (1985) also

reports that even systems with viscosities as high as 40 cp reach equilibrium after passing through 1 cm of solution. Solutions having viscosities greater than 50 cp were found to be problematic. The main concerns were that the stirring was ineffective and that the liquids tend to foam.

3.5.2.6 Bubble Size

Previous studies undertaken by Richon et al. (1993) showed that bubble sizes less than 2 mm were most appropriate for a bubble rise height in solution of more than 3 cm. Thus the dispersion device must maintain bubble diameters below a certain maximum diameter that depends ultimately on the bubble rise height in the cell. For good mass transfer and to ensure that equilibrium conditions for the experiment are met, the bubble rise height must be more than sufficient and the bubbles must be smaller than a certain maximum. Fine bore capillaries seem to work well but any dispersion device that maintains small bubble diameters in the equilibrium cells will satisfy. For any gas dispersion device the cells must be designed for the largest bubbles, formed at the highest operating flow rates.

3.5.2.7 The Infinite Dilution Activity Coefficient

The design of the cell depends on the value of the infinite dilution activity coefficient. The effect of a large infinite dilution activity coefficient on the rate of solute mass transfer can be significant. The infinite dilution activity coefficient has no effect on solute diffusion. The applicability of the cell used in this project is limited by the value of the infinite dilution activity coefficient. Systems such as non-electrolytes in water (discussed by Li et al. (1993)) have values of infinite dilution activity coefficient that are of the order of several thousands and require that the cell be revised to ensure adequate approach to equilibrium.

3.6 Advantages and Disadvantages of the Inert Gas Stripping Method

The IGS technique has its pros and cons but its advantages out-weigh its disadvantages making it a method that is superior to others in terms of the range of systems that can be analysed.

3.6.1 Advantages

- Can be used to determine infinite dilution activity coefficients for systems with high and low volatility solvents.
- A single experiment can allow for the investigation of multiple solutes.

- It is a direct method for determining limiting activity coefficients.
- There is no need for detector calibration especially if a gas chromatograph is used as the means of analysis.

3.6.2 Disadvantages

- High purity solutes and solvents are required.
- Sufficient gas-liquid contact is required for accurate results.
- Systems with low volatility solutes are difficult to analyse.

3.7 Review of Previous IGS Apparatus

Over the years various different dilutor cells have been designed for various systems. An illustration and description of dilutor cells have been outlined below.

3.7.1 Leroi et al. (1977)

The most basic dilutor cell is the cell designed by Leroi et al. (1977). Since then various cells have been designed to handle different solutions that would be more difficult to analyse using the basic cell design of Leroi et al. (1977). The cell designed by Leroi et al. (1977), most closely describes the cells used for all systems in this dissertation. An illustration of this cell is shown in Figure 3-4.

The dilutor cell (Figure 3-4) could hold about 25 cm^3 of solvent and the liquid solute was introduced into the cell by means of a 10 µl syringe through the septum. This would have resulted in an initial mole fraction of solute, which is small enough to observe no significant deviation of the activity coefficient from its limiting value. The carrier gas passed through a fritted disk where it was dispersed into fine bubbles.

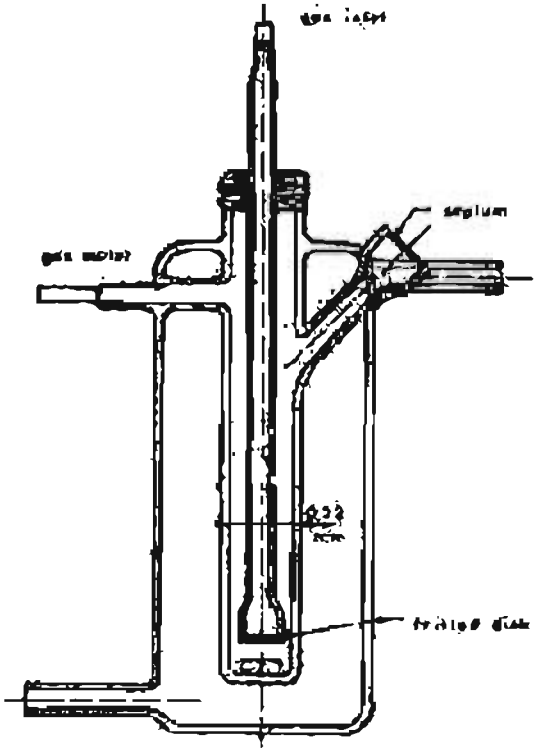

Figure 3-4: Experimental dilutor cell used by Leroi et al. (1977), which was made of Pyrex glass.

3.7.2 Richon et al. (1980)

A few years later Richon, Antoine and Renon, improved the dilutor cell to calculate infinite dilution activity coefficients for linear and branched alkanes from single carbon (C1) to nine carbon (C9) alkanes. The cell is similar to the cell developed by Leroi et al. (1977) except for the following improvements and differences. The carrier gas is introduced at the bottom of the cell by capillaries, of which, gas bubbles of equal size form slowly at the extremities. This modification improves the mass transfer of solute and solvent into the bubble. The new glass cell was built with a concentric gas inlet and outlet. The outlet gas collector is conical to prevent liquid entrainment. Fine capillaries were chosen as the gas dispersion device. Apart from the reasons above it also gives even bubble size distribution. The dilutor cell by Richon et al. (1980) is shown in Figure 3-5.

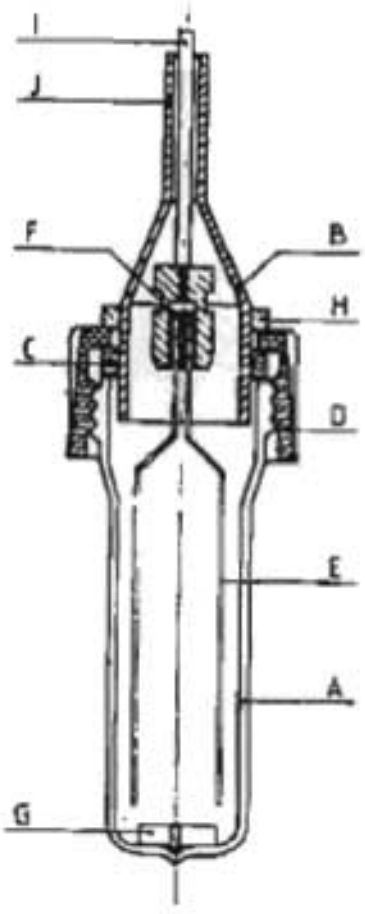

Figure 3-5: Dilutor cell used by Richon et al. (1980)

A – glass still body, B – conical collector of gas outlet, C – gasket, D – plug, E – capillaries, F – Teflon seal, G – magnetic stirrer, H – metallic ring to adjust the depth of the conical collector B in the still, I – tube for carrier gas inlet, J – gas outlet.

3.7.3 Richon and Renon (1980)

In the same year Richon and Renon designed a cell for the determination of activity coefficients for light hydrocarbons. This is a completely new cell design and the operation of which requires the filling of the cell to a liquid level not less than 1 cm from the top of the cell, reducing the volume of the vapour phase considerably. The collector has also been modified to obtain a simple geometric shape for the vapour phase. The dilutor cell is shown below:

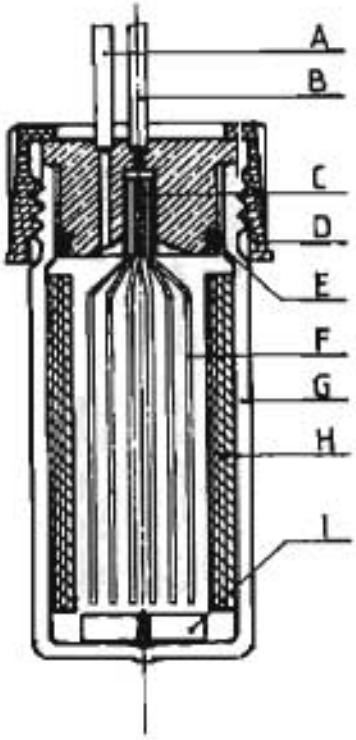

Figure 3-6: Equilibrium cell designed by Richon and Renon (1980).
A – vapour-phase outlet, B – inert gas inlet, C – Teflon seal, D – plug, F – capillaries, G – glass still body, H – baffles, I –magnetic stirrer.

3.7.4 Legret et al. (1983)

Legret et al. (1983) designed a cell for use with the IGS technique specifically for the determination of partition coefficients for use with the inert gas stripping technique. Partition coefficients are closely related to limiting activity coefficients. The gas flow is dispersed at the bottom of the cell by means of vertical capillaries open at the bottom of the cell. The dilutor and pre-saturator cells used for their experiments were of similar design with 20 capillaries of 3×10^{-4} m internal diameter used in the saturator cell and 50 capillaries of 10^{-4} m internal diameter used in the dilutor cell. They were also able to immerse the cells in an oil bath and regulate the temperature of the oil keeping the contents of the cells at the experimental temperature. The cells each contained about 40 cm^3 of solvent which was well mixed by small magnets rotating in magnetic fields by means of external permanent magnets rotating in turbines. An illustration of the dilutor cell appears in Figure 3-7.

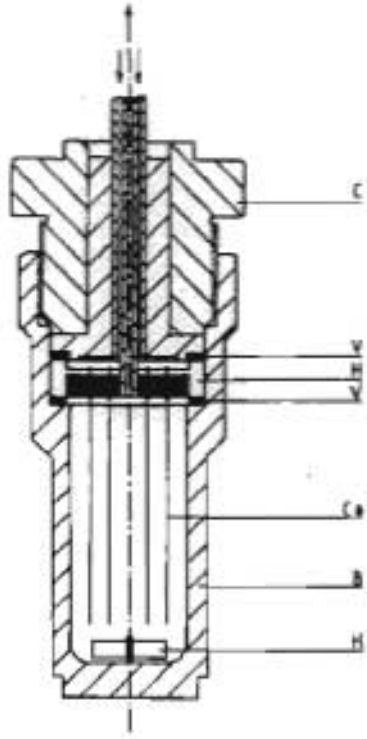

Figure 3-7: Dilutor cell for the determination of partition coefficients for alkanes

B – body, C – cap, Ca – capillaries, H – capillary holder, M – magnet, V – Viton "O"-ring

3.7.5 Richon et al. (1985)

Richon et al. (1985) took dilutor cell design to another level when they designed a cell for the determination of limiting activity coefficients for viscous and foaming mixtures. All the previous cells were limited to the study of non-foaming mixtures with low viscosity due to the design of the dilutor cell. An illustration of this cell is shown in Figure 3-8.

The cell shown in Figure 3-8 is composed of a glass tube (K) closed at each extremity by plugs (G), and the corresponding sealing being achieved by using soft gaskets (D). At the lower extremity of the glass tube the carrier gas inlet (M) holding the capillary injectors (L) can be found. At the other extremity is the vapour phase outlet (A), a deflector (B), a foam-breaking device (E) and a bladed screw (H). The bladed screw is used to prevent liquid rotation in the cell and promote the coalescence of gas bubbles. Between the two extremities, two pivots maintain an Archimede's screw. It is activated by means of magnet (F) and is used to circulate the liquid from top to bottom inside the internal cylinder (J).

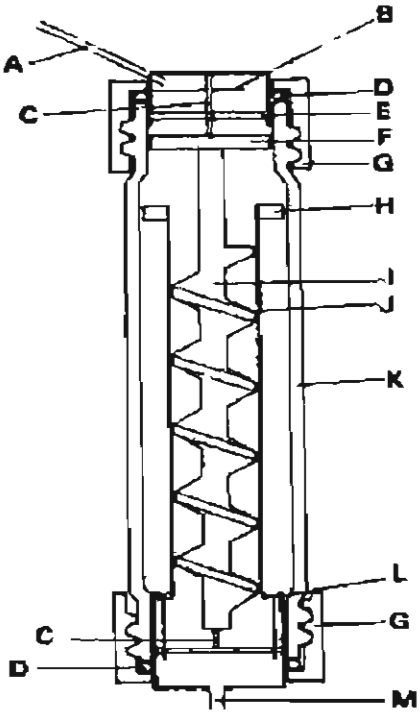

Figure 3-8: New type of dilutor cell designed by Richon et al. (1985) for viscous and foaming mixtures.

A – vapour phase outlet, B – deflector, C – pivot, D – gasket, E – foam-breaking device, F – permanent magnet, G – plug, H – bladed screw, I – Archimede's screw, J – internal cylinder, K – dilutor cell, L – carrier gas capillary injectors and M – carrier gas inlet.

3.7.6 Boa et al. (1994)

Boa et al. (1994) designed a dilutor cell for various types of systems. The equilibrium cell consists of a liquid-conducting tube as shown in Figure 3-9. The tube enhances mass transfer and makes the stripping process more efficient by generating a counter current flow of circulating solution to the stripping bubbles. Stainless steel capillaries of 10^{-4} m internal diameter were used to generate small bubbles.

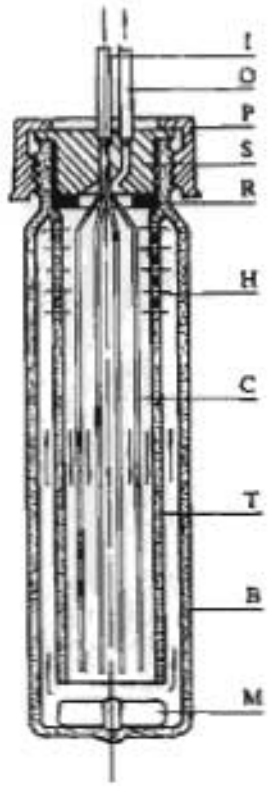

Figure 3-9: Equilibrium cell designed by Bao et al. (1994).
B – body, C – capillaries, H – small holes, I – inert gas inlet, M – magnet, O – vapour phase outlet, P – plug, R – PTFE "O"-ring, T – liquid-conducted-tube.

3.7.7 Hovorka et al. (1997)

Hovorka et al. (1997) designed a cell for the determination of activity coefficients at infinite dilution, for use in the determination of air-water partitioning coefficients of volatile halogenated hydrocarbons. The equilibrium stripping cell is an all-glass jacketed device composed of the pre-saturator (P) and the dilution cell (D) as shown Figure 3-10. The stripping gas first enters the pre-saturator (P). Its compartment is divided by fritted glass disks into several plates to achieve efficient pre-saturation with the solvent vapour, yet keeping a small pressure drop across the pre-saturator. The pre-saturated gas then passes into the solution in the dilutor cell (D) through a fine porosity fritted glass tip where it is dispersed into bubbles with small diameters. The solution is vigorously mixed with an efficient magnetic stirrer (S), which extends considerably the path and the residence time of the bubbles in the solution. The vapour space of the cell and a special design of the gas outlet prevent liquid droplet entrainment. An illustration of the cell is shown below.

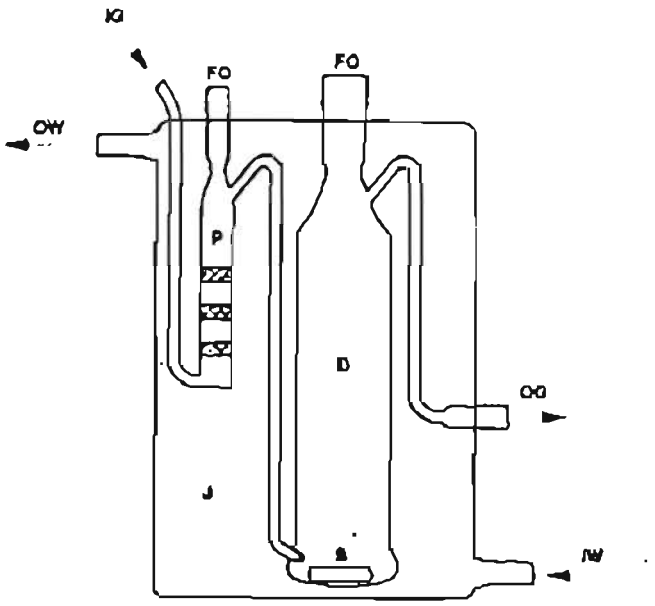

Figure 3-10: Equilibrium cell designed by Hovorka et al. (1997).

P – pre-saturator with fritted glass disks, D – dilutor cell, S – stirrer, J – thermo-statted jacket, IW – input of thermo-statted water, OW – output of thermo-statted water, IG – input of stripping gas, OG – outlet of saturated stripping gas, FO – filling openings.

3.7.8 Miyano et al. (2003)

Miyano et al. (2003) designed a cell to determine activity coefficients at infinite dilution for the determination of Henry's constants for solutes such as alkanes and alkenes in solvent alcohols. Henry's constants are closely related to limiting activity coefficients as discussed in Chapter 6. The experimental gas stripping cell is shown in Figure 3-11. The equilibrium cell has a volume of 44 cm^3. The cell contains an inner glass tube and a magnetic stirrer. The inner tube ensures good mixing of the whole solution, and also creates a counter flow of liquid against the rising bubbles. This results in the vapour-liquid contacting times becoming longer. The exit port of the inert gas in the dilutor cell is made of a stainless tube with inner diameter of 0.14 mm.

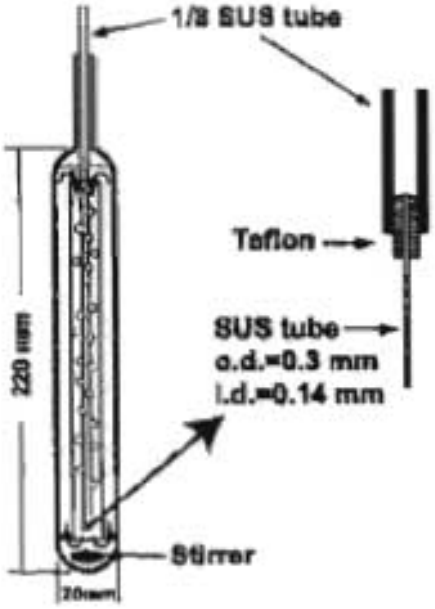

Figure 3-11: Equilibrium cell designed by Miyano et al. (2003) for the determination of Henry's constants using the inert gas stripping technique.

Chapter IV - Equipment and Experimental Procedure

In the preceding chapters the critical design parameters were discussed. The scope of this project involved the design, construction and commissioning of a suitable inert gas stripping equipment for thermodynamic measurements of activity coefficients at infinite dilution. The design of the IGS apparatus was limited due to financial constraints. As a result less robust equipment was used resulting in a very basic design. Though the apparatus used was not as automated and in some instances less efficient than some of the other previous designs on which it was based, it is still adequate for obtaining favourable results. Material selection was based on availability, cost, inertness to the effects of various chemicals such as acids and strength of materials. The specification of the equipment assembled is comparable to equipment designed by other researchers.

4.1 Process Description

The flow of material through the system can be difficult to describe and is best shown in the form of a comprehensive flow diagram. The illustration, Figure 4-1, shows the various flows of materials and all the major equipment used for this study.

Nitrogen gas flows out the regulator of the nitrogen tank (A) to a smaller regulator (T) which maintains a constant flow of nitrogen to the control valve (P). The control valve sets the flow rate of nitrogen into the system for a particular run with the help of the soap bubble flow meter (O). Once the flow rate has been set the gas enters a long copper coil (Q1 - ¼ inch ID) immersed in a water bath (B1) which allows the gas to equilibrate to the set-point temperature. This set-point temperature is the system temperature i.e. the temperature of the pre-saturator cell (C) and the dilutor cell (D). A Grant temperature controller (Type: GD 120) keeps the water in the water bath at the constant system set-point temperature. The water surfaces in the water baths are completely covered with polystyrene chips to reduce heat loss to the atmosphere. The Grant temperature controller has a built-in pump and pumps water into the jackets around the equilibrium cells and to the heat exchanger (L) keeping them at system temperature. All the relevant piping is well insulated reducing any heat losses.

After the gas flows through the heating coil it enters the pre-saturator cell through a steel pipe (¼ inch ID) through the centre of the cell and is distributed through ten capillaries ($^{1}/_{32}$ inch ID) at the bottom of the cell.

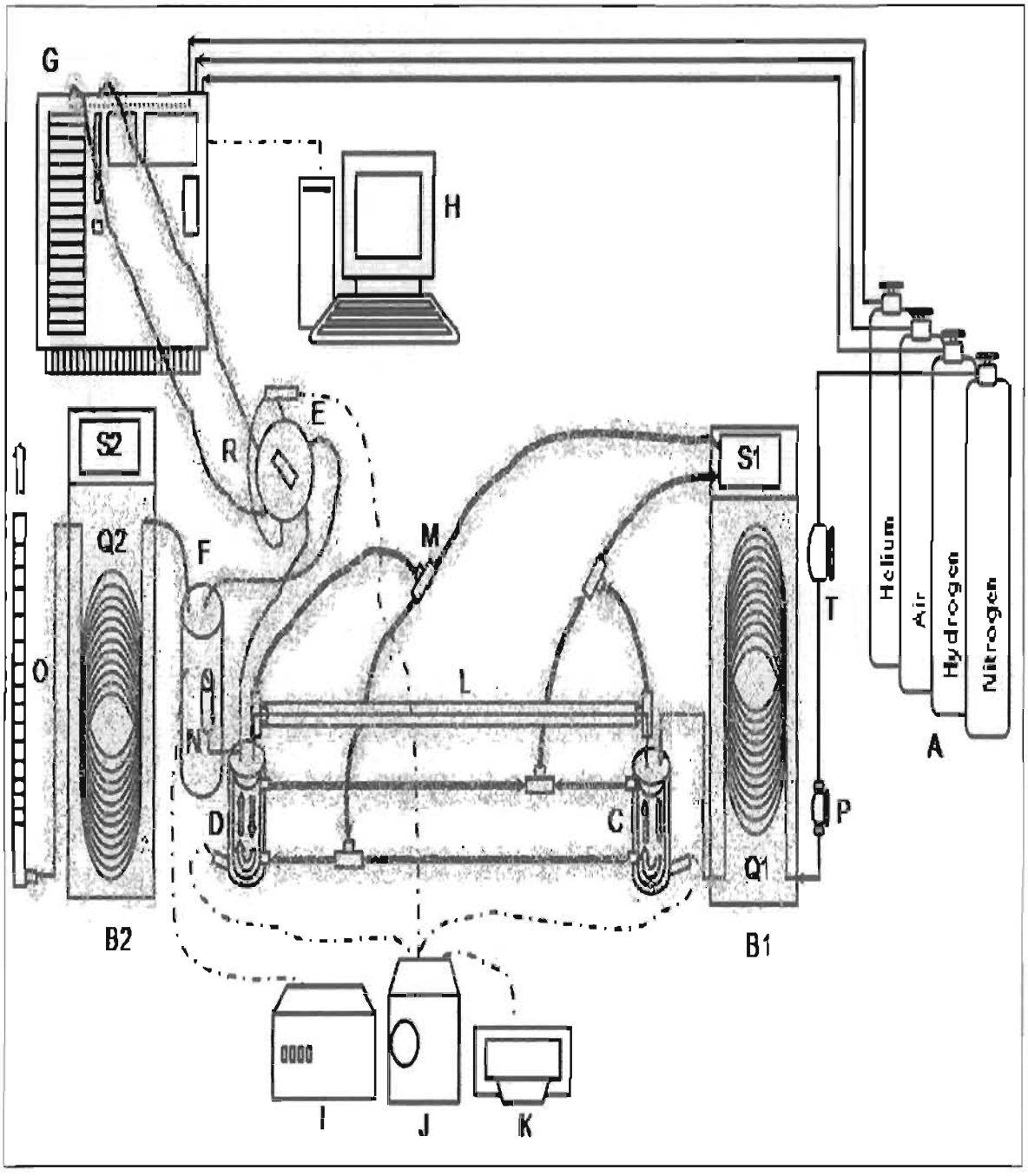

Figure 4-1: Process flow diagram of experimental setup used for the determination of limiting activity coefficients. The grey spots show where glass wool or polystyrene was used as insulation and where there was thermo regulation in the process

A – gas tanks, B – water baths, C – pre-saturator cell, D – dilutor cell, E – six-port gas-sampling valve, F – cold trap, G – Varian 3300 GC, H – computer, I – Sensotec pressure display, J – selector switch, K – temperature display, L – heat exchanger, M – t-piece, N – Sensotec pressure transducer, O – soap bubble flow meter, P – flow control valve, Q – coil tubes, R – sample loop, S – temperature controller with built-in pump, T - regulator

These capillaries ensure constant and optimal bubble size for good mass transfer. The pre-saturator cell contains a known amount of solvent. The solvent enters the bubble phase as the bubbles rise up into the vapour phase in the cell before entering the inner tube of the heat exchanger (L). The heat exchanger keeps the saturated nitrogen gas at the system temperature and prevents condensation of solvent before entering the dilutor cell (D). Water from the water bath (B1) is used to maintain the temperature of the gas flowing through the heat exchanger. The heat exchanger is well insulated to prevent any heat losses that might occur through the outer tube. An illustration of the heat exchanger is shown in Figure 4-2.

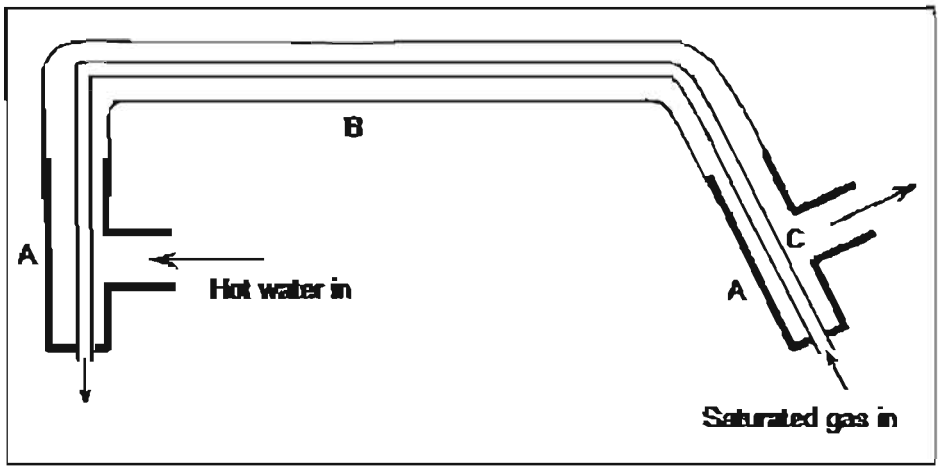

Figure 4-2: Heat exchanger fitted on the gas line between the two equilibrium cells.
A – T-pieces ceiled at one end with silicon, B – Outer plastic tube (½ inch ID) of 0.5 *m* in length and C – Inner steel tube (¼ inch ID)

The saturated gas enters the dilutor cell in a similar fashion to the way it enters the pre-saturator cell. The dilutor cell contains a known amount of solvent as well as a drop of solute just enough to be detected. The contents of both cells are stirred by means of magnetic stirrers. The cells are also well insulated using glass wool to prevent heat loss from its outer jackets. Gas bubbles form as the gas passes through the 10 capillaries ($^{1}/_{32}$ inch ID) and rise to the top of the cell into the vapour phase, stripping the solute from the solution in the dilutor flask. The nitrogen gas containing the solute and solvent then enters port 1 of a Valco 6-port gas-sampling valve (E) through a $^{1}/_{8}$ inch ID heated pipe about 40 cm long. The line is heated using nichrome wire inserted into a jacket and wrapped around the pipe with thermal tape. A voltage is applied across the both ends of the wire using a Major Tech variac which heats up the line to a temperature set at 40 °C above the system temperature in order to prevent condensation in the line. Attached along the same line is a Sensotec pressure transducer (N) which measures the pressure in the dilutor cell. The signal from the Sensotec transducer is sent to the Sensotec

pressure display (I). The transducer was calibrated using a reference transducer in order to obtain correct pressure readings in kPa.

Once the gas reaches the 6-port gas-sampling valve the flow can either be sent to the GC or else be vented. The valve has two configurations, the "fill" and "inject" positions, as shown below:

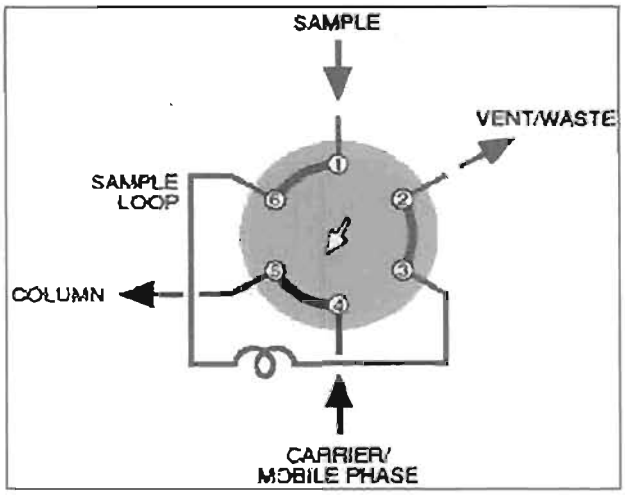

Figure 4-3: (a) The "fill" position.[2]

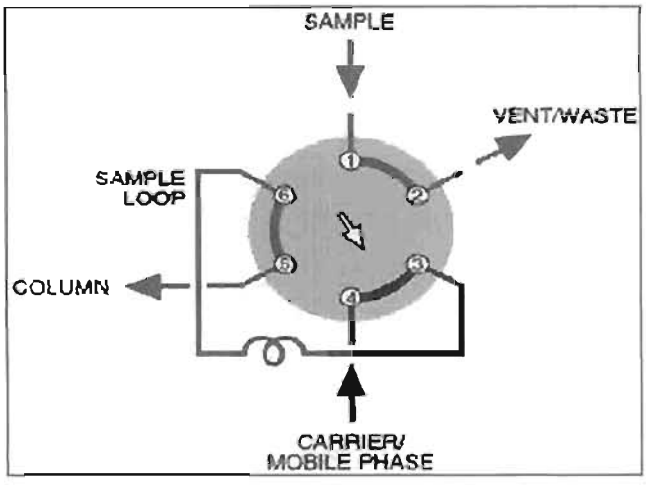

Figure 4-4: (b) The "inject" position.

[2] Pictures taken from www.vici.com/support/app/app11j.php

In position (a), known as the "fill" position, the gas sample enters port 1 flows through to port 6 and then through the external loop known as the sample loop (R) through to port 3 and then out port 2 where it flows into a cold trap (F). This is know as the fill position, as the sample loop is filled with the flowing gas from the dilutor cell that must analysed while the carrier gas (helium) enters port 4 and leaves through port 5 to the GC column. The helium gas was diverted from a line in the gas chromatograph (G – Varian 3300) just before it enters the column and re-enters the gas chromatograph (GC) along the same break in the original line. In this position the carrier gas does not come in contact with any of the sample. In position (b), known as the "inject" position, the sample contained in the sample loop is injected directly into the gas chromatograph for analysis. The carrier gas entering port 4 now moves to port 3 and through the sample loop to port 6 and then to port 5 and into the GC. In the mean time the gas from the dilutor cell entering port 1 now enters port 2 directly and moves to the cold trap. All the lines entering or leaving the 6-port sampling valve are heated using nichrome wire to a temperature approximately 40 °C above the system temperature and well insulated with glass wool to prevent heat loss as well as cold spots.

Two separate flows of material take place at this point in the process; the gas entering the cold trap and the helium gas with or without sample entering the gas chromatograph. The cold trap is filled with an ice - acetone solution, and reaches temperatures between 2 to 5 °C. The purpose of the cold trap is to condense the stripped components in the nitrogen gas entering the cold trap so that only the nitrogen gas passes to the soap bubble flow meter for determination of the flow rate of pure nitrogen flowing through the cells. In this way accurate measurement of the nitrogen gas flow rate can be obtained. The nitrogen gas leaving the cold trap enters a copper coil (Q2) inserted into a water bath (B2) where it is heated to system temperature again before reaching the soap bubble flow meter (O) so that the correct flow rate of nitrogen gas can be measured. The water in water bath (B2) is maintained at constant temperature using a BC (Model: BTC 901) temperature controller. After the nitrogen passes through the soap bubble flow meter it is vented to the atmosphere.

When the gas-sampling valve is moved to the inject position the helium gas carries with it all the contents of the sample loop into the GC for analysis. The sample content gets separated in the capillary column of the GC and usually the volatile solute reaches the detector before the less volatile solvent. Upon reaching the detector a signal is sent to a computer (H) where the integration program Clarity determines the peak areas and residence times.

As mentioned before a Major Tech variac sets the system temperatures and two Class A Pt-100's measures the temperatures in the two equilibrium cells. A Pt-100 is a temperature

dependent resistor. The resistance at 0 °C is 100 Ohm. The temperature coefficient is approximately 0.38 Ohm/K. Pt-100's are used to measure temperatures of -200 to 850 °C.

The temperatures are displayed up to two decimal points on a Eurotherm temperature display. The line temperatures are set using other similar variacs and measured using Class A Pt-100's fitted into metal jackets. The temperatures are read off the same Eurotherm display by the use of a Wika Tronic Line selector switch. The Pt-100 devices are calibrated before use in order to obtain accurate temperatures. A typical calibration curve for the dilutor cell Pt-100 is shown in Figure 4-5. The accuracy of the Pt-100's in determining temperature is only as accurate as the calibration probe used to calibrate it. Figure 4-5 shows the deviation of the dilutor Pt-100 from the actual system temperature. This deviation was used to plot a calibration cure for the Pt-100 which resulted in a straight line with all points lying on the line.

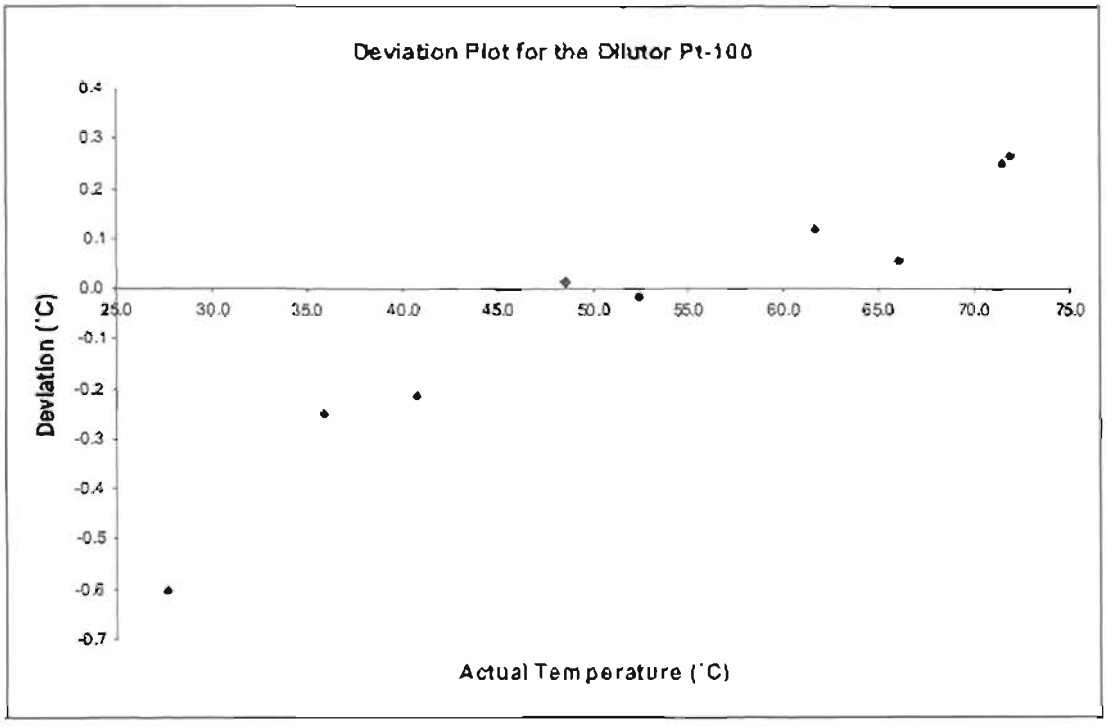

Figure 4-5: Plot showing deviation of the dilutor cell Pt-100 temperature from the actual system temperature.

4.2 Description of Important Equipment and their Functionality in the Process

This section describes some the more important equipment used in the process of the IGS technique for the determination of limiting activity coefficients.

4.2.1 The Pre-saturator and Dilutor Cells

The equilibrium cells are probably the two most important pieces of equipment as they are responsible for thermodynamic equilibrium. Other important conditions to fulfil within the cells include a large total transfer area and a sufficiently long contact time. These factors serve to ensure that the gas leaving the cell is in thermodynamic equilibrium with the liquid phase. The cells are a modification of the apparatus designed by Leroi et al. (1977) in that the gas is distributed by fine capillaries instead of a fritted disk. An illustration of a single cell is shown in Figure 4-6. Both pre-saturator and dilutor cells are of similar design and operate in similar fashion although they have totally different purposes in the process.

Figure 4-6: Equilibrium cell used in this study

A – Stripping gas inlet, B – Stripping gas outlet, C – Teflon plug, D – O-ring seals, E – Circulating water inlet, F – Capillaries, G – Thermowell, H – Magnetic stirrer

Gas enters the capillaries (G) in the cell at the gas inlet (A) and is distributed at the bottom of the inner cell just above the magnetic stirrer (H). The capillaries are fastened within the Teflon plug (C) by a clay based adhesive and Loctite™. The Teflon plug is not thermo-regulated but is in contact with the walls of the cell and the fittings attached to it are heated to system temperature. This ensures that the Teflon plug is also heated to system temperature. The Teflon plug is well insulated using glass wool ensuring that it at system temperature at all times and that none of the vapour condenses when in contact with it. The small gas bubbles rise to the top of the cell and leave the cell at the gas outlet (B). The cell is contained in a water jacket to allow for isothermal operation. Water enters the inlet at (E) and leaves at (I) maintaining a constant temperature in the inner cell. A Teflon plug is fitted on top of the cell. The o-ring seals on the plug serve to prevent the upward movement of the plug due to possible pressure build-up in the

cell and prevent any gas from escaping the cell. A class A Pt-100 is inserted into a stainless steel shell placed in thermowell (H) and is in direct contact with the solution in order to accurately determine the temperature of the solution in equilibrium in the cell. The Pt-100 sends a small current to the selector switch which in turn sends a signal to the temperature display. During operation the cell is completely isolated from the atmosphere using glass wool. This assists in preventing any heat loss from the jackets outer surface and helps avoid temperature fluctuations which make it difficult to get a constant temperature reading.

4.2.2 Cold Trap

The limiting activity coefficient is very sensitive to the value of the nitrogen gas flow rate. It is therefore essential that the cold trap is working properly. The gas entering the cold trap consists of solute, solvent and nitrogen. If the gas is allowed to pass through to the soap bubble flow meter without passing through the cold trap it would result in a flow rate reading that is higher than the actual nitrogen gas flow rate. Also the temperature of the gas is higher than system temperature because it passes through the heated lines before getting to the cold trap. The cold trap cools the gas condensing all the condensable vapour and trapping it as liquid.

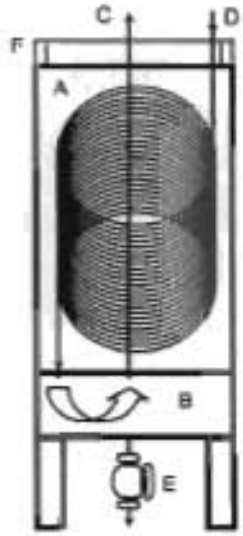

Figure 4-7: Cross Section of the cold trap to illustrate its inner workings.
A – upper chamber, B – lower chamber, C – gas inlet, D – non-condensable gas outlet, E – release valve, F – lid

Gas enters a ¼ inch ID copper coil through (D) which passes through a hole in lid (F). The coil is completely immersed in an ice - acetone solution in chamber (A). The cold trap allows for the complete condensation of the solute and solvent vapour flowing with the nitrogen into the coil.

The condensate makes its way to chamber (B) where it is trapped. In the meantime the cold nitrogen gas makes its way to exit pipe (C) out of the cold trap into another copper coil where it is heated to system temperature again. The liquid entrained in chamber (B) can be drained out by opening valve (E).

4.2.3 The Bubble Flow meter

A simple bubble flow meter was used to measure the inert gas flow rate in the absence of a gas rotameter. A soapy solution was used to fill the lower reservoir attached to the glass tube which is actually a rubber teat. The gas flowing from the IGS apparatus is connected just above the reservoir containing the soapy solution. The gas travels through the glass flow tube which is essentially a burette-like tube that has volume increments. At this point, the rubber teat is either manually squeezed or a clamp is used to continuously generate bubbles that travel at the same speed as the gas. The bubble flow meter requires timing of the bubble ring movement with a stopwatch and noting the resultant bubble rise volume.

The water vapour pressure is not taken into account to correct for inert gas flow rate calculation due to the design of the apparatus. The gas first passes through a cold trap which condenses any water vapour, solute and solvent that may be present and trapping it. The cooled non condensable gas which is mostly nitrogen is heated to system temperature before measurement at the soap bubble flow meter. There is therefore no need to account for water vapour pressure when determining the inert gas flow rate for this experimental set-up.

4.2.3.1 Advantages

- The major advantage of the soap bubble meter for gases is that it is not affected by the gas composition.
- A single bubble flow meter can be used for ordinary gases such as N_2, O_2, H_2, CO_2, and for measuring a unique gas mixture. There is no need for re-calibration when using different gases. Thus equipment costs are reduced.
- Bubble flow meters are now available for expanded flow rate-ranges. The gas flow meter has a range of 0.1 to 25 L/min.

4.2.3.2 Disadvantages

- Bubble meters are not well suited for continuous, in-line monitoring. In some applications, the use of a bubble solution could be a minor inconvenience, since it needs to be cleaned up after the measurement. This was not a problem in this study.

- There is also the problem of reaction time and error of parallax when taking measurements of this nature and this could result in huge errors when using this technique.

4.2.3.3 Applications

Bubble flow meters are commonly used in the chemical laboratory and in low flow research applications. Their use in more industrial applications is extremely limited. Some applications include:

- Accurate flow measurement of gas mixtures without recalibration
- Chromatography column, detector, and carrier-gas measurement
- Calibration and flow verification for variable area and electronic flow meters
- Supercritical fluid extraction
- Accurate flow measurement of changing gas concentrations

4.2.4 Gas Chromatography (GC)

A Varian 3300 GC was used to analyse the gas in the sample loop of the 6-port gas sampling valve. The sample gas enters the CG at some point before the Injector. The sample passes into a long capillary column where separation of the gases takes place. A flame ionization detector (FID) was used to analyse the gas instead of a thermocouple detector (TCD). The flame ionization detector is much more sensitive to the injected sample than a TCD. It is advised that a FID be used due to the low concentration of solute in the gas sample.

4.2.4.1 Gas Chromatography Sampling Techniques

There are two types of injections one can perform when using the inert gas stripping technique. Depending on the system, choosing the right type of injection method can save time. However both types of injection methods are equally suitable. The injection method in Figure 4-10 is suitable if the solvent does not have large residence time compared to the solute.

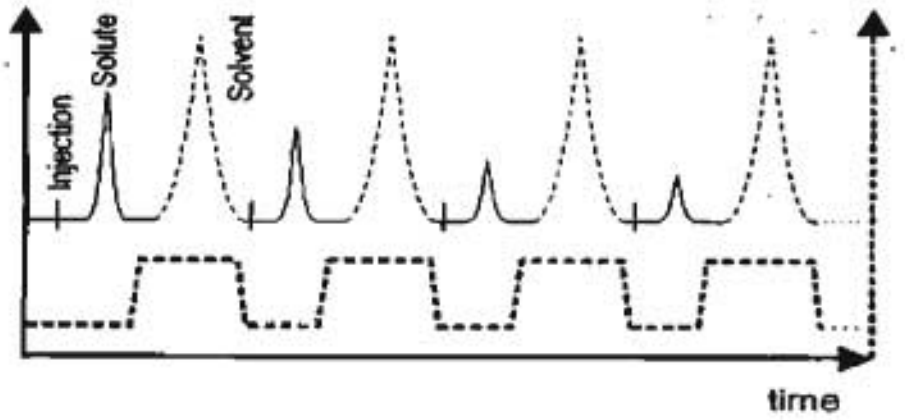

Figure 4-10: Peak profile of the injection method where the solvent peak follows after the solute peak (picture taken from Krummen et al. (2000)).

The figure below (Figure 4-11) shows an injection method for the case when the solvent has a very long residence time during gas chromatographic analysis. A number of injections can be made before the solvent peak shows up at the detector. Using this type of method for solvents that have long residence times would save on experimental time. For both techniques the solvent can be ramped out by using a suitable temperature program for the GC. The residence time of the solvent can be reduced by increasing the carrier gas flow rate but this would affect the shape of the solute peak to an extent where a spike rather than a rounded peak is obtained. This would make integration very difficult and it would also be difficult to differentiate between the solute peak and the peaks resulting from impurities.

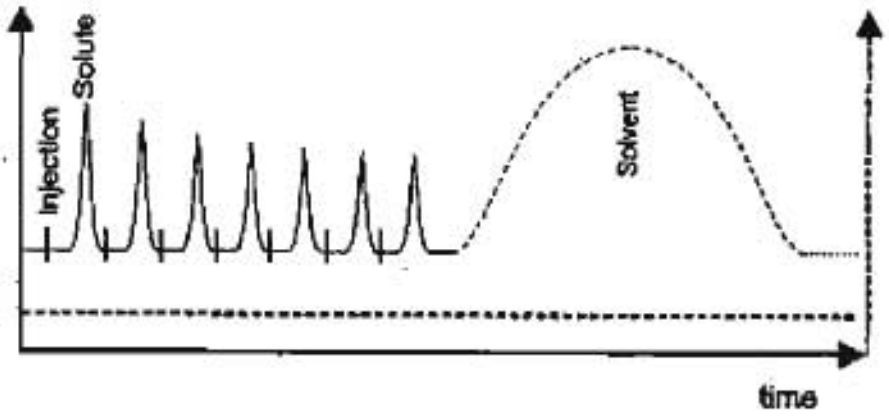

Figure 4-11: Peak profile for an injection method where the solvent residence time is long (picture taken from Krummen et al. (2000)).

4.3 Experimental Procedure

a. All electrical equipment is switched on.
b. Open the GC gases. Set the method on the GC for the particular system to be analysed. Ignite the flame.
c. All water baths are allowed to equilibrate to the set-point temperature which is the system temperature by turning on the temperature controllers immersed in the water. The set point temperature is the temperature at which the limiting activity coefficient is to be evaluated. When the controllers are switched on the built-in pumps are automatically turned on allowing a flow rate of water into the cell jackets and the heat exchanger.
d. The cold trap is filled with a mixture of acetone and ice.
e. All lines between the cell, the sampling valve and the GC are heated by turning on the variacs to ensure that no partial condensation takes place in these lines. This takes approximately 3 hours to stabilise. Pt-100's are inserted along the lines to check if the temperature is constant. It is vital to ensure that the lines have reached their equilibrium temperatures otherwise the amount of sample injected into the GC will vary giving inaccurate results. The time it takes to reach equilibrium temperature can be reduced by increasing the voltage on the variacs and then dropping it to the original value once the temperature is close to the set point temperature.
f. While the lines are heating up the nitrogen gas flow rate can be set to the desired value by changing the control valve and measuring the flow rate at the soap bubble flow meter. This can only be done once the water bath temperatures have reached their set points.
g. Check for leaks along all the gas line containing fittings as there may be leaks at different operating temperatures. If there any leaks it must be stopped before continuing with the experiment. Also check the GC injector for any leaks as a result of previously injected samples.
h. Two beakers are each filled with approximately 250 ml of solvent and weighed to determine initial mass of solvent usually by difference after filling the cells.
i. Once the cells are filled with solvent. A drop of solute from a fine tipped dropper is placed in the dilutor cell only. This should ensure that the mole fraction is less than 10^{-3}.
j. The Teflon lids are placed onto the cells sealing them preventing any gas from escaping and the stirrers are switched on.
k. Ensure that the heating medium (water) is circulating in the system and that the lines are not blocked
l. The sampling valve is set to the "fill" position, which allows the stripped gas to flow through the gas-sampling valve.

m. Once the GC has reached its temperatures and the system is in equilibrium the sampling valve is then set to the "inject" position for approximately 2 to 3 minutes and then set back to the "fill" position once the sample has successfully been analysed.

n. As soon as the baseline has reached its set-point value the temperature can be ramped so that the solute passes through much faster than it normally would thus reducing the experimental time. A new baseline is now obtained and once the solute passes through the GC, the temperatures can be brought back down to the original temperatures and another sample can be taken.

o. This procedure is repeated periodically (usually taking at intervals of 1 hour) until sufficient peaks are obtained.

p. After sufficient data (solute peak areas) has been obtained, the experiment is stopped. Around 5 to 6 points is enough for a straight line The GC temperatures are set to ambient, the nitrogen gas tank is shut off and all electrical equipment are switched off.

q. The experiment is repeated to ensure that the obtained results for the infinite dilution activity coefficient do not differ significantly for the various flow rates and that the data is reproducible.

r. The measurement procedure starts with flushing the clean equilibrium cells and all the adjoining pipelines thoroughly with the inert gas.

Chapter V – Mass Transfer and Equilibrium Cell Design Considerations

The design of the equilibrium cells is based primarily on the rate of mass transfer taking place in the cells. A condition of validity of the present method is that thermodynamic equilibrium must be reached between the saturated gas leaving the cell and the liquid. When the stripping gas passes through the solvent-solute mixture, the solute is transferred from the mixture to the gas through the interface of the bubbles in two steps as discussed below. The interested reader is referred to the work of Richon et al. (1980) for details. The system was designed on the basis of the results of similar calculations.

5.1 Mass Transfer in the Equilibrium Cell

The following calculation derived by Richon et al. (1980) for mass transfer of solute was used to design the dilutor and pre-saturation cells. The solute is transferred from the solvent to the gas through the interface of the bubbles in two steps.

5.1.1 Mass Transfer in the Liquid Phase

Some of the assumptions that Richon et al. (1985) made in deriving these working expressions are:

- The solute is considered as the only component which is exchanged between the liquid and the gas bubbles
- The bubble diameters are constant
- The modification of the liquid concentration is negligible while the gas bubbles are in the solution and are supposedly perfectly stirred.
- At the gas-liquid interface equilibrium is achieved

A diagram illustrating a typical bubble in a solution showing some of the major variables has been provided (Figure 5-1). The concentration profile is for time (t) far from equilibrium. At equilibrium a completely different concentration profile exists. C_i^L is the concentration of solute in the liquid phase and $C_{i,s}^L$ is the solute concentration in the liquid at the interface on the liquid side, while $C_{i,s}^G$ is the solute concentration at the interface on the vapour side and C_i^G is the

solute concentration in the vapour which changes with radius (r) as indicated for all r. The three quantities C_i^L, $C_{i,s}^L$ and $C_{i,s}^G$ are time dependant while C_i^G is dependant on time and distance to the centre of the gas bubble.

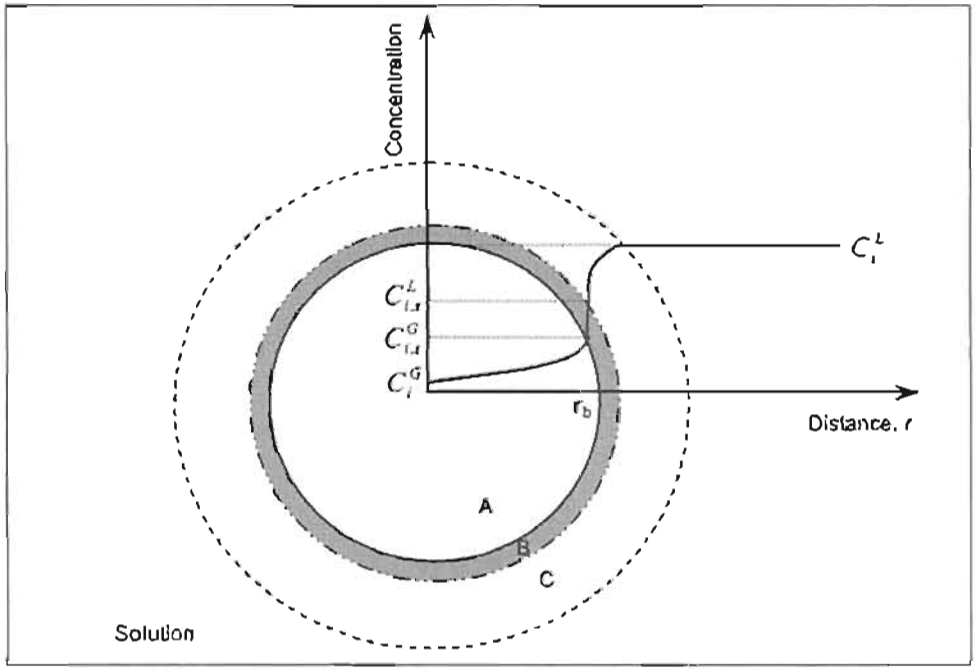

Figure 5-1: Concentration profile of solute in and around a gas bubble immersed in solution, where A – gas bubble; B – Interface (Exaggerated to illustrate $C_{i,s}^L$ and $C_{i,s}^G$); C - Immediate layer of solution around the gas bubble.

Therefore the number of moles of solute (dn_i) passing through the interface during a time dt is given by

$$dn_i = 4k_L \pi R_b^2 \left(C_i^L - C_{i,s}^L\right) dt \qquad 5.1$$

k_L is the mass transfer coefficient and can be calculated by means of a correlation by Cheh and Tobias (1968) which relates three adimensional numbers.

$$Sh = 2k_L \left(R_b / D_{ij}^L \right) \qquad Sh = \left(\frac{3}{4\pi} \right)^{0.5} I(Re) Pe^{0.5}$$

$$I(Re) = 2\left(4/3 - 6.82\,Re\right)^{-0.5} \qquad \mathrm{Re} = 2P_L \upsilon^{\infty} R_b / \mu_L \qquad Pe = 2\upsilon^{\infty} R_b / D_{ij}^L$$

For computation of k_L, it is necessary to know the liquid diffusion coefficient D_{ij}^L of the solute (i) in solvent (j) which can be estimated from the correlation of Wilke and Chang (1955). A variety of correlations is available to calculate the molecular diffusivities of solutes in liquids. The determination of the liquid diffusivity coefficient is not limited to the equation by Wilke and Chang (1955). Any appropriate equation may be used for the system. When written at infinite dilution the concentrations C_i^L and $C_{i,s}^G$ are related at the interface, by the equilibrium relation 5.2.

$$C_{i,s}^L = \frac{M_G}{\rho_G}\frac{\rho_L}{M_L}\frac{1}{\gamma^\infty}\frac{P}{P_i^s}C_{i,s}^G = AC_{i,s}^G \qquad 5.2$$

n_i, is related to the average concentration in a bubble by

$$n_i = \overline{C}_i^G \frac{M_G}{\rho_G}\frac{P}{RT}V_b \qquad 5.3$$

Therefore $$\frac{dn_i}{dt} = \frac{M_G}{\rho_G}\frac{P}{RT}V_b\frac{d\overline{C}_i^G}{dt} \qquad 5.4$$

Assuming that diffusion in the gas phase of the bubble is very fast (Richon et al. (1980))

$$\overline{C}_i^G(r,t) = C_{i,s}^G(t) \qquad 5.5$$

Equations 5.2, 5.4, and 5.5 combined with 5.1 lead to the following differential equation

$$\frac{dC_{i,s}^G(t)}{C_i^L - AC_{i,s}^G(t)} = \frac{3}{R_b}k_L\frac{\rho_G}{M_G}\frac{RT}{P}dt = B\,dt \qquad 5.6$$

B is assumed constant because variations of k_L, P and physical constants of the gas and liquid are negligible for bubbles going up the cell. Taking account of all those hypotheses, the integration of Equation 5.6 between concentration 0 and $C_{i,s}^G(t)$ gives

$$\frac{AC_{i,s}^{G}(t)}{C_i^{L}} = 1 - exp\left[-\left(\frac{3}{R_b}\frac{\rho_L}{M_L}k_L\frac{RT}{P_i^{s}\gamma^{\infty}}\frac{h}{\upsilon^{\infty}}\right)\right] = \tau_L \qquad 5.7$$

τ_L, is an estimation of the approach to equilibrium between bubbles and solution as a function of the time spent by bubbles in solution. υ^{∞} (limiting speed for bubbles in solution), is obtained through the equation for the intermediate law (Richon et al. (1980)).

$$\left(\upsilon^{\infty}\right)^{1.4} = 7.2\times10^{-2}\,\nu_L^{-0.6}D_b^{1.6}g \qquad 5.8$$

Richon et al. (1980) did some analysis for the system n-heptane (1) in n-methyl-2-pyrrolidone (2) at 25 °C and 1 atm with the carrier gas being helium forming bubble diameters of 1.5 mm. Using Equation 5.7 to determine the minimum height of the cell required for equilibrium conditions in the cell, taking into account liquid phase resistance only, allows for the generation of the following graphs.

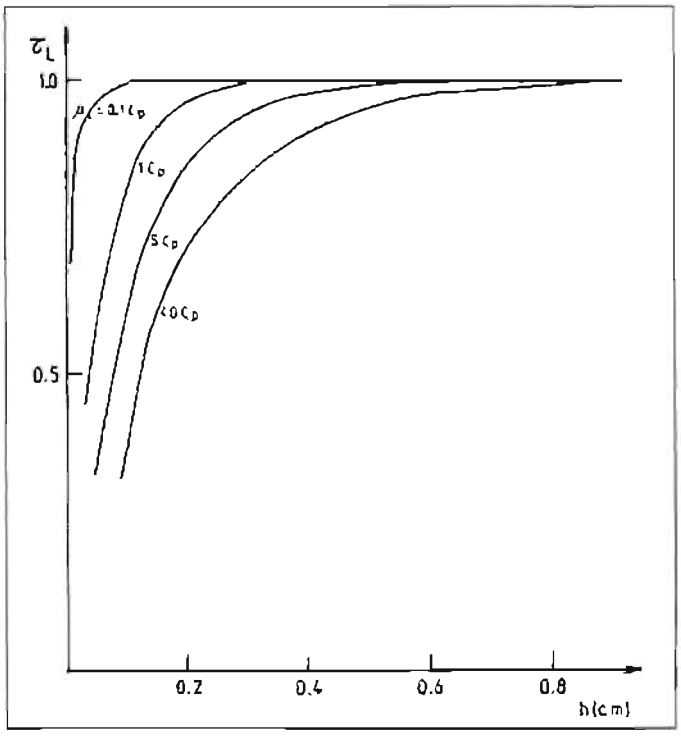

Figure 5-2: Plots of τ_L versus height at different dynamic viscosities for the solute n-heptane (1) and solvent NMP (2) system (Richon et al. (1980)).

Figure 5-2 shows that viscosity is not the limiting factor because even with μ_L = 40 cP, a state 99 % from equilibrium is achieved after only passing through 1 cm of solution. The small influence of viscosity on τ_L is due to compensating effects, i.e. when viscosity increases k_L increases but the velocity of the bubble in solution decreases and time spent in solution increases (Richon et al. (1980)).

The effect of bubble diameter can also be investigated as the behaviour of τ_L against path length of the bubbles in solution for different bubble diameters. Richon et al. (1980) found that for the system n-heptane (1) + NMP (2) at similar conditions as above, bubble diameters of approximately 4.5 mm result in a τ_L close to one for a solution height of only 5 cm (see Figure 5-3). This means that an equilibrium cell that allows for a solution height greater than 5 cm will allow for equilibrium if only liquid phase resistance is taken into account. A second set of conditions need to be evaluated before the minimum solution height (also the minimum cell height) can be determined, which takes into account gas phase diffusion only. The limiting of the two scenarios will result in the correct bubble path height for equilibrium conditions in the cell.

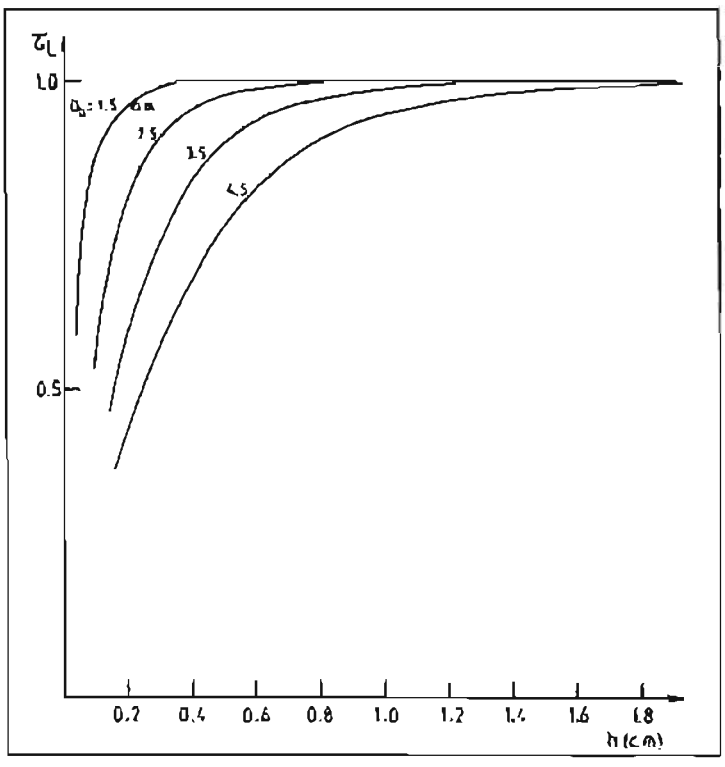

Figure 5-3: Plots of τ_L against path length for different bubble diameters for the system n-heptane (1) + NMP (2) at a viscosity of 1 cP. (Graph taken from Richon et al. (1980))

5.1.2 Diffusion in the Gas Phase

Crank (1956) gives the following relation for the solute concentration in gaseous bubbles not being stirred by convection movements at a distance r from a bubble centre at time t

$$C_i^G(r,t) = C_{i,s}^G\left[1 + \frac{2R_b}{\pi r}\sum_{l=1}^{\infty}\frac{(-1)^l}{l}\sin\frac{l\pi r}{R_b}\exp\left(-\frac{D_{ij}^G l^2\pi^2 t}{R_b^2}\right)\right] \qquad 5.9$$

D_{ij}^G, is the diffusion coefficient of solute i in gas j, and is given by Slattery and Bird (1958).

$$D_{ij}^G = \frac{1}{P}a\left(\frac{T}{(T_{Ci}T_{Cj})^{0.5}}\right)^b (P_{Ci}P_{Cj})^{\frac{1}{3}}(T_{Ci}T_{Cj})^{\frac{5}{12}}\left(\frac{1}{M_i}+\frac{1}{M_j}\right)^{0.5} \qquad 5.10$$

$a = 2.745\times10^{-4}$

$b = 1.823$

Mass of solute in the bubble at time t is given by the integral,

$$m(t) = 4\pi m_i\int_0^{R_b} r^2 C_i^G(r,t)\,dr \qquad 5.11$$

When $t \to \infty$

$$C_i^G(r) \to C_{i,s}^G \qquad 5.12$$

So substituting

$$m^{\infty} = \frac{4}{3}\pi R_b^3 m_i C_{i,s}^G \qquad 5.13$$

The approach to equilibrium (τ_G) is defined as the ratio of $m(t)$ over m^{∞}

$$\tau_G = 1 - \frac{6}{\pi^2}\sum_{l=1}^{\infty}\frac{1}{l^2}\exp\left[-\frac{D_{ij}^G l^2\pi^2 h}{R_b^2 v^{\infty}}\right] \qquad 5.14$$

The influence of bubble diameters on the diffusion rate can now be investigated using Equation 5.14. According to the analysis of Richon et al. (1980) if the bubble diameter is less than 2.5 mm, time for gas phase diffusion can be neglected compared to time for liquid mass transfer, but if the bubble diameter is greater than 4 mm the calculations of τ_L is not valid because Equation 5.5 does not hold and gaseous diffusion becomes a limiting factor for mass transfer.

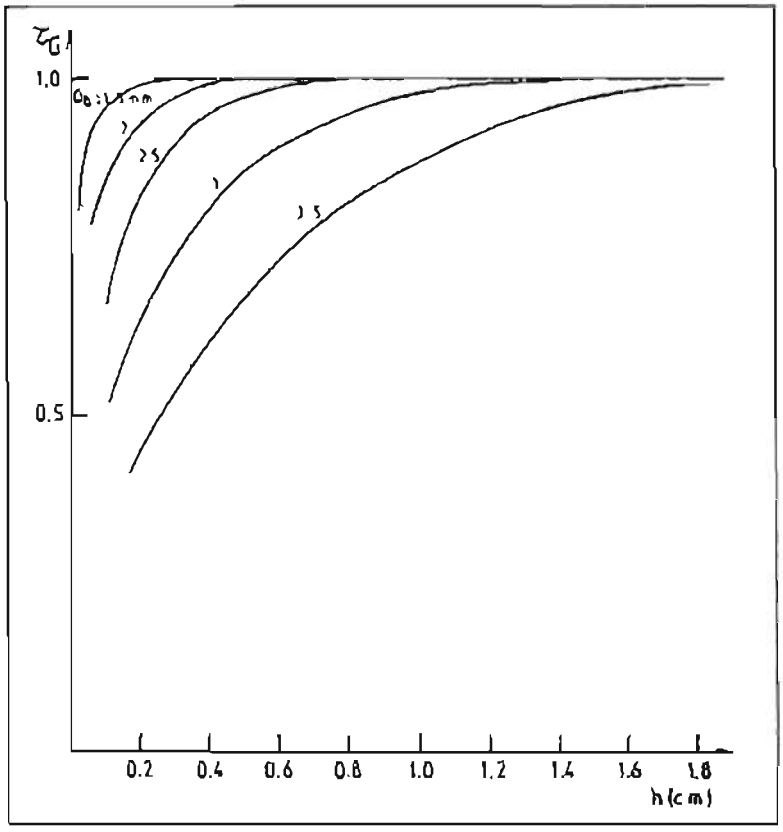

Figure 5-4: Effect of different bubble diameters on τ_G versus path length (h) of bubbles in liquid at 25 °C and 1 atm with viscosity taken as 1 cP, for the system n-heptane (1) + NMP (2) (picture taken from Richon et al. (1980))

Similar calculations need to be performed for all systems under investigation in order to determine the height required for the bubbles to reach equilibrium. One equilibrium cell can be designed for all the systems under investigation by designing the cell for system that requires the greatest path length for the bubbles to reach equilibrium. To ensure thermodynamic equilibrium the cells must accommodate a path length for the bubbles that is greater than that determined using the equations above.

Richon et al. (1980) has taken a very basic modelling approach to determine cell height for thermodynamic equilibrium. There are other methods for modelling a rising bubble in a solution

but they are very tedious (Korlie (2000) and Krepper et al. (2005)). The method used by Richon et al. (1980) to determine solution height works well for most systems and has been used by many other researchers. The influence of other variables can also be investigated. Richon et al. (1985) made some plots to investigate the effects of some of these variables.

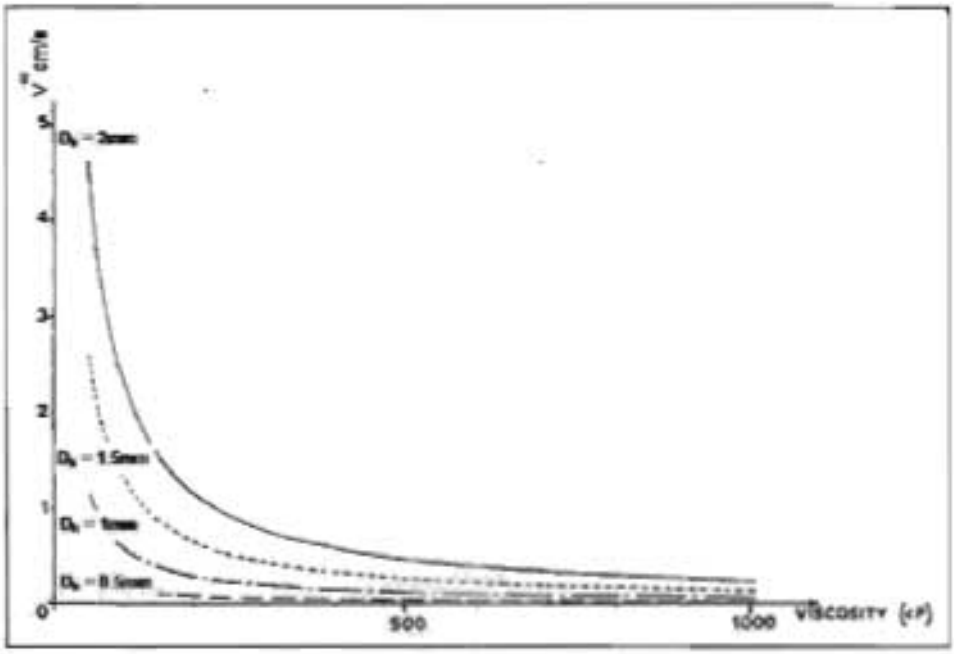

Figure 5-5: Influence of viscosity on the limiting bubble speed for different gas bubble diameters (Richon (1985))

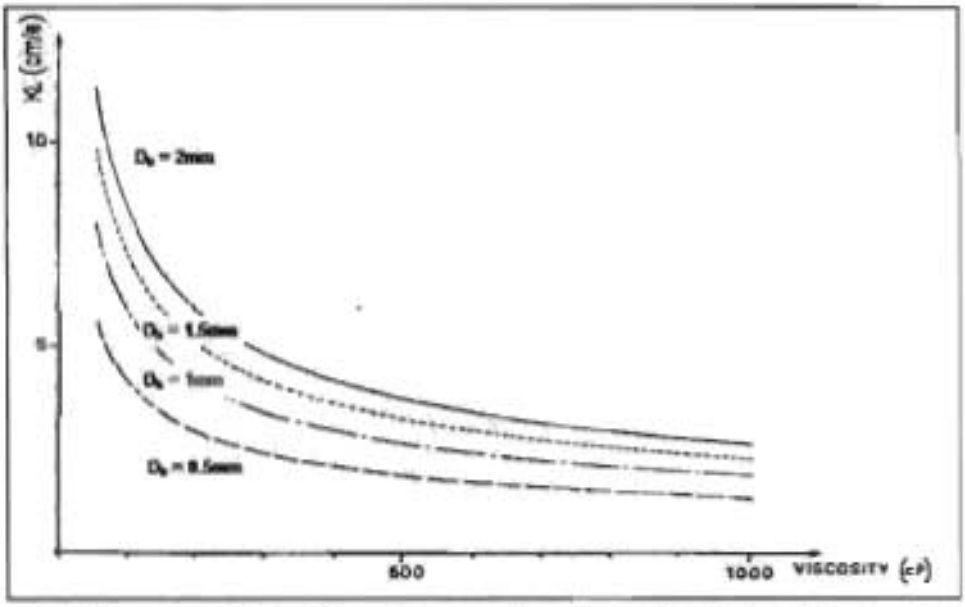

Figure 5-6: Influence of viscosity on the mass-transfer coefficient for different gas bubble diameters (Richon (1985))

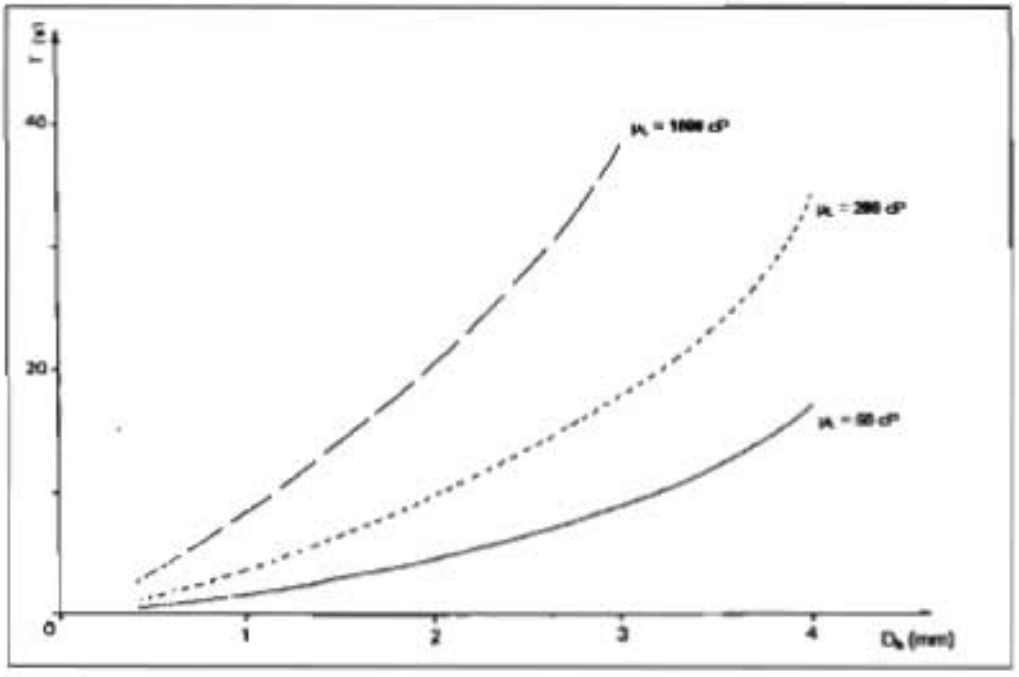

Figure 5-7: Influence of bubble diameter on the time necessary to reach equilibrium for different liquid viscosities (Richon (1985))

Chapter VI – Principles and Theory

The principle of the IGS method was described in detail by Leroi et al. (1977) and in Chapter 4. Leroi et al. (1977) also derived a very simple equation for the determination of limiting activity coefficients. These equations are however limited to a few types of systems based on the nature of the components. Beyond that, equations were derived taking into account the vapour phase correction that is important for solutes with higher volatilities (Duhem and Vidal (1978)). This chapter summarizes the newly derived equation by Krummen et al. (2000) which requires the use of a saturation cell. Hovorka and Dohnal (1997) also derived a set of equations for use with the inert gas stripping technique. All significant developments in the determination of limiting activity coefficients are outlined in this chapter.

The limiting activity coefficient is related to other well known parameters used for designing highly specialized equipment. Its relation to these parameters is outlined to stress the importance of accurately knowing limiting activity coefficients. Thereafter the derivations of the various equations for the determination of limiting activity coefficients are outlined. These equations can only be used with the inert gas stripping technique.

6.1 Activity Coefficients, Selectivity, Capacity and Selection Factor

The limiting activity coefficient is related to other well known parameters namely selectivity, capacity and selection factor. These factors are very important for the separation of high purity chemicals because removal of the last traces of impurities requires the greatest separation effort. The limiting activity coefficient is required to select entrainers for separation processes and to check for separation problems such as azeotropes and miscibility gaps, aiding in the design of various separation units. Accurate knowledge of the limiting activity coefficient makes these parameters, which are important for the economics of a separation process, easy to calculate.

The measurement of limiting activity coefficients (γ_i^∞) in multi-component systems are of great interest, because the addition of small amounts of a solvent to an entrainer has a considerable effect on the activity coefficient at infinite dilution and thus on the selectivity $\left(S_{ij}^\infty = \gamma_i^\infty / \gamma_j^\infty\right)$ and capacity $\left(k_i^\infty = 1/\gamma_i^\infty\right)$ of the entrainer. This is useful knowledge for the separation of mixtures.

The addition of an entrainer or of a solvent mixture can simplify the separation considerably. The selectivity can be increased by the addition of a second solvent. An increase in the selectivity often leads to a decrease in the capacity of a solvent or solvent mixture; however it is important for the economic efficiency of a separation process.

The activity coefficient at infinite dilution (γ_i^{∞}) is an important parameter, particularly for the reliable design of thermal separation processes such as extractive distillation. Thus the synthesis, simulation and optimization factors (α_{ij}) which, depending on pressure, temperature and the composition of the mixture, can be calculated across the complete concentration range using the following simplified equation:

$$\alpha_{ij} = \frac{\gamma_i P_i^{sat}}{\gamma_j P_j^{sat}} \qquad 6.1$$

where i is the low boiling component and j is the high boiling component and P^{sat} is the saturated pure component pressure. It is seen that the separation of the final traces of a component requires the greatest effort because the least favourable values of the separation factor occur at high dilution. In the case of positive deviations from Raoult's Law ($\gamma_i > 1$) the greatest separation effort is required at the top of the column ($x_j \rightarrow 1$). In such cases the relation below applies.

$$\alpha_{ij}^{\infty} = \frac{P_i^{sat}}{\gamma_j^{\infty} P_j^{sat}} \qquad 6.2$$

At the bottom of the column ($x_j \rightarrow 1$) the effort involved in the separation is largest for negative deviations from Raoult's Law ($\gamma_i < 1$). In such cases the relation below applies.

$$\alpha_{ij} = \frac{\gamma_i^{\infty} P_i^{sat}}{P_j^{sat}} \qquad 6.3$$

The effect necessary for the separation is determined by the value of $\alpha - 1$. To avoid an over design of a distillation column and to minimize the investment and operating costs, reliable

knowledge of the separation factor at high dilution (α_{ij}^{∞}) is important. Taking into account limiting activity coefficients also improves the reliability of the description in the dilute region when reliable g^E model parameters are to be fitted or in the development and improvement of group contribution methods. In addition, it is possible to obtain reliable values for Henry's constants and partition coefficients as shown later.

Some very basic equations were formulated by Leroi et al. (1977) in order to determine activity coefficients at infinite dilution for solutes that are volatile in nature. These equations, depending on the nature of the solvent, can be used to calculate limiting activity coefficients for most systems. Duhem and Vidal (1978) and Boa and Han (1995) modified the Leroi et al. (1977) equations taking into account some of the simplifying assumptions that are usually not valid for most systems. The derivations of all these important equations together with assumptions are outlined below.

6.2 Thermodynamic Formulations for the Leroi et al. (1977), Duhem and Vidal (1978) and Boa and Han (1995) Equations

Assuming that the gas phase is in equilibrium with the liquid phase, it is possible to write the equilibrium equations for each component: solute (sol), solvent (s) and carrier gas (CG) as follows.

$$x_{sol}\gamma_{sol}f_{sol}^{OL*}I_{sol} = y_{sol}\varphi_{sol}P \qquad 6.4$$

$$x_s\gamma_s f_s^{OL*}I_s = y_s\varphi_s P \qquad 6.5$$

$$x_{CG}H_{CG} = y_{CG}\varphi_{CG}P \qquad 6.6$$

where x is the mole fraction in the liquid phase, y is the mole fraction in the vapour phase, f is the fugacity, f^{OL*} is the reference fugacity for a liquid at pure state and zero pressure, I is the Poynting correction, φ is the fugacity coefficient, P is the pressure, γ is the activity coefficient and H is the Henry's constant. For both solvent and solute, the reference state is the pure liquid at zero pressure. For equilibrium at low pressure, which is mainly studied here, vapour phase corrections φ_i can be derived from second virial coefficients.

$$ln\,\varphi_i = 2\sum_{j=1}^{n}\left(y_j B_{ij} - B_M\right)\frac{P}{RT} \qquad 6.7$$

$$B_M = \sum_i \sum_j y_i y_j B_{ij} \qquad 6.8$$

B_{ij}, is the virial coefficient characterizing bimolecular interaction between molecule i and molecule j, while B_M is the mixture second virial coefficient, T is the temperature and R is the Universal gas constant. Reference fugacity's f_i^{OL*} are obtained from the equation

$$f_i^{OL*} = P_i^v \varphi_i^0\left(T, P_i^v\right)\exp\left(-\frac{v_i^{OL*} P_i^v}{RT}\right) \qquad 6.9$$

where v_i^{OL*} is the molar volume, f_i^{OL*} is the reference fugacity for the i^{th} component of the pure liquid at zero pressure, P_i^v is the vapour pressure and φ_i^0 is the fugacity coefficient in the vapour phase at saturation. If the solute is highly dilute in the solvent and if the solubility of the carrier gas in the liquid phase is negligible, the solute activity coefficient may be approximated by its value at infinite dilution. It can be shown that in most cases this approximation is valid if the mole fraction of the solute x_{sol} is less than 10^{-3} (Leroi et al. (1977)). The solvent mole fraction in the liquid phase and the activity coefficient γ_s may be taken equal to 1 in Equation 6.5, under the same conditions. If the vapour phase corrections are neglected then the following equations apply.

$$x_{sol}\gamma^{\infty} P_{sol}^v = y_{sol} P \qquad 6.10$$

$$P_s^v = y_s P \qquad 6.11$$

If n and N are respectively the total number of moles of solute and solvent in the equilibrium cell at time t, the quantities $(-dn)$ and $(-dN)$ withdrawn from the solution during dt by the carrier gas flow are

$$dn = -y_{sol} P\frac{D_2 dt}{RT} \qquad 6.12$$

$$dN = -y_s P \frac{D_2 dt}{RT} \qquad 6.13$$

D_2 is the total volumetric rate of gas flowing out of the still converted to pressure (P) and temperature (T). From Equations 6.10 to 6.13 it can be deduced that

$$\frac{dn}{dt} = -x_{sol} \gamma^{\infty} P_{sol}^{v} \frac{D_2}{RT} \qquad 6.14$$

$$\frac{dN}{dt} = -P_s^{v} \frac{D_2}{RT} \qquad 6.15$$

An overall mass balance around the dilution still gives

$$D_2 = D - \frac{RT}{P}\left(\frac{dn}{dt} + \frac{dN}{dt}\right) \qquad 6.16$$

where D is the pure carrier gas flow rate measured at system temperature (T) and system pressure (P). Combining Equations 6.16, 6.14 and 6.15 yields

$$D_2 = \frac{D}{1 - x_{sol} \gamma^{\infty} \frac{P_{sol}^{v}}{P} - \frac{P_s^{v}}{P}} \qquad 6.17$$

If D_2 is replaced by Equation 6.17 in Equations 6.14 and 6.15 and if x_{sol} is replaced by Equation 6.18 at infinite dilution

$$x_{sol} = \frac{n}{n+N} \cong \frac{n}{N} \qquad 6.18$$

where n is the molar amount of solute in the still and N is the molar amount of solvent in the still, as mentioned before. If the vapour and liquid phases are in equilibrium in the dilutor cell, neglecting vapour phase corrections and carrier gas solubility in the liquid phase and in the highly diluted range, then the basic differential equations relating the variations of the amounts of solute and solvent with time are the following:

$$\frac{dn}{dt} = -\frac{n}{N}\gamma_{sol}^{\infty}\frac{P_{sol}^{sat}}{RT}\frac{D}{1-\frac{n}{N}\gamma_{sol}^{\infty}\frac{P_{sol}^{sat}}{P}-\frac{P_{s}^{sat}}{P}} \qquad 6.19$$

$$\frac{dN}{dt} = -\frac{P_{s}^{sat}}{RT}\frac{D}{1-\frac{n}{N}\gamma_{sol}^{\infty}\frac{P_{sol}^{sat}}{P}-\frac{P_{s}^{sat}}{P}} \qquad 6.20$$

where P_i^{sat} is the pressure of component i at saturation.

The equations used in the activity coefficient calculation procedure are based on the following two assumptions:

- Ideal vapour phase
- Negligible solubility of inert gas in the liquid

A further assumption is that the solution of these equations depends on the type of solvent.

6.2.1 Leroi et al. (1977) Equations

The above equations lead to two very simple equations derived by Leroi et al. (1977). These equations are the simplest equations to date and give accurate results. The assumptions made when deriving these equations are justified by experimental conditions.

6.2.1.1 Non-volatile Solvent

A simplifying assumption is made in the next development by neglecting the term

$$\frac{n}{N}\gamma_{sol}^{\infty}\frac{P_{sol}^{sat}}{P}$$

It should be justified by experimental conditions.

The integration of the differential Equations 6.19 and 6.20 is simplified if N can be assumed constant. This condition is satisfied if the solvent is non-volatile. All solvents studied here had a vapour pressure lower than 1 mmHg and are within this limit of non-volatility for all experimental

conditions. A non-volatile solvent can be described as a solvent having a vapour pressure less than 1 mmHg and thus with a non-volatile solvent $P_s^v/P << 1$. Assuming that the term $\frac{n}{N}\gamma_{sol}^{\infty}\frac{P_{sol}^{sat}}{P}$ can be ignored and that N can be taken as constant, the solution to Equation 6.19 is:

$$ln\frac{n}{n_0} = -\frac{D}{RT}\frac{P_{sol}^{sat}}{N}\gamma_{sol}^{\infty}t \qquad 6.21$$

where n_0 is the initial amount of solute in the cell. As the sample loop of the gas sampling valve is maintained at constant temperature, the amount of solute injected into the chromatographic column is proportional to the solute partial pressure over the solution and since detector linearity is satisfied, it can be deduced that

$$A_{sol} = \kappa y_{sol} P \qquad 6.22$$

A_{sol} is the area of the solute peak from GC analysis and κ is the proportionality constant. Finally from Equations 6.10, 6.18, 6.21 and 6.22

$$\ln\frac{A}{A_0} = -\frac{D}{RT}\frac{P_{sol}^{sat}}{N}\gamma_{sol}^{\infty}t \qquad 6.23$$

Equation 6.23 indicates an exponential variation of A_{sol} with time.[3] This equation is used for systems where the solvent volatility is low (less than 1 mmHg).

6.2.1.2 Volatile Solvent

In this case, N is not constant and Equations 6.19 and 6.20 have to be solved simultaneously. The solution has the form:

[3] These results are obtained when the solute mole fraction in the liquid phase is calculated from the ratio of n (total number of moles of solute) to N (total number of moles of solvent). So when applying the dilutor technique to high value limiting activity coefficients, such an assumption does not hold and the n/N ratio will be substituted as shown in Section 6.2.2.

$$\ln\frac{A}{A_0}=\left(\frac{\gamma_{sol}^{\infty}P_{sol}^{sat}}{P_s^{sat}}-1\right)\ln\left(1-\frac{P}{P-P_s^{sat}}\frac{DP_s^{sat}}{N_0RT}t\right) \qquad 6.24$$

6.2.2 Duhem and Vidal (1978) Correction

Duhem and Vidal state that the term $\frac{n}{N}\gamma_{sol}^{\infty}\frac{P_{sol}^{sat}}{P}$ cannot be neglected, and that the assumptions of Leroi et al. (1977) are not valid for large values of the infinite dilution activity coefficient. They then derived another equation to determine limiting activity coefficients for systems where the solvent is non-volatile, taking into account the term $\frac{n}{N}\gamma_{sol}^{\infty}\frac{P_{sol}^{sat}}{P}$.

6.2.2.1 Non-volatile Solvent

Since the term $\frac{n}{N}\gamma_{sol}^{\infty}\frac{P_{sol}^{sat}}{P}$ is not neglected, and the ratio $\frac{n}{N}$ is replaced by $x_{sol}=\frac{n}{N\left(1+\frac{V_G}{RT}\frac{P_{sol}^{sat}\gamma_{sol}^{\infty}}{N}\right)}$ in Equation 6.19, these authors obtained:

$$\frac{dn}{dt}=-\frac{n}{N\left(1+\frac{V_G}{RT}\frac{P_{sol}^{sat}\gamma_{sol}^{\infty}}{N}\right)}\gamma_{sol}^{\infty}P_{sol}^{sat}\frac{D}{RT\left(1-\frac{n}{N\left(1+\frac{V_G}{RT}\frac{P_{sol}^{sat}\gamma_{sol}^{\infty}}{N}\right)}\gamma_{sol}^{\infty}\frac{P_{sol}^{sat}}{P}\right)} \qquad 6.25$$

where V_G is the volume of vapour space in the still. Integration of the above equation is possible provided that either D or D_2 is assumed to be constant. According to the experimental setup, the measured gas flow D_2 at the exit of the dilutor cell, after condensing volatile solute, or the gas flow D entering the still, can be constant. They differ by the carrier gas accumulation in the dilutor cell:

$$D_2 = D - \frac{dN_{CG}}{dt}\frac{RT}{P} = D + \frac{P_{sol}^{sat}\gamma_{sol}^{\infty}}{P}\frac{V_G}{N\left(1+\frac{V_G}{RT}\frac{P_{sol}^{sat}\gamma_{sol}^{\infty}}{N}\right)}\frac{dn}{dt} \qquad 6.26$$

If D_2 is constant, the integration yields:

$$\ln\frac{A}{A_0} - \frac{1}{kP}(A - A_0) = -\frac{D_2 P_{sol}^{sat}}{RTN\left(1+\frac{V_G}{RT}\frac{P_{sol}^{sat}\gamma_{sol}^{\infty}}{N}\right)}\gamma_{sol}^{\infty} t \qquad 6.27$$

where k is the detector calibration constant.

If D is constant, we have:

$$\ln\frac{A}{A_0} - \frac{1}{kP\left(1+\frac{V_G}{RT}\frac{P_{sol}^{sat}\gamma_{sol}^{\infty}}{N}\right)}(A - A_0) = -\frac{DP_{sol}^{sat}}{RTN\left(1+\frac{V_G}{RT}\frac{P_{sol}^{sat}\gamma_{sol}^{\infty}}{N}\right)}\gamma_{sol}^{\infty} t \qquad 6.28$$

However, such a distinction is seldom allowed by experimental precision. Using Equation 6.27 or 6.28 implies a detector calibration. On the other hand, from the experimental data, it can be observed a linear variation of $\ln A/A_0$ verses time. Therefore Duhem and Vidal (1978) introduced a constant and mean value for the corrective term of Equation 6.25, the integration of which yields:

$$\ln\frac{A}{A_0} = -\frac{D}{NRT\left(1+\frac{V_G}{RT}\frac{P_{sol}^{sat}\gamma_{sol}^{\infty}}{N}\right)}\frac{P_{sol}^{sat}}{1-\frac{\tilde{n}}{N\left(1+\frac{V_G}{RT}\frac{P_{sol}^{sat}}{N}\right)}\frac{\gamma_{sol}^{\infty}P_{sol}^{sat}}{P}}\gamma_{sol}^{\infty} t \qquad 6.29$$

where $\tilde{n} = \dfrac{n - n_0}{\ln\dfrac{n}{n_0}}$ 6.30

From a comparison between Equations 6.25 and 6.27, it can be shown that $\tilde{n}$ must be evaluated by logarithmic means. In order to evaluate $\tilde{n}$ the initial amount of solute n_0 placed into the dilutor cell must be known. V_G is the volume of the vapour space above the liquid in the dilutor cell. This can be determined from an equation proposed by Bao et al. (1993a):

$$V_G = V_c - \frac{m_s}{\rho_s} \qquad 6.31$$

V_c is the dilutor cell volume while m_s and ρ_s are the solvent mass and density respectively. Equation 6.25 is especially accurate for systems with large infinite dilution activity coefficients.

6.2.3 Bao and Han (1995) Derivation for a Volatile Solvent

Bao and Han (1995) suggested a solution for Equations 6.19 and 6.20, provided that the equation suggested by Duhem and Vidal (1978) is used to calculate the mole fraction of the solute, i.e.

$$x_{sol} = \frac{n}{N\left(1 + \frac{V}{RT}\frac{P_{sol}^{sat}\gamma_{sol}^{\infty}}{N}\right)} \qquad 6.32$$

With the corrective term neglected, the solution is:

$$\ln\frac{A}{A_0} = \left(\frac{1}{1 + \frac{\gamma_{sol}^{\infty} P_{sol}^{sat} V_G}{N_0 RT}}\frac{\gamma_{sol}^{\infty} P_{sol}^{sat}}{P_s^{sat}} - 1\right)\ln\left(1 - \frac{P_s^{sat}}{P - P_s^{sat}}\frac{PD}{N_0 RT}t\right) \qquad 6.33$$

Equations 6.23, 6.24, 6.29 and 6.33 are the four proposed equations covering most non-idealities for the determination of limiting activity coefficients. These four equations have been used to determine limiting activity coefficients in Chapter 7.

6.3 Derivation of the Equation Proposed by Krummen et al. (2000)

The saturation fugacity coefficient φ_{sol}^{sat} is taken into account by Krummen et al. (2000) in the derivation of the equation for the limiting activity coefficient which would otherwise lead to an approximate error of 4 % if ignored. Krummen et al. (2000) furthermore takes into account the increase of the carrier gas stream caused by the saturation of the carrier gas with the solvent. In order to determine the activity coefficient at infinite dilution, it must be assumed that the gas phase is in equilibrium with the liquid phase. According to Gmehling et al. (1992) the following relation applies for the highly dilute component (solute *sol*):

$$x_{sol}\gamma_{sol}\varphi_{sol}^{sat}P_{sol}^{sat}Poy_{sol} = y_{sol}\varphi_{sol}^{*}P \qquad 6.34$$

where φ_{sol}^{*} is the fugacity of solute in the vapour phase. Analogous to the previous equation, the following equation applies for the pure solvent (s):

$$x_s\gamma_s\varphi_s^{sat}P_s^{sat}Poy_s = y_s\varphi_s^{v}P \qquad 6.35$$

The following is further assumed:

a) The solute is present in infinite dilution ($x_{sol} < 10^{-3}$). Thus,

$$\gamma_{sol} = \gamma_{sol}^{\infty}$$

For the pure solvent,

$$\gamma_s = 1 \qquad (x_s \approx 1)$$

This is assumed because the liquid phase consists of almost only solvent.

b) The Poynting factor (Poy_{sol}) takes into account the change of the fugacity upon expansion or compression, and can be neglected at low temperature or at low pressure differences ($P - P_{sol}^{sat}$). Thus, the approximation $Poy_{sol} \approx 1$ applies.

c) The solubility of the carrier gas in the liquid phase can be neglected.

d) The fugacity coefficients (φ_{sol}^{*}) for nitrogen as the carrier gas has a value of approximately unity, therefore $\varphi_{sol}^{*} \approx 1$.

For the solvent it is assumed that

$$\frac{\varphi_s^{sat} P o y_s}{\varphi_s^{v}} \approx 1 \qquad 6.36$$

It thus follows for the phase equillbrium of the solute that

$$x_{sol}\gamma_{sol}\varphi_{sol}^{sat}P_{sol}^{sat} = y_{sol}P \qquad 6.37$$

And for the solvent

$$P_s^{sat} = y_s P \qquad 6.38$$

As mentioned previously, the measurement principle is based on the fact that the carrier gas (here nitrogen) removes the highly dilute component from the dilutor cell. If the stream of carrier gas entering the dilutor cell (D_1) is considered, it is clear that this is made up of the nitrogen carrier gas stream entering the saturation cell (D) and the solvent gas stream (D_s) obtained by the saturation process. Thus, for D_1

$$D_1 = D + D_s \qquad 6.39$$

The solvent flow arises from the saturation vapour pressure of the solvent and the flow velocity of the nitrogen gas entering the saturator. The vapour pressure of the solvent depends on the temperature in the saturation cell. It thus follows that

$$D_s = Dy_s \qquad 6.40$$

When Equations 6.38 to 6.40 are combined and rewritten, the following expression for the carrier gas stream entering the measurement cell (D) is obtained:

$$D_1 = D\left(1 + \frac{P_s^{sat}}{P}\right) \qquad 6.41$$

The solvent content is particularly important for measurements in which the saturation vapour pressure of the solvent cannot be neglected ($P_s^{sat} > 5mbar$). The carrier gas stream leaving the dilutor cell (D_2) is the sum of the gas streams entering the cell (D_1) and the solute gas stream D_{sol}. The amount of solute decreases with time, as a steady removal of the highly dilute component from the cell occurs. Assuming that the ideal gas law can be applied, the following expression applies for the solute gas stream (D_{sol}):

$$D_{sol} = -\frac{RT}{P}\frac{dn_{sol}}{dt} \qquad 6.42$$

It thus follows that the gas stream leaving the dilutor cell is thus:

$$D_2 = D_1 - \frac{RT}{P}\frac{dn_{sol}}{dt} \qquad 6.43$$

As already mentioned, the variation of the amount of solute in the measurement cell is measured as a function of time. The following equation for this variation applies:

$$\frac{dn_{sol}}{dt} = -y_{sol}\frac{PD_2}{RT} \qquad 6.44$$

Because of the pre-saturation, the change in the amount of solvent present can be neglected. If Equation 6.44 is used in Equation 6.43 and combining this new equation with Equation 6.37, the resulting expression for the carrier gas stream leaving the dilutor cell is Equation 6.45.

$$D_2 = \frac{D_1}{1 - \frac{x_{sol} y_{sol}^{\infty} \varphi_{sol}^{sat} P_{sol}^{sat}}{P}} \qquad 6.45$$

If the expression for D_2 is used in Equation 6.44 and combined with Equation 6.37, the result is Equation 6.46.

$$\frac{dn_{sol}}{dt} = -x_{sol}\gamma_{sol}^{\infty}\varphi_{sol}^{sat}P_{sol}^{sat}\frac{1}{\left(1-\frac{x_{sol}\gamma_{sol}^{\infty}\varphi_{sol}^{sat}P_{sol}^{sat}}{P}\right)}\frac{D_1}{RT} \qquad 6.46$$

For relatively volatile solutes i.e. at high saturation vapour pressures of the solvent or large infinite dilution activity coefficients, it is advisable to take into account only the solute content in the liquid phase (n_{sol}^{L}) when defining the molar fraction. This means that the content in the gas phase must be subtracted. In this case,

$$n_{sol} = n_{sol}^{L} + n_{sol}^{V} = x_{sol}n_s + n_{sol}^{V} \qquad 6.47$$

The content of the solute in the gas phase can be described as follows, assuming ideal gas behaviour:

$$n_{sol}^{V} = y_{sol}\frac{PV_G}{RT} \qquad 6.48$$

The combination of Equations 6.48 and 6.37 and insertion into Equation 6.47 leads to

$$x_{sol} = \frac{n_{sol}}{n_s\left(1+\frac{\gamma_{sol}^{\infty}\varphi_{sol}^{sat}P_{sol}^{sat}V_G}{n_sRT}\right)} \qquad 6.49$$

If this expression for the molar fraction (Equation 6.49) is used in Equation 6.46, the result is:

$$\frac{dn_{sol}}{dt} = -\frac{n_{sol}}{n_s\left(1+\frac{\gamma_{sol}^{\infty}\varphi_{sol}^{sat}P_{sol}^{sat}V_G}{n_sRT}\right)}\gamma_{sol}^{\infty}\varphi_{sol}^{sat}P_{sol}^{sat}\left[\frac{1}{\left(1-\frac{\gamma_{sol}^{\infty}\varphi_{sol}^{sat}P_{sol}^{sat}n_{sol}}{Pn_s\left(1+\gamma_{sol}^{\infty}\varphi_{sol}^{sat}P_{sol}^{sat}V_G/(n_sRT)\right)}\right)}\right]\frac{D_1}{RT} \qquad 6.50$$

The reduction in solute concentration during a measurement leads to a corresponding reduction in the solute gas stream. However, this variation can be neglected (with respect to the carrier gas stream) under the conditions used in this work, i.e. the value of the correction term approaches unity. This term therefore does not need to be taken into account in the following integration. The integration of the simplified equation then leads to:

$$\ln\left(\frac{n_{sol}}{n_o}\right) = -\frac{\gamma_{sol}^{\infty}\varphi_{sol}^{sat}P_{sol}^{sat}}{n_s\left(1+\frac{\gamma_{sol}^{\infty}\varphi_{sol}^{sat}P_{sol}^{sat}V_G}{n_s RT}\right)}\frac{D_1}{RT}t \qquad 6.51$$

The sample loop and all other tubing connected after the dilutor cell must be thermo-statted to avoid condensation effects. This is accomplished by heating the lines to 40 °C above the entering gas stream. Also, if the amounts of solute injected into the gas chromatograph are proportional to the partial pressure of the solute over the solution, then Equation 6.22 applies once again. In the dilute range the linearity of the detector is assured. If it were not, it would be necessary to carry out time-consuming calibrations. If Equations 6.49, 6.37 and 6.22 are combined, a relationship between the peak area A_{sol} and the number of moles of solute (n_{sol}) can be obtained:

$$A_{sol} = \kappa\frac{\gamma_{sol}^{\infty}\varphi_{sol}^{sat}P_{sol}^{sat}}{n_s\left(1+\frac{\gamma_{sol}^{\infty}\varphi_{sol}^{sat}P_{sol}^{sat}V_G}{n_s RT}\right)}n_{sol} \qquad 6.52$$

Apart from the molar quantity of the solutes (n_{sol}), the quantities on the right hand side of the equation do not vary during the measurements. If n_{sol} from Equation 6.52 is used in Equation 6.51, the result is

$$\frac{\ln\left(A_{sol}/A_o\right)}{t} = -\frac{\gamma_{sol}^{\infty}\varphi_{sol}^{sat}P_{sol}^{sat}}{n_s\left(1+\frac{\gamma_{sol}^{\infty}\varphi_{sol}^{sat}P_{sol}^{sat}V_G}{n_s RT}\right)}\frac{D_1}{RT} \qquad 6.53$$

With slope $a = ln\left(A_{sol}/A_o\right)/t$ 6.54

If the equation is solved for γ_{sol}^{∞} and using Equation 6.41 we obtain:

$$\gamma_{sol}^{\infty} = -\frac{n_s RT}{\varphi_{sol}^{sat}P_{sol}^{sat}\left(\frac{D\left(1+P_s^{sat}/P\right)}{a}+V_G\right)} \qquad 6.55$$

Equation 6.55 is used in Chapter 7 to determine limiting activity coefficients for three test systems in order to verify the correct operation of the equipment used. There is sufficient recent literature data available for limiting activity coefficients calculated from this equation by Krummen et al. (2004).

When solvent mixtures are used, it is necessary to use the sum of the partial pressures of the components of the solvent mixture rather than the saturation vapour pressure of the solvent in the saturator (there will be the same acceptance made as that for pure solvent); that is

$$P_s^{sat} = \sum_{1}^{i} p_{s(i)} \qquad 6.56$$

$$n_s = \sum_{1}^{i} n_{s(i)} \qquad 6.57$$

In the analysis of the gas injected into the gas chromatograph the highly dilute component must always be separated from the solvent component, which is also removed from the cell. The separation is often time-consuming because the determination of the limiting activity coefficient requires the determination of at least 5 measurement values so that the decrease in the solute concentration can be reliably determined.

The limiting activity coefficient is determined with the help of the experimentally determined slope *a*. The slope is obtained by plotting $ln(A_{sol}/A_s)$ against time which would give a perfect straight line. The calculable quantities for the saturation vapour pressures of the solvent P_i^{sat} and the solute P_{sol}^{sat} were obtained using a group contribution method derived by Nanoolal et al. (in preparation) for vapour pressures. This newly derived method gives a better estimate of the vapour pressure than the well known Antoine equation, determined by fitting curves to literature data in the Dortmund Data Bank (DDB).

$$log(P_i^{sat}) = (4.1012 + dB)\left(\frac{T_{rb} - 1}{T_{rb} - \frac{1}{8}}\right) \qquad 6.58$$

$$T_{rb} = \frac{T}{T_b} \qquad 6.59$$

The vapour pressure (P_i^{sat}) calculated using Equation 6.58 is in atmospheres while T (in Kelvin) is the temperature at which the vapour pressure is to be evaluated. The boiling point temperature (T_b) also in Kelvin was obtained from the DDB together with dB values which is a constant specific for each pure component (computed from a group contribution method). T_{rb} is a dimensionless number and is essentially the ratio of system temperature to component boiling point.

The saturation fugacity coefficient (φ_{sol}^{sat}) was obtained using a widely used equation of state developed specifically for vapour liquid equilibrium (VLE) calculations. The saturation fugacity coefficient φ_{sol}^{sat} is determined using the Soave/Redlich/Kwong (SRK) equation.[4] Details of the calculation and all equations used can be found in Appendix A. The vapour volume in the dilutor cell (V_G) is obtained from the density of the solvent or solvent mixture (at the temperature of measurement) and its mass. The necessary data for the pure substances, such as critical data were taken from Reid et al. (1966).

An important quantity in the data evaluation is the carrier gas flow rate (D). This can be obtained with the help of a soap bubble flow meter or a rotameter. The condition of the carrier gas at the exit of the system must be the same as that at the inlet of the system when measuring its value. An alternative method of determining the carrier gas flow rate is to saturate the non condensable gas with water and then take into account the water vapour in the gas stream using Equation 6.60. The conversion of the gas stream D^{exp} determined at the soap bubble flow meter to the cell conditions is carried out as follows:

$$D = D^{exp} \frac{T}{T_{FM}} \frac{P_{FM} - P_{H_2O}^{sat}}{P_{cell}} \qquad 6.60$$

where T_{FM} is the temperature at the flowmeter, P_{FM} is the pressure at the flowmeter, P_{cell} is the pressure in the measurement cell, D^{exp} is the carrier gas flow at the flowmeter and $P_{H_2O}^{sat}$ is the water vapour pressure at T_{FM} . A water vapour volume flow must be added to the carrier gas flow because of the pre-saturation. Apart from the flow rate (D) which is corrected experimentally for the cell conditions, the pressure (P), the temperature (T) in the measurement

[4] Soave (1972)

cell and the mass of the solvent are the experimental quantities required for determining the limiting activity coefficient using Equation 6.55.

6.4 Equation Proposed by Hovorka and Dohnal (1997)

The equations proposed by Leroi et al. (1977) are specially suited for the determination of limiting activity coefficients, but Hovorka and Dohnal (1997) developed corrections to account for certain experimental conditions and non-idealities. These equations are to be used in conjunction with the equations derived by Leroi et al. (1977). The corrections were originally derived to determine limiting activity coefficients for volatile halogenated hydrocarbons. Such chemicals are produced on a large scale and used in many manufacturing industries as solvents, extractants, dry cleaning agents, metal degreasers, aerosol propellants and chemical intermediates.

Most pollutants are toxic and have carcinogenic and/or mutagenic potential. They are discharged into the environment through evaporation and spills and in wastewater effluents, resulting in exposure to the population. For environmental transport and fate studies and for design of water remediation processes, knowledge of air-water partitioning and aqueous solubility of these pollutants is indispensable. The fundamental thermodynamic quantity to characterize air-water partitioning is the limiting activity coefficient of the solute in water. The Henry's constant (H_{12}) and the air-water partitioning coefficient (K_{aw}) are closely related to the limiting activity coefficient, and under the assumption that the vapour phase behaves as an ideal gas they are given by

$$H_{12} = \gamma_{sat}^{\infty} P_{sol}^{sat} \qquad 6.61$$

$$K_{aw} = \frac{\gamma_{sol}^{\infty} P_{sol}^{sat} \upsilon_w^L}{RT} \qquad 6.62$$

P_{sol}^{sat} and υ_w^L denote the saturated vapour pressure of the pure liquid solute and the liquid molar volume of pure water, respectively and T is the absolute temperature. The systems under investigation may not be a treat to the environment at present but the corrections do apply. In fact the corrections will apply to any system to which the equations derived by Leroi et al. (1977) apply. It is shown in this chapter that the corrections apply to systems with high solute volatility and low solvent volatility.

The inert gas stripping technique is favoured over some of the other methods for the determination of γ_i^{∞} because of its applicability to a broad range of solute volatilities (10 kPa < H_{12} < 10^5 kPa) and its precision (1 to 2 %). There is also no need for calibration of the gas chromatographic detector and no or rather marginal importance of knowing exactly the initial solute concentration.

As shown by Leroi et al. (1977) when the partial pressure of the solute is small compared to the total pressure, the rate of solute elution from a non-volatile solute follows a simple exponential first-order kinetics pattern. Vapour-phase non-ideality corrections and the effect of the vapour space in the cell are neglected. Provided the detector response is linear, the limiting activity coefficient can be determined from the following equation.

$$\gamma_{sol}^{\infty} = \frac{NRT}{P_{sol}^{sat} D}\left(-\frac{d \ln A_{sol}}{dt}\right) \qquad 6.63$$

The above equation applies to the single cell technique. For the double cell technique, i.e. when a pre-saturation cell is in place, usually for solvents of appreciable volatility, Equation 6.63 does not apply due to the amount of solvent decreasing in the cell. Another more complicated relation to calculate γ_i^{∞} is required. In order to keep the amount of solvent (N) in the equilibrium cell constant a second cell (pre-saturation cell), is used. Upon pre-saturation, the flow rate of the stripping gas entering the cell changes by a factor of $1/\left(1 - P_i^{sat}/P\right)$, where P_i^{sat} is the pure solvent vapour pressure. The formula to calculate the activity coefficient at infinite dilution in the pre-saturation mode becomes

$$\gamma_{sol}^{\infty} = \frac{NRT}{P_{sol}^{sat} D}\left(-\frac{d \ln A_{sol}}{dt}\right)\left(1 - \frac{P_i^{sat}}{P}\right) \qquad 6.64$$

The first order approximation provided by Equations 6.63 and 6.64 is often sufficiently accurate, but if the simplifying assumptions are violated appreciably, this leads to the involved and rather complex Equations 6.29 (derived by Duhem and Vidal (1978)) and 6.33 (derived by Boa and Han (1995)). Alternatively, using the perturbation approach Hovorka and Dohnal (1997) derived separate corrections to each of the simplifying assumptions in the form of correction factors (k_i). This resulted in the second order approximation $\gamma_{sol}^{\infty,II}$ of the limiting activity coefficient value as

$$\gamma_{sol}^{\infty,II} = \gamma_{sol}^{\infty} \prod_{i}^{4} k_i \qquad 6.65$$

where $\gamma_{sol}^{\infty,II}$ is the corrected activity coefficient at infinite dilution and represents the solutes actual activity coefficient value at infinite dilution. It is obvious that if the individual corrections are not too high, then their interference is negligible and the perturbation formula (Equation 6.65) yields almost exact results as Equations 6.63 and 6.64.

6.4.1 Important Corrections

The correction factors k_i were derived by Hovorka and Dohnal (1997) and are to be used as a simplified way to account for deviations in Equations 6.63 and 6.64.

6.4.1.1 Change of Stripping Gas Flow Rate due to Saturation in the Cell

For inert gas stripping without the pre-saturation of the stripping gas by the solvent vapour (γ_{sol}^{∞} calculated from Equation 6.63) the correction factor is given by

$$k_1 = 1 - \left(\frac{\overline{n}_{sol}}{N}\right)\gamma_{sol}^{\infty}\left(\frac{P_{sol}^{sat}}{P}\right) - \frac{P_s^{sat}}{P} \qquad 6.66$$

With the use of the pre-saturation cell (γ_1^{∞} calculated from Equation 6.64) the correction factor is given by Equation 6.67.

$$k_1 = \left[1 - \left(\frac{\overline{n}_{sol}}{N}\right)\gamma_{sol}^{\infty}\left(\frac{P_{sol}^{sat}}{P}\right) - \frac{P_s^{sat}}{P}\right] \Bigg/ \left(1 - \frac{P_s^{sat}}{P}\right) \qquad 6.67$$

Here $\overline{n}_{sol}$ is the mean amount of solute in the cell during the measurement, obtained from Equation 6.68.

$$\overline{n}_{sol} = n_{sol}^{o}\left(\frac{A_{sol}^{f}}{A_{sol}^{o}} - 1\right) \Bigg/ \ln\left(\frac{A_{sol}^{f}}{A_{sol}^{o}}\right) \qquad 6.68$$

where n_{sol}^{o} is the initial amount of solute in the cell, A_{sol}^{f} and A_{sol}^{o} are the GC responses to the solute at the end and at the beginning of the experiment, respectively. The correction factor k_1 is always less than 1. Its importance becomes greater with increasing volatility of the solute and the solvent.

6.4.1.2 Removal of the Solvent due to its Volatility

The correction factor without pre-saturation of the inert gas is

$$k_2 = 1 - \left(\frac{P_s^{sat} Dt}{2N_0 RT} \right) \qquad 6.69$$

where N_0 is the initial amount of the solvent in the cell and t is the total stripping time. The correction factor k_2 is less than 1, and its importance rises with increasing solvent volatility and decreasing cell volume, thus when the stripping gas is pre-saturated with the solvent, $k_2 = 1$. If k_2 is evaluated for a system with a pre-saturation cell in place, despite the logic, its calculated value will be very close to 1.

6.4.1.3 Amount of Solvent in the Vapour Space of the Cell

If complete mixing of the vapour space of the cell is assumed, the appropriate correction factor can be written as

$$k_3 = \left[1 - \left(\frac{\gamma_{sol}^{\infty} P_{sol}^{sat} V_G}{NRT} \right) \right]^{-1} \qquad 6.70$$

where V_G is the vapour space volume in the cell. The correction factor k_3 is always greater than 1 and rises with the solute volatility and with the increasing ratio of the vapour space volume to the amount of solvent in the cell.

6.4.1.4 Vapour-phase Non-ideality

Using the virial equation of state, the vapour phase non-ideality correction factor is

$$k_4 = \left[1 + \frac{B_{33}P}{RT}\right] \exp\left\{\frac{P\left[\left(2B_{13} - B_{33} - v_{sol}^{L}\right) - P_{sol}^{sat}\left(B_{11} - v_{sol}^{L}\right)\right]}{RT}\right\} \qquad 6.71$$

where v_{sol}^{L} is the pure solute liquid molar volume and B_{ij} are the second virial coefficients; the components 1, 2, 3 being the solute, the solvent and the stripping gas, respectively. The vapour-phase non-ideality correction factor can be either greater or smaller than 1 depending on the system and its conditions.

The virial coefficients B_{ij} required for the evaluation of Equation 6.71 can be calculated using the following equation:

$$B_{ij} = \frac{RT_{Cij}}{P_{Cij}}\left(B_0 + \omega_{ij}B_1\right) \qquad 6.72$$

The critical properties of components were taken from Reid et al. (1966) and the Dortmund Data Bank (DDB). B_0 and B_1 are functions of reduced temperature (Equations 6.73 and 6.74).

$$B_0 = 0.083 - \frac{0.422}{T_{rij}^{1.6}} \qquad 6.73$$

$$B_1 = 0.139 - \frac{0.172}{T_{rij}^{4.2}} \qquad 6.74$$

where $T_{rij} = \frac{T}{T_{Cij}}$.

The combining rules proposed by Smith, Van Ness and Abbott (1996) for calculations of ω_{ij}, T_{Cij}, P_{Cij}, Z_{Cij} and V_{Cij} are:

$$\omega_{ij} = \frac{\omega_i + \omega_j}{2} \qquad 6.75$$

$$T_{Cij} = \left(T_{Ci}T_{Cj}\right)^{0.5}\left(1 - k_{ij}\right) \qquad 6.76$$

In Equation 6.76, k_{ij} is an empirical interaction parameter specific to an $i-j$ molecular pair. When $i=j$ and for chemically similar species, $k_{ij}=0$. Otherwise, it is a small positive number evaluated from minimal PVT data or in the absence of data as in the case with all chemical species used here, k_{ij} is set equal to 0.

$$P_{Cij}=\frac{Z_{Cij}RT_{Cij}}{V_{Cij}} \qquad 6.77$$

$$Z_{Cij}=\frac{Z_{Ci}+Z_{Cj}}{2} \qquad 6.78$$

$$V_{Cij}=\left(\frac{V_{Ci}^{1/3}+V_{Cj}^{1/3}}{2}\right)^3 \qquad 6.79$$

When $i=j$ all the equations reduce to the appropriate values for a pure species. When $i \neq j$ these equations define a set of interaction parameters having no physical significance. This is a very basic method used to predict virial coefficients. Other more complex methods for determining virial coefficients may be used if they lead to more accurate results. For this study this predictive method for virial coefficients were applied in all the calculation procedures.

6.5 Henry's Law Constants and IGS

The inert gas stripping technique described in the previous chapters is well suited for the determination of activity coefficients at infinite dilution. The inert gas stripping method has also been extended to the accurate measurement of Henry's constants. Henry's Law Constants characterize the equilibrium distribution of dilute concentrations of volatile, soluble chemicals between gas and liquid. In other words the Henry's constant is the ratio of the concentration of a chemical substance in air to the concentration in an aqueous solution at equilibrium. It can be used as a qualitative measure of the volatility of a substance and its whereabouts in nature.

Waste water treatment is another research area where Henry's law constants are needed since solubility affects volatilization of toxic compounds into the air. Henry's constants are useful in providing design data for absorption processes, as well as, indirectly, in aiding the analysis of molecular interactions in solutions. Solubility data will be useful to develop prediction methods, especially for group contribution methods, where it may also be necessary to take into account

the differences between isomers. For developing the molecular theory, the accurate intermolecular potential is necessary. The Henry's constant is directly related to the residual chemical potential of the solute at infinite dilution. This is evaluated from the intermolecular potential between a solute molecule and a solvent molecule. Therefore, the Henry's constant is a suitable macroscopic property for testing the intermolecular potential between different kinds of molecules.

Henry's constants (solubilities) are useful data for oil recovery or transportation problems. A fast and accurate method is required to investigate numerous solvents. For this purpose, the gas stripping method is particularly convenient, but a special equilibrium cell must be used and certain experimental conditions fulfilled. The liquid level in the cell should not be lower than 1 cm from the top of the cell. It is also necessary to place two baffles in the glass cell body to achieve efficient stirring of the liquid phase. Equilibrium between liquid and vapour phases is reached only with these special conditions of cell design. An illustration of the equilibrium cell can be found in Chapter 3, Figure 3-3.

Henry's constants can be calculated using an equation proposed by Duhem and Vidal (1978) and was successfully used by Richon and Renon (1980) for light hydrocarbons as the solute and is shown below:

$$H_{s,i}^{\infty} = -\frac{1}{t} ln \frac{A}{A_0} \frac{RTN}{D + \frac{V_G}{t} ln \frac{A}{A_0}} \qquad 6.80$$

A special dilutor cell, very different from the one used here was used by Richon and Renon (1980) to determine Henry's constants of light hydrocarbons in more heavier alkanes such as n-hexadecane, n-octadecane and 2,2,4,4,6,8,8-heptamethylnonane. An illustration of the dilutor cell used is shown in Figure 3-3. Equation 6.80 was also used by Richon et al. (1980) to determine infinite dilution activity coefficients of linear and branched alkanes in n-hexadecane but by using a different dilutor cell as shown in Figure 3-5.

Recently, extensive studies have been undertaken by Miyano et al. (2003) to determine Henry's constants for gases like C_4 using the inert gas stripping technique. In light of this recent work the rest of this chapter is an understudy of the work done by Miyano et al. (2003 – 2005).

6.5.1 Equation for Determining Henry's Constants

Only key equations proposed for the determination of Henry's constants by Miyano et al. (2003) can be found in this chapter. A full derivation of all proposed equations and details of all calculation methods can be found in the journal article by Miyano et al. (2003).

The gas stripping method originally proposed by Leroi et al. (1977) is based on the variation of vapour phase composition when the highly diluted solute of the liquid mixture is stripped from the solution by a constant flow of inert gas. The approximated equation to express the relationship between the solute peak area (A) the gas volume flowing out of the equilibrium cell, and the total volume of nitrogen (Dt) flowing out of an equilibrium cell at time t is given by Equation 6.29. The peak solute area (A) is measured by gas chromatography. The gas volume out of the equilibrium cell is proportional to the vapour phase composition stripped from the solution. Equation 6.29, which was derived under some assumptions reported above, may therefore not be used for highly volatile mixtures.

The equation to determine Henry's constants derived by Miyano et al. (2003) requires a number of assumptions. If the solute is highly diluted in the solvent and if the solubility of the inert gas in the liquid phase is negligible, the mole fraction and the activity coefficient of the solvent may be taken equal to 1. The existence of the inert gas must not affect the equilibrium between solute and solvent. The mole fraction of solute in the liquid phase must be very small (less than 10^{-3}). The peak area (A_0) of the solute detected by gas chromatography is proportional to solute partial pressure.

$$ln\frac{A}{A_0}=\left(\frac{H_{sol}\varphi_s^V}{\varphi_{sol}^V(1+\alpha)f_s^{L,0}-\alpha\varphi_s^V H_{sol}}-1\right)ln\left(1-\frac{\left[(1+\alpha)f_s^{L,0}/\varphi_s^V\right]-\left(\alpha H_{sol}/\varphi_{sol}^V\right)}{ZRT\left[N_0+\left(H_{sol}V_{GP,0}/\varphi_{sol}^V ZRT\right)\right]}V\right) \quad 6.81$$

Equation 6.81 can be used when the volume (V) of the saturated gas flowing out of the equilibrium cell is used. If the volume of vapour phase in the cell is negligible ($V_{GP,0}$ = 0 and α = 0),

$$ln\frac{A}{A_0}=\left(\frac{H_{sol}\varphi_s^V}{\varphi_{sol}^V f_s^{L,0}}-1\right)ln\left(1-\frac{f_s^{L,0}}{\varphi_s^V ZRTN_0}V\right) \quad 6.82$$

Furthermore, if the vapour phase can be treated as an ideal gas ($\varphi_g^V = \varphi_s^V = Z = 1$) and using an approximation of $f_s^{L,0}$

$$ln\frac{A}{A_0} = \left(\frac{H_{sol}}{P_s^{sat}} - 1\right) ln\left(1 - \frac{P_s^{sat}}{N_0 RT} V\right) \qquad 6.83$$

This equation is similar to Equation 6.29 proposed by Duhem and Vidal which is a modification of the Leroi et al. (1977) equations. When the vapour pressure of solute is negligibly small, the $PDt/\left(P - P_s^{sat}\right)$ term in Equation 6.29 is approximately equal to the volume of the saturated vapour (V). $H_{sol} \approx \gamma^{\infty} P_{sol}^{sat} P_i^{sat}$ then becomes the vapour pressure of pure component i.

6.5.2 Realizations by Miyano et al. (2003)

After careful consideration, numerous experiments and manipulation of results by Miyano et al. (2003) it was realized that certain assumptions outlined above were not entirely true. The effect of two assumptions on the final outcome of the Henry's constant has been outlined below together with some alterations to the above equations.

6.5.2.1 Volume Effect of Vapour Phase

In general, the existence of vapour phase in the cell affects the evaluation of the Henry's constants for the gas stripping method. When a solution contacts a fresh inert gas, some amounts of solute and solvent in the solution will move into the inert gas bubbles to keep the equilibrium. If there is a space to keep the vapour in the cell, the solute can stay there for its residence time, and some amounts of them will dissolve into the solution again. This will reduce the rate of stripping. Therefore, the evaluated Henry's constant without the correction of the volume effect of vapour phase will become smaller than the true value.

The difference in the Henry's constants is mainly proportional to the initial volume of the vapour phase in the cell. Therefore, the initial volume of the vapour phase should be made as small as possible. In addition, the volume effect will depend on the total volume of the cell and the flow rate of the inert gas. If the solute is non-volatile, the volume effect will be reduced.

6.5.2.2 Effects of Non-ideality

Miyano et al. (2003) found that the fugacity coefficients of solute in the vapour phase were almost one and the fugacity coefficients of solvent in vapour phase differed from one by about 2 % at the higher temperatures. Sorting out this problem requires taking the ratio of the fugacity of solvent at the reference state and the fugacity coefficient of solvent in vapour phase:

$$\frac{f_s^{L,0}}{\varphi_s^V} = P_s^{sat} \qquad 6.84$$

At infinite dilution of solute, the solvent can be treated as a pure substance and the above relationship (Equation 6.84) can be used. Thus Equation 6.81 can be re-written as:

$$ln\frac{A}{A_0} = \left(\frac{\left(H_{sol}/\varphi_{sol}^V\right)}{(1+\alpha)P_s^{sat} - \alpha\left(H_{sol}/\varphi_{sol}^V\right)} - 1\right) ln\left(1 - \frac{(1+\alpha)P_s^{sat} - \alpha\left(H_{sol}/\varphi_{sol}^V\right)}{ZRTN_0 + V_{GP,0}\left(H_{sol}/\varphi_{sol}^V\right)} V\right) \qquad 6.85$$

This means that the ratio may not be affected by the non-ideality and the Henry's constant will depend only on the non-ideality of the solute, φ_g^V. Equation 6.85 can successfully be used to determine Henry's Law constants with the aid of the IGS technique.

The rigorous formula (Equation 6.85) to evaluate the Henry's constants from the IGS experiments has been proposed by Miyano et al. (2003). When using this formula, the effects of non-ideality of fluids and the existence of gas phase in the cell has been discussed. In general, the Henry's constants do not depend on the non-ideality so much, while the activity coefficients strongly depend on the non-ideality of solute at the reference state. Experiments could not be conducted here to determine Henry's constants due to the highly specialized dilutor cells required. The simple cells in this study were not designed for this purpose.

Chapter VII – Experimental Results

Part I: Test Systems

Three test systems were chosen for which limiting activity coefficients have already been determined by Krummen et al. (2004) using the IGS technique. The three test systems were n-heptane (1) in N-methyl-2-pyrrolidone (NMP) (2), cyclohexane (1) in N-methyl-2-pyrrolidone (2) and n-hexane (1) in N-methyl-2-pyrrolidone (2), (1 refers to the solute while 2 refers to the solvent). The limiting activity coefficients obtained from experiments using the IGS technique were compared to literature data published by Krummen et al. (2004) obtained from experiments using the same technique. Once it was established that the data was good and reliable, unknown systems were attempted and the results of which can be found in Part 2 of this chapter.

7.1 Limiting Activity Coefficients - Krummen et al. (2000)

The double cell technique was used for the analysis of all test systems, but for the n-hexane (1) + NMP (2) system the single cell technique was also used and the results for the two techniques were compared. The limiting activity coefficients were evaluated for all the equations outlined in the previous chapter. The results for the Krummen et al. (2000) proposed equation (Equation 6.55) are reported, followed by that for Leroi et al. (1977) based equations (Equations 6.23, 6.24, 6.29 and 6.33) and lastly for the Hovorka and Dohnal (1997) derived equation (Equation 6.65).

7.1.1 Test System 1: Cyclohexane (1) + NMP (2)

Before one can forge ahead with the experimental determination of activity coefficients a suitable inert gas flow rate needs to be determined. The higher the flow rate, the less likely it is that the system will reach equilibrium. There is a maximum flow rate that must not be exceeded when using the IGS technique for a particular system. If experiments are performed at flow rates beyond this maximum flow rate there will be large errors in the limiting activity coefficients as equilibrium conditions will not be obtained. There would be a loss of accuracy and precision which would lead to inconclusive results. At the same time, operating at a very low flow rate would result in a poor variation of solute peak areas with time. It would not be possible to obtain a good representation of data for slope in a short period of time especially for non-volatile solutes, but for highly volatile solutes low flow rates are ideal. As a result there needs to be a suitable balance between flow rate and experimental time with regard to solute volatility.

The solute peak areas and residence times were obtained from the GC program Clarity which is an integration program that analyses the signal coming from the FID detector of the Varian 3300 gas chromatograph. This was done with the aid of a computer. The solute peak areas and residence times are used to determine the slope (a). The peak areas need to be represented before a plot can be made. The peak areas A_i are divided by the initial area A_0 and the logarithm of the resultant ratio is plotted against time to give a straight line. The gradient a of the line is used in Equation 6.55 to determine γ_i^{∞}. All plots and data manipulations were done in Microsoft Excel unless otherwise stated. MATLAB was used to determine vapour pressures and fugacity coefficients.

The system cyclohexane (1) + NMP (2) was used in order to determine the inert gas flow rate range necessary for accurate results. Five flow rates between 4 and 50 millilitres per minute were chosen to determine a suitable operating range for the system. Nitrogen was the chosen inert gas used for all experiments. A plot showing the slopes for the system cyclohexane (1) + NMP (2) at different nitrogen gas flow rates (D) is illustrated in Figure 7-1. Experiments were done in order to find a suitable range for the flow rate. The equipment was not able to handle flow rates greater than 50 ml/min and the bubbles formed by the capillaries were becoming large.

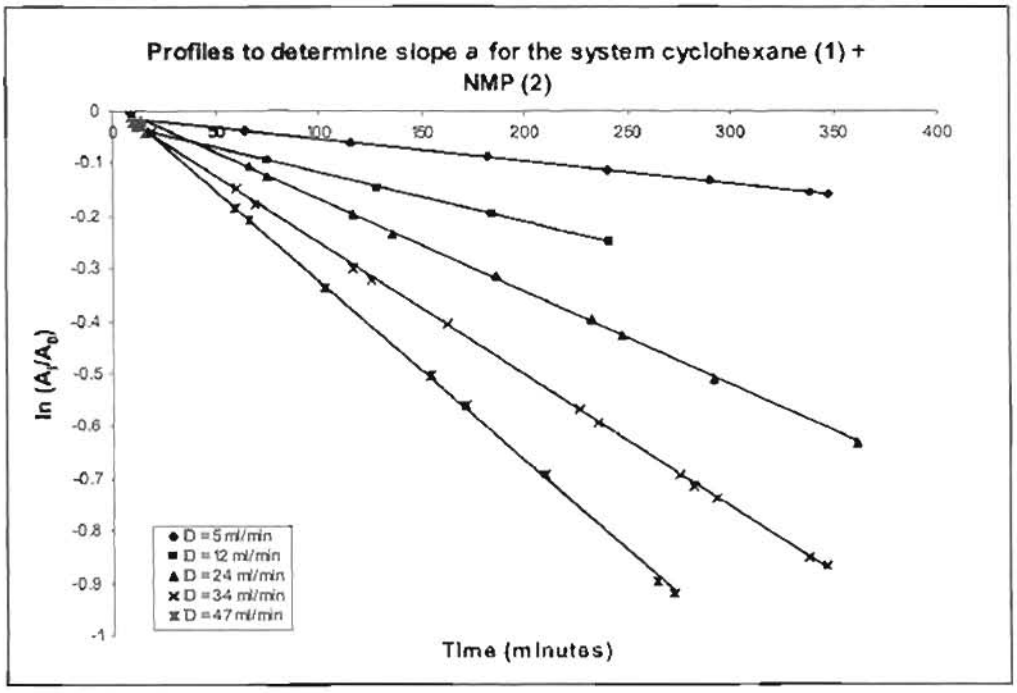

Figure 7-1: Straight line plots showing slope *a*. The slope was used to determine limiting activity coefficients at constant temperature from Equation 6.55.

It is recommended that higher flow rates be used for systems where the solute volatility is very low in order to reduce experimental time. Temperature, time between injections, solute volatility and inert gas flow rate effect the variation of solute in the dilutor cell, with time. A good variation of solute peak areas with time is required for a reasonable plot to determine the slope. High temperatures, longer stripping times, high volatility solutes and high inert gas flow rates contribute to larger variations of the solute peaks with time. High temperatures and gas flow rates as well as long stripping times between injections work against highly volatile solutes as most of the solute is stripped before a well represented plot can be made. Therefore, a balance between these variables must be found, usually by logical deduction or trial and error.

From Figure 7-1 the profound effect that the inert gas flow rate has on the slope can be seen. As the flow rate increases the slope also increases. This shows that the higher the inert gas flow rate, the higher the stripping rate which will be expected. The resulting limiting activity coefficients due to varying flow rate and keeping temperature constant is shown in Table 7-1.

Flowrate (D)	Temperature (T)	Limiting Activity Coefficients		Deviation
(ml/min)	(°C)	$\gamma^{\infty}_{Experimental}$	$\gamma^{\infty}_{Literature}$	%
5.83	50.16	6.67	6.7	-0.48
12.65	50.16	6.67	6.7	-0.45
24.43	50.23	6.65	6.7	-0.72
34.59	50.17	6.68	6.7	-0.30
47.47	50.30	6.64	6.7	-0.89

Table 7-1: Activity coefficients at infinite dilution for the system cyclohexane (1) + NMP (2) at a temperature of approximately 50 °C and at different inert gas flow rates chosen in the range 4 to 50 ml/min.

The literature value for the γ^{∞} for cyclohexane in NMP at 50.2 °C is 6.7 as determined by Krummen et al. (2004) using the IGS technique with flow rates between 30 and 40 ml/min. It can be seen that the values obtained using the newly designed equipment gives values close to the value obtained by Krummen et al. (2004). Even with inert gas flow rates as high as 47 ml/min the deviation from the literature value is small. However it was then decided to operate the equipment at flow rates in the range 10 to 30 ml/min. This was done in order to minimize the pressure build-up in the pre-saturator as the "O"-ring seals were not able to keep the Teflon plug in place. The effect of temperature on the limiting activity coefficients for the system cyclohexane (1) + NMP (2) was then investigated.

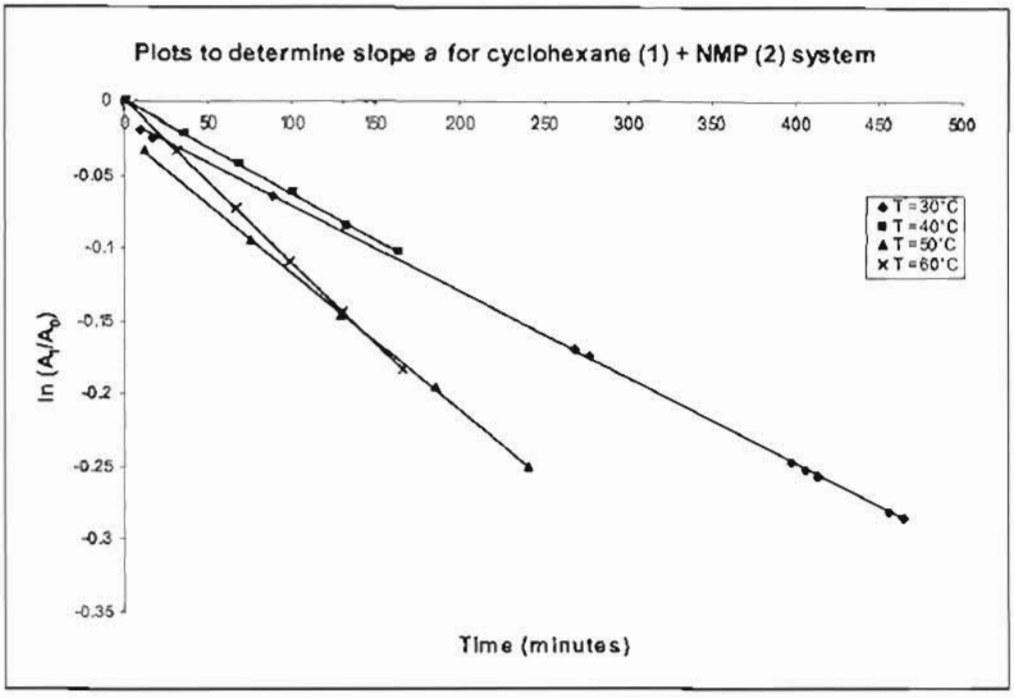

Figure 7-2: GC solute peak areas that have been represented to give straight line plots for the determination of slope *a*, at different temperatures for the system cyclohexane (1) + NMP (2).

Figure 7-2 shows the effect that temperature has on the slope and thus the stripping rate. As temperature increases the slopes increase, which means that the stripping rate increases. This means that more solute is going into the bubble phase. This makes sense due to the fact that the volatilities of the solute and solvent in the equilibrium cells are a function of temperature. The higher the temperature the more volatile the components in the cell become and thus readily move into the gas phase. The effect that temperature has on the limiting activity coefficients at constant nitrogen gas flow rate is shown in Table 7-2.

Literature Data		Experimental Values			Deviation
T (°C)	$\gamma^{\infty}_{Literature}$	D (ml/min)	T (°C)	$\gamma^{\infty}_{Experimental}$	(%)
30.1	7.8	14.89	30.08	7.77	-0.43
40.2	7.19	11.77	40.03	7.21	0.32
50.1	6.7	12.65	50.16	6.73	0.42
60.2	6.23	11.77	60.06	6.20	-0.49

Table 7-2: Experimental limiting activity coefficients for cyclohexane (1) + NMP (2) evaluated at different temperatures. Also tabulated are literature values at similar temperatures, determined by Krummen et al. (2004).

The calculated deviation shown in Table 7-2 is not a true measure of the accuracy of the results because the temperatures at which the experiments have been performed are not exactly the same as the literature temperatures. Instead a plot of the experimental results and literature values gives a better indication of the accuracy and is a far better comparison. Deviations will not be shown in tables; instead a plot, such as that in Figure 7-3 shows clearly the accuracy of the results when compared to literature.

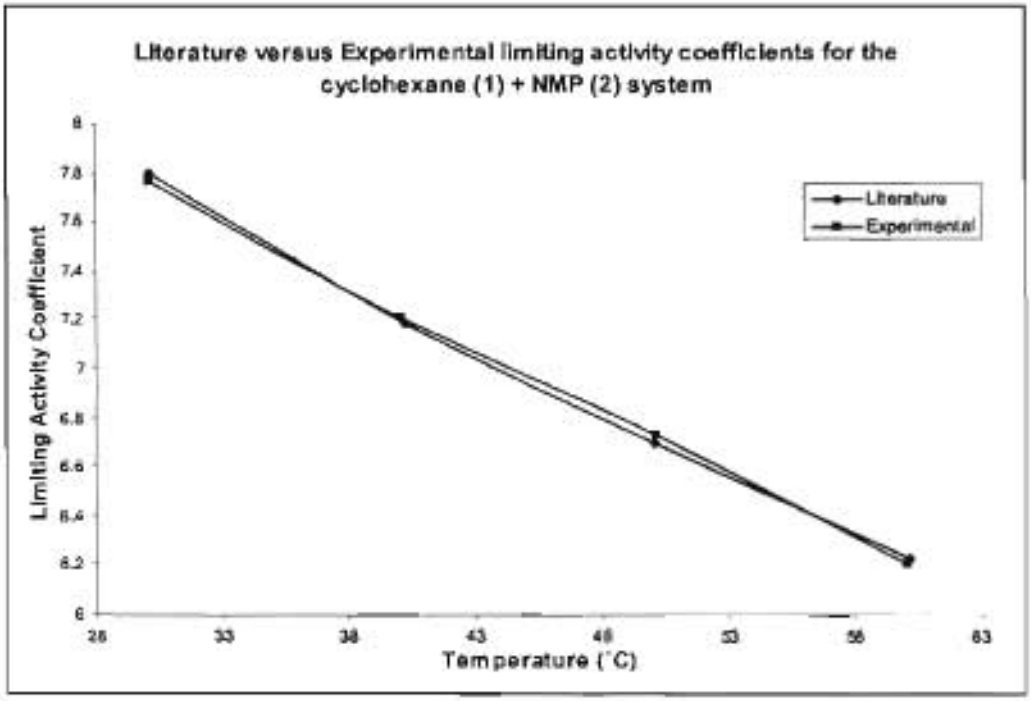

Figure 7-3: Comparison of experimental and literature values of limiting activity coefficients for the system cyclohexane (1) + NMP (2) from Equation 6.55.

The flow rate is not consistent for the four experimental runs for this system because at the time of the measurements a pressure regulator was not in place at the gas inlet to the system. This resulted in the flow rate changing due to others using nitrogen gas from the same tank on different days. However, the flow rate during the experimental run was the same throughout the run. The actual value of the limiting activity coefficients is not significantly affected by inert gas flow rate as long as it is constant throughout the entire period of analysis and equilibrium conditions are maintained in the cells. Once the regulator was in place disturbances in the nitrogen gas line did not affect the flow of nitrogen out of the regulator. This was true only if these disturbances did not result in a pressure that was below the set pressure on the regulator.

The results show that the experimental setup is well suited for the determination of activity coefficients at infinite dilution for the cyclohexane (1) + NMP (2) system. The obtained results

are in strong agreement with already published literature data. The trend for γ^{∞} as a function of temperature confirms the general trend for these types of systems. The results for this system determined from other proposed equations follow later in the chapter.

7.1.2 Test System 2: n-heptane (1) + NMP (2)

The next test system studied was n-heptane (1) in NMP (2). The limiting activity coefficients for the system n-heptane in NMP evaluated from Equation 6.55 can be found in this section. The results for other equations are reported later in the chapter. The various plots to determine slope *a*, is shown in Figure 7-4.

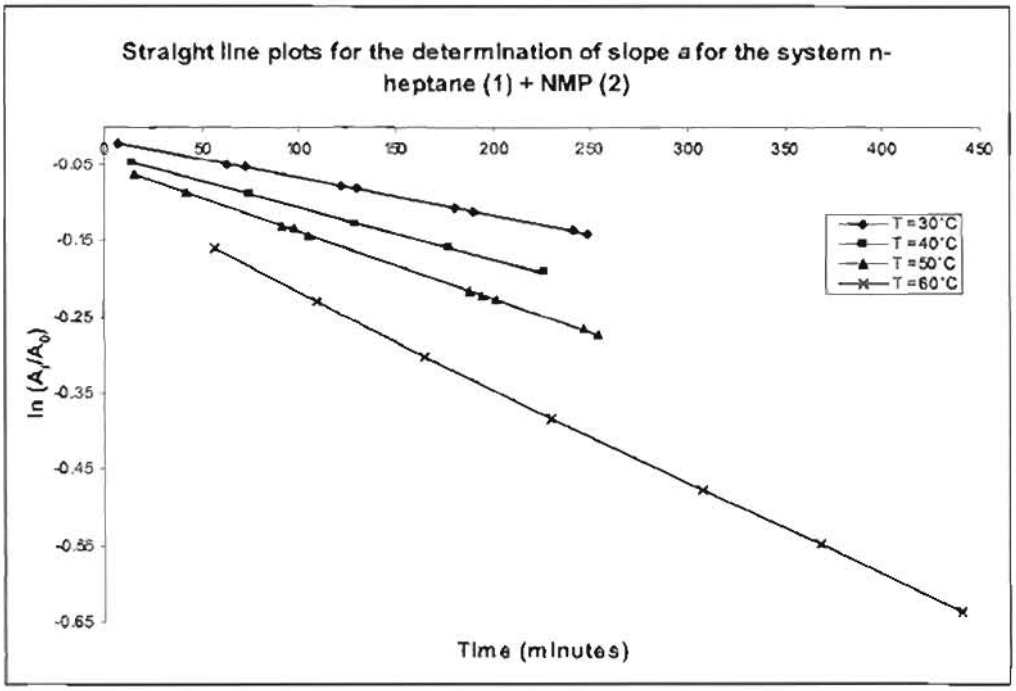

Figure 7-4: Temperature effect on the straight line plots for the system n-heptane (1) + NMP (2) for use with Equation 6.55 to determine limiting activity coefficients.

The effect of temperature on the slope *a*, for this system is similar to that for the system cyclohexane (1) + NMP (2). The slope gradually increases as temperature increases, but this has an opposite effect on the limiting activity coefficient itself. The limiting activity coefficient has an inverse relationship with temperature i.e. as temperature increases the solute limiting activity coefficient decreases. This is true for most systems and the effect can be clearly seen in the table below.

Literature Values		Experimental Values		
T (°C)	$\gamma^{\infty}_{Literature}$	D (ml/min)	T (°C)	$\gamma^{\infty}_{Experimental}$
30	14.9	11.06	30.12	14.92
40.2	13.7	11.13	39.83	13.72
50.2	12.4	11.08	50.51	12.43
60.2	11.5	11.46	60.19	11.46

Table 7-3: Calculated limiting activity coefficients for the system n-heptane (1) + NMP (2) with corresponding literature values at similar temperatures obtained from Equation 6.55.

The experimental values are in strong agreement with recently published literature values by Krummen et al. (2004). After installing the pressure regulator the nitrogen gas flow rate was constant for the different runs done on different days, despite use from the same source by other researchers. This is clearly depicted in Table 7-3 for the four runs done over four days. The flow rate is very difficult to set at a specific value using a simple needle valve. An electronic mass flow device can be used to control the inert gas flow rate but this equipment is very expensive. A clear indication of the effect of temperature on γ^{∞} is seen in Figure 7-5.

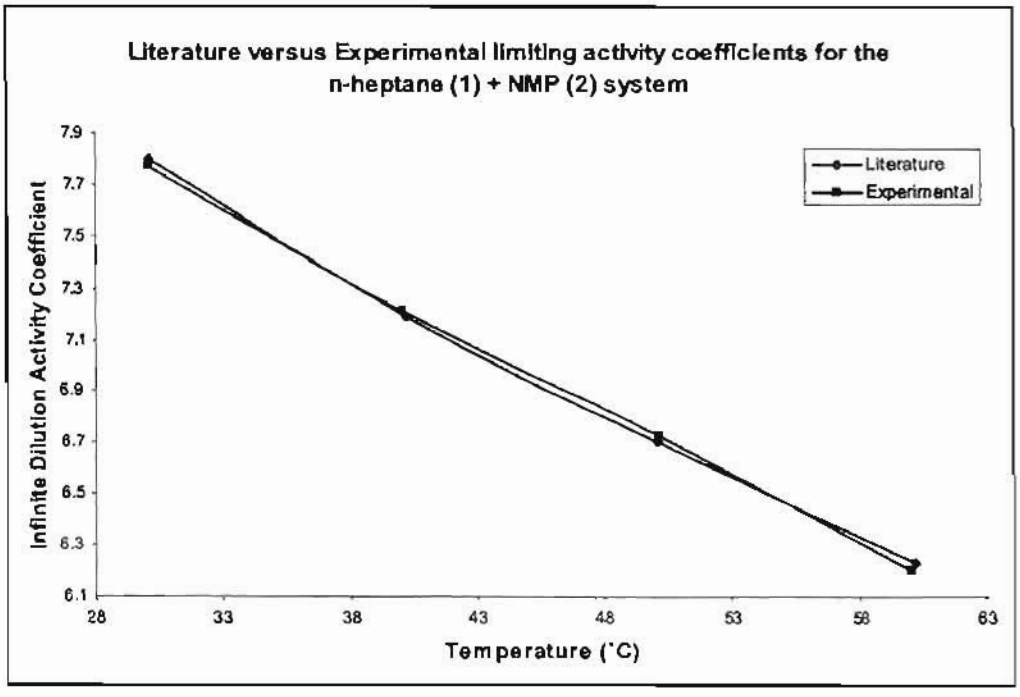

Figure 7-5: Limiting activity coefficients for the system n-heptane (1) + NMP (2) as a function of temperature and comparison with published literature data by Krummen et al. (2004).

The limiting activity coefficient is strongly affected by temperature, as seen by the results of the two test systems.

7.1.3 Test System 3: n-hexane (1) + NMP (2)

For the third test system the effect of using one cell (SCT) and two cells (DCT) was investigated. The nature of the components determines which technique to use. Due to the low volatility (less than 1 mm Hg) of the solvent NMP in these systems the SCT can be successfully used. Another prerequisite is that the solvent must be a single component and not a mixture of components otherwise the concentration might change considerably in the dilutor cell due to the fact that the rate at which each component is stripped may vary. In that case the DCT must be used to ensure accurate results. The DCT slope plots for the system n-hexane (1) + NMP (2) is shown in Figure 7-6.

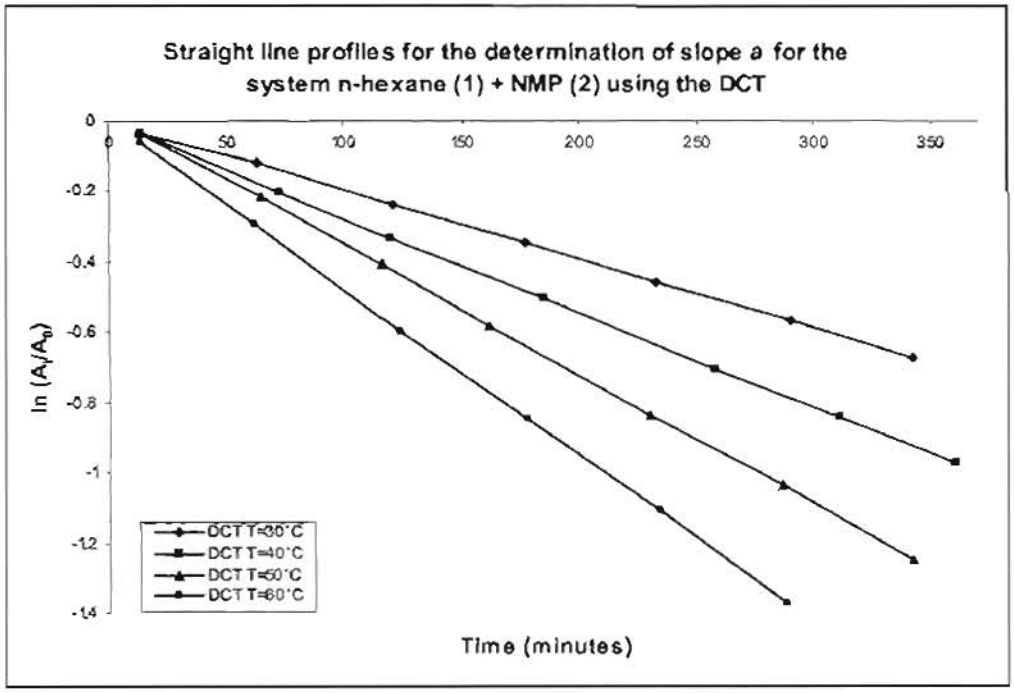

Figure 7-6: Plots for the determination of slope (*a*) at different temperatures and constant flow rate for the system n-hexane (1) + NMP (2) using the double cell technique

The affect of temperature on the system n-hexane (1) + NMP (2) is similar to the other two test systems. Since the slope (*a*) greatly influences the limiting activity coefficient it is expected that the affect of temperature on γ^{∞} should be similar to that of the other two test systems as shown in Table 7-4.

Double Cell Technique				
Literature Data		Experimental Data		
T (°C)	$\gamma^{\infty}_{Literature}$	D (ml/min)	T (°C)	$\gamma^{\infty}_{Experimental}$
30.1	12.7	19.42	30.13	12.65
40.2	11.6	19.91	40.12	11.59
50.2	10.7	19.95	50.34	10.64
60.2	9.9	19.93	60.61	9.88

Table 7-4: Comparison of literature and experimental data for the system n-hexane (1) + NMP (2) obtained using the double cell technique.

A higher flow rate than for the other two test systems was used for the determination of γ^{∞} in order to check the effect it would have on the activity coefficient for this system. The higher flow rate of 20 ml/min still allows for equilibrium in the dilutor cell as determined with the cyclohexane (1) + NMP (2) system for flow rates up to 47 ml/min. The double cell technique clearly works well for systems will low solvent volatility and high solute volatility and to check if the single cell technique works just as well as the DCT, it was used to determine limiting activity coefficients at similar temperatures. The slopes obtained for the determination of γ^{∞} for such an analysis is shown in Figure 7-7.

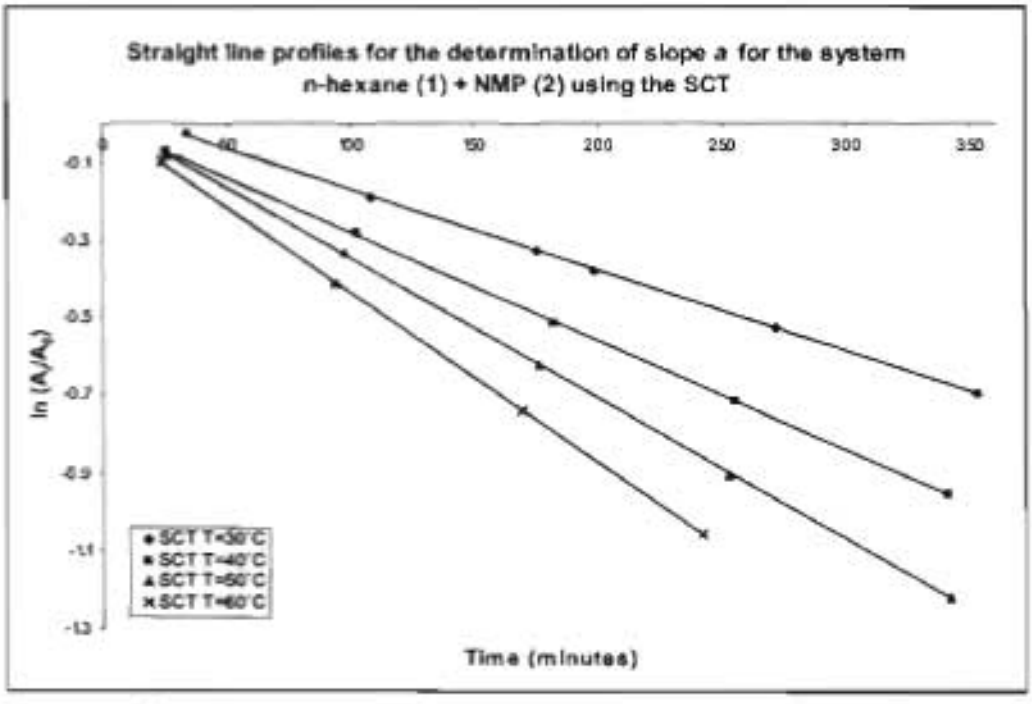

Figure 7-7: Plots for the determination of slopes *a*, for the evaluation of limiting activity coefficients using Equation 6.55 and for the SCT.

The slopes for the single cell technique have a similar trend to that for the double cell technique with the effect of temperature. The flow rates of inert gas for both techniques are similar and the limiting activity coefficients with their corresponding temperatures and flows are shown in Table 7-5.

Single Cell Technique		
D (ml/min)	T (°C)	$\gamma^{\infty}_{Experimental}$
20.23	30.15	12.69
20.62	39.93	11.55
20.64	50.23	10.64
19.38	60.62	9.89

Table 7-5: Limiting activity coefficients at different temperatures for the system n-hexane (1) + NMP (2) obtained using the SCT.

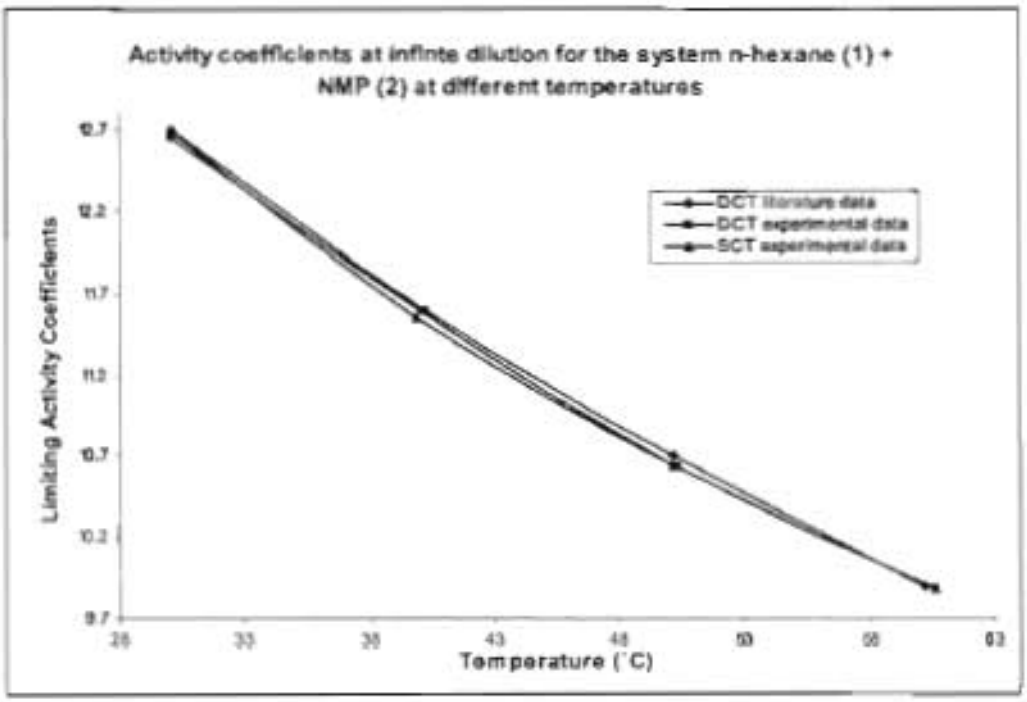

Figure 7-8: Activity coefficients at infinite dilution for the system n-hexane (1) + NMP (2) using the SCT and DCT, and compared to literature data for the DCT by Krummen et al. (2004).

The limiting activity coefficients determined using the SCT is similar to that for the DCT. This shows that the SCT works just as well as the DCT for systems where solvent volatility is low and solute volatility is high. The difference in the experimental values of γ^{∞} from published literature

values of Krummen et al. (2004) is shown in Figure 7-8. These graphs show how close the experimental results are in comparison to published literature data for the DCT.

Both techniques seem to work just as well and have deviations in γ^{∞} from each other and from literature values of less than 1 %. A sensitivity analysis was performed to check the effect small deviations in the measurable variables would have on the limiting activity coefficient. The results of this are discussed in Chapter 8. Systems involving n-hexene, o-cresol and NMP in different combinations were further attempted and the results of which can be found in Part 2 of Chapter 7. The next two sections deal with limiting activity coefficients calculated from equations proposed by other researchers using the same experimental data.

7.2 Limiting Activity Coefficients - Leroi et al. (1977), Duhem and Vidal (1978) and Boa and Han (1995)

In this section activity coefficients at infinite dilution were evaluated using Equations 6.23, 6.24, 6.29 and 6.33 which are the Leroi et al. (1977) based equations. They are used to evaluate limiting activity coefficient for the same test systems as above. All these equations were derived for the determination of limiting activity coefficients for use with the inert gas stripping technique by various researchers already mentioned. Limiting activity coefficients are evaluated for the test systems using the four equations and compared with γ_i^{∞} calculated from Equation 6.55 and the literature data of Krummen et al. (2004). Limiting activity coefficients as a result of different inert gas flow rates, evaluated using the four equations for the test system cyclohexane (1) + NMP (2) can be found in Table 7-6.

7.2.1 Results for the test system: cyclohexane (1) + NMP (2)

Experimental Conditions		Limiting Activity Coefficients Calculated Using Equation				
D (ml/min)	T (°C)	6.55	6.23	6.24	6.29	6.33
5.83	50.16	6.67	6.63	6.62	6.62	6.62
12.65	50.16	6.67	6.63	6.62	6.62	6.62
24.43	50.23	6.65	6.61	6.60	6.60	6.60
34.59	50.17	6.68	6.64	6.62	6.63	6.63
47.47	50.30	6.64	6.60	6.58	6.59	6.59

Table 7-6: Limiting activity coefficients at various inert gas flow rates and at constant temperature for the four Leroi et al. (1977) based equations.

Equations 6.23, 6.24, 6.29 and 6.33 predict limiting activity coefficients that are similar to that determined above using Equation 6.55. All the γ_i^∞ determined using the four Leroi et al. (1977) based equations are slightly lower than that determined by Equation 6.55 and the literature value of 6.7 at 50.2 °C by Krummen et al. (2004). The difference between the experimental γ_i^∞ is however not greater than 0.91 % and not greater than 1.79 % when compared to literature values. The nitrogen gas flow rate appears to have no significant affect on γ_i^∞ at the experimental conditions concerned. The effect temperature has on the γ_i^∞ for the system cyclohexane (1) + NMP (2), as predicted by the Equations 6.23, 6.24, 4.6 and 6.33, is shown in Table 7-7.

Experimental Conditions		Limiting Activity Coefficients Calculated Using Equation				
T (°C)	D (ml/min)	6.55	6.23	6.24	6.29	6.33
30.08	14.89	7.77	7.74	7.74	7.73	7.74
40.03	11.77	7.21	7.15	7.15	7.14	7.15
50.16	12.65	6.73	6.63	6.68	6.68	6.68
60.06	11.77	6.20	6.17	6.14	6.15	6.15

Table 7-7: Limiting activity coefficients calculated using Equations 6.23, 6.24, 6.29 and 6.33 for different temperatures and compared to limiting activity coefficients calculated using Equation 6.55, derived by Krummen et al. (2000).

The limiting activity coefficients calculated using Equations 6.23, 6.24, 6.29 and 6.33 have good agreement with each other and are all lower, although close to the literature values and to those values calculated using Equation 6.55. The greatest deviation in the calculated values from the four Leroi et al. (1977) based equations and Equation 6.55 is 1.48 %. Between the four equations themselves the deviation is only 0.75 %. A clearer indication of how close the values really are is shown in Figure 7-9.

Figure 7-9 shows that the limiting activity coefficients determined using the well known Equations 6.23 and 6.24 derived by Leroi et al. (1977) are very good. Even the simplest of the equations (Equation 6.23) gives values that are in good agreement with the more complex ones. Duhem and Vidal, and Boa and Han's slightly more complex equations (Equations 6.29 and 6.33) also give acceptable values for the system cyclohexane (1) + NMP (2). Equations 6.24 and 6.33 are for use with volatile solvents, but the results are as justifiable as the more appropriate Equations 6.23 and 6.29 which were derived specifically for non-volatile solvents. A non-volatile solvent is classified here as a solvent whose vapour pressure is less than 1 mmHg under all experimental temperatures and pressures of concern, which was true for all the solvents used.

If it is difficult to classify a solute as volatile or non-volatile; it would be safer to treat it as volatile and use Equations 6.24 and 6.33 for the determination of limiting activity coefficients. Using the non-volatile solvent Equations 6.23 and 6.29 for a volatile solvent would result in inaccurate activity coefficients. All equations work well here because all the solvents used are non-volatile in nature and have vapour pressures well below 1 mm Hg in the temperature region of interest.

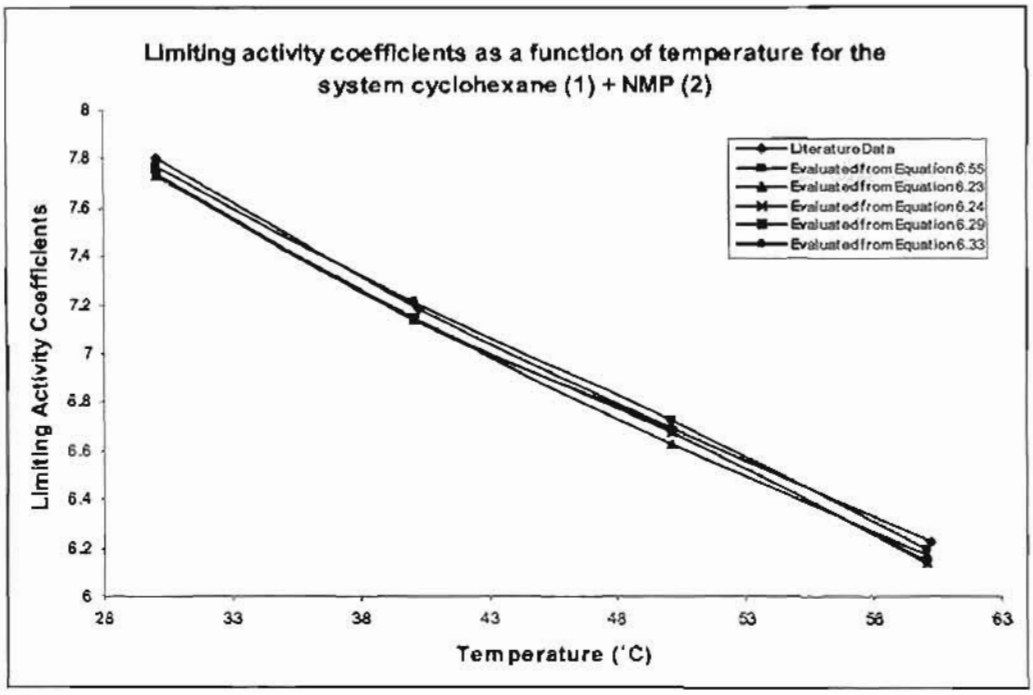

Figure 7-9: Comparison of all calculated activity coefficients at infinite dilution for the system cyclohexane (1) + NMP (2) with predetermined literature values.

Equations 6.23, 6.24, 6.29 and 6.33 are suited for systems with low solvent volatility and high solute volatility, as seen for the test system cyclohexane (1) + NMP (2). The next two test systems also confirm this. The system n-heptane (1) + NMP (2) is better suited for use with the IGS technique due to the highly reproducible data obtained. The calculated limiting activity coefficients are similar for all equations, some of which are shown in Table 7-8.

7.2.2 Results for test system: n-heptane (1) + NMP (2)

The results for this system are exceptional for all equations concerned. The deviation in reported limiting activity coefficients is less than 0.8 %.

Experimental Conditions		Limiting Activity Coefficients Calculated Using Equation				
D (ml/min)	T (°C)	6.55	6.23	6.24	6.29	6.33
11.06	30.12	14.92	14.89	14.88	14.88	14.89
11.13	39.83	13.72	13.68	13.67	13.67	13.68
11.08	50.51	12.43	12.38	12.35	12.36	12.36
11.46	60.19	11.46	11.42	11.37	11.40	11.39

Table 7-8: Limiting activity coefficients for the system *n*-heptane (1) + NMP (2) evaluated for different temperatures and constant nitrogen flow rate.

The maximum deviation in γ_i^{∞} from Equation 6.55 and all other calculated values for the system n-heptane in NMP is 0.8 %, for the same experimental conditions. There is excellent agreement between all five equations. The limiting activity coefficient values for a specific experimental condition in Table 7-8 do not differ by more than 0.43 % for the Leroi et al. (1977) based equations. The accuracy of the resulting γ_i^{∞} values can be seen in Figure 7-10.

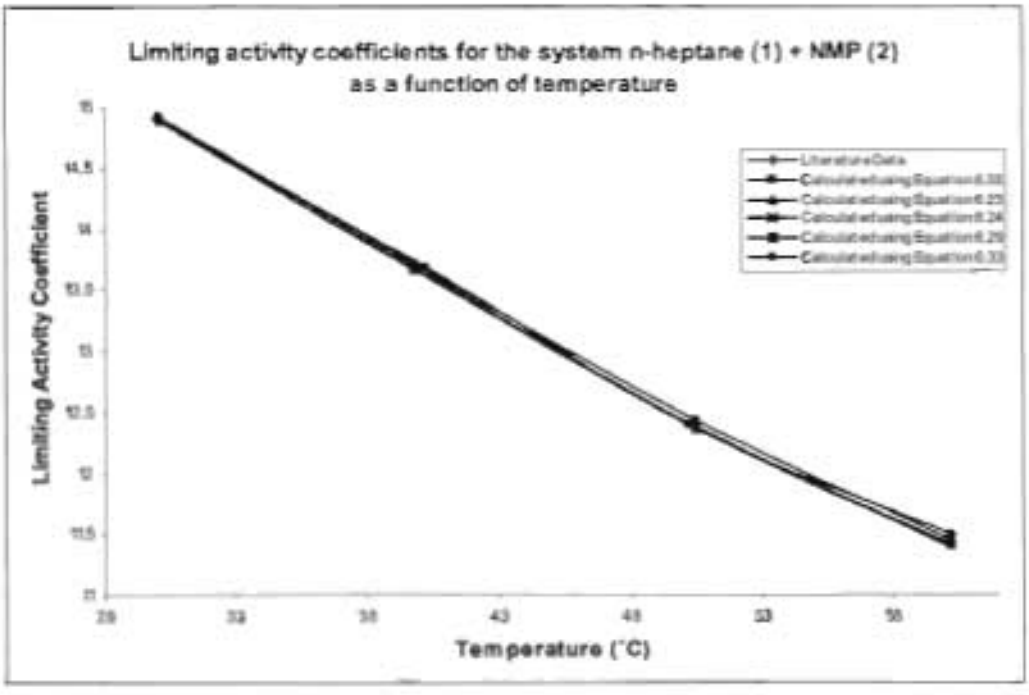

Figure 7-10: Comparison of limiting activity coefficients showing the accuracy of results at different temperatures for the system n-heptane (1) + NMP (2).

The limiting activity coefficients calculated here are in good agreement with literature values and with each other. So far, there is no reason to reject any equation as they all give reasonably accurate results. The next system under investigation was n-hexane (1) + NMP (2) where the DCT and the SCT was used. The DCT results are shown in Table 7-9 below.

7.2.3 Results for test system: n-hexane (1) + NMP (2)

Double Cell Technique						
Experimental Conditions		Limiting Activity Coefficients Calculated Using Equation				
D (ml/min)	T (°C)	6.55	6.23	6.24	6.29	6.33
19.42	30.13	12.65	12.56	12.55	12.55	12.56
19.91	40.12	11.59	11.48	11.46	11.46	11.47
19.95	50.34	10.64	10.52	10.49	10.51	10.51
19.93	60.61	9.88	9.74	9.68	9.71	9.70

Table 7-9: Limiting activity coefficients determined using the DCT for the system n-hexane (1) + NMP (2) at different temperatures and constant inert gas flow rates.

The limiting activity coefficients are in good agreement, but not as good as that for the system n-heptane (1) + NMP (2). This shows that the IGS method is system dependant and thus what works for one system may not work for another similar system. The calculated values of γ_i^∞ are acceptable as the maximum deviation between all γ_i^∞ at any experimental condition in Table 7-9 does not exceed 2 %. The maximum deviation between calculated γ_i^∞ using Equations 6.23, 6.24, 6.29 and 6.33 is 0.62 %. This is clearly seen in Figure 7-11.

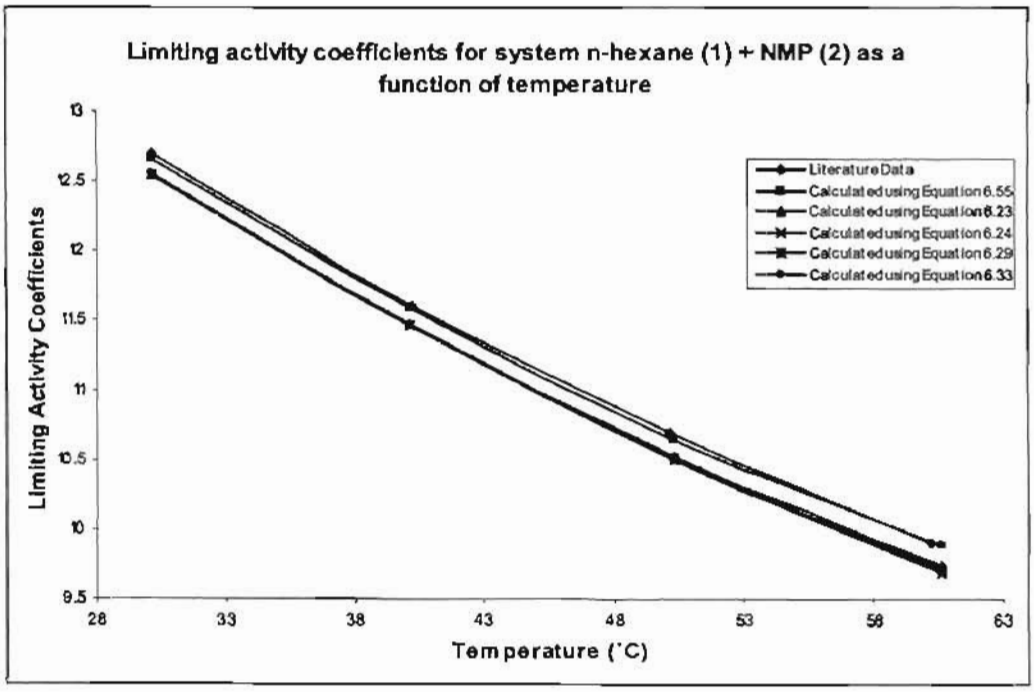

Figure 7-11: Comparison of all calculated limiting activity coefficients for the system n-hexane (1) + NMP (2) for different system temperatures.

The graphs show fairly good agreement within reasonable tolerance. There is a clear indication that Equation 6.55 predicts a slightly higher value for the limiting activity coefficient as can be seen by the clear segregation between the graphs in Figure 7-11. There is remarkable similarity between the γ_i^{∞} calculated from Equations 6.23, 6.24, 6.29 and 6.33. This could be due to the fact that a similar approach was taken in the derivation of these equations by the researchers Leroi et al., Duhem and Vidal and Boa and Han. The results for the SCT can be found below in Table 7-10.

Single Cell Technique						
Experimental Conditions		Limiting Activity Coefficients Calculated Using Equation				
D (ml/min)	T (°C)	6.55	6.23	6.24	6.29	6.33
20.23	30.15	12.69	12.60	12.59	12.59	12.60
20.62	39.93	11.55	11.44	11.43	11.43	11.44
20.64	50.23	10.64	10.51	10.48	10.50	10.49
19.38	60.62	9.89	9.74	9.69	9.71	9.70

Table 7-10: Limiting activity coefficients for the system n-hexane (1) + NMP (2) using the SCT at different system temperatures and relatively constant inert gas flow rates.

The single cell technique gives results similar to that of the double cell technique for this system. The maximum deviation in γ_i^{∞} from that calculated using Equation 6.55 is also 2 %, the same as that for the DCT. Due to the nature of the components both techniques work well giving accurate results. Equations 6.23, 6.24, 6.29 and 6.33 predicts γ_i^{∞} for the single cell technique just as accurately as that for the double cell technique. These equations predict limiting activity coefficients easily without the need for lengthy calculations as for Equation 6.55. The accuracy of the SCT results is shown in Figure 7-12.

It is important to note that the SCT is extremely sensitive to the nature of the solvent used. If the solvent is multi-component with at least two components having appreciably different volatilities these components will be stripped at different rates in the dilutor still. The concentration of the solvent mixture in the dilutor still will vary with time and thus the limiting activity coefficient will also vary with time. Even with a solvent mixture consisting of low volatility solvents such as o-cresol and NMP the effect on the limiting activity coefficient is significant. Evidence of this is shown in Chapter 8 with the system n-hexene (1) + 20 %($^m/_m$) o-cresol (2) + 80 %($^m/_m$) NMP (2).

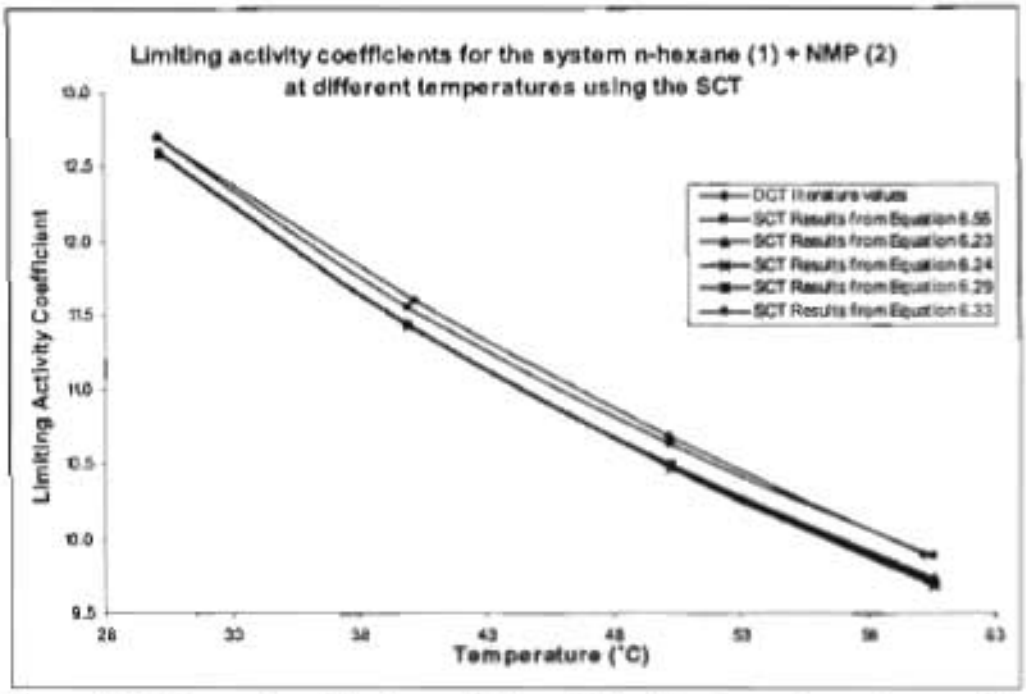

Figure 7-12: Comparison of limiting activity coefficients for the system n-hexane (1) + NMP (2) using the SCT at different temperatures and constant inert gas flow rates.

The accuracy seen between the five equations and the literature data of Krummen et al. (2004) calculated using Equation 6.55 is acceptable. The SCT results differ from the DCT results for the limiting activity coefficient by not more than 0.35 % for this binary system.

7.3 Limiting Activity Coefficients - Hovorka and Dohnal (1997)

In this last section the results for the equations proposed by Hovorka and Dohnal (1997) are reported. Hovorka and Dohnal (1997) proposed Equation 6.65 for the determination of limiting activity coefficients. The validity of the equation and the effect that flow rate and temperature has on systems with low solvent volatility and high solute volatility was investigated. Limiting activity coefficients for multi-component solvent systems using Equation 6.65 is investigated in Chapter 7 - Part 2. The effect that flow rate has on the system cyclohexane (1) + NMP (2) is shown in Table 7-11.

7.3.1 Results for test system: cyclohexane (1) + NMP (2)

Clearly the results thus far show negligible effect of flow rate on the limiting activity coefficient as long as equilibrium conditions are maintained in the cell. Errors in the reading of the flow rate will however have a significant effect on the γ_i^{∞} as determined by sensitivity analysis in Chapter 8.

Experimental Conditions		γ_{sol}^{∞}	Correction Factors				$\gamma_{sol}^{\infty,II}$
D (ml/min)	T (°C)		k_1	k_2	k_3	k_4	
5.83	50.16	6.61	0.998	1	1.000	1.005	6.63
12.65	50.16	6.61	0.998	1	1.001	1.005	6.63
24.43	50.23	6.59	0.998	1	1.000	1.005	6.62
34.59	50.17	6.62	0.998	1	1.000	1.005	6.64
47.47	50.30	6.58	0.998	1	1.000	1.005	6.60

Table 7-11: Limiting activity coefficients for the system cyclohexane (1) + NMP (2) using the DCT at a temperature of approximately 50 °C and at flow rates between 5 and 48 ml/min. Also shown are values for the correction factors (k_i).

γ_{sol}^{∞} **and** $\gamma_{sol}^{\infty,II}$ are evaluated using Equations 6.64 and 6.65 respectively. The correction factors except for k_2 are evaluated from Equations 6.67, 6.70 and 6.71. Flow rate does not seem to have an effect on the limiting activity coefficient in the range of interest. The difference between the largest and lowest limiting activity coefficient is 0.6 %, but in the chosen flow rate range of 10 to 30 ml/min it is only 0.3 %. The limiting activity coefficients determined using Equation 6.65 are similar to the values determined in the other sections. The correction factors (k_i) are very close to 1 indicating that the system is well suited to the IGS technique and that ideal conditions are maintained in the cells. The ability of Equation 6.65 to predict limiting activity coefficients at different temperatures and constant flow rate is investigated below.

Experimental Conditions		γ_{sol}^{∞}	Correction Factors				$\gamma_{sol}^{\infty,II}$
T (°C)	D (ml/min)		k_1	k_2	k_3	k_4	
30.08	14.89	7.73	0.999	1	1.000	0.993	7.68
40.03	11.77	7.14	0.998	1	1.000	0.999	7.12
50.16	12.65	6.67	0.998	1	1.001	1.005	6.69
60.06	11.77	6.13	0.997	1	1.001	1.013	6.20

Table 7-12: Limiting activity coefficients as a function of temperature for the system cyclohexane (1) + NMP (2) using the DCT.

A clear observation between the limiting activity coefficients of Equation 6.65 and those of the Leroi et al. based equations is that at the higher temperatures Equation 6.65 gives values that are closer to the literature values determined by Krummen et al. (2004). The correction factor k_1 decreases with increasing temperature and k_4 increases with increasing temperature while k_3 remains fairly constant. The correction factor k_2 is not affected by temperature at this stage

due to the pre-saturator in place. Equation 6.65 is well suited for the determination of γ_i^{∞} for the system cyclohexane (1) + NMP (2). The accuracy of the results is shown in Figure 7-13.

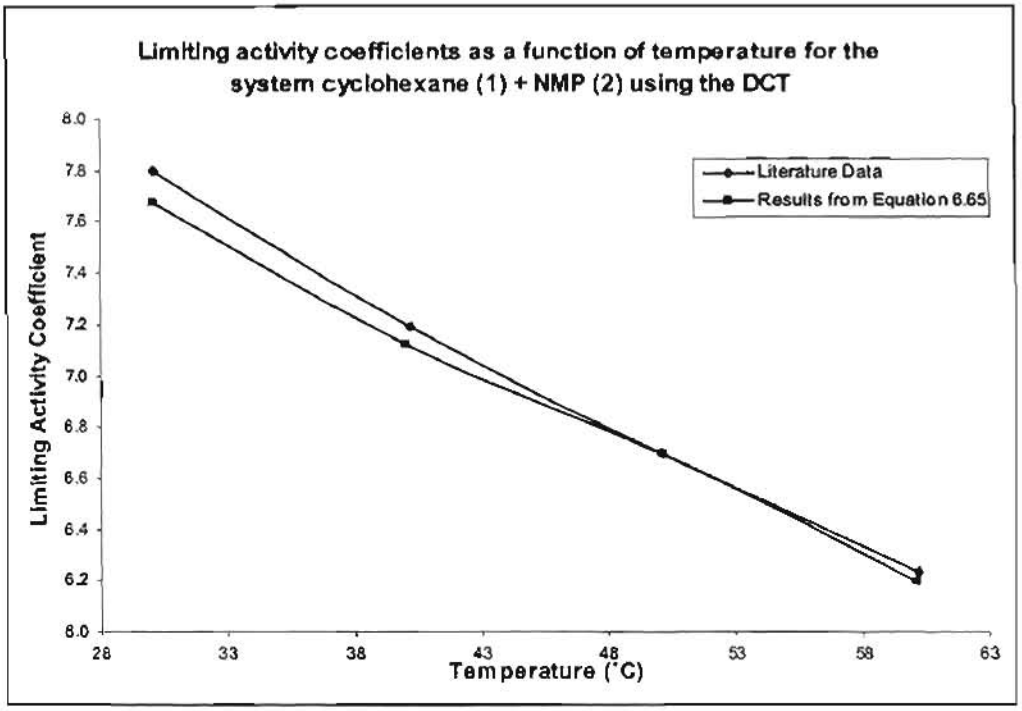

Figure 7-13: Comparison of literature values for limiting activity coefficients with those determined from Equation 6.65 for the system cyclohexane (1) + NMP (2) using the DCT.

There is a slight deviation between the graphs at the lower temperatures; however this deviation is not greater than 1.54 %. The second test system under investigation was n-heptane (1) + NMP (2) and the results of the investigation are shown below in Table 7-13.

7.3.2 Results for test system: n-heptane (1) + NMP (2)

Experimental Conditions		γ_{sol}^{∞}	Correction Factors				$\gamma_{sol}^{\infty,II}$
D (ml/min)	T (°C)		k_1	k_2	k_3	k_4	
11.06	30.12	14.88	0.999	1	1.001	0.988	14.69
11.13	39.83	13.66	0.998	1	1.001	0.993	13.55
11.08	50.51	12.34	0.998	1	1.001	1.000	12.32
11.46	60.19	11.36	0.996	1	1.001	1.003	11.37

Table 7-13: Limiting activity coefficients for the system n-heptane (1) + NMP (2) determined using the DCT and evaluated using Equation 6.65 at constant flow rates and different temperatures

The correction factors display a similar trend for this system as for the system cyclohexane (1) + NMP (2), but the limiting activity coefficient values are lower than the literature values determined by Krummen et al. (2004), as shown in Figure 7-14.

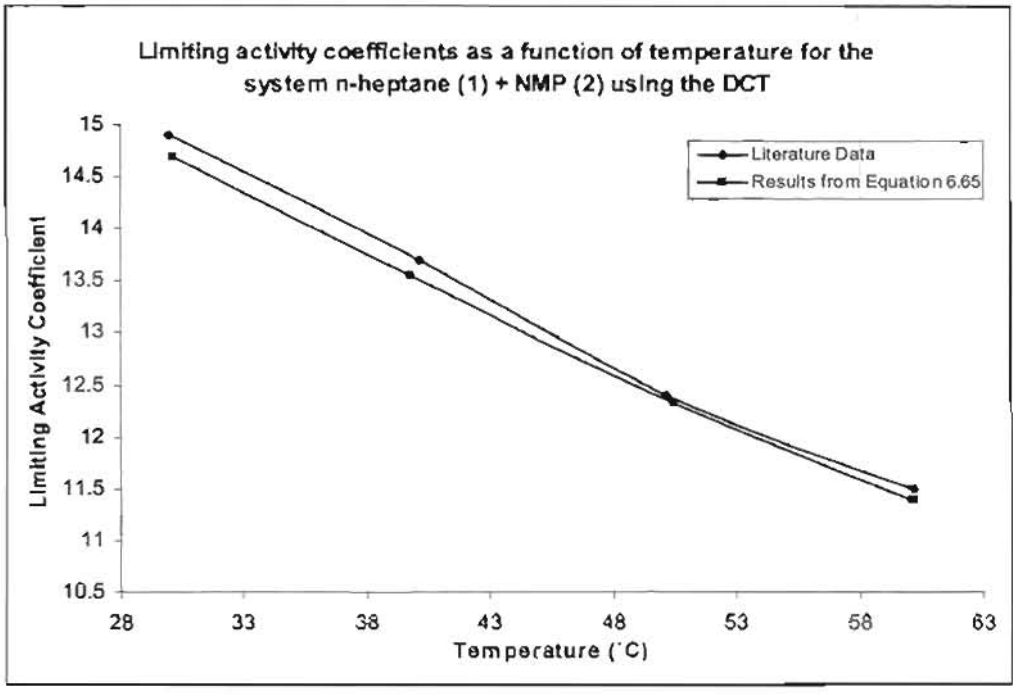

Figure 7-14: Comparison of limiting activity coefficients of Equation 6.65 with literature values for the system n-heptane (1) + NMP (2) using the DCT at constant flow rate.

The limiting activity coefficients evaluated using Equation 6.65 all lie lower than their literature values, but have a better trend line with regards to temperature than the literature values. The graph shows a distinct inverse relationship of limiting activity coefficient and temperature with a smooth trend line. There is some agreement between the literature γ_i^{∞} and the experimental γ_i^{∞} calculated using Equation 6.65 at 50 °C. At this point the limiting activity coefficients obtained using Equation 6.65 may give a better representation of the actual values due to the smooth curve formed as apposed to the dip in the curve at 50 °C for the literature data. The third test system under investigation is n-hexane (1) + NMP (2) and the limiting activity coefficients are found in Table 7-14 for the DCT.

7.3.3 Results for test system: n-hexane (1) + NMP (2)

Double Cell Technique							
Experimental Conditions		γ_{sol}^{∞}	Correction Factors				$\gamma_{sol}^{\infty,II}$
D (ml/min)	T (°C)		k_1	k_2	k_3	k_4	
19.42	30.13	12.55	0.998	1	1.000	1.000	12.54
19.91	40.12	11.46	0.996	1	1.001	1.008	11.53
19.95	50.34	10.48	0.997	1	1.002	1.018	10.66
19.93	60.61	9.68	0.994	1	1.003	1.029	9.93

Table 7-14: Limiting activity coefficients calculated from Equation 6.65 for the system n-hexane (1) + NMP (2) using the DCT at constant inert gas flow rates and temperatures.

There is greater deviation for the correction factors from their ideal value of 1 at higher temperatures. This means that there is a greater deviation from ideal conditions at higher temperatures. The correction factors thus, give rise to limiting activity coefficients that are probably more accurate than those calculated in the previous sections from the other equations. The other equations only take some of these corrections into account in their derivation. This is the only equation (Equation 6.65) that accounts for every possible non-ideality or deviation encountered thus far.

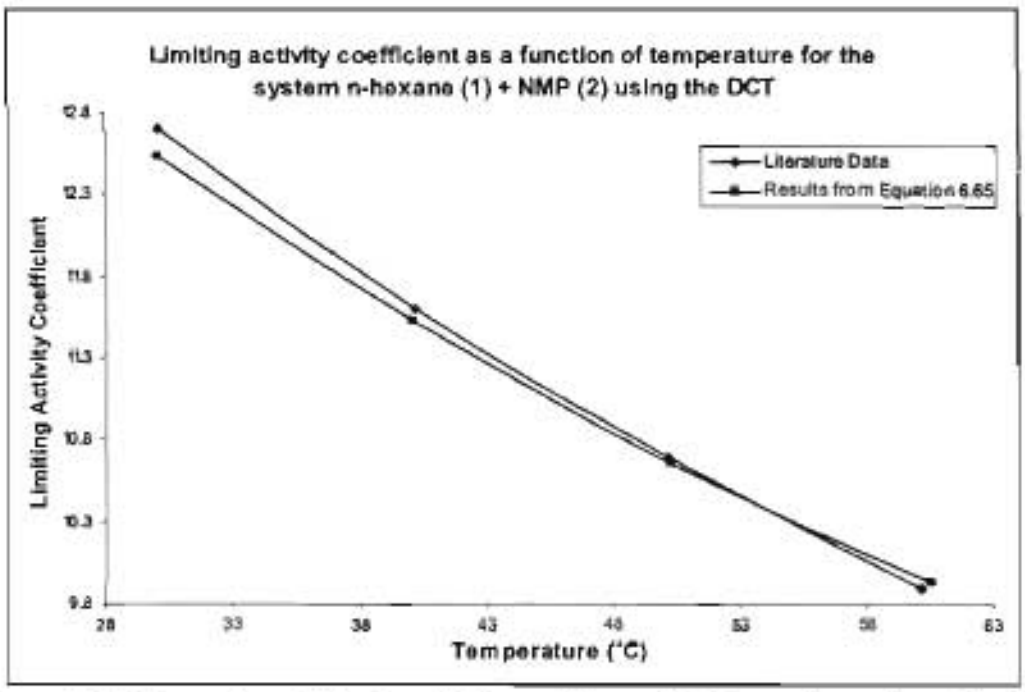

Figure 7-15: Comparison of literature limiting activity coefficients and experimental values for the system n-hexane (1) + NMP (2) using the DCT at constant inert gas flow rate.

Equation 6.65 seems to under-predict limiting activity coefficients at low temperatures and over-predicts it at higher temperatures when compared to literature values determined by Krummen et al. (2004). The trend line produced is still a smooth curve. Equation 6.65 is well suited for the prediction of limiting activity coefficients using the DCT. The deviation from literature values of Krummen et al. (2004) is less than 1.3 %. Equation 6.65 can also be used to predict limiting activity coefficients for the SCT as shown in Table 7-15.

Single Cell Technique							
Experimental Conditions		γ_{2e}^{∞}	Correction Factors				$\gamma_{2e}^{\infty,II}$
D (ml/min)	T (°C)		k_1	k_2	k_3	k_4	
20.23	30.15	12.60	0.998	1.000	1.001	1.000	12.58
20.62	39.93	11.44	0.996	1.000	1.001	1.008	11.50
20.64	50.23	10.51	0.994	1.000	1.001	1.018	10.64
19.38	60.62	9.74	0.990	1.000	1.001	1.029	9.93

Table 7-15: Limiting activity coefficients for the system *n*-hexane (1) + NMP (2) using the SCT at a constant flow rate and at different temperatures.

The correction factor k_2 accounts for the change of stripping gas flow rate due to saturation in the cell. There seems to be no significant change in the stripping gas flow rate due to saturation. This is expected as the solvent (NMP) volatility is very low (less than 1 mm Hg). The effect the SCT has on the limiting activity coefficients is shown in Figure 7-16 together with a comparison to literature values for the DCT and experimental values calculated using Equation 6.65 for the DCT.

Figure 7-16 shows how close the calculated limiting activity coefficients are for the SCT and the DCT. A comparison to literature values obtained using the DCT (Krummen et al. (2004)) is also depicted in Figure 7-16. There is remarkable consistency between the two techniques (DCT and SCT) for the system *n*-hexane (1) + NMP (2) in terms of the calculated limiting activity coefficients. The SCT can be used instead of the DCT for systems where the solvent volatility is low and solute volatility is high to save on costs, as some chemicals may be extremely expensive at the high purities required for the IGS technique. There is a maximum deviation in limiting activity coefficients of 0.4 % for the two techniques and this deviation decreases as system temperature increases.

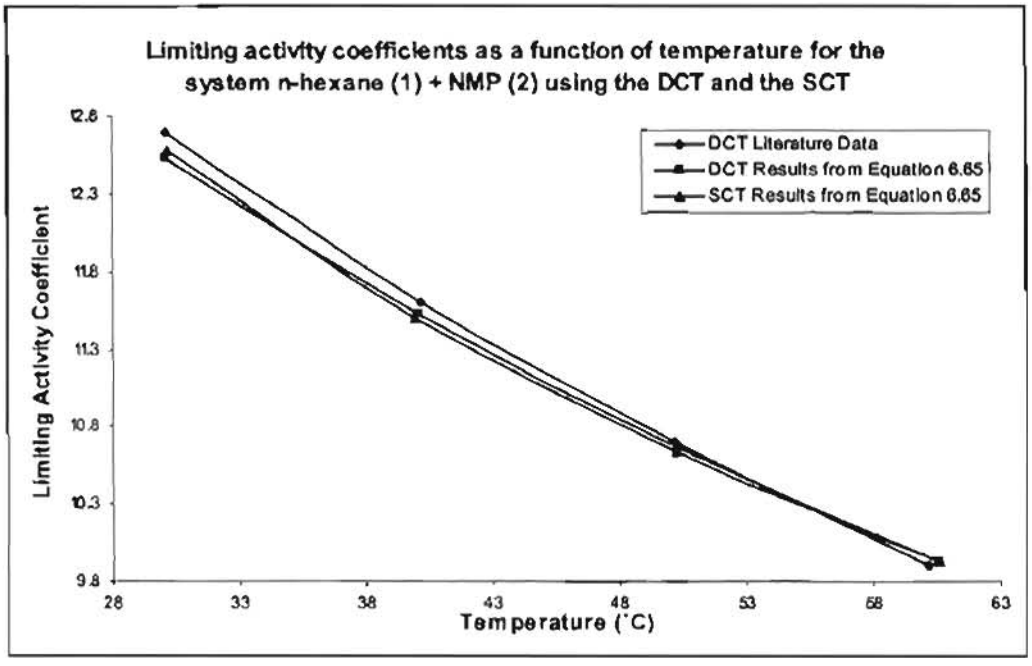

Figure 7-16: Comparison of limiting activity coefficients calculated using Equation 6.65 for the DCT and SCT with literature values for the system n-hexane (1) + NMP (2) at constant inert gas flow rates.

Chapter VII – Experimental Results

Part II: New Systems

The positive conclusions drawn from the test systems show that the newly designed equipment works well and is suitable for the determination of limiting activity coefficients for binary systems. The various equations used to determine limiting activity coefficients predict values that agree with each other and with the literature values where possible within certain tolerances. Limiting activity coefficients play a major role in accounting for the non-ideality that certain chemicals experience in relation to their surroundings and their accuracy must be extremely high. The equations used must predict limiting activity coefficients with a maximum error of 1 % when compared to literature values and with each other.

A more demanding task than evaluating limiting activity coefficients for binary systems is evaluating it for ternary systems and higher order systems. The challenge here is getting good separation in the GC column for all components and maintaining a constant solvent concentration in the dilutor cell. The solute limiting activity coefficient changes as the solvent concentration changes, especially for multi-component solvent systems. A way of working around this is to always use the DCT. The SCT will also work with systems of extremely low solvent volatility.

This chapter deals with the evaluation of limiting activity coefficients for the ternary system n-hexene (1) + NMP (2) + o-cresol (2) for which there are no published limiting activity coefficient data using the IGS method at the conditions of interest. NMP and o-cresol make up the solvent, and the limiting activity coefficient is evaluated for different concentrations of NMP and o-cresol using the various equations derived by researchers in the previous few chapters. The different concentrations involve mass percentages of o-cresol in NMP between 0 and 100 % in multiples of 20. Two of these percentages (0 and 100%) result in binary systems. These two systems are n-hexene (1) + NMP (2) and n-hexene (1) + o-cresol (2).

The n-hexene (1) + NMP (2) system has been investigated before by Krummen et al. (2004) at different experimental conditions from those in this study. Experiments on this system have been repeated for completeness rather than using the available literature values. The other binary system has no published data to date for limiting activity coefficients using the IGS technique. The results for the binary systems are shown first, followed by the results for the ternary

systems, for each equation used to determine the limiting activity coefficient. All experiments were repeated for four different temperatures and three different inert gas flow rates.

7.4 System - n-hexene (1) + NMP (2)

Limiting activity coefficients were evaluated at three different flow rates for this system i.e. 10, 20 and 30 ml/min and at four different temperatures 35, 45, 55 and 65 °C using the DCT. The results for the equation proposed by Krummen et al. (2000) (Equation 6.55) is shown in Table 7-16 for the system n-hexene (1) + NMP (2).

7.4.1 Results for Equation 6.55

Literature Data		Experimental Data		$\gamma^{\infty}_{experiment}$
T (°C)	$\gamma^{\infty}_{Literature}$	D (ml/min)	T (°C)	
30.1	6.46	10.13	35.02	6.28
40.2	6.12	10.12	45.01	5.97
50.2	5.84	10.01	55.03	5.68
60.2	5.56	10.00	64.98	5.41
		20.07	35.01	6.27
		20.16	45.00	5.99
		20.22	55.00	5.71
		20.06	65.00	5.44
		29.99	34.99	6.30
		29.82	45.01	6.01
		29.48	55.03	5.70
		29.90	64.98	5.42

Table 7-16: Limiting activity coefficients obtained using the DCT for the binary system n-hexene (1) + NMP (2).

It is clear, as a confirmation of the assumption that the method is based on, that flow rate does not have a significant effect on the limiting activity coefficient as long as equilibrium conditions remain in the cell. The maximum deviation for limiting activity coefficients in the region 10 to 30 ml/min is 0.7 %. The experiments were done at different temperatures from the literature values in order to maintain consistency with the o-cresol systems as o-cresol is a solid at temperatures lower than 32 °C at 99.5 % purity. The accuracy of the results can be seen in Figure 7-1 when compared to the literature data.

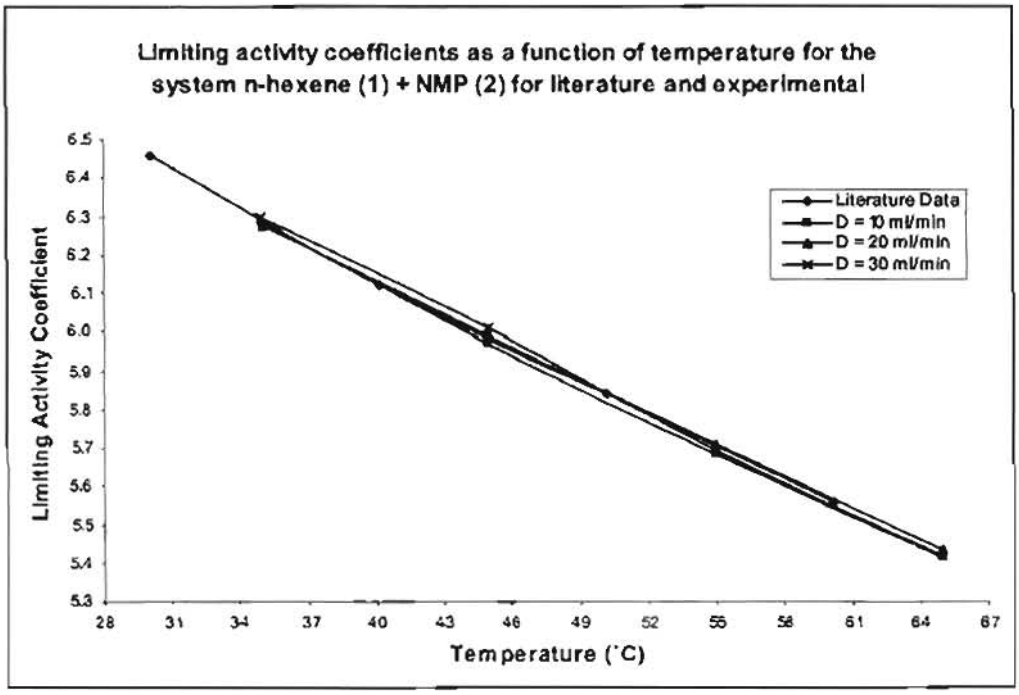

Figure 7-17: Comparison of literature and experimental limiting activity coefficients for the system n-hexene (1) + NMP (2).

The experimental limiting activity coefficients agree strongly with the literature values determined by Krummen et al. (2004). There is a maximum deviation that is less than 1 % for all values.

7.4.2 Results for Equations 6.23, 6.24, 6.29 and 6.33

This section reports limiting activity coefficients for the system n-hexene (1) + NMP (2) obtained by using the Leroi et al. (1977) based equations. The results for the four equations are compared against each other and with the literature values from above. The limiting activity coefficients evaluated for a flow rate of 10 ml/min and for the four different temperatures are shown in Table 7-17.

Experimental Conditions		Limiting Activity Coefficients Calculated Using Equation			
D (ml/min)	T (°C)	6.23	6.24	6.29	6.33
10.13	35.02	6.22	6.22	6.21	6.22
10.12	45.01	5.90	5.89	5.89	5.89
10.01	55.03	5.59	5.58	5.58	5.58
10.00	64.98	5.31	5.28	5.30	5.29

Table 7-17: Limiting activity coefficients for the n-hexene (1) + NMP (2) system evaluated at a constant flow rate of approximately 10 ml/min.

A comparison of this data with literature data can be found in Figure 7-18.

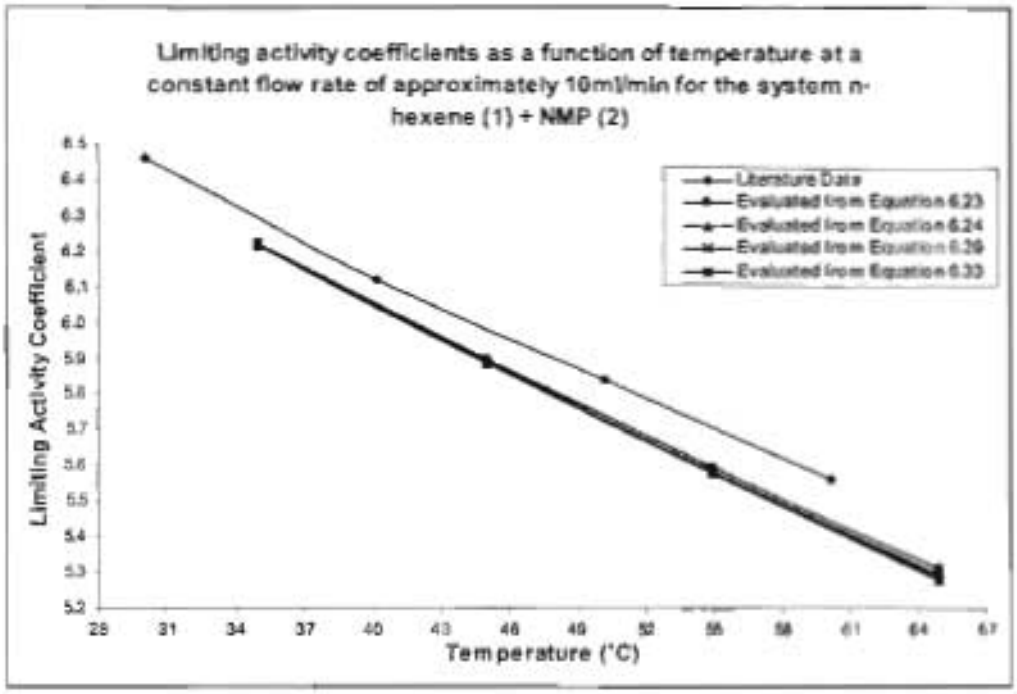

Figure 7-18: Comparison of experimental limiting activity coefficients with literature values for the system n-hexene (1) + NMP (2).

The limiting activity coefficients evaluated at a flow rate of approximately 20 ml/min and at different temperatures for the system n-hexene (1) + NMP (2) can be found in Table 7-18.

Experimental Conditions		Limiting Activity Coefficients Calculated Using Equation			
D (ml/min)	T (°C)	6.23	6.24	6.29	6.33
20.07	35.01	6.21	6.21	6.21	6.21
20.16	45.00	5.92	5.91	5.91	5.91
20.22	55.00	5.62	5.60	5.61	5.61
20.06	65.00	5.34	5.35	5.37	5.36

Table 7-18: Limiting activity coefficients at a constant flow of 20 ml/min and at four different temperatures for the system n-hexene (1) + NMP (2).

Comparison of the limiting activity coefficient data with literature values determined by Krummen et al. (2004) is shown in Figure 7-19 below.

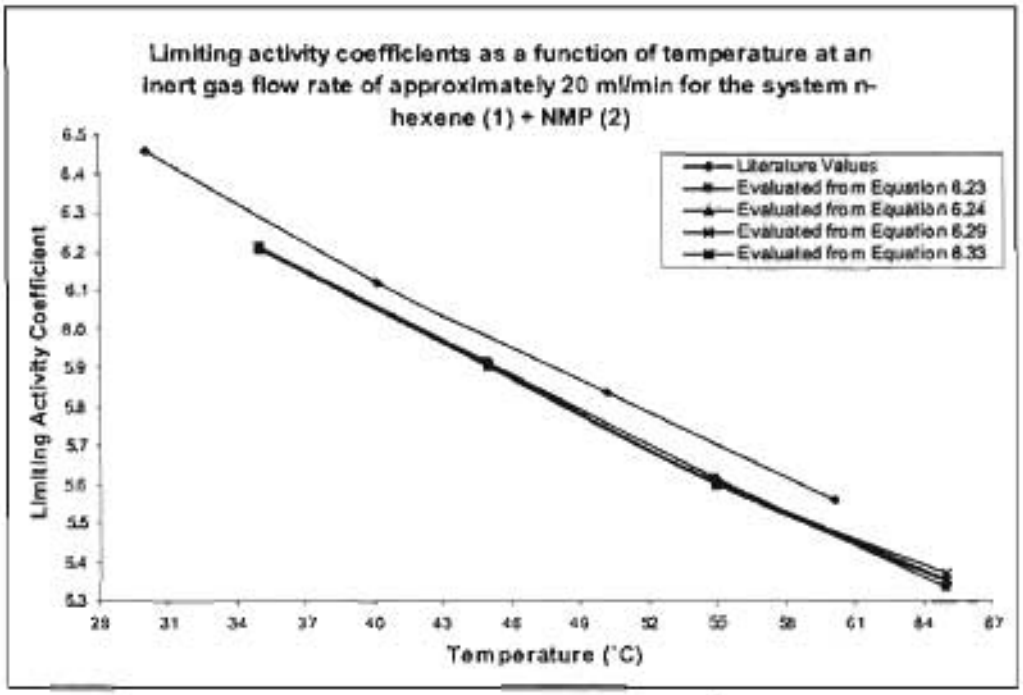

Figure 7-19: Comparison of experimental limiting activity coefficients with literature values for the system n-hexene (1) + NMP (2).

Limiting activity coefficients for the system n-hexene (1) + NMP (2) at a constant flow rate of 30 ml/min and at four different temperatures can be found in Table 7-19.

Experimental Conditions		Limiting Activity Coefficients Calculated Using Equation			
D (ml/min)	T (°C)	6.23	6.24	6.29	6.33
29.99	34.99	6.24	6.23	6.23	6.24
29.82	45.01	5.94	5.93	5.93	5.93
29.48	55.03	5.61	5.59	5.60	5.59
29.90	64.98	5.32	5.28	5.31	5.29

Table 7-19: Limiting activity coefficients for the system n-hexene (1) + NMP (2) for 30 ml/min and at four different temperatures.

A comparison of experimental values at 30 ml/min with literature values can be found in Figure 7-20. This figure shows the accuracy and precision of the results. Precision refers to how close the limiting values evaluated from the different equations are to each other for the same experimental conditions.

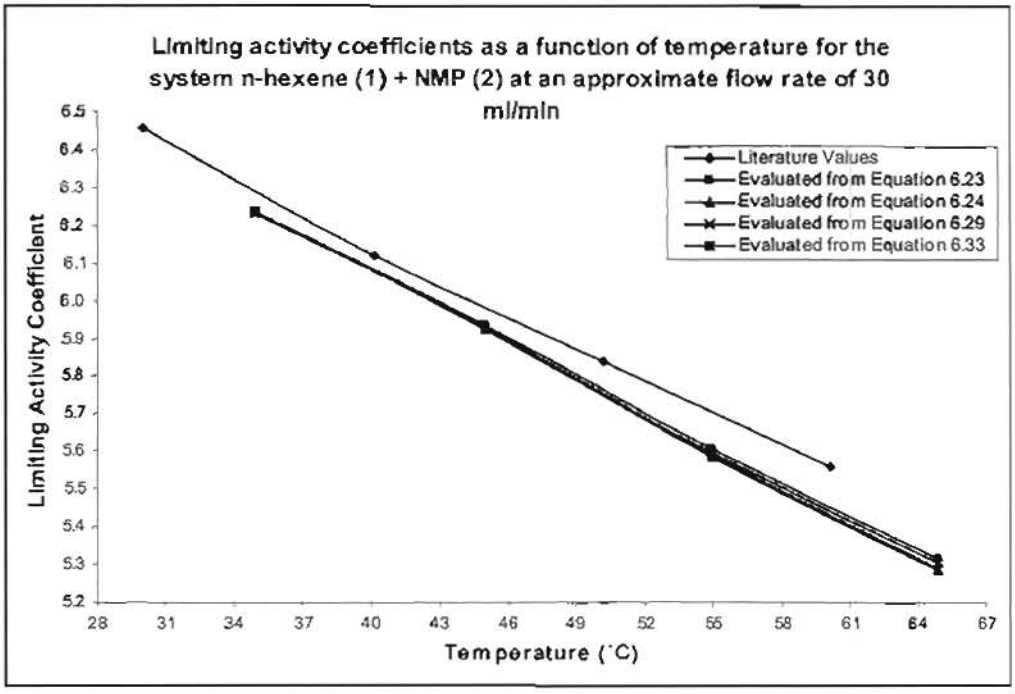

Figure 7-20: Comparison of literature and experimental limiting activity coefficients for the system n-hexene (1) + NMP (2) at a constant flow rate of 30 ml/min.

The limiting activity coefficients evaluated from Equations 6.23, 6.24, 6.29 and 6.33 all agree with each other, with a maximum deviation of 0.65 % for any set condition. These values are however lower than the values determined using Equation 6.55 and lower than the literature values. The difference in limiting activity coefficients evaluated from the Leroi et al. (1977) based equations and that of Equation 6.55 is small and lies within an acceptable range within certain tolerances.

7.4.3 Results for Equation 6.65

The limiting activity coefficients evaluated using Equation 6.65 is closer to literature values than the limiting activity coefficients evaluated using any of the other equations. Since the DCT technique was used the correction factor k_2 is always 1. The other correction factors seem to account more for the non-ideality of this system. Equation 6.65 seems to give better estimates of the limiting activity coefficient at higher temperatures when compared to literature data. The limiting activity coefficients as a result of Equation 6.65 can be found in Table 7-20.

Experimental Conditions		γ_{sol}^{∞}	Correction Factors				$\gamma_{sol}^{\infty,II}$
D (ml/min)	T (°C)		k_1	k_2	k_3	k_4	
10.13	35.02	6.21	0.998	1	1.001	1.008	6.25
10.12	45.01	5.88	0.997	1	1.001	1.017	5.97
10.01	55.03	5.57	0.996	1	1.001	1.028	5.71
10.00	64.98	5.27	0.993	1	1.001	1.040	5.45
20.07	35.01	6.21	0.998	1	1.001	1.008	6.25
20.16	45.00	5.90	0.997	1	1.001	1.017	5.99
20.22	55.00	5.60	0.997	1	1.001	1.028	5.74
20.06	65.00	5.34	0.991	1	1.001	1.040	5.52
29.99	34.99	6.23	0.998	1	1.001	1.008	6.27
29.82	45.01	5.92	0.997	1	1.001	1.017	6.01
29.48	55.03	5.58	0.997	1	1.001	1.028	5.73
29.90	64.98	5.28	0.992	1	1.001	1.040	5.46

Table 7-20: Limiting activity coefficients evaluated using Equation 6.65 for the system n-hexene (1) + NMP (2) using the IGS technique at different inert gas flow rates and temperatures.

A comparison of the new values of limiting activity coefficients for the three flows and four temperatures, with the literature values of Krummen et al. (2004) is shown in Figure 7-21 below.

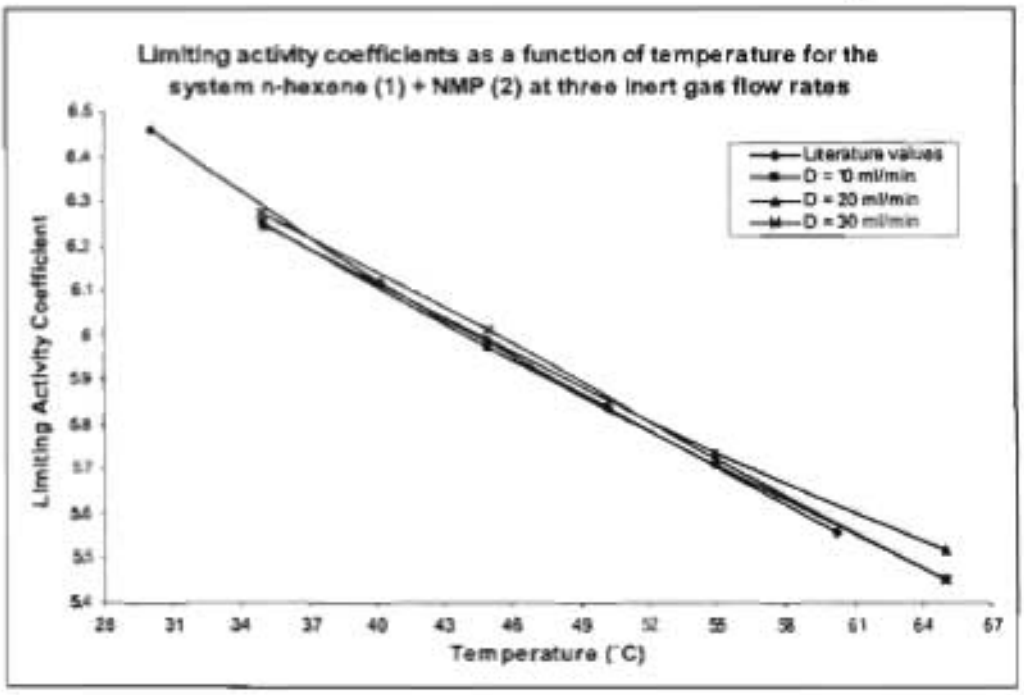

Figure 7-21: Comparison of literature data with limiting activity coefficients evaluated using Equation 6.65 for the system n-hexene (1) + NMP (2).

The inert gas stripping technique is able to accurately determine activity coefficients at infinite dilution for the system n-hexene (1) + NMP (2). The calculated limiting activity coefficients agree strongly with the already published literature data of Krummen et al. (2004). The next system under investigation has no limiting activity coefficient data available for the inert gas stripping technique to date. The system n-hexene (1) + o-cresol (2) has never been attempted using the inert gas stripping technique.

7.5 System - n-hexene (1) + o-cresol (2)

The chemical o-cresol is extremely dangerous at high purity and one must follow all the safely procedures when working with this chemical. The material safety data sheet (MSDS) must be obtained and read before working with o-cresol. The o-cresol vapours are extremely dangerous and can cause all kinds of respiratory problems and organ failures at very low concentrations in air if inhaled for a prolonged period of time.

7.5.1 Results for Equation 6.55

The proposed equation by Krummen et al. (2000) was used in order to determine limiting activity coefficients and the results tabulated below.

Experimental Data		$\gamma^{\infty}_{experiment}$
D (ml/min)	T (°C)	
10.01	34.99	5.68
9.95	45.00	5.22
9.91	54.97	4.91
10.01	64.95	4.74
19.44	34.98	5.66
19.23	45.03	5.22
19.97	55.02	4.92
19.66	65.02	4.73
29.79	34.98	5.68
29.43	45.01	5.23
30.08	54.99	4.92
29.96	64.98	4.75

Table 7-21: Limiting activity coefficients evaluated using Equation 6.55 for the system n-hexene (1) + o-cresol (2) at different flow rates and temperatures.

The assumption based on the method that inert gas flow rate does not seem to have a significant effect on the limiting activity coefficient for the system n-hexene (1) + o-cresol (2) is confirmed, however, as temperature increases the limiting activity coefficient decreases. This was also observed previously with the other systems studied. The effect of temperature on the limiting activity coefficient can be clearly seen in Figure 7-22.

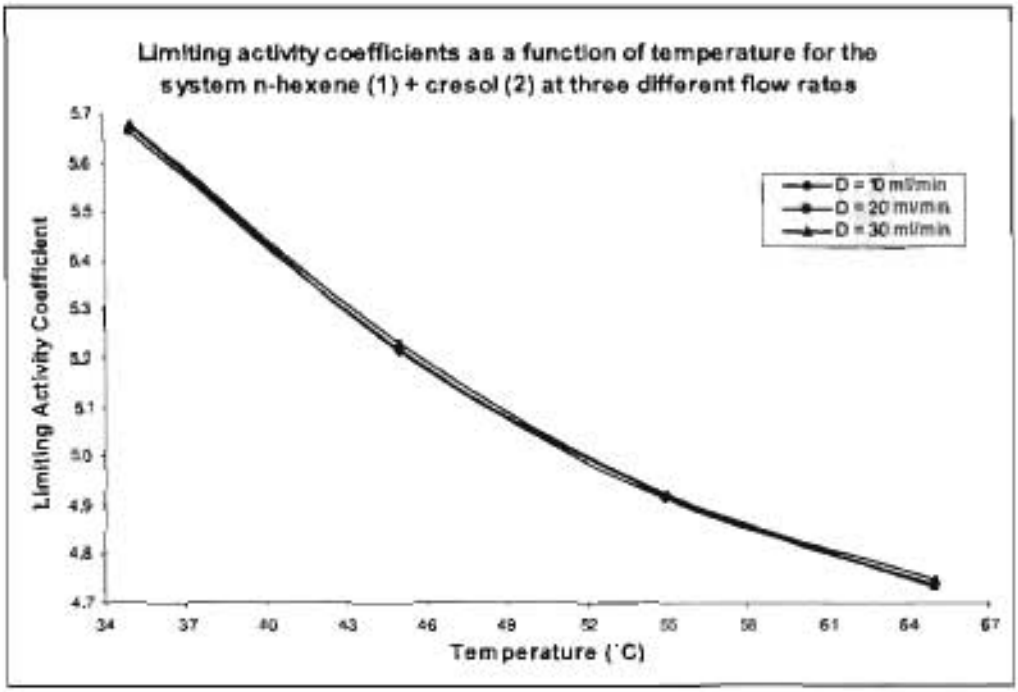

Figure 7-22: Comparison of limiting activity coefficients at three different flow rates for the system n-hexene (1) + o-cresol (2).

The fact that flow rate does not significantly effect the limiting activity coefficient (as seen in Figure 7-22) implies that equilibrium is achieved and maintained within the cells. The limiting activity coefficients show excellent agreement for the three flow rates at corresponding temperatures. This implies that the experimental set-up gives results that are reproducible and repeating the experiment at three different temperatures serves as a check in order to ascertain as to whether the data obtained is reliable or not.

7.5.2 Results for Lerol et al. (1977) based equations.

Equations 6.23, 6.24, 6.29 and 6.33 are used for the evaluation of limiting activity coefficients in Tables 7-22 to 7-24. Each Table (7-22 to 7-24) has limiting activity coefficients and correction factors for a different inert gas flow rate, but at similar temperatures. Temperatures were

maintained within 0.1 degrees Celsius of their set point values. The results for a flow rate of 10 ml/min are found in Table 7-22.

Experimental Conditions		Limiting Activity Coefficients Calculated Using Equation			
D (ml/min)	T (°C)	6.23	6.24	6.29	6.33
10.01	34.99	5.62	5.62	5.61	5.62
9.95	45.00	5.15	5.14	5.15	5.15
9.91	54.97	4.84	4.82	4.83	4.83
10.01	64.95	4.66	4.62	4.64	4.63

Table 7-22: Limiting activity coefficients for the system n-hexene (1) + o-cresol (2) at an inert gas flow rate of approximately 10 ml/min and at different temperatures.

It is very difficult to get flow rates and temperatures at exactly the set-point value with the current experimental set-up and a slight deviation of no more than 0.1 °C for temperature and 0.8 ml/min for flow rate was observed from the set-point values. It has been established already as part of the assumption that the method is based on that flow rate does not seem to have an adverse effect on the limiting activity coefficient if equilibrium conditions are maintained in the cells and as long as the flow rate is constant throughout the experiment. It is therefore difficult to compare limiting activity coefficients without the aid of graphs for different but similar temperatures.

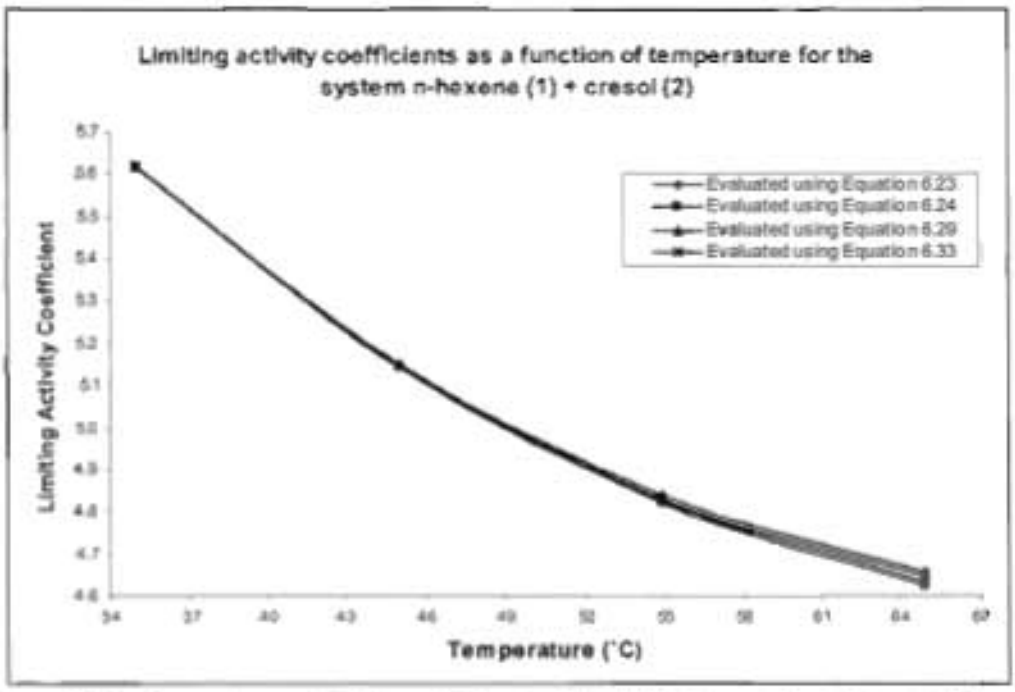

Figure 7-23: Comparison of limiting activity coefficients for the system n-hexene (1) + o-cresol (2) at an approximate inert gas flow rate of 10 ml/min.

Figure 7-23 compares the limiting activity coefficients evaluated using the Leroi et al. based equations at the exact same experimental conditions. There appears to be some disagreement between the limiting activity coefficients evaluated at 65 °C, but the deviation between the maximum and minimum value is only 0.85 %. This deviation is negligible and the data is reliable. The limiting activity coefficients for a flow of 20 ml/min are shown in Table 7-23.

Experimental Conditions		Limiting Activity Coefficients Calculated Using Equation			
D (ml/min)	T (°C)	6.23	6.24	6.29	6.33
19.44	34.98	5.61	5.61	5.60	5.61
19.23	45.03	5.15	5.15	5.15	5.15
19.97	55.02	4.84	4.83	4.84	4.83
19.66	65.02	4.65	4.61	4.63	4.62

Table 7-23: Limiting activity coefficients for the system n-hexene (1) + o-cresol (2) evaluated at a flow rate of approximately 20 ml/min.

The limiting activity coefficients evaluated using 6.23, 6.24, 6.29 and 6.33 at the constant flow rate of 20 ml/min is similar to those for a flow rate of 10 ml/min, as expected. A comparison for the limiting activity coefficients evaluated from the four equations for the system n-hexene (1) + o-cresol (2) is shown in Figure 7-24.

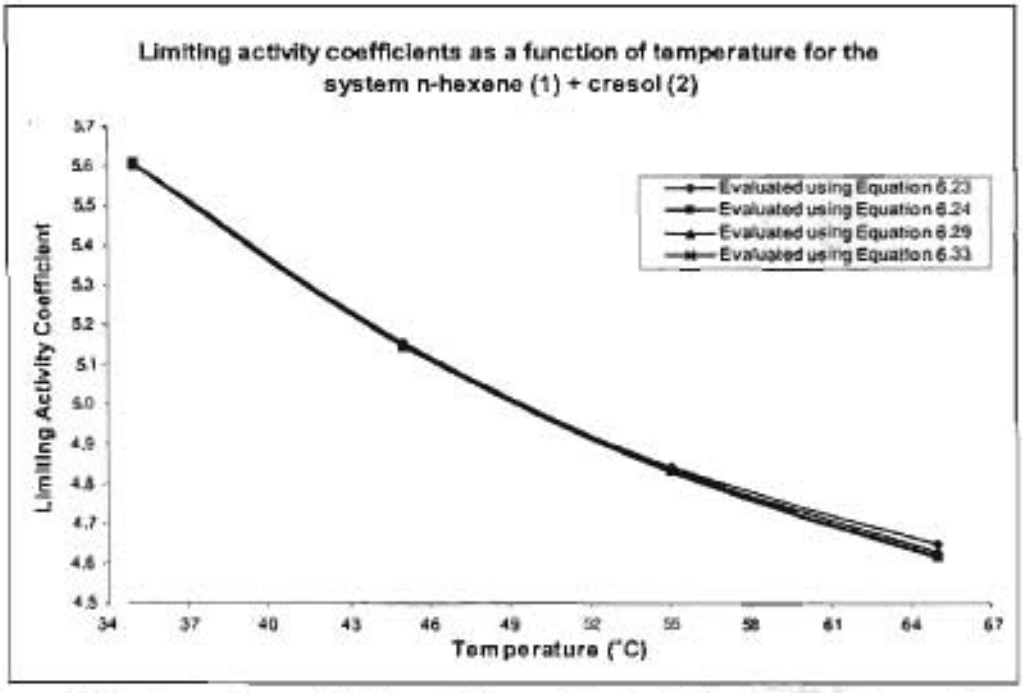

Figure 7-24: Comparison of limiting activity coefficients for the system n-hexene (1) + o-cresol (2) evaluated at a flow rate of approximately 20 ml/min.

The limiting activity coefficients evaluated at 65 °C have the largest deviation from each other when using the four Leroi et al. (1977) based equations. The deviation between the largest and smallest value of limiting activity coefficients is 0.86 %. Since there are no literature data available for this system the mean value of 4.63 should give an accurate estimation of its true value at 65 °C. This then gives a maximum deviation from the mean of 0.42 %. The limiting activity coefficients for a flow rate of 30 ml/min are shown in Table 7-24.

Experimental Conditions		Limiting Activity Coefficients Calculated Using Equation			
D (ml/min)	T (°C)	6.23	6.24	6.29	6.33
29.79	34.98	5.63	5.62	5.62	5.63
29.43	45.01	5.17	5.16	5.16	5.16
30.08	54.99	4.85	4.83	4.84	4.84
29.96	64.98	4.66	4.63	4.65	4.64

Table 7-24: Limiting activity coefficients for the system n-hexene (1) + o-cresol (2) at a flow rate of approximately 30 ml/min evaluated at different temperatures.

The accuracy of the equations in determining the limiting activity coefficients is shown in Figure 7-25 for the four temperatures.

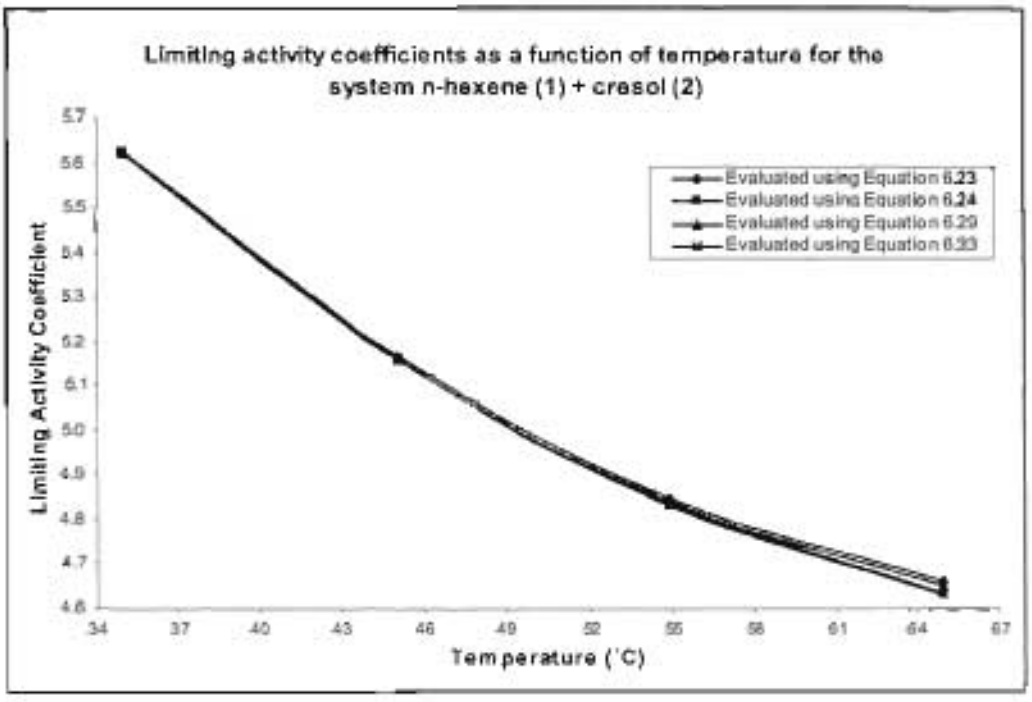

Figure 7-25: Comparison of limiting activity coefficients for the system n-hexene (1) + o-cresol (2) at 30 ml/min.

There is a maximum deviation of 0.34 % between the limiting activity coefficients for similar temperatures across the three flow rates and when compared to the same equation from which the activity coefficients were calculated. This shows that the data is reproducible when taking into account that flow rate does not affect the limiting activity coefficient as long as equilibrium is maintained in the cells.

7.5.3 Results for Equation 6.65

The limiting activity coefficients calculated using Equation 6.65 can be found in Table 7-25.

Experimental Conditions		γ_{sol}^{∞}	Correction Factors				$\gamma_{sol}^{\infty,II}$
D (ml/min)	T (°C)		k_1	k_2	k_3	k_4	
10.01	34.99	5.61	0.998	1	1.001	1.008	5.65
9.95	45.00	5.14	0.997	1	1.001	1.017	5.22
9.91	54.97	4.82	0.997	1	1.001	1.028	4.94
10.01	64.95	4.62	0.994	1	1.001	1.040	4.78
19.44	34.98	5.60	0.998	1	1.001	1.008	5.64
19.23	45.03	5.14	0.998	1	1.001	1.017	5.22
19.97	55.02	4.82	0.997	1	1.001	1.028	4.95
19.66	65.02	4.61	0.994	1	1.001	1.040	4.77
29.79	34.98	5.62	0.998	1	1.001	1.008	5.66
29.43	45.01	5.15	0.998	1	1.001	1.017	5.23
30.08	54.99	4.83	0.997	1	1.001	1.028	4.95
29.96	64.98	4.62	0.993	1	1.001	1.040	4.78

Table 7-25: Limiting activity coefficients for the system n-hexene (1) + o-cresol (2) evaluated using the equation proposed by Hovorka and Dohnal (1997) for different experimental conditions.

The limiting activity coefficients calculated from Equation 6.65 are similar to the values calculated using the equation proposed by Krummen et al. (2000) (Equation 6.55). There is a maximum deviation of 0.85 % between the limiting activity coefficients of Equation 6.65 and those of Equation 6.55. The limiting activity coefficients for 45 °C are identical to those calculated from Equation 6.55. The correction factors are all very close to unity. This means that under the experimental conditions chosen the system does not significantly deviate from ideal conditions. This was observed for all systems in this study. A comparison of the limiting activity coefficients for the three flows is shown in Figure 7-25.

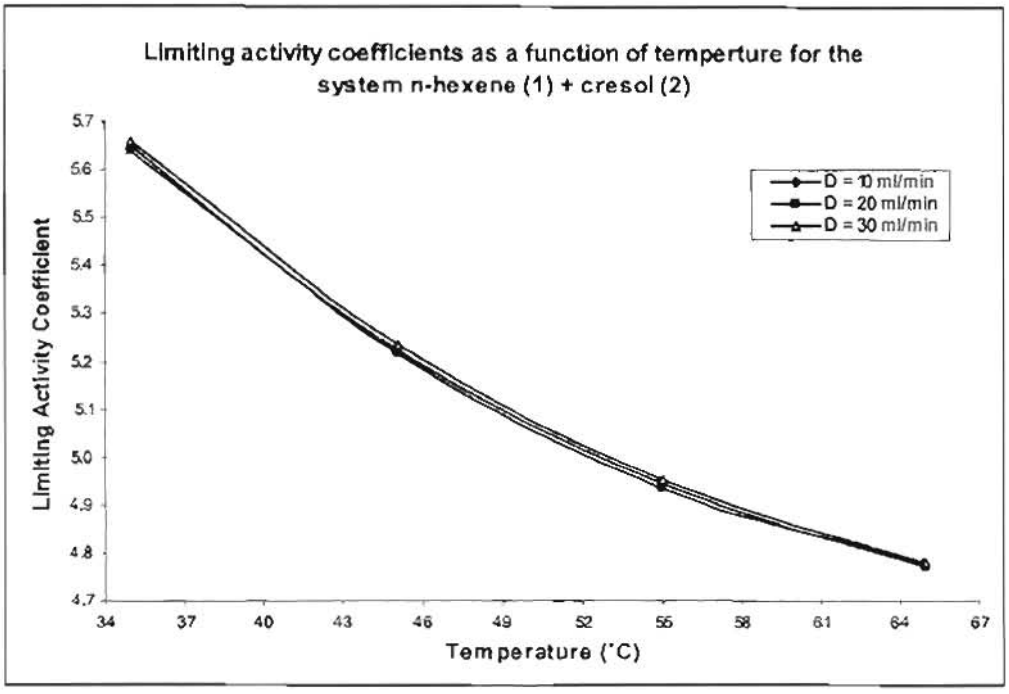

Figure 7-26: Comparison of limiting activity coefficients for the system n-hexene (1) + o-cresol (2) at three flows and four temperatures.

The inert gas stripping technique is well suited for the determination of activity coefficients at infinite dilution for the system n-hexene (1) + o-cresol (2) as n-hexene can be regarded as a volatile solute while o-cresol can be classified as a non-volatile solvent having vapour pressures less than 1 mmHg at all system temperatures studied here. All the limiting activity coefficients calculated for the system n-hexene (1) + o-cresol (2) show strong agreement with each other.

7.6 Results for the ternary systems n-hexene (1) + o-cresol (2) + NMP (2)

Binary systems are the easiest systems to work with when determining limiting activity coefficients for most techniques, but the IGS technique can easily handle ternary systems as well. The next few sections are dedicated to determining limiting activity coefficients for ternary systems involving the solute n-hexene and the solvents o-cresol and NMP at different concentrations on a mass basis.

7.6.1 System n-hexene (1) + 20 %($^m/_m$) o-cresol (2) + 80 %($^m/_m$) NMP (2)

The 20 %($^m/_m$) o-cresol + 80 %($^m/_m$) NMP solvent was formed by weighing out predetermined masses of o-cresol and NMP to form a total mixture volume of 230 ml for the two cells. The solid o-cresol was then heated to 50 °C to form a liquid and the two chemicals were well mixed to

form the solvent mixture. The total volume of solvent required to fill the two cells for experimental analysis is around 220 ml. Activity coefficients at infinite dilution are evaluated for all the equations discussed in Chapters 6.

7.6.1.1 Results for Equation 6.55

This type of system has never been reported in literature before and there are therefore no data available to compare results. Due to the nature of the components under investigation it would not be a problem to accurately determine limiting activity coefficients. The precision of the results evaluated using Equation 6.55 is shown in Table 7-26.

Experimental Data		$\gamma^{\infty}_{experiment}$
D (ml/min)	T (°C)	
9.81	35.07	7.34
9.97	45.00	7.07
10.01	55.06	6.78
9.97	65.06	6.55
19.93	35.09	7.36
19.34	45.12	7.06
19.33	55.13	6.80
19.26	65.25	6.57
29.36	35.06	7.38
29.73	44.99	7.06
30.08	54.98	6.80
29.23	65.00	6.56

Table 7-26: Limiting activity coefficients for the system n-hexene (1) + 20 %($^{m}/_{m}$) o-cresol (2) + 80 %($^{m}/_{m}$) NMP (2) at three inert gas flow rates and four temperatures.

The evaluated limiting activity coefficients for this ternary system are higher than that for the binary systems n-hexene (1) + o-cresol (2) and n-hexene (1) + NMP (2). One would expect the limiting activity coefficients to be in a range similar to that of the limiting activity coefficients for the binary systems. The limiting activity coefficients should be closer to the values for the system n-hexene (1) + NMP (2) since there is 80 % NMP in the solvent on a mass basis, but that is not the case. The limiting activity coefficients for the system n-hexene (1) + 20 %($^{m}/_{m}$) o-cresol (2) + 80 %($^{m}/_{m}$) NMP (2) have their own unique values not related in any way to values evaluated for their binary counterparts. The relationship between temperature and limiting activity coefficients is the same as for previous systems, as well as the effect of flow rate on the limiting activity coefficients as seen in Figure 7-27.

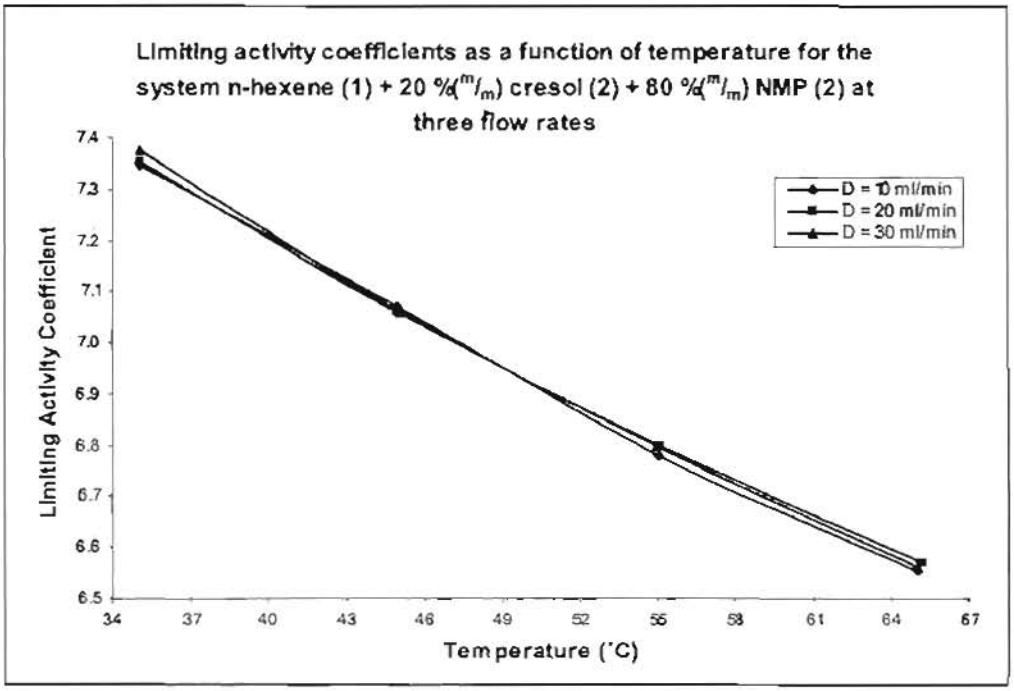

Figure 7-27: Comparison of limiting activity coefficients for the system n-hexene (1) + 20 %($^{m}/_{m}$) o-cresol (2) + 80 %($^{m}/_{m}$) NMP (2) for the three flow rates and at four temperatures.

There is good agreement between the limiting activity coefficients for the three flows as can be seen in Figure 7-27. There is a maximum deviation of 0.45 % between limiting activity coefficients for the three flows. The average of the limiting activity coefficient for the three flows should give the best representation of the actual and is reported in Chapter 8.

7.6.1.2 Results for Equations 6.23, 6.24, 6.29 and 6.33

Limiting activity coefficients for the same experimental conditions as those for Equation 6.55, but evaluated using the four Leroi et al. (1977) based equations for an inert gas flow rate of approximately 10 ml/min is shown in Table 7-27.

Experimental Conditions		Limiting Activity Coefficients Calculated Using Equation			
D (ml/min)	T (°C)	6.23	6.24	6.29	6.33
9.81	35.07	7.28	7.27	7.28	7.29
9.97	45.00	6.99	6.98	6.99	6.99
10.01	55.06	6.68	6.65	6.67	6.67
9.97	65.06	6.44	6.40	6.44	6.43

Table 7-27: Limiting activity coefficients for the system n-hexene (1) + 20 %($^{m}/_{m}$) o-cresol (2) + 80 %($^{m}/_{m}$) NMP (2) at a flow rate of approximately 10 ml/min.

The activity coefficients evaluated using Equations 6.23, 6.24, 6.29 and 6.33 are all still lower than those determined from the equation proposed by Krummen et al. (2000). This deviation between limiting activity coefficients is approximately 1 %. There is excellent agreement between the limiting activity coefficients evaluated from the four equations.

Experimental Conditions		Limiting Activity Coefficients Calculated Using Equation			
D (ml/min)	T (°C)	6.23	6.24	6.29	6.33
19.93	35.09	7.29	7.28	7.29	7.29
19.34	45.12	6.97	6.96	6.97	6.97
19.33	55.13	6.70	6.68	6.70	6.69
19.26	65.25	6.46	6.42	6.46	6.44

Table 7-28: Limiting activity coefficients for the system n-hexene (1) + 20 %($^m/_m$) o-cresol (2) + 80 %($^m/_m$) NMP (2) at constant inert gas flow rate of approximately 20 ml/min for different temperatures.

The γ^{∞} evaluated here are similar to that for the inert gas flow rate of 10 ml/min. This is an indication that the data is reproducible. The results can be seen graphically in Figure 7-28. Again an average would still be the best indication of the true value of the limiting activity coefficient at each experimental condition.

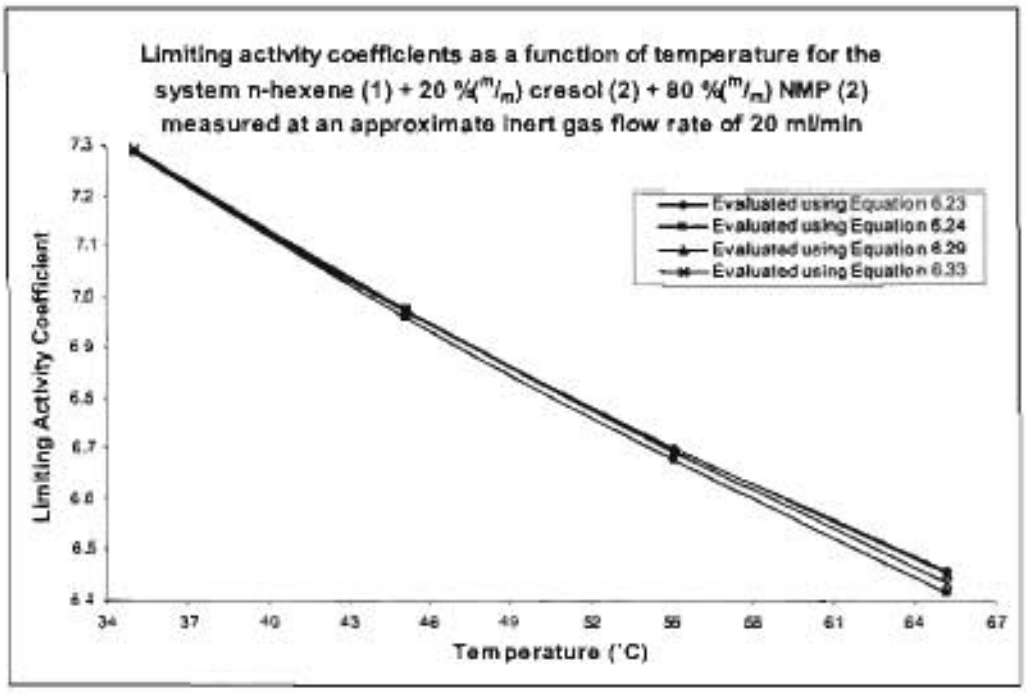

Figure 7-28: Activity coefficients at infinite dilution for the system n-hexene (1) + 20 %($^m/_m$) o-cresol (2) + 80 %($^m/_m$) NMP (2) at a flow rate of 20 ml/min.

The deviation of limiting activity coefficients at 65 °C, which can be seen in Figure 7-28, is only 0.62 % between the largest and smallest limiting activity coefficient. This deviation is rather small and is probably due to deviations in the assumptions used to derive the equations. It is also possible that at the higher temperatures there may be interference caused by the impurities as the chemicals used were not 100 % pure. The limiting activity coefficients measured at a flow rate of 30 ml/min is shown in Table 7-29.

Experimental Conditions		Limiting Activity Coefficients Calculated Using Equation			
D (ml/min)	T (°C)	6.23	6.24	6.29	6.33
29.36	35.06	7.30	7.31	7.31	7.32
29.73	44.99	7.00	6.97	6.98	6.98
30.08	54.98	6.70	6.68	6.70	6.70
29.23	65.00	6.45	6.41	6.45	6.43

Table 7-29: Activity coefficients at infinite dilution for the system n-hexene (1) + 20 %($^m/_m$) o-cresol (2) + 80 %($^m/_m$) NMP (2) measured at four temperatures at a flow rate of approximately 30 ml/min

A comparison of the limiting activity coefficients for the four equations is shown below.

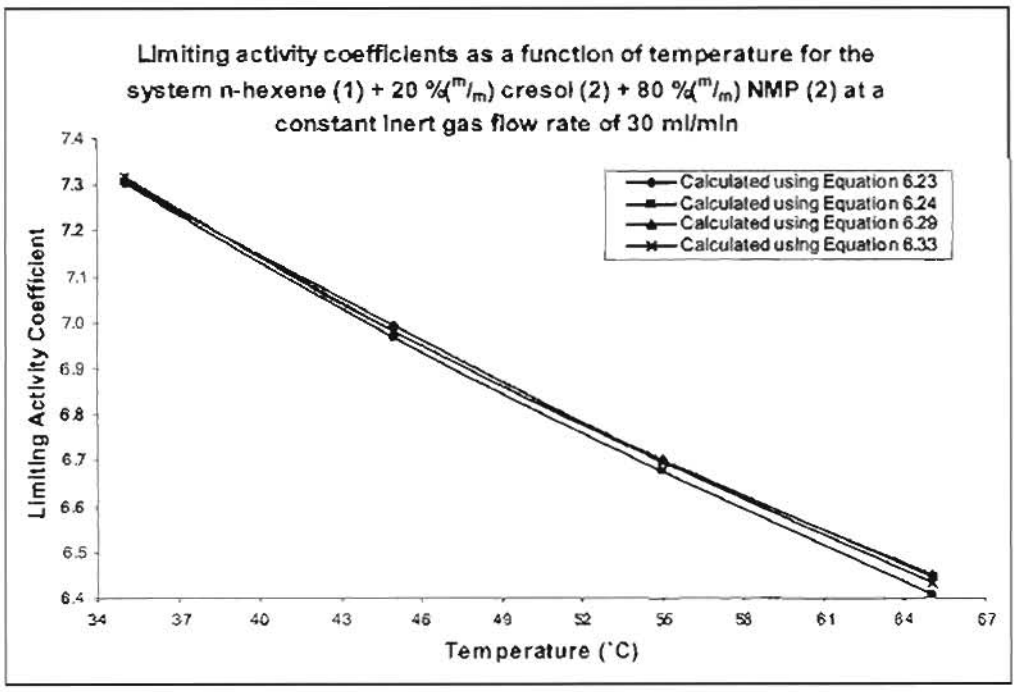

Figure 7-29: Comparison of limiting activity coefficients for the system n-hexene (1) + 20 %($^m/_m$) o-cresol (2) + 80 %($^m/_m$) NMP (2) measured at a flow rate of approximately 30 ml/min.

7.6.1.3 Results for Equation 6.65

Equation 6.65 used in conjunction with Equation 6.64 and the correction factors determines limiting activity coefficients that are closer to the limiting activity coefficients determined by Equation 6.55 for the binary systems. The same applies for the ternary systems as shown in Table 7-30.

Experimental Conditions		γ_{sol}^{∞}	Correction Factors				$\gamma_{sol}^{\infty JI}$
D (ml/min)	T (°C)		k_1	k_2	k_3	k_4	
9.81	35.07	7.27	0.998	1	1.002	1.008	7.32
9.97	45.00	6.98	0.997	1	1.002	1.017	7.09
10.01	55.06	6.65	0.996	1	1.003	1.028	6.83
9.97	65.06	6.40	0.995	1	1.004	1.040	6.64
19.93	35.09	7.28	0.998	1	1.001	1.008	7.33
19.34	45.12	6.96	0.997	1	1.002	1.017	7.07
19.33	55.13	6.67	0.997	1	1.003	1.028	6.85
19.26	65.25	6.41	0.995	1	1.003	1.040	6.66
29.36	35.06	7.30	0.998	1	1.002	1.008	7.36
29.73	44.99	6.97	0.998	1	1.002	1.017	7.08
30.08	54.98	6.67	0.995	1	1.003	1.028	6.84
29.23	65.00	6.41	0.990	1	1.004	1.040	6.62

Table 7-30: Limiting activity coefficients for the system n-hexene (1) + 20 %($^{m}/_{m}$) o-cresol (2) + 80 %($^{m}/_{m}$) NMP (2) measured at three flow rates and four temperatures.

There are two sets of equations for the correction factors; one for use with the DCT and the other for the SCT. These equations are not interchangeable and the appropriated set of equations must be used depending on the experimental set-up. At nearly ideal conditions such as this there is very little difference if the wrong equations are used. If the DCT is used, k_2 is always equal to one. To be on the safe side the DCT must be used for multi-component systems irrespective of the nature (volatilities) of the components under investigation.

The inert gas stripping technique appears to be well suited for the determination of activity coefficients at infinite dilution for the system n-hexene (1) + 20 %($^{m}/_{m}$) o-cresol (2) + 80 %($^{m}/_{m}$) NMP (2) based on the shape of the curves and the precision of the results. The different equations used to determine limiting activity coefficients for this system shows good agreement with each other. A comparison of the results in Table 7-30 for the three flows is shown in Figure 7-30.

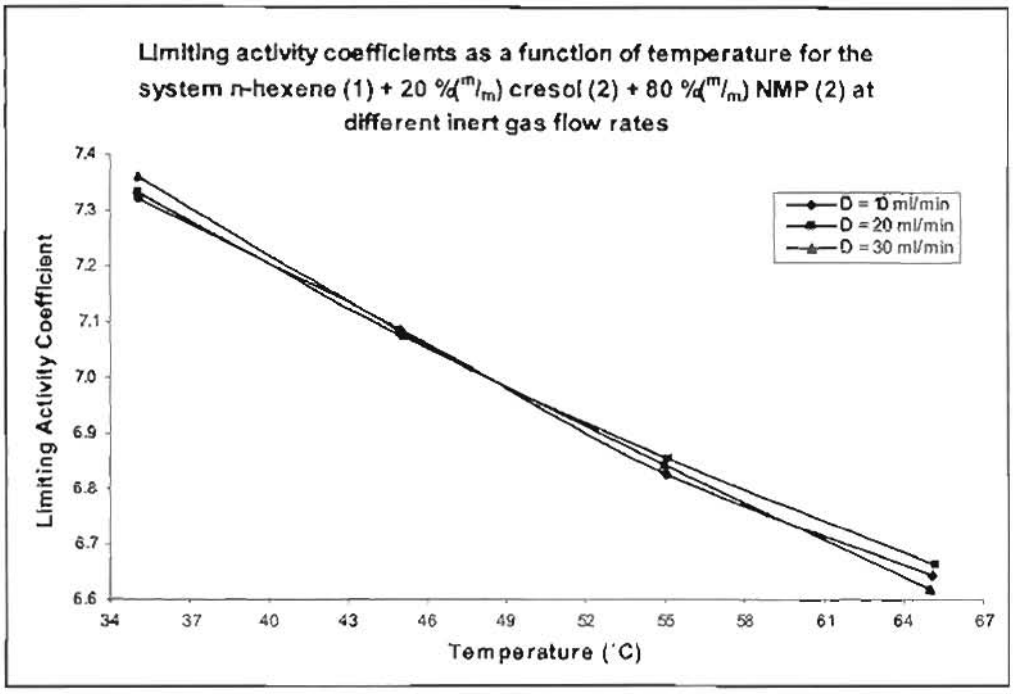

Figure 7-30: Comparison of activity coefficients at infinite dilution for the system n-hexene (1) + 20 %($^m/_m$) o-cresol (2) + 80 %($^m/_m$) NMP (2) evaluated using Equation 6.65.

Equation 6.65 predicts limiting activity coefficients that are similar to that determined by Equation 6.55 and there are smaller deviations between the values at the higher temperatures. The next system under investigation is similar to this one, except the solvent consists of more o-cresol and lesser NMP.

7.6.2 System n-hexene (1) + 40 %($^m/_m$) o-cresol (2) + 60 %($^m/_m$) NMP(2)

The effect of varying the solvent concentration on the limiting activity coefficient can now be observed for the ternary system n-hexene (1) + o-cresol (2) + NMP (2). It would be interesting to see if the limiting activity coefficients tend towards the values of their binary counter parts i.e. since the binary system with the solvent o-cresol has lower activity coefficients than that for the solvent NMP by itself, it would be logical to assume that by adding more o-cresol into the solvent mixture the limiting activity coefficients will now decease slightly from the system n-hexene (1) + 20 %($^m/_m$) o-cresol (2) + 80 %($^m/_m$) NMP (2).

7.6.2.1 Results for Equation 6.55

Equation 6.55 proposed by Krummen et al. (2000) predicts activity coefficients that show excellent agreement with each other for all systems studied thus far. The limiting activity coefficients for this system are shown in Table 7-31.

Experimental Data		$\gamma^{\infty}_{experiment}$
D (ml/min)	T (°C)	
9.99	34.99	7.24
9.88	44.99	7.05
9.77	55.06	6.93
9.92	64.96	6.84
20.07	34.95	7.22
20.05	44.98	7.04
20.07	55.07	6.91
19.99	65.02	6.85
29.17	35.05	7.24
28.55	45.04	7.05
27.53	55.06	6.93
26.60	64.98	6.86

Table 7-31: Limiting activity coefficients for the system n-hexene (1) + 40 %($^{m}/_{m}$) o-cresol (2) + 60 %($^{m}/_{m}$) NMP (2) from Equation 6.55 at different flow rates and temperatures

The limiting activity coefficients are indeed lower than that for the system n-hexene (1) + 20 %($^{m}/_{m}$) o-cresol (2) + 80 %($^{m}/_{m}$) NMP (2). Varying the solvent concentration does indeed have an effect on the limiting activity coefficients. Certain chemicals can increase or decrease the limiting activity coefficient of the solute thus enabling it to be easily separated from a mixture or making separation more difficult altogether. Determining limiting activity coefficients in this fashion can make entrainer selection easier to aid in the breaking of azeotropes allowing for greater separation between certain components in a mixture.

The limiting activity coefficients are shown as a function of temperature in Figure 7-31. The graph shows excellent agreement between all values at similar experimental temperatures. Flow rate does not seem to have any significant effect on the limiting activity coefficient based on the assumption of the IGS method. Any deviations are due to experimental errors rather than due to a change in flow rate. A maximum deviation of 0.2 % is observed between limiting activity coefficients at similar temperatures. This type of precision is extremely high and required for determining limiting activity coefficients at infinite dilution.

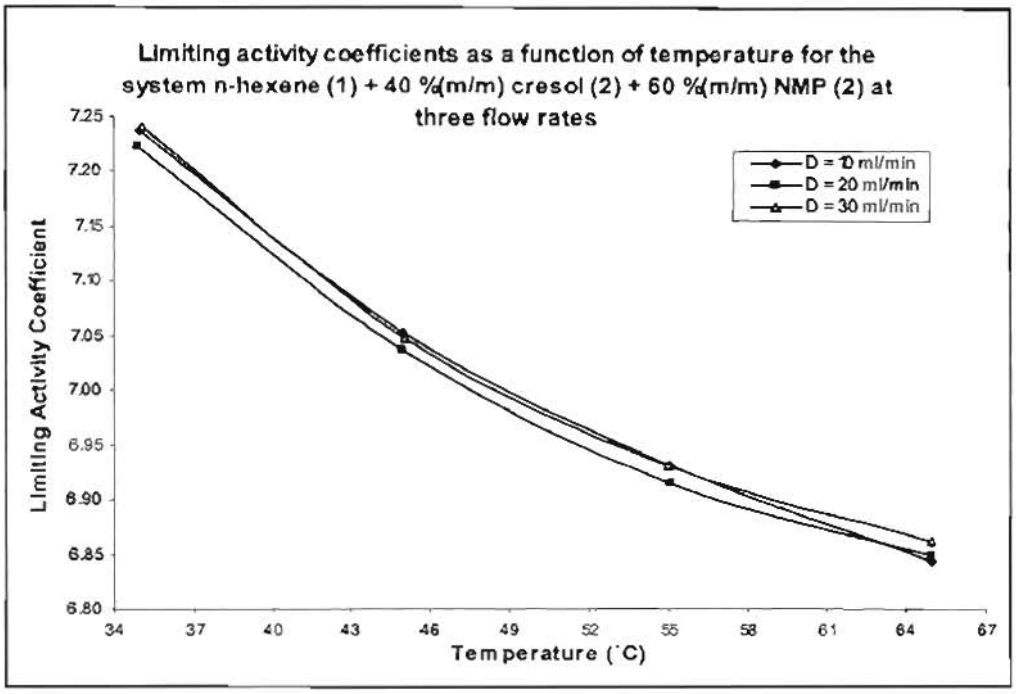

Figure 7-31: Comparison of limiting activity coefficients for the system n-hexene (1) + 40 %($^m/_m$) o-cresol (2) + 60 %($^m/_m$) NMP (2) measured at different flows and temperatures.

The graphs may not appear to be that coherent, but they are plotted on a highly expanded scale, as can be seen by the values on both axis.

7.6.2.2 Results for Equations 6.23, 6.24, 6.29 and 6.33

The limiting activity coefficients evaluated from the four equations can be found in Table 7-32 for an inert gas flow rate of approximately 10 ml/min.

Experimental Conditions		Limiting Activity Coefficients Calculated Using Equation			
D (ml/min)	T (°C)	6.23	6.24	6.29	6.33
9.99	34.99	7.17	7.17	7.17	7.18
9.88	44.99	6.97	6.96	6.96	6.97
9.77	55.06	6.83	6.81	6.82	6.82
9.92	64.96	6.73	6.68	6.72	6.70

Table 7-32: Limiting activity coefficients for the system n-hexene (1) + 40 %($^m/_m$) o-cresol (2) + 60 %($^m/_m$) NMP (2) at a constant inert gas flow rate of approximately 10 ml/min and at different temperatures.

The limiting activity coefficients evaluated between the four equations show excellent agreement although the values are slightly lower than the values determined using Equation 6.55. The results are shown graphically in Figure 7-32.

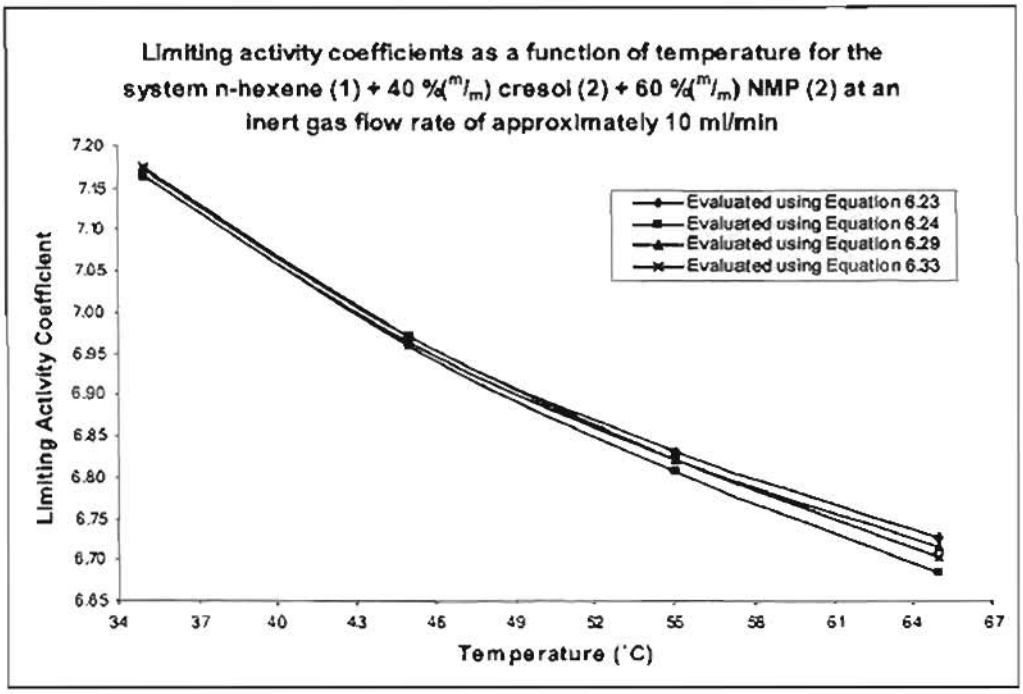

Figure 7-32: Comparison of limiting activity coefficients for the system n-hexene (1) + 40 %($^{m}/_{m}$) o-cresol (2) + 60 %($^{m}/_{m}$) NMP (2) at an approximate flow rate of 10 ml/min.

The largest deviations are observed at the higher temperatures once again. This deviation however is not greater than 0.67 % between the largest calculated value of 6.73 and the smallest value of 6.68. This deviation is rather small and an average would result in limiting activity coefficients that are closer to the true value.

Experimental Conditions		Limiting Activity Coefficients Calculated Using Equation			
D (ml/min)	T (°C)	6.23	6.24	6.29	6.33
20.07	34.95	7.16	7.15	7.15	7.16
20.05	44.98	6.95	6.94	6.95	6.95
20.07	55.07	6.82	6.79	6.81	6.81
19.99	65.02	6.74	6.69	6.73	6.71

Table 7-33: Limiting activity coefficients for the system n-hexene (1) + 40 %($^{m}/_{m}$) o-cresol (2) + 60 %($^{m}/_{m}$) NMP (2) measured at an inert gas flow rate of approximately 20 ml/min.

The limiting activity coefficients measured at a flow rate of approximately 20 ml/min are similar to those for a flow rate of approximately 10 ml/min as expected. Graphically the results can be found in Figure 7-33.

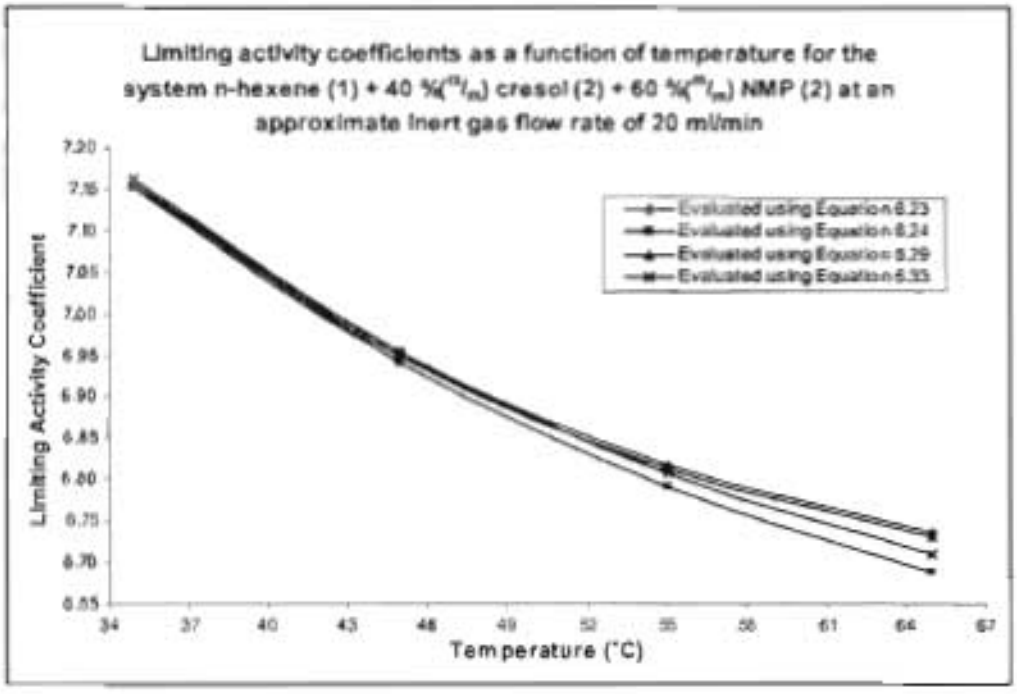

Figure 7-33: Comparison of activity coefficients at infinite dilution for the system n-hexene (1) + 40 %(m/m) o-cresol (2) + 60 %(m/m) NMP (2) measured at approximately 20 ml/min.

There is some variation occurring between the limiting activity coefficients at higher temperatures. Equations 6.23 and 6.24 give remarkably similar results that differ slightly from the other two equations, which in tern have values that differ from each other for the same experimental conditions. The values differ by a maximum deviation of 0.7 % only. Limiting activity coefficients evaluated at an inert gas flow rate of 30 ml/min is shown below in Table 7-34.

Experimental Conditions		Limiting Activity Coefficients Calculated Using Equation			
D (ml/min)	T (°C)	6.23	6.24	6.29	6.33
29.17	35.05	7.18	7.17	7.17	7.18
28.55	45.04	6.97	6.95	6.96	6.96
27.53	55.06	6.83	6.81	6.83	6.82
26.60	64.98	6.75	6.70	6.75	6.72

Table 7-34: Limiting activity coefficients for the system n-hexene (1) + 40 %(m/m) o-cresol (2) + 60 %(m/m) NMP (2) measured at flow rates of approximately 30 ml/min.

The limiting activity coefficients are similar to those calculated for flows of 10 and 20 ml/min and graphically the curves have the same trends as before shown in Figure 7-34.

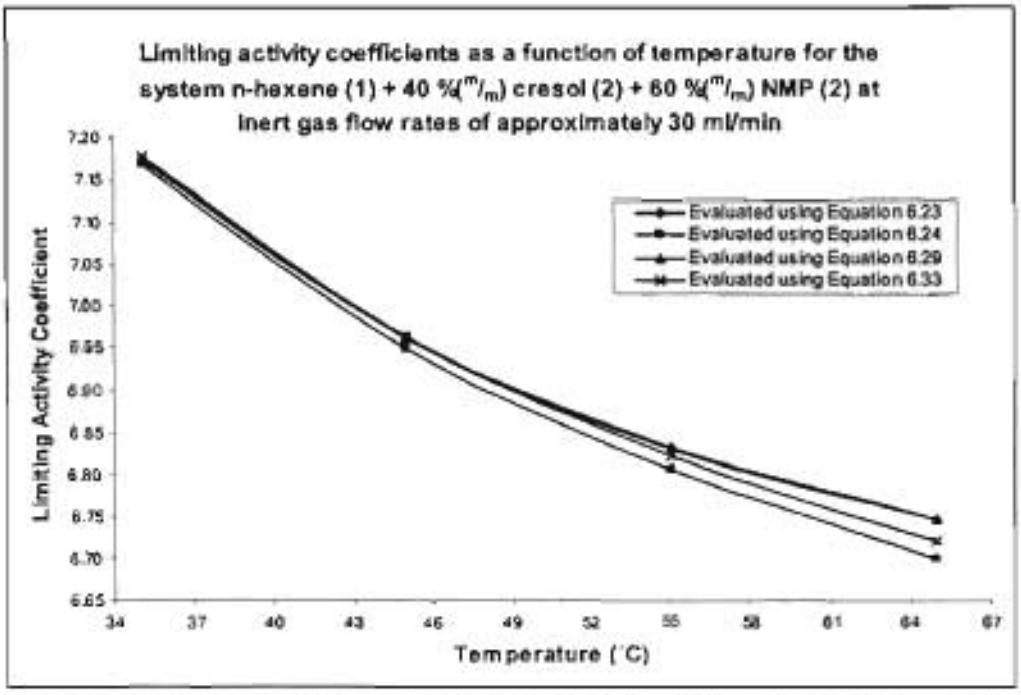

Figure 7-34: Comparison of activity coefficients at infinite dilution for the system n-hexene (1) + 40 %(m/m) o-cresol (2) + 60 %(m/m) NMP (2) at flow rates of approximately 30 ml/min.

The limiting activity coefficients at 35 °C and 45 °C for all flows have excellent agreement. The maximum deviation of values in this temperature range is 0.21 %. Extrapolating limiting activity coefficients from Figures 7-32, 7-33 and 7-34 may lead to inconclusive results. Since the graphs are spread sufficiently far apart at 65 °C it will lead to large errors when extrapolating; instead a plot of $\ln(\gamma^{\infty})$ against $1/T$ should result in a straight line that can be used for extrapolation. If not a plot of the average limiting activity coefficients for each experimental condition must be used when extrapolating and interpolating

7.6.2.3 Results for Equation 6.65

Limiting activity coefficients evaluated from Equation 6.65 can be found in Table 7-35 along with the correction factors evaluated under the experimental conditions. Once again the correction factors are very close to unity but leaving them out would results in deviations that are greater than 1 %.

Experimental Conditions		γ_{sol}^{∞}	Correction Factors				$\gamma_{sol}^{\infty,II}$
D (ml/min)	T (°C)		k_1	k_2	k_3	k_4	
9.99	34.99	7.16	0.998	1	1.001	1.008	7.21
9.88	44.99	6.95	0.997	1	1.002	1.017	7.06
9.77	55.06	6.80	0.994	1	1.002	1.028	6.96
9.92	64.96	6.68	0.989	1	1.003	1.040	6.89
20.07	34.95	7.15	0.998	1	1.001	1.008	7.20
20.05	44.98	6.94	0.997	1	1.002	1.017	7.05
20.07	55.07	6.79	0.995	1	1.003	1.028	6.96
19.99	65.02	6.68	0.996	1	1.003	1.040	6.90
29.17	35.05	7.17	0.998	1	1.001	1.008	7.22
28.55	45.04	6.95	0.997	1	1.002	1.017	7.06
27.53	55.06	6.80	0.995	1	1.003	1.028	6.98
26.60	64.98	6.70	0.992	1	1.003	1.040	6.91

Table 7-35: Limiting activity coefficients for the system n-hexene (1) + 40 %($^{m}/_{m}$) o-cresol (2) + 60 %($^{m}/_{m}$) NMP (2) measured at different flow rates and temperatures.

The precision (in terms of how close the limiting activity coefficients are to each other for the similar temperatures) of the results for Equation 6.65 is shown Figure 7-35. The correction factors are of similar magnitude as that for all the other systems studied thus far.

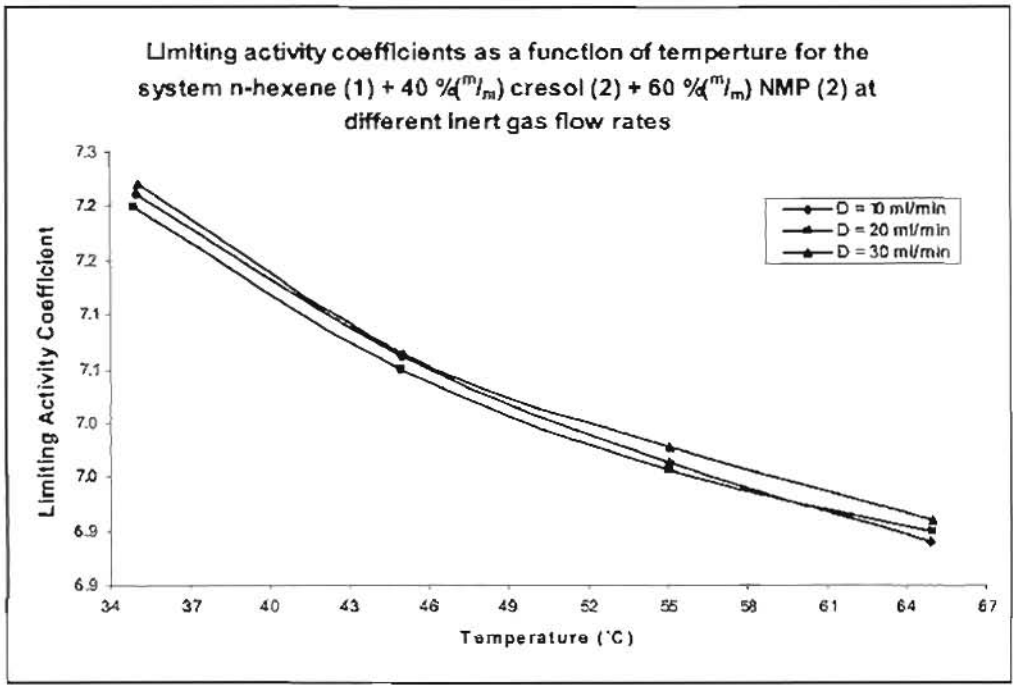

Figure 7-35: Comparison of limiting activity coefficients for the system n-hexene (1) + 40 %($^{m}/_{m}$) o-cresol (2) + 60 %($^{m}/_{m}$) NMP (2) measured at different flows and temperatures.

The deviation between the limiting activity coefficients in Figure 7-35 is relatively small and the results can be considered as sufficiently accurate.

7.6.3. System n-hexene (1) + 60 %($^m/_m$) o-cresol (2) + 40 %($^m/_m$) NMP (2)

The addition of more o-cresol to the solvent in order to obtain a solution of 60 %($^m/_m$) o-cresol should result in limiting activity coefficients that are closer to the binary system n-hexene (1) + o-cresol (2) than the previous system with 40 %($^m/_m$) o-cresol in the solvent. This is the observable trend thus far, but as seen in Table 7-36 this is not the case.

7.6.3.1. Results for Equation 6.55

Experimental Data		$\gamma^{\infty}_{experiment}$
D (ml/min)	T (°C)	
10.04	34.98	7.54
10.07	44.97	7.31
10.13	55.01	7.11
9.97	64.97	6.95
20.41	34.98	7.54
20.30	45.02	7.32
20.80	55.01	7.10
20.57	65.01	6.93
29.59	35.00	7.55
28.93	45.00	7.32
29.54	55.03	7.10
28.40	64.97	6.91

Table 7-36: Limiting activity coefficients for the system n-hexene (1) + 60 %($^m/_m$) o-cresol (2) + 40 %($^m/_m$) NMP (2) measured at different flows and temperature.

The limiting activity coefficients obtained for the system n-hexene (1) + 60 %($^m/_m$) o-cresol (2) + 40 %($^m/_m$) NMP (2) is higher than that for all the systems above. There seems to be a jump in the limiting activity coefficients at this point. There is no observable trend when looking at the concentration profiles formed by plotting limiting activity coefficients against concentration at this point. It is shown elsewhere (Chapter 8) that it is actually the previous system (n-hexene (1) + 40 %($^m/_m$) o-cresol (2) + 40 %($^m/_m$) NMP (2)) that has values that are inconsistent with the rest of the data for two temperatures only. There is actually a distinct trend for limiting activity coefficient and concentration as there is a distinct trend between limiting activity coefficient and temperature as seen in Figure 7-36.

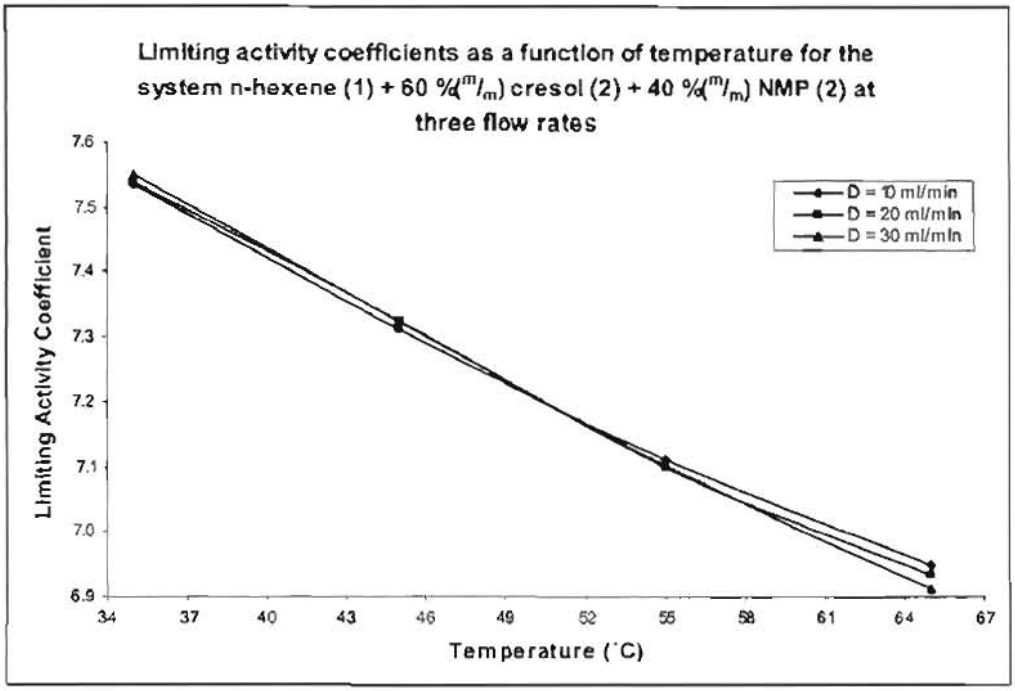

Figure 7-36: Comparison of activity coefficients at infinite dilution for the system n-hexene (1) + 60 %($^m/_m$) o-cresol (2) + 40 %($^m/_m$) NMP (2) for the three flows.

There is excellent agreement between the limiting activity coefficients evaluated using Equation 6.55 for the three inert gas flow rates. Some deviation is observable at 65 °C but as discussed previously this deviation is small and negligible and taking the average for that condition would give the best representation of the results.

7.6.3.2 Results for Equations 6.23, 6.24, 6.29 and 6.33

The four equations above predict similar values for the limiting activity coefficients as Equation 6.55 for the system n-hexene (1) + 60 %($^m/_m$) o-cresol (2) + 40 %($^m/_m$) NMP (2) at the same experimental conditions.

Experimental Conditions		Limiting Activity Coefficients Calculated Using Equation			
D (ml/min)	T (°C)	6.23	6.24	6.29	6.33
10.04	34.98	7.47	7.46	7.46	7.47
10.07	44.97	7.23	7.21	7.21	7.22
10.13	55.01	7.08	7.05	7.06	7.07
9.97	64.97	6.80	6.75	6.78	6.77

Table 7-37: Activity coefficients at infinite dilution for the system n-hexene (1) + 60 %($^m/_m$) o-cresol (2) + 40 %($^m/_m$) NMP (2) at a flow rate of approximately 10ml/min.

The limiting activity coefficients evaluated using Equations 6.23, 6.24, 6.29 and 6.33 are lower than that determined using Equation 6.55. This trend is also similar for all the other systems mentioned thus far. The maximum difference in limiting activity coefficients between the four equations and Equation 6.55 is not greater than 2.85 %. The limiting activity coefficients measured at a flow rate of approximately 20 ml/min is shown in Table 7-38.

Experimental Conditions		Limiting Activity Coefficients Calculated Using Equation			
D (ml/min)	T (°C)	6.23	6.24	6.29	6.33
20.41	34.98	7.47	7.46	7.46	7.47
20.30	45.02	7.24	7.22	7.23	7.23
20.80	55.01	6.99	6.97	6.98	6.98
20.57	65.01	6.81	6.76	6.80	6.78

Table 7-38: Limiting activity coefficients for the system n-hexene (1) + 60 %($^{m}/_{m}$) o-cresol (2) + 40 %($^{m}/_{m}$) NMP (2) at a flow rate of approximately 20 ml/min.

There is a maximum difference of 2.45 % between limiting activity coefficients in Table 7-38 and Table 7-36 evaluated at similar conditions. This is a large discrepancy in the results for activity coefficients. The results for a flow rate of 30 ml/min are shown in Table 7-39.

Experimental Conditions		Limiting Activity Coefficients Calculated Using Equation			
D (ml/min)	T (°C)	6.23	6.24	6.29	6.33
29.59	35.00	7.48	7.47	7.47	7.48
28.93	45.00	7.26	7.22	7.23	7.23
29.54	55.03	7.00	6.97	6.99	6.98
28.40	64.97	6.79	6.74	6.78	6.76

Table 7-39: Limiting activity coefficients for the system n-hexene (1) + 60 %($^{m}/_{m}$) o-cresol (2) + 40 %($^{m}/_{m}$) NMP (2) measured at a flow rate of approximately 30 ml/min and evaluated using the Leroi et al. (1977) based equations.

The difference in limiting activity coefficients between the four equations and Equation 6.55 is rather large, however the limiting activity coefficients evaluated from Equations 6.23, 6.24, 6.29 and 6.33 have excellent precision, similar to that of Figure 7-36.

7.6.3.3 Results for Equation 6.65

Table 7-40 has limiting activity coefficients evaluated from Equation 6.65 measured at three flows and four temperatures.

Experimental Conditions		γ_{tol}^{∞}	Correction Factors				$\gamma_{tol}^{\infty,II}$
D (ml/min)	T (°C)		k_1	k_2	k_3	k_4	
10.04	34.98	7.46	0.998	1	1.001	1.008	7.50
10.07	44.97	7.21	0.997	1	1.001	1.017	7.32
10.13	55.01	7.05	0.982	1	1.002	1.028	7.12
9.97	64.97	6.74	0.983	1	1.002	1.040	6.91
20.41	34.98	7.46	0.998	1	1.001	1.008	7.51
20.30	45.02	7.22	0.997	1	1.001	1.017	7.33
20.80	55.01	6.96	0.996	1	1.002	1.028	7.14
20.57	65.01	6.76	0.990	1	1.002	1.040	6.90
29.59	35.00	7.47	0.998	1	1.001	1.008	7.52
28.93	45.00	7.22	0.997	1	1.001	1.017	7.33
29.54	55.03	6.97	0.995	1	1.002	1.028	7.13
28.40	64.97	6.74	0.991	1	1.002	1.040	6.91

Table 7-40: Limiting activity coefficients for the system n-hexene (1) + 60 %($^m/_m$) o-cresol (2) + 40 %($^m/_m$) NMP (2) measured at different flows and temperatures.

The limiting activity coefficients determined here are very precise as shown Figure 7-37.

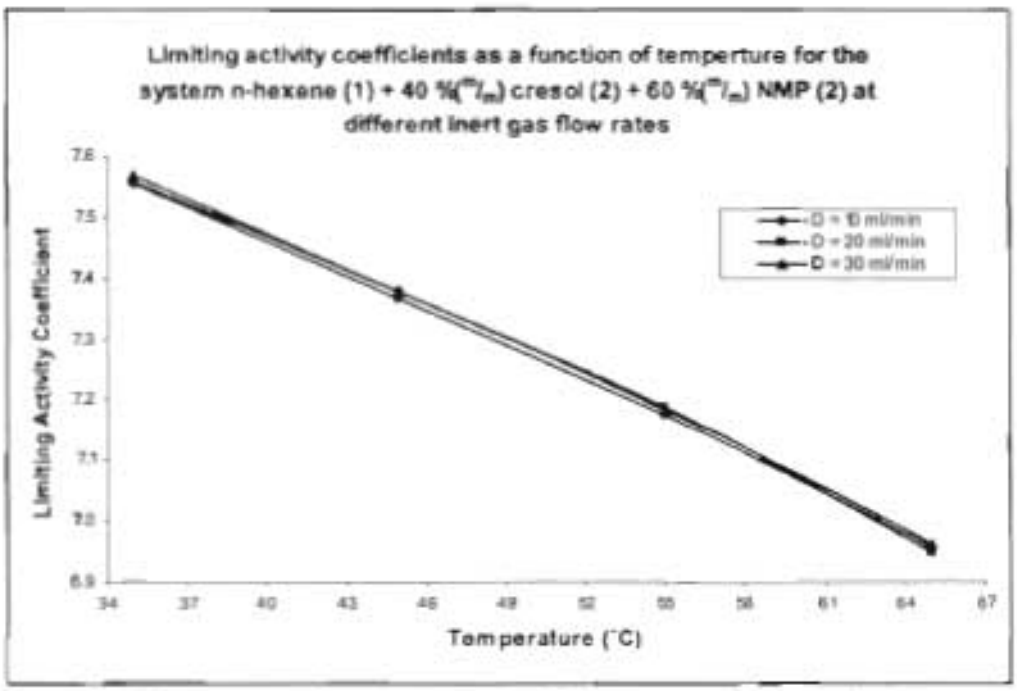

Figure 7-37: Comparison of limiting activity coefficients for the system n-hexene (1) + 60 %($^m/_m$) o-cresol (2) + 40 %($^m/_m$) NMP (2) measured at three flows.

The results for the system n-hexene (1) + 60 %($^m/_m$) o-cresol (2) + 40 %($^m/_m$) NMP (2) from Equation 6.65 has to be the most precise in terms of predictability of limiting activity coefficients for all the systems studied thus far. There is excellent agreement at higher temperatures using Equation 6.65 unlike for the other equations as shown in Figure 7-37.

7.6.4 System n-hexene (1) + 80 %($^m/_m$) o-cresol (2) + 20 %($^m/_m$) NMP (2)

The final system studied is n-hexene (1) + 80 %($^m/_m$) o-cresol (2) + 20 %($^m/_m$) NMP (2). At this concentration o-cresol is still potentially dangerous and the necessary precautions need to be taken when handling the solvent especially at the higher temperatures.

7.6.4.1 Results for Equation 6.55

There is a considerable drop in the limiting activity coefficient for this system when compared to the previous system as shown in Table 7-41.

Experimental Data		$\gamma^{\infty}_{experimental}$
D (ml/min)	T (°C)	
9.26	34.95	7.19
9.30	44.98	7.00
9.37	55.01	6.79
9.41	65.04	6.62
20.05	35.03	7.19
20.14	45.03	6.98
19.80	55.01	6.81
19.95	64.99	6.63
30.17	34.99	7.19
30.25	44.98	6.97
30.33	55.04	6.81
30.25	65.04	6.64

Table 7-41: Limiting activity coefficients for the system n-hexene (1) + 80 %($^m/_m$) o-cresol (2) + 20 %($^m/_m$) NMP (2) measured at three flow rates and different temperatures.

The deviation between the limiting activity coefficients for the system n-hexene (1) + 80 %($^m/_m$) o-cresol (2) + 20 %($^m/_m$) NMP (2) is very small. The results are similar to that for the system n-hexene (1) + 40 %($^m/_m$) o-cresol (2) + 60 %($^m/_m$) NMP (2). There is no distinct trend obtained with the effect of varying concentration. The precision of the results can be found in Figure 7-38.

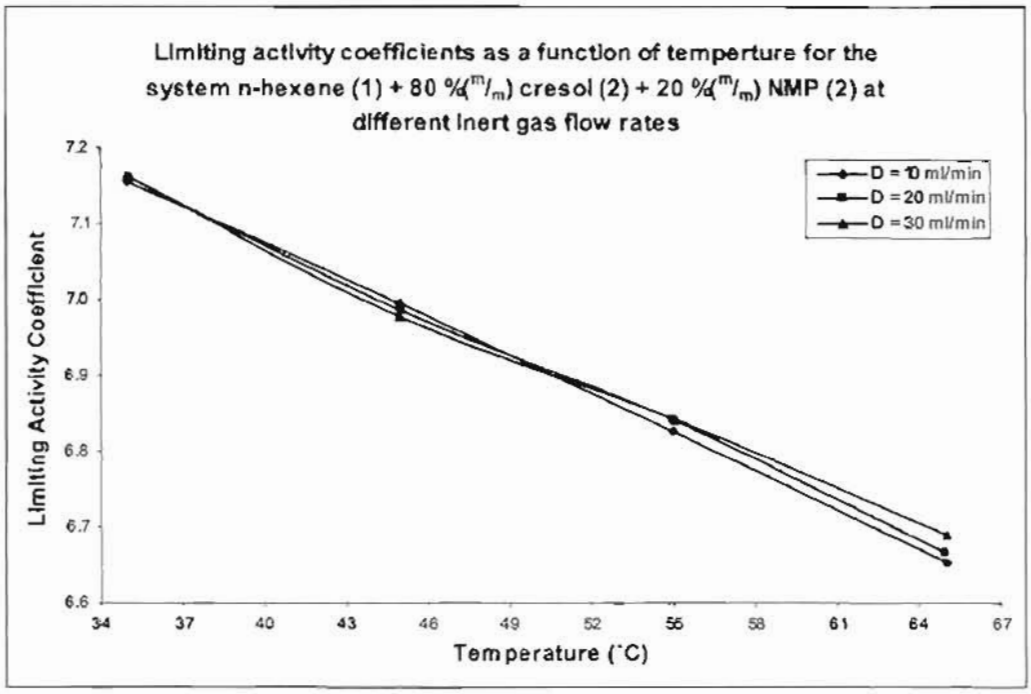

Figure 7-38: Comparison of limiting activity coefficient for the system n-hexene (1) + 80 %($^{m}/_{m}$) o-cresol (2) + 20 %($^{m}/_{m}$) NMP (2) for the three flows.

Averaging of the limiting activity coefficients evaluated from Equation 6.55 would result in values that are close to their actual values. The results are very precise and once again show that the data is reproducible.

7.6.4.2 Results for Equations 6.23, 6.24, 6.29 and 6.33

Tabulated in Table 7-42 are limiting activity coefficients for the system n-hexene (1) + 80 %($^{m}/_{m}$) o-cresol (2) + 20 %($^{m}/_{m}$) NMP (2) measured at 10 ml/min and evaluated using the Leroi et al. (1977) based equations.

Experimental Conditions		Limiting Activity Coefficients Calculated Using Equation			
D (ml/min)	T (°C)	6.23	6.24	6.29	6.33
9.26	34.95	7.12	7.11	7.11	7.12
9.30	44.98	6.91	6.90	6.90	6.90
9.37	55.01	6.69	6.67	6.67	6.68
9.41	65.04	6.51	6.46	6.49	6.47

Table 7-42: Activity coefficients at infinite dilution for the system n-hexene (1) + 80 %($^{m}/_{m}$) o-cresol (2) + 20 %($^{m}/_{m}$) NMP (2) at a flow rate of approximately 10 ml/min.

The trends formed as a result of varying temperature are similar to that for the other systems where these equations were used to evaluate limiting activity coefficients. There are larger deviations at higher temperatures than at the lower temperatures as shown in Figure 7-39.

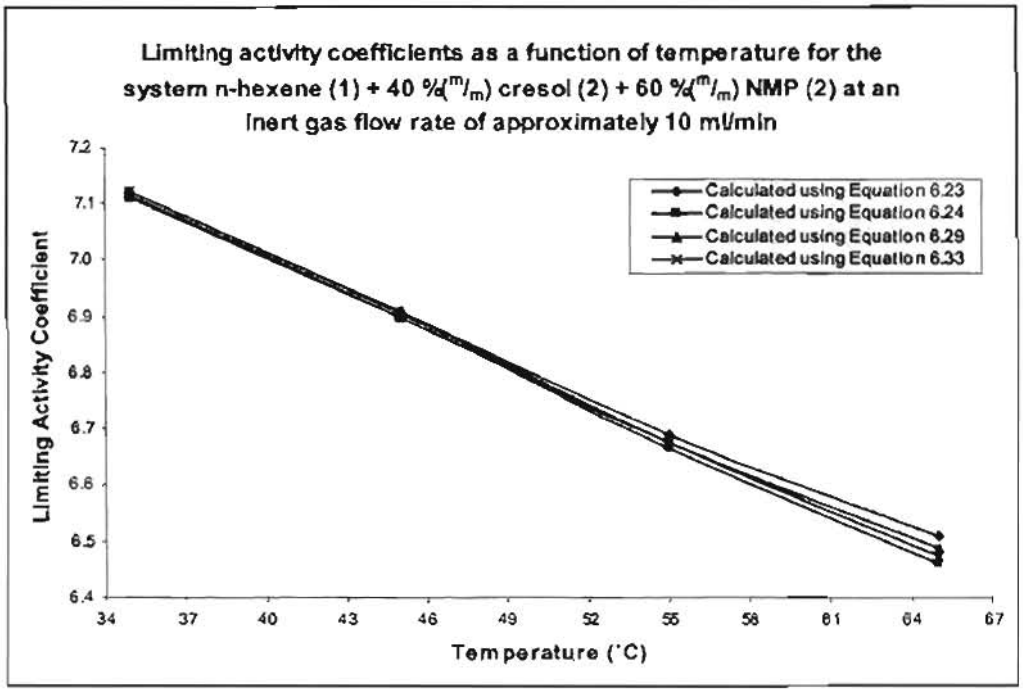

Figure 7-39: Comparison of limiting activity coefficients for the system n-hexene (1) + 80 %($^m/_m$) o-cresol (2) + 20 %($^m/_m$) NMP (2) measured at approximately 10 ml/min.

The four equations have some difficulty in determining limiting activity coefficients at higher temperatures. Although acceptable in the temperature range of interest it might lead to large errors when extrapolating (Refer to discussion for extrapolation and interpolation techniques). Limiting activity coefficients measured at approximately 20 ml/min is shown in Table 7-43.

Experimental Conditions		Limiting Activity Coefficients Calculated Using Equation			
D (ml/min)	T (°C)	6.23	6.24	6.29	6.33
20.05	35.03	7.12	7.12	7.11	7.12
20.14	45.03	6.90	6.88	6.89	6.89
19.80	55.01	6.70	6.68	6.69	6.69
19.95	64.99	6.51	6.46	6.50	6.48

Table 7-43: Limiting activity coefficients for the system n-hexene (1) + 80 %($^m/_m$) o-cresol (2) + 20 %($^m/_m$) NMP (2) measured at approximately 20 ml/min.

The trend obtained for limiting activity coefficients as a function of temperature is similar to that of Figure 7-39. The limiting activity coefficients for a flow rate of 30 ml/min are tabulated below.

Experimental Conditions		Limiting Activity Coefficients Calculated Using Equation			
D (ml/min)	T (°C)	6.23	6.24	6.29	6.33
30.17	34.99	7.13	7.12	7.12	7.12
30.25	44.98	6.89	6.87	6.88	6.88
30.33	55.04	6.71	6.68	6.70	6.69
30.25	65.04	6.52	6.47	6.51	6.49

Table 7-44: Activity coefficients at infinite dilution for the system n-hexene (1) + 80 %($^m/_m$) o-cresol (2) + 20 %($^m/_m$) NMP (2) measured at approximately 30 ml/min.

7.6.4.3 Results for Equation 6.65

The results obtained using Equation 6.65 is close to the results for Equation 6.55. The maximum deviation between these two equations is 1 % for any set of experimental conditions.

Experimental Conditions		γ_{exp}^{∞}	Correction Factors				$\gamma_{sol}^{\infty,II}$
D (ml/min)	T (°C)		k_1	k_2	k_3	k_4	
9.26	34.95	7.11	0.998	1	1.001	1.008	7.16
9.30	44.98	6.89	0.997	1	1.001	1.017	7.00
9.37	55.01	6.66	0.996	1	1.001	1.028	6.83
9.41	65.04	6.46	0.989	1	1.002	1.040	6.65
20.05	35.03	7.11	0.998	1	1.001	1.008	7.16
20.14	45.03	6.88	0.997	1	1.001	1.017	6.99
19.80	55.01	6.67	0.996	1	1.001	1.028	6.84
19.95	64.99	6.46	0.990	1	1.002	1.040	6.67
30.17	34.99	7.12	0.998	1	1.001	1.008	7.16
30.25	44.98	6.87	0.997	1	1.001	1.017	6.98
30.33	55.04	6.68	0.995	1	1.001	1.028	6.84
30.25	65.04	6.47	0.992	1	1.002	1.040	6.69

Table 7-45: Activity coefficients at infinite dilution for the system n-hexene (1) + 80 %($^m/_m$) o-cresol (2) + 20 %($^m/_m$) NMP (2) measured at different flows and temperatures.

A better indication of the precision of the results is shown in Figure 7-40. The inert gas stripping technique has proved to be a very reliable technique for determining limiting activity coefficients. The results obtained for the various systems are proof of this, especially for the systems whose results were comparable to literature.

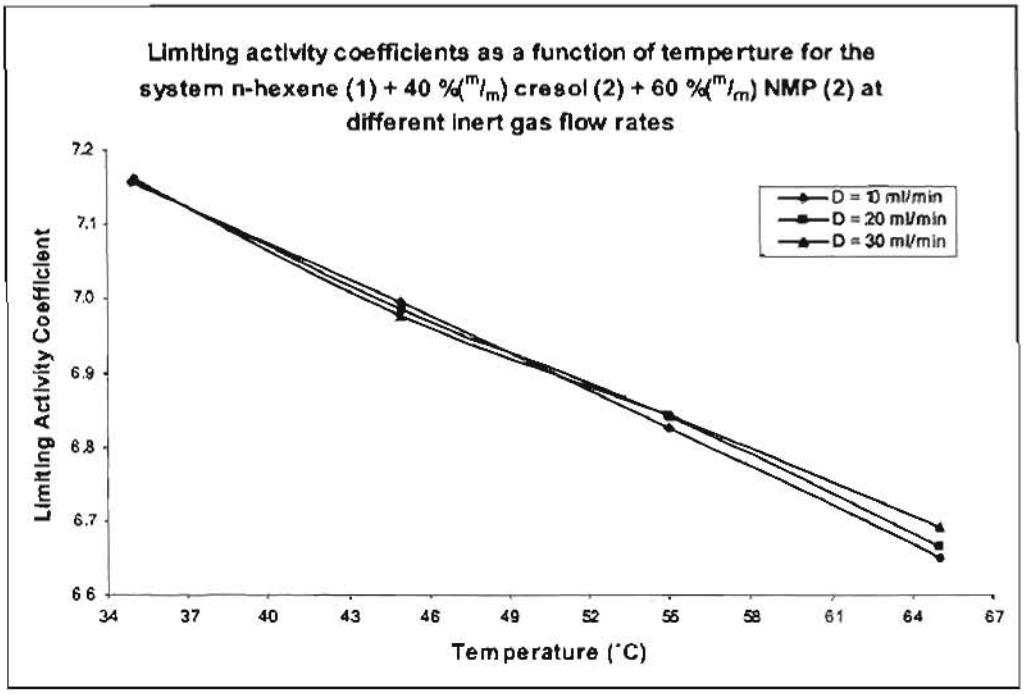

Figure 7-40: Comparison of limiting activity coefficients for the system n-hexene (1) + 80 %($^{m}/_{m}$) o-cresol (2) + 20 %($^{m}/_{m}$) NMP (2) for three flows.

Chapter VIII – Discussion

8.1 Discussion

The objectives of this study were to design, construct and commission a suitable inert gas stripping apparatus for the determination of limiting activity coefficients for binary and multi-component systems. The acquired data was for use by Sasol, since cresols are commonly found in crude oil and end up in exhaust fumes. The design and construction of the apparatus was based on a similar setup by Leroi et al. (1977). The apparatus was commissioned using three test systems for which chemicals were readily available. The three test systems chosen were cyclohexane (1) + NMP (2), n-heptane (1) + NMP (2) and n-hexane (1) + NMP (2), where (1) refers to the solute and (2) refers to the solvent.

8.1.1 Equilibrium Conditions

Literature data for the test systems were sourced from a recently published article by Krummen et al. (2004). They also used the inert gas stripping technique to determine limiting activity coefficients with inert gas flow rates in the region of 30 ml/min. Using this as a guide, a flow rate range was determined for the new apparatus using the test system cyclohexane (1) + NMP (2). Flow rate does not significantly affect the limiting activity coefficient as long as equilibrium conditions are maintained in the cells. The inert gas flow rate was varied for different experiments while keeping all other parameters constant to observe the effect on the resulting limiting activity coefficients. In Table 7-1 it shows that in the range 5 to 48 ml/min the limiting activity coefficient varies from the literature value of 6.7 by less than 1 %.

It thus shows that equilibrium conditions are maintained in the cells for the system cyclohexane (1) + NMP (2). This is expected as the height of the equilibrium cells are much greater than the minimum height of 5 cm calculated for bubble diameters less than 4.5 mm by Richon et al. (1980) for the system n-heptane (1) + NMP (2). The bubbles formed by the capillaries in this study were around 1 mm in diameter (based on observation) which is far smaller than that used in the calculation by Richon et al. (1980). This means that equilibrium conditions were easily achieved within the cells.

The resulting equilibrium conditions in the cells allows for accurate determination of the limiting activity coefficients and the represented solute peak areas (refer to Table 8-2) form a straight

line when determining slope *a*. The solute peak areas would be erratic if equilibrium conditions were not maintained and this was not observed after the equipment was properly insulated. The operating flow rate range is totally system dependant and may vary for other systems. For this reason it was decided to operate at low flow rates in the range 10 to 30 ml/min. The lower the flow rates the better the chances of reaching equilibrium. Also more solute peaks can be obtained within the experimental time which would result in smooth plots of the depletion rate of the solute in the solvent and ultimately for the accurate determination of slope *a*.

8.1.2 Experimental Conditions

All chemicals for use with the inert gas stripping technique need to be of extremely high purity as the impurities can interfere with the solute peak areas in the dilute region. It is recommended that there be no impurities in the chemicals used. If the impurity is inert and has very low volatility then the presence of small quantities of this will be acceptable. Depending on the chemical the price usually escalates drastically as the purity increases. It may also be very difficult to obtain chemicals with 100 % purity and to ensure that it remains pure when handling it. Chemicals were sourced from different companies and the purities in Table 8-1 are the minimum purities for the chemicals. All chemicals were analysed to check for purity using a GC and it was found that the impurities were difficult to detect as in all cases there was only one noticeable peak. Special care was not taken to check if the solvents and solutes did contain impurities whose peaks could overlap with solute peaks.

Chemicals	Source	Purity	Method Used
n-heptane	Saarchem(Pty) Ltd	99.5%	GC
n-hexane	SKYCHEM	99.8%	GC
n-hexene	FLUKA	99.8%	GC
cyclohexane	AnalaR	99.5%	GC
NMP	MERCK	99.5%	GC
o-cresol	FLUKA	99.5%	GC

Table 8-1: Chemicals used together with their source, purity and the method used to determine the purity as supplied by the manufacturers

When using inert gas stripping to determine limiting activity coefficients, there are two techniques to consider the SCT and DCT. The DCT was used for all systems and in the case of the system n-hexane (1) + NMP (2) the SCT was also used to compare results between the two techniques. This was done because both techniques are applicable for systems with low volatility solvents. It was found that both techniques yield good results that strongly agree with literature values. The SCT however has the added benefit of using less solvent which is useful

when using speciality chemicals or high purity chemicals which are very expensive. From the results of the test systems it is evident that the apparatus is operating properly and can be used to determine limiting activity coefficients with high accuracy and precision, despite its relatively simple design.

The experimental measurements undertaken in this study were primarily that of the measurement of limiting activity coefficients. These experiments were performed under two conditions, with the outcome of observing its effect on three variables, temperature, inert gas flow rate and solvent concentration for the ternary systems. Temperature was observed to have a considerable effect on the limiting activity coefficients, while the inert gas flow rate does not seem to have any effect on the limiting activity coefficient as long as equilibrium conditions are maintained in the cells. For all the systems, three different flow rates were used merely to serve as a consistency test i.e. to see whether the data would be reproducible.

The test systems were used to determine limiting activity coefficients at 4 different temperatures and it was found that the values obtained strongly agreed with literature values. The temperature of concern is the system temperature which is the temperature at which the limiting activity coefficients are to be determined. The system temperatures should not exceed the boiling point of the lowest component in the solute + solvent mixture, bearing in mind that the boiling points of the components in the mixture are not the same as pure component boiling points, but they should however not differ drastically. If one of the components starts to boil the stripping rate would be affected by evaporation and the method would fail.

For all systems studied the limiting activity coefficient decreases as temperature increases. Since the limiting activity coefficient accounts for the non-ideality of a system, this means that at higher temperatures the system becomes more ideal. The purpose of the limiting activity coefficient among other things is to account for deviations from ideal behaviour at low temperatures and high pressures. Since all experiments were done close to atmospheric pressure which is considered low, the only factor affecting the limiting activity coefficient, based on the method used is temperature. Therefore all figures of concern in Chapter 7 show a true reflection of the effect of temperature on the limiting activity coefficient.

8.1.3 Effect of Design Parameters

A suitable operating range for the inert gas flow rate really depends on the height of the equilibrium cells, the size of the bubbles and to a lesser extent the degree of mixing in the cells. The minimum height of the cells and bubble diameters in turn depends on the volatility of the

solute and solvent, or mixture of these, in the cells. Richon et al. (1980) and Li et al. (1993) took the nature of the solute and bubble diameter into consideration for the design of the equilibrium cells in order to determine the minimum cell height required to achieve thermodynamic equilibrium in the cells. The cell height, bubble diameter, temperature, inert gas flow rate, solute and solvent volatility and mixing in the cells affects the thermodynamic equilibrium. A significant change in any of these variables will affect the outcome of the results. The effect of cell height, bubble diameter and mixing in the cell are all design parameters that need to be considered when constructing the equilibrium cells.

8.1.4 Effect of Inert Gas Flow Rate

The operating flow rate range that is suitable for ensuring equilibrium conditions in the cells has to be determined experimentally. This was done by running experiments at some initial reasonably low flow rate (5 ml/min) and thereafter increasing the flow rate until equilibrium is disrupted. The disruption can be observed by erratic solute peak areas of injected samples into the GC. This would result in a plot that would not give a straight line when determining slope (a). The limiting activity coefficient data would also not be reproducible. This is a simple way to determine a suitable operating flow rate range. The flow rate range is sensitive to the type of system studied and this procedure may have to be performed for each system under investigation. This is necessary if the systems differ significantly from each other with respect to volatility especially for solutes with low volatility. With this experimental set-up it was not possible to determine the maximum flow rate. When exceeding flow rates of 50 ml/min there was considerable pressure build up in the cells. The concern was that the "O"-rings may not be able to contain the pressure.

When the flow rate range was determined logical deduction was used to choose which flow rates in that range would be most suitable to use for all experiments. A too low flow rate will result in long experimental times as the method is based on the variation of stripped solute with time. A good variation of the stripped solute in the dilute region needs to be obtained. The variation of solute with time depends largely on the volatility of the solute. This means that solutes with low volatility will require higher operating flow rates than solutes with high volatility. Also the mixing in the dilutor cell must be sufficiently high in order to have a uniform solution at high flow rates. Similarly, too high flow rates will cause most of the solutes to be stripped out before a suitable curve can be obtained especially for solutes with high volatility. After much consideration to the design capabilities of the equipment it was decided that flow rates in the range 10 to 30 ml/min would be most suitable. Thus for all the systems the inert gas (nitrogen) flow rates used were 10,

20 and 30 ml/min. From Table 7-1 the difference in the limiting activity coefficients for this flow rate range is very small.

8.1.5 Effect of Solvent Concentration

The concentration of components making up the solvent also affects the limiting activity coefficient. Figure 8-1 shows the affect that different o-cresol concentrations have on the limiting activity coefficient at similar temperatures and flow rates. For the 40 % concentration there is a maximum deviation of 1 % obtained from repeating the experiment at different flow rates.

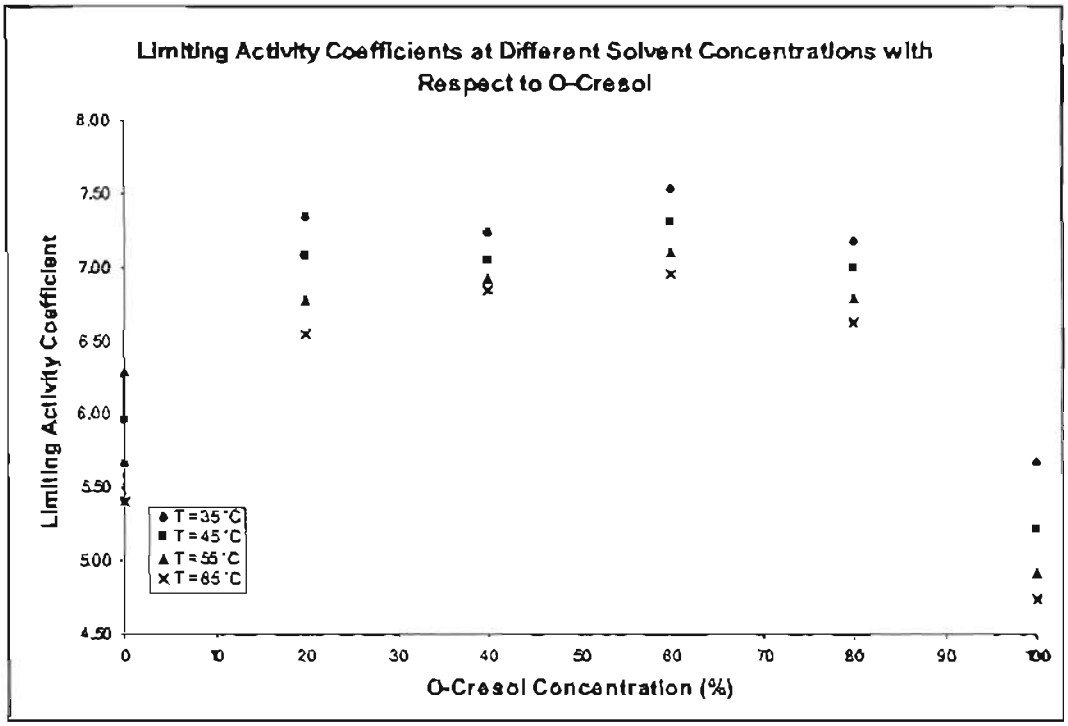

Figure 8-1: Variation of limiting activity coefficients at different o-cresol concentrations in the solvent on mass percent basis.

The other component making up the solvent is NMP. From the graph it is observed that the relationship between limiting activity coefficient and solvent concentration is quiet different from that of temperature and limiting activity coefficient. An o-cresol and NMP solvent mixture results in solute (hexane) limiting activity coefficients that are higher than if they were used as solvents on their own i.e. binary systems. The limiting activity coefficient is expected to be different as the interaction between the o-cresol and the NMP changes the properties of the solvent considerably. The limiting activity coefficients do however approach towards the binary system

values when the concentration of o-cresol in the solvent is very high or when the concentration of NMP is very high.

8.1.6 Effect of Pressure and Leaks

The other experimental parameter that needs to be considered is pressure. The pressures encountered were close to atmospheric pressure for all the experiments and this pressure is actually the pressure in the dilutor cell. The pressure is affected by the flow rate of the inert gas, as well as leaks in the system. It was observed that the higher the flow rate the higher the pressure. The pressure increases by approximately 1 mmHg for every 10 ml/min increase in inert gas flow rate for this experimental set-up. It is important to accurately know the pressure as it affects the vapour pressure calculations required to determine the limiting activity coefficient. Leaks along any of the gas lines caused erratic pressure readings. Any soapy solution can be used to detect the presence of leaks but most will leave a residue when it dries. This can contaminate the lines and interfere with the solute peaks. Snoop which does not leave any residue was used to locate any leaks before commencing with the experiment.

Leaks at different locations in the experimental set-up have different effects on the results, all of which impact negatively on the results. If there is a leak before the gas enters the cells then this would result in the flow rate changing throughout the experiment. If there are leaks after the gas has passed through the dilutor cell and before the injection point some of the stripped solute will be lost and this would result in inaccurate solute concentrations. Also any leak after the gas has passed through the dilutor cell will result in an incorrect flow rate reading at the bubble flow meter. The pressure readings are very stable and the presence of any leaks would result in erratic pressure readings which were observed whenever there was a leak in the equipment.

8.1.7 Effect of Slope

Another variable that affects the limiting activity coefficient is the slope (a) from the straight line plots. This was observed when leaving out peaks that do not lie on the curve. The slope changes and the limiting activity coefficients are extremely sensitive to the slope. Usually when leaving out peaks (in most cases the first one or two peaks were left out) the resulting limiting activity coefficients became more accurate. It is obvious that if peaks are left out towards the end and beginning of the slope there will be a more drastic change in the gradient than when removing peaks from the middle. Since peaks were only left out at the beginning of the experiment the results will be more accurate as the solute is more dilute in the solvent. Five to six peaks lying in a straight line are sufficient to obtain good results. At least 10 injections need

to be performed in order to achieve this as there may be some other reasons for leaving out peaks during the experiment such as interference during the analysis or a good split may not have been achieved for a certain injected sample.

8.1.8 Equations

Each of the equations used have different terms for predicting limiting activity coefficients and although they do not predict exactly the same values there is agreement to a certain extend between the values obtained from the different equations. Equation 6.23 is the simplest equation for determining limiting activity coefficients and must be used for systems with non-volatile solutes only. Despite its simplicity it is very good in predicting limiting activity coefficients especially for systems with high solute volatility and low solvent volatility. Equation 6.55 is also used for systems where the solvent volatility is low (less than 1mm Hg). Equations 6.24 and 6.33 can be used for any system even though they were derived for volatile solvents as shown in Chapter 6.

Equations 6.55 and 6.65 were derived to account for all kinds of systems. The saturation fugacity coefficient is taken into account with Equation 6.55 and the effect the value of the coefficient has on the limiting activity coefficient increases as temperature increases. If ignored there would be large errors at the higher temperatures. It is expected that Equations 6.23, 6.24, 6.29 and 6.33 would give less accurate limiting activity coefficients at very high temperatures. Since temperatures did not exceed 65 °C for all experiments the integrity of these equations were not compromised.

8.1.8.1 Applicability of the Equations

The equations (Leroi et al. (1977), Duhem and Vidal (1978), Boa and Han (1995), Krummen et al. (2000) and Hovorka and Dohnal (1997)) used for the determination of limiting activity coefficients were specifically derived for use with the inert gas stripping technique. Some equations were for use with systems where the solvent is volatile (Leroi et al. (1977) and Boa and Han (1995)), while others were derived for non-volatile solvents (Leroi et al. (1977) and Duhem and Vidal (1978)). All systems studied had non-volatile solvents which are classified as having vapour pressures less than 1 mmHg at all experimental temperatures.

In this regard the non-volatile equations will always apply when determining the limiting activity coefficient. The equations derived for volatile solvents would also apply for non-volatile solvent systems. The effect of the term that accounts for volatility of the solvent in the equation would be

negligible. This makes the equations for volatile solvents similar to the equations for the non-volatile solvent. These equations would then yield results similar to that for the equation for non-volatile solutes. Equations for both volatile and non-volatile solvents were used to determine their validity.

8.1.8.2 Rearrangement of Equations

In all cases the equations had to be rearranged in order to make the limiting activity coefficient easier to calculate. The experimental technique for obtaining data for the calculation of limiting activity coefficients from all the equations is the same. For Equations 6.23, 6.29, 6.55 and 6.65 the slope (a) was obtained by plotting $ln(A/A_0)$ against time (t) and for Equations 6.24 and 6.33 the slope was obtained from plots of $ln(A/A_0)$ versus $ln\left(1-\frac{PDP_s^{sat}t}{(P-P_s^{sat})NRT}\right)$. The resulting limiting activity coefficients were calculated very differently for each equation. The equations used to determine the limiting activity coefficients are shown in Table 8-2.

Equation Number	Limiting Activity Coefficient Equation
6.23	$\frac{aNRT}{DP_{sol}^{sat}}$
6.24	$(a+1)\frac{P_s^{sat}}{P_{sol}^{sat}}$
6.29	$\frac{a}{\frac{-DP_{sol}^{sat}}{NRT}-a\left(\frac{V_G P_{sol}^{sat}}{NRT}-\frac{\tilde{n}P_{sol}^{sat}}{NP}\right)}$
6.33	$\frac{1}{\frac{P_{sol}^{sat}}{P_s^{sat}(a+1)}-\frac{P_{sol}^{sat}V_G}{NRT}}$
6.55	$\frac{NRT}{\varphi_{sol}^{sat}P_{sol}^{sat}\left(\frac{D(1+P_s^{sat}/P)}{a}+V_G\right)}$
6.65	$\frac{aNRT}{P_{sol}^{sat}D}\left(1-\frac{P_s^{sat}}{P}\right)k_1k_2k_3k_4$

Table 8-2: Equations for the determination of limiting activity coefficients after linearization to determine slope a.

8.1.8.3 Quantifying Equation Variables

The experimental pressure (P) was obtained by using a calibrated Sensotec transducer with a read-out in kPa. The inert gas flow rate (D) was obtained by taking the average of 3 readings from a soap bubble flow meter at the start, the middle and the end of the experiment. This was done also to observe that the flow rate was constant throughout the experiment. The saturated solute and solvent pressures were calculated using a newly derived equation by Nannoolal et al. (in preparation) and the pressures were compared using the well known Antoine equation. The pressures from the two equations are very similar.

The initial moles of solute (N) were obtained by measuring the mass of solvent added into the still and converted to moles by dividing by the molar mass. The temperature (T) was obtained using a Class A Pt-100 inserted into a jacket that fits into the cells. The areas (A) and time (t) was obtained from the integration program Clarity as a result of periodically injecting samples into the GC. All values were converted to SI units before calculating the limiting activity coefficients from the equations. This is important since there would be large inaccuracies.

8.1.9 Acquiring Solute Peak Areas

All plots to determine slope *a* are straight line plots formed with at least 5 points that lie on the line. In most cases all the points did lie along a straight line especially after taking the average of the areas obtained in a certain interval due to the injection method used. The experiments were repeated when this was not the case and usually it was due to contamination in the lines from chemicals that was used in the previous experiment. Compressed air was used to get rid of the trapped chemicals in the lines. For all the systems the solvents had a long residence time when compared to the solutes. As a result 3 to 4 injections could be made before the solvent reached the detector. Since there was a ramping program in place for the GC, 3 to 4 solute peaks (around 3 to 4 minutes apart) could be obtained and then the GC was ramped to higher temperatures for the faster movement of the solvent to the detector. The normal, ramped and column cleaning methods used for the Varian 3300 are shown in Table 8-3.

Device	Normal (°C)	Ramped (°C)	Cleaning (°C)
Column	110	200	220
Injector	180	210	230
Detector	190	215	230

Table 8-3: GC methods used for all systems under study

The four solute injections had to be completed within 20 minutes, after which the solvent peak from the first injection would appear. Without ramping it took around 1 hour for the solvent peak to completely pass through the column. With the effect of ramping the GC temperatures, it took around 20 minutes for the solvent to be removed completely. Another 10 minutes gets the temperature back to the original setting and the next injection can thus be made. These solute areas along with the residence times were then averaged resulting in a single area and residence time. Thus a single point on any of the slope plots took around 1 hour to obtain. The times mentioned are subject to GC settings and will vary for different GC's and columns. This approach was used for all the systems under investigation. The number of peaks that can be obtained depends on the carrier gas flow rate and the length of the column. Low flow rates and long columns will result in longer solvent residence times.

8.1.10 Analysis of Results - Test Systems

The proof of the pudding is in the analysis of the results. All the test systems have experimental values that have been compared to literatures values (Krummen et al. (2004)) where as far as possible the same conditions were maintained for consistency. For the test system cyclohexane (1) + NMP (2) there are deviations from literature values of no more than 0.49 % for all temperatures (Table 7-2), however the experimental temperatures are not exactly the same as the temperatures reported in literature. This is not a true reflection of the difference between experimental and literature values. If the experimental limiting activity coefficients were extrapolated or interpolated to obtain values at exactly the literature temperatures the deviation would be far less than 1 %. This was also true for the test systems n-heptane (1) + NMP (2) and n-hexane (1) + NMP (2). The maximum error tolerance allowed for limiting activity coefficients for all systems under investigation was 1 %.

A comparison of Tables 7-2, 7-7 and 7-12 show that the limiting activity coefficients calculated from Equations 6.23, 6.24, 6.29 and 6.33 are all lower than the limiting activity coefficients calculated from Equations 6.55 and 6.65. The difference between the limiting activity coefficients calculated from Equations 6.23, 6.24, 6.29 and 6.33 is very small and not greater than 0.5 % for all systems studied. There is very strong agreement between the limiting activity coefficients from these four equations as can be seen in Tables 7-7 to 7-9. This is expected because these equations are based on a similar derivation by Leroi et al. (1977) and were solved differently to eliminate some of the assumptions that were made. Also the types of systems studied favour all the equations. Equations 6.23 and 6.29 would not give accurate values of limiting activity coefficients if the systems studied consisted of solvents that are volatile, since it was derived for use with non-volatile solvents.

The ultimate challenge with the inert gas stripping technique was for multi-component systems. The technique and experimental set-up was put to the test with ternary systems where the solvent consisted of two non-volatile components, o-cresol and NMP (results in Chapter 7: Part 2). Also in this chapter are the two binary systems n-hexene (1) + NMP (2) and n-hexene (1) + o-cresol (2). The n-hexene + NMP system has literature values for limiting activity coefficients (Krummen et al (2004)), but here it was investigated at different temperatures. In essence this system can also be considered as a test system. The ternary systems and the n-hexene + o-cresol system have no known published data for limiting activity coefficients using this technique and possibly any other technique.

An indication of how close the experimental limiting activity coefficients for the system n-hexene (1) + NMP (2) is to the literature values within extrapolation and interpolation capacities is shown in Figures 7-17 and 7-21. The deviation when interpolating is not greater than 1 % for Equations 6.55 and 6.65. For the other equations (6.23, 6.24, 6.29 and 6.33) there is a considerable deviation (see Figures 7-18 to 7-20) from literature values of Krummen et al. (2004). One can only assume that this system somehow does not agree with the simplifying assumptions used to derive these equations.

8.1.11 Analysis of Results - New Systems

The systems involving o-cresol have no reported literature values for the limiting activity coefficient. A comparison of the experimentally obtained values with literature data was unfortunately not possible. Predictive methods or other experimental methods for the determination of limiting activity coefficients must be performed in order to confirm the accuracy of the results obtained. However due to time constraints, this was not possible. The limiting activity coefficients obtained for the new systems show no significant deviations from the trends obtained for the test systems and it has already been established that the calculated limiting activity coefficients for the test systems have excellent agreement with literature values.

From Figure 8-1 there is a clear trend for the n-hexene limiting activity coefficient against solvent concentration. There are two points that do not agree with the trend, the 35 and 45 °C values for the solvent system containing 40 % o-cresol. The rest if the data lie on a smooth parabolic curve. There may be some experimental errors which resulted in inaccuracies with regards to limiting activity coefficients at these conditions. When taking the average of the n-hexene limiting activity coefficients for the o-cresol systems and plotting that against o-cresol concentration a different situation arises (refer to Figure 8-9).

It can only be deduced from the accuracy of the test systems that the limiting activity coefficients for the new o-cresol systems are fairly accurate since the test systems were used to establish whether the equipment was working properly or not. There were no difficulties experienced with separation of the different components in the GC column. The solute peak areas obtained showed smooth curves when plotted against time. There is no reason to dismiss the results for the new systems until further work is done to verify the data.

The correction factors for Equation 6.65 give an indication of the system behaviour. There is a slight change of the stripping gas flow rate due to saturation in the cell as seen by k_1 being less than 1. There is very little solvent in the vapour space in the cell since k_3 is slightly greater than 1 and does not significantly affect the value of the limiting activity coefficient if left out. This is expected due to the low volatilities of the solvents. A significant change in k_4 shows that there is vapour-phase non-ideality. Only k_1 and k_4 significantly affect the limiting activity coefficients for all the systems studied. This work has added to the plethora of thermodynamic data available today. A summary of the results for the new systems is shown later in this chapter.

8.1.12 SCT versus DCT

The effect of using the SCT and DCT was also investigated. The binary system n-hexane (1) + NMP (2) was chosen to perform this task. From the results reported in Chapter 7, there is no significant evidence that the one technique is better or more suitable than the other. It was established that due to the nature of the components (the solvent having a low volatility and the solute a relatively high volatility) that both methods would be ideally suited. From literature it has been established that in most cases the SCT is not suited for multi-component solvent systems (Boa and Han (1995)), as the rate at which each component making up the solvent may be stripped differently, thus changing the concentration of the contents in the dilutor cell which will result in errors in the limiting activity coefficient. This theory was tested using the system n-hexene (1) + 20 %(m/m) o-cresol (2) + 80 %(m/m) NMP (2), the results of which have not been reported in Chapter 7.

Figure 8-2 shows a comparison of the results for the two techniques. The shape of the curve for the single cell technique is not reproducible for different flow rates as the solvent concentration is changing at different rates in the dilutor since the saturation cell in not present. The curve will probably have similar shape if experiments were performed using the same flow rate, but this is still to be confirmed as no such experiments were performed here.

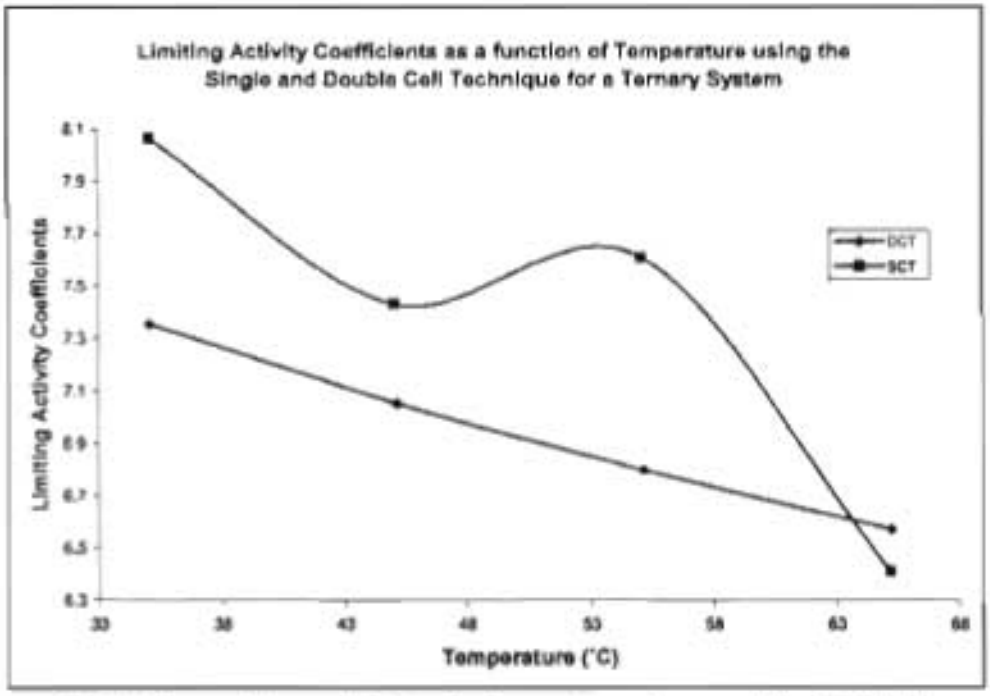

Figure 8-2: Limiting activity coefficients for the system n-hexene (1) + 20 %($^m/_m$) o-cresol (2) + 80 %($^m/_m$) NMP (2) obtained by using the single and double cell techniques.

The graph clearly shows that the single cell technique should not be used to determine limiting activity coefficients for these types of systems. For multi-component solvent systems this technique must be avoided at all costs. The overall scheme by Boa and Han (1995) should be followed in order to determine which technique to use. If there is still uncertainty as to which technique to use the double cell technique must be used.

For all systems studied the limiting activity coefficient decreases as temperature increases. When temperature increases the slope increases and the limiting activity coefficient should increase but the saturation fugacity coefficient and the solute saturation pressure decreases and the limiting activity coefficient ends up decreasing because of this. The saturation vapour pressure of non-volatile solutes do not affect the limiting activity coefficient as much as a volatile solvent. Therefore Equation 6.23 which does not even have the saturated solvent pressure term in it gives just as good results as the equations with the term. For highly volatile solutes Equation 6.23 cannot be used to determine limiting activity coefficients.

Equation 6.55 is the only equation that incorporates the saturation fugacity term into its expression, but Equation 6.65 accounts for non-idealities that may exist. For the highly non-ideal systems the other equations may result in large errors. Equations 6.55 and 6.65 should be considered for such systems. For the systems studied here all equations are suitable and have

been used with great success in terms of the results obtained. These equations have also been derived with some assumptions and one needs to bare in mind some of those assumptions when using the technique for various systems. The dilutor technique is only as good as the equations used to predict the limiting activity coefficients.

8.1.13 Extrapolation and Interpolation

It is often desired to extrapolate/interpolate limiting activity coefficients for other temperatures from the experimental data. This can be done either when using plots of limiting activity coefficient against temperature or from plots of ln (γ^{∞}) against inverse temperature. For the latter it is not always possible to regress the data linearly. If a re-representation of the data is required in order to extrapolate or interpolate for other experimental conditions then it should result a straight line. A plot of ln (γ^{∞}) against $100/T$ would result in a straight line that can be used for extrapolating or interpolating data (see Figures 8-3 to 8-4). This straight line effect was not observed for all the systems containing NMP as seen in Figure 8-3.

Clearly the best representation of the points is not a straight line but rather a third order polynomial. The literature values obtained from Krummen et al. (2004) show the same trend as that for the experimental values in Figure 8-3. For many systems in literature a straight line is observed (Gruber et al. (1999), Krummen and Gmehling (2004), Krummen et al. (2002) and Vrbka et al. (2002)) but this was not the case for all the systems containing NMP. However for the system n-hexene (1) + o-cresol (2) a straight line was observed. Figure 8-4 shows the result of this. This was the only system that was best represented by a straight line when plotting ln (γ^{∞}) against $100/T$. The ternary systems also resulted in a curve which was best represented by a second order polynomial.

This does not mean that the data is incorrect. For many systems this straight line effect is not observed (Miyano et al. (2004)). The obtained data is system dependant and in the case that linear regression gives a straight line it should be used for interpolation and extrapolation.

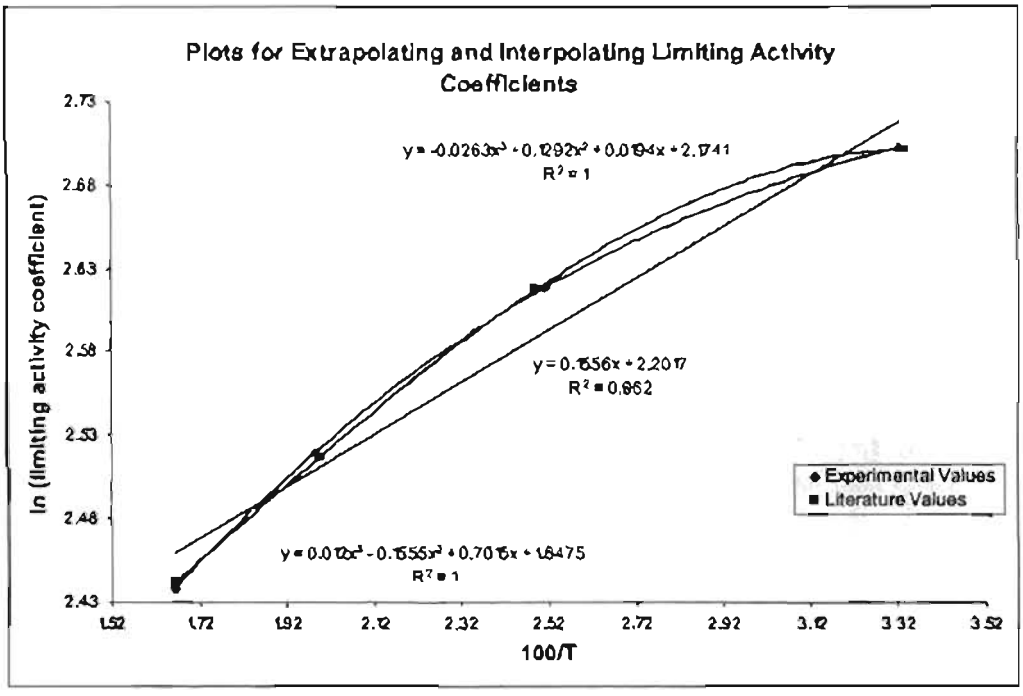

Figure 8-3: Re-represented activity coefficients for the test system n-heptane (1) + NMP (2) for extrapolation (original data can be found in Table 7.3)

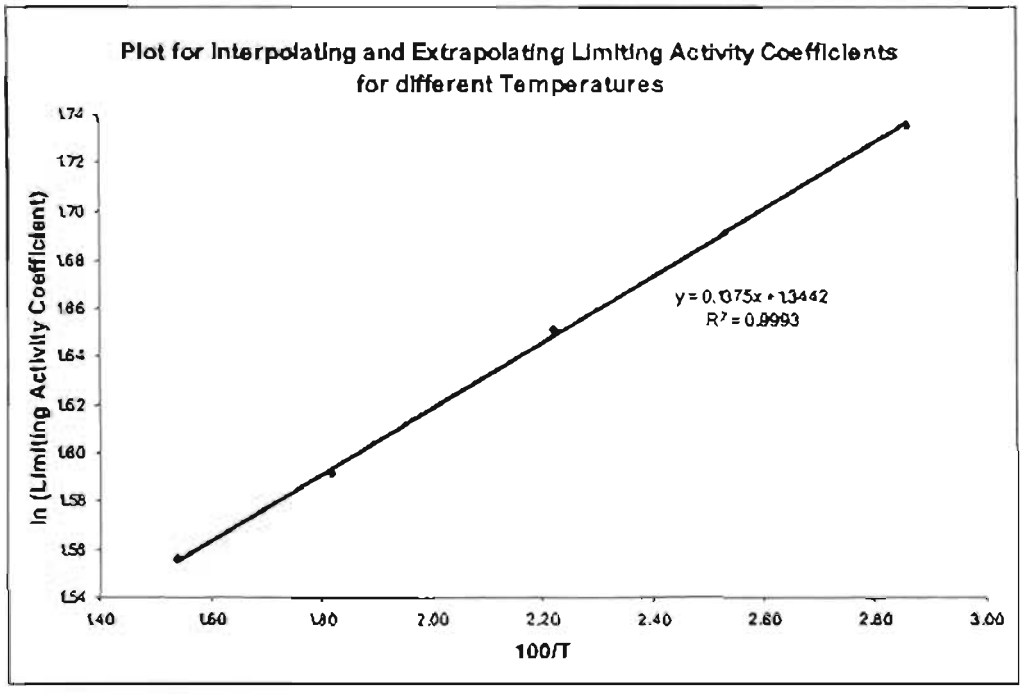

Figure 8-4: Straight line plot for extrapolating and interpolating limiting activity coefficients from Equation 6.55 for the binary system n-hexene (1) + o-cresol (2) at 10 ml/min. (See Table 7-21 for the original data)

8.1.14 Average Limiting Activity Coefficients

In Chapter 7 there are limiting activity coefficients reported for three different flow rates (approximately 10, 20 and 30 ml/min) and four temperatures (approximately 35, 45, 55 and 65 °C) and evaluated for 6 different equations (6.23, 6.24, 6.29, 6.33, 6.55 and 6.65). With so many limiting activity coefficient values, which one do you use as the correct value? An attempt has been made to average the limiting activity coefficients and have one value for the exact temperatures 35.00, 45.00, 55.00 and 65.00 °C. In order to do this tedious task, intense interpolation and extrapolation was done in order to get limiting activity coefficients at the same temperature for each system. This was then averaged for the different flow rates and corresponding temperatures to get one limiting activity coefficient for each temperature and equation. This can be done since based on the assumption of the method flow rate should not affect the limiting activity coefficient and was only varied to see if the data was reproducible.

All the averaged limiting activity coefficients were then averaged again across each equation to get one limiting activity coefficient that would best describe the system. Since for equations 6.23, 6.24, 6.29 and 6.33 the difference in limiting activity coefficients is less than 0.5 % this was averaged first and then interpolation or extrapolation was performed to get limiting activity coefficients at the desired temperatures. The calculation procedure is shown in Appendix B. Table 8-4 shows the results of this calculation for the system n-hexene + NMP.[5]

T (°C)	Average, Interpolated/Extrapolated γ^{∞}			Average γ^{∞}
	Krummen et al.	Leroi et al. based[5]	Hovorka and Dohnal	
25	6.59	6.55	6.53	6.56
35	6.29	6.22	6.26	6.26
45	5.99	5.90	5.99	5.96
55	5.70	5.59	5.73	5.68
65	5.43	5.29	5.48	5.40
75	5.16	5.01	5.24	5.14

Table 8-4: Average limiting activity coefficients for the system n-hexene (1) + NMP (2)
(Original data can be found in Tables 7-16 to 7-20)

The average limiting activity coefficients calculated from Equations 6.23, 6.24, 6.29 and 6.33 were not taken into account for the calculation of the average limiting activity coefficient in column 5 of Table 8-3. The deviation of the limiting activity coefficients between these equations with Equations 6.55 and 6.65 is greater than 1 %. Limiting activity coefficients for 25 and 75 °C

[5] The Leroi et al. based equations include the equations derived by Duhem and Vidal (1978) and Boa and Han (1995)

were obtained by extrapolating limiting activity coefficients for each equation and flow rate. The new trend of limiting activity coefficient with temperature for the system n-hexene + NMP is shown in Figure 8-5. Figure 8-5 is the best representation of the data since the limiting activity coefficients have been averaged across each equation and flow rate.

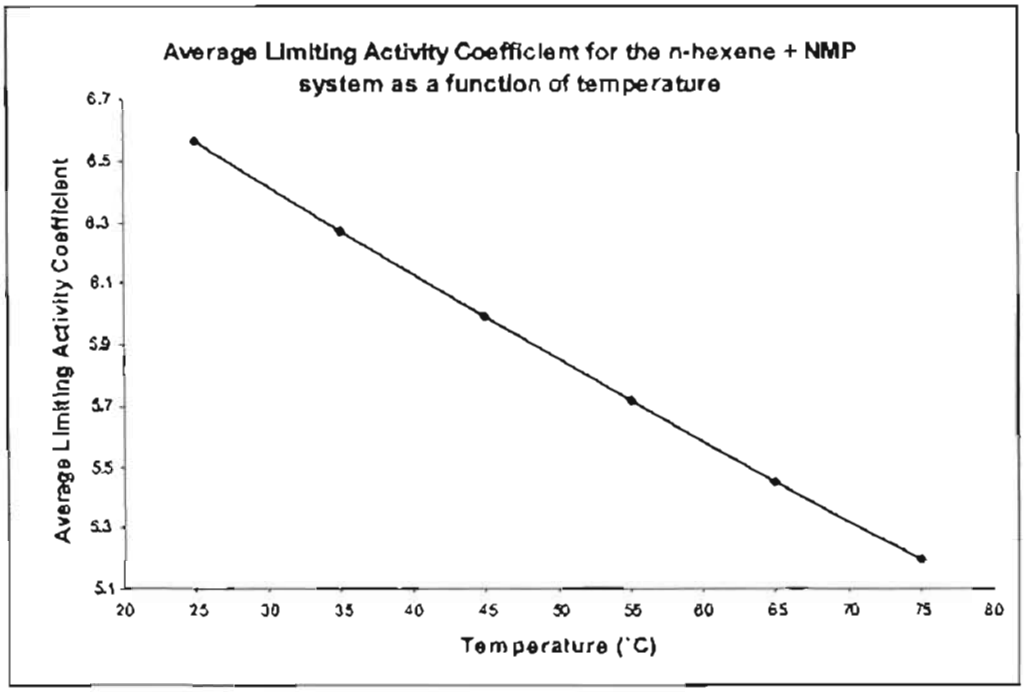

Figure 8-5: Average limiting activity coefficients for the system n-hexene + NMP evaluated from equations by Krummen et al. (2000) and Hovorka and Dohnal (1997)

The next system under investigation was n-hexene + o-cresol and for this system all the systems from hereon, the limiting activity coefficients from every equation was taken into consideration for the average limiting activity coefficient. For the system containing solvent o-cresol only, a plot of $\ln(\gamma^{\infty})$ against the inverse of temperature resulted in a straight line (Figure 8-4) unlike for the systems containing NMP. These plots were used for interpolating and extrapolating.

T (°C)	Average, Interpolated/Extrapolted γ^{∞}			Average γ^{∞}
	Krummen et al.	Lerol et al. based	Hovorka and Dohnal	
35	5.68	5.46	5.51	5.55
45	5.21	5.03	5.13	5.12
55	4.93	4.77	4.89	4.86
65	4.74	4.60	4.74	4.69

Table 8-5: Average limiting activity coefficients for the system n-hexene (1) + o-cresol (2). (Data used from Tables 7-21 to 7-25)

Figure 8-6 shows a plot of average limiting activity coefficients where the data has been extrapolated in order to obtain activity coefficients for 25 and 75 °C.

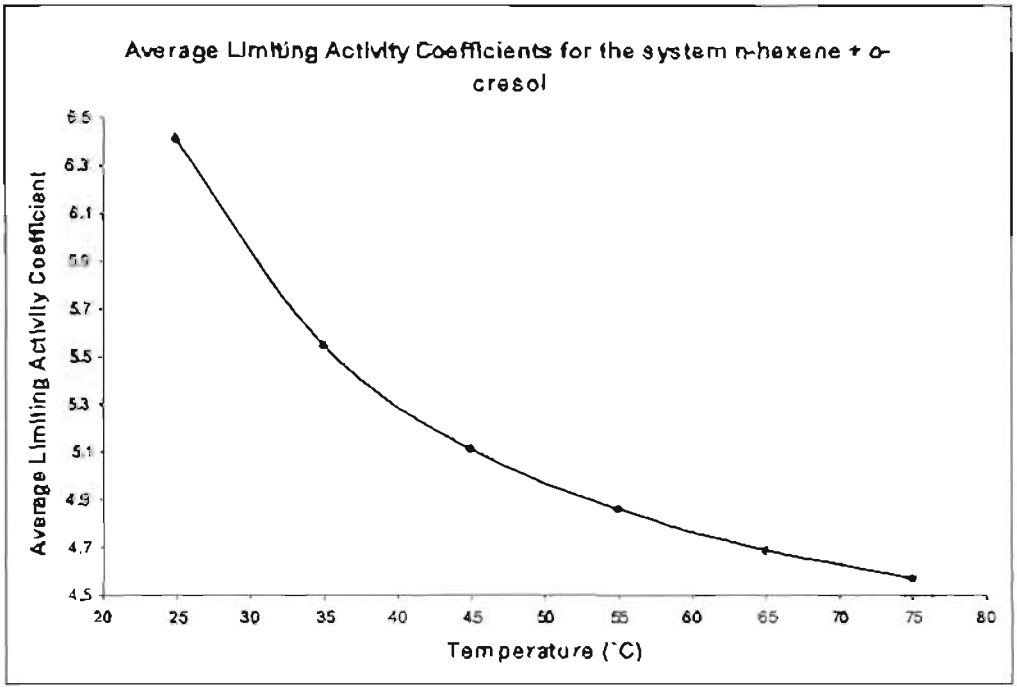

Figure 8-6: Trend of average limiting activity coefficients with the effect of temperature for the system n-hexene (1) + o-cresol (2)

The average limiting activity coefficients for the system n-hexene (1) + 20 %($^m/_m$) o-cresol (2) + 80 %($^m/_m$) NMP (2) can be found in Table 8-6.

T (°C)	Average, Interpolated/Extrapolated γ^∞			Average γ^∞
	Krummen et al.	Leroi et al. based	Hovorka and Dohnal	
25	7.69	7.65	7.62	7.66
35	7.36	7.30	7.32	7.33
45	7.06	6.99	7.04	7.03
55	6.79	6.71	6.79	6.76
65	6.55	6.46	6.57	6.53
75	6.35	6.25	6.37	6.32

Table 8-6: Average limiting activity coefficients for the system n-hexene (1) + 20 %($^m/_m$) o-cresol (2) + 80 %($^m/_m$) NMP (2). (Data re-represented from Tables 7-26 to 2-30)

For this system a plot of limiting activity coefficient against temperature is shown in Figure 8-7. Also in Figure 8-7 are two additional points obtained via extrapolation as shown below.

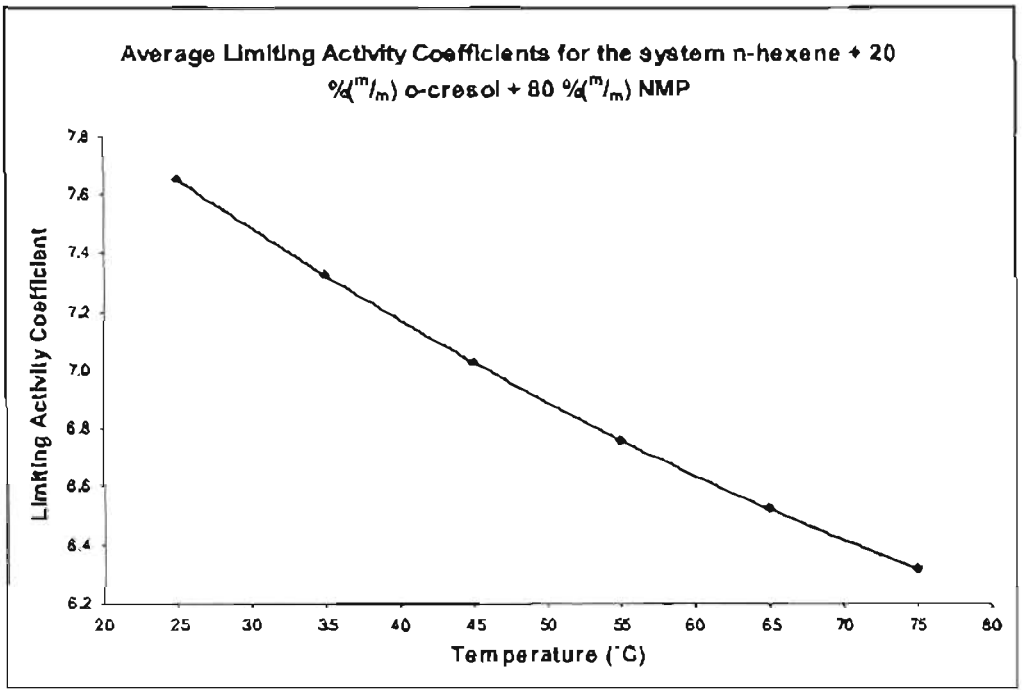

Figure 8-7: Average limiting activity coefficients as a function of temperature for the system n-hexene (1) + 20 %($^{m}/_{m}$) o-cresol (2) + 80 %($^{m}/_{m}$) NMP (2)

Average limiting activity coefficients for the system n-hexene (1) + 40 %($^{m}/_{m}$) o-cresol (2) + 60 %($^{m}/_{m}$) NMP (2) is shown in Table 8-7.

T (°C)	Average, Interpolated/Extrapolated γ^{∞}			Average γ^{∞}
	Krummen et al.	Leroi et al. based	Hovorka and Dohnal	
25	7.46	7.42	7.39	7.42
35	7.21	7.16	7.19	7.19
45	7.02	6.96	7.03	7.00
55	6.87	6.80	6.91	6.86
65	6.78	6.70	6.84	6.77
75	6.75	6.66	6.80	6.73

Table 8-7: Average limiting activity coefficients for the system n-hexene (1) + 40 %($^{m}/_{m}$) o-cresol (2) + 60 %($^{m}/_{m}$) NMP (2). (Data averaged from Tables 7-31 to 7-35)

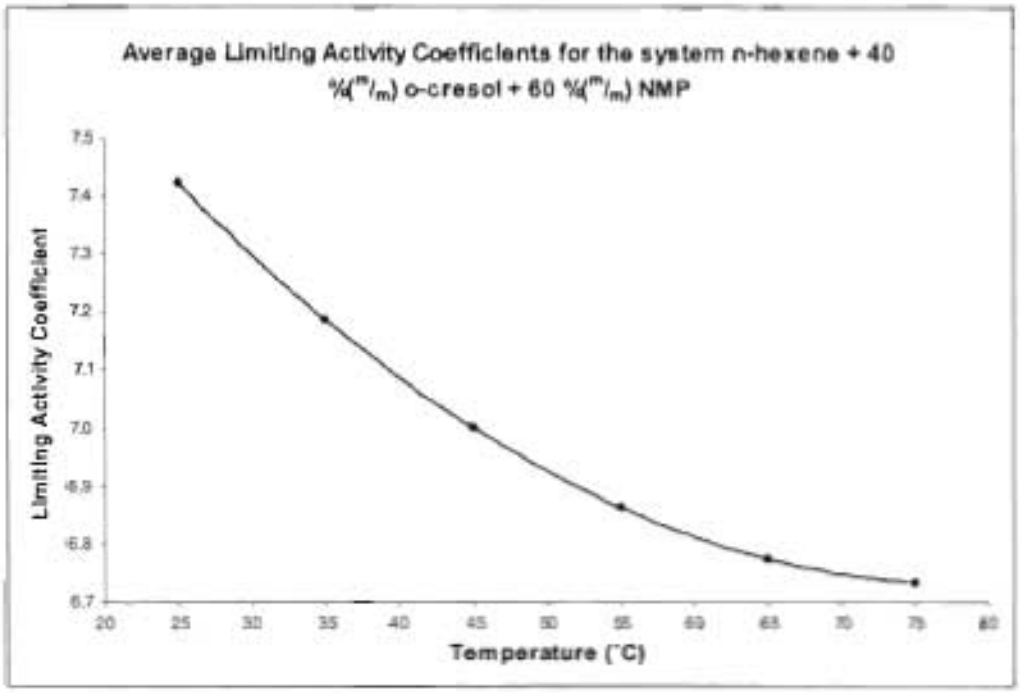

Figure 8-8: Trend of average limiting activity coefficients for the system n-hexene (1) + 40 %(m/m) o-cresol (2) + 60 %(m/m) NMP (2)

Average limiting activity coefficients for the system n-hexene (1) + 60 %(m/m) o-cresol (2) + 40 %(m/m) NMP (2) is shown in Table 8-8.

T (°C)	Average, Interpolated/Extrapolated γ^{∞}			Average γ^{∞}
	Krummen et al.	Leroi et al. based	Hovorka and Dohnal	
25	7.80	7.70	7.68	7.73
35	7.56	7.47	7.53	7.52
45	7.33	7.24	7.36	7.31
55	7.14	7.02	7.18	7.11
65	6.97	6.80	6.98	6.91
75	6.83	6.58	6.76	6.72

Table 8-8: Average limiting activity coefficients for the system 60 %(m/m) o-cresol (2) + 40 %(m/m) NMP (2) (Limiting activity coefficients averaged from Tables 7-36 – 7-40)

Average limiting activity coefficients for the system n-hexene (1) + 80 %(m/m) o-cresol (2) + 20 %(m/m) NMP (2) is shown in Table 8-9.

T (°C)	Average, Interpolated/Extrapolated γ^{∞}			Average γ^{∞}
	Krummen et al.	Leroi et al. based	Howorka and Dohnal	
25	7.41	7.35	7.18	7.31
35	7.18	7.11	6.95	7.08
45	6.97	6.88	6.73	6.86
55	6.78	6.67	6.51	6.65
65	6.60	6.47	6.29	6.45
75	6.44	6.29	6.08	6.27

Table 8-9: Average limiting activity coefficients for the system -hexene (1) + 80 %($^{m}/_{m}$) o-cresol (2) + 20 %($^{m}/_{m}$) NMP (2) (Limiting activity coefficients averaged from Tables 7-36 to 7-40)

A plot of average limiting activity coefficients against o-cresol concentration results in the system for the 60 % o-cresol solvent displaying some interesting behaviour as shown in Figure 8-9.

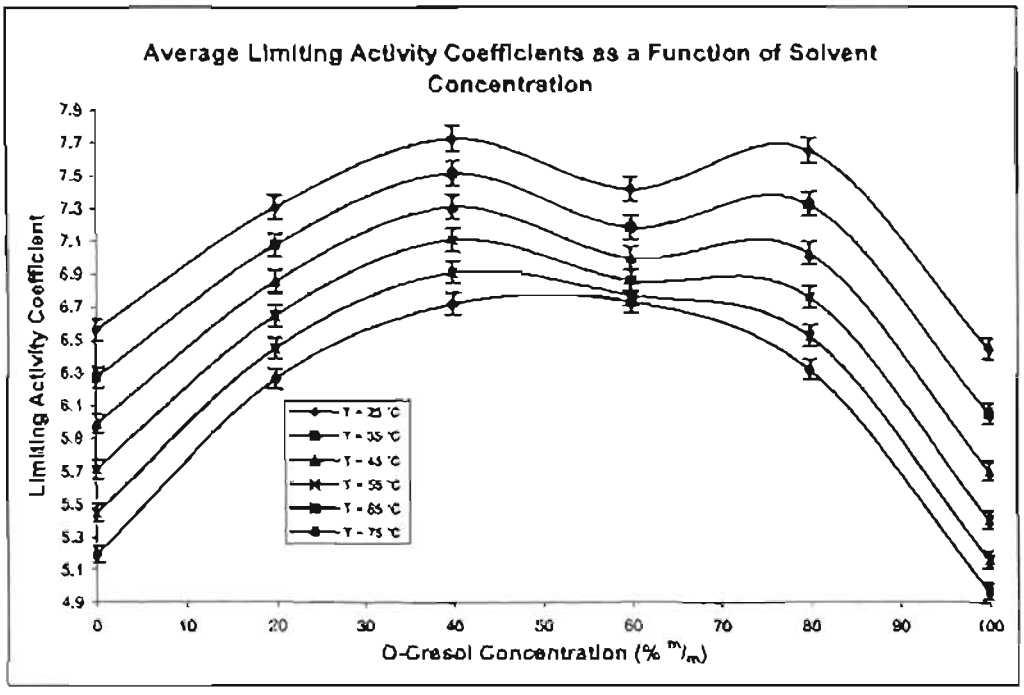

Figure 8-9: Average limiting activity coefficients for each temperature as a function of o-cresol concentration in the solvent mixture

The shape of the graph is reliable as reproducibility tests have been done and it was found that a deviation of less than 1 % was observed for all data points on Figure 8-9. At the lower temperatures the activity coefficients do not agree with the trend but as temperature increases the deviation from the apparent trend decreases. At 75 °C the deviation is no longer there and a smooth curve is obtained. The slightly lower activity coefficients for this system mean that it is more ideal at lower temperatures than expected from the trend in Figure 8-9.

8.1.15 Sensitivity Analysis

A sensitivity analysis was performed in order to check what effect errors in the measured variables (pressure, temperature, solvent mass in the dilutor cell and inert gas flow rate) would have on the limiting activity coefficient. After some careful consideration it was determined that the pressure in the cell does not vary by more than 150 Pa (> 1 mmHg). The limiting activity coefficients obtained due to an increase and decrease in pressure by 150 Pa resulted in no significant deviation in the limiting activity coefficient. It was only at pressure changes of around 10000 Pa that significant changes were observed in the limiting activity coefficients obtained from Equation 6.55. An error of this magnitude is not possible with a Sensotec pressure transducer.

8.1.15.1 Uncertainty in Temperature Readings

With regard to temperature it was established that there may be a small error that can be attributed to the Class A Pt-100. The Class A Pt-100 has an accuracy that can be described using Equation 8.1.

$$Error\ in\ K = 0.15 + \left(0.002 \times \left|T(^{\circ}C)\right|\right) \qquad 8.1$$

Equation 8.1 gives the maximum error in Kelvin for a Class A Pt-100.[6] The maximum error would thus result for the highest operating temperature which was 65 °C. This would result in an error of ± 0.28 K. The errors in the limiting activity coefficient are shown below:

Experimental Data		Pt-100 Error	Corrected	Deviation
T (°C)	γ^{∞}	(K)	γ^{∞}	(%)
35.35	6.282	0.221	6.286	0.06
45.18	5.971	0.240	5.976	0.08
55.04	5.685	0.260	5.689	0.07
64.82	5.414	0.280	5.417	0.06
35.35	6.282	-0.221	6.277	-0.08
45.18	5.971	-0.240	5.967	-0.07
55.04	5.685	-0.260	5.680	-0.09
64.82	5.414	-0.280	5.408	-0.11

Table 8-10: Deviation of limiting activity coefficients for the system n-hexene (1) + NMP (2) due to errors in temperature when using a Pt-100.

[6] www.leiderdorpinstruments.nl/International%20web/Temperatuursensoren

A negative deviation means that the limiting activity coefficient is smaller than the original value. A maximum positive error of 0.08 % and a maximum negative error of -0.11 % can be attributed to errors in the temperature readings. This is not a significant error. Temperature affects the solute and solvent vapour pressures as well as the saturated fugacity coefficient and these calculated variables affect the limiting activity coefficient significantly. The limiting activity coefficient is extremely sensitive to the solute saturation pressure which in turn, due to the high volatility of the solute, is very sensitive to temperature.

8.1.15.2 Uncertainty in Mass Readings

The precision of measurements made with a digital instrument, such as a mass balance, is based predominantly on the reading uncertainty. The uncertainty in reading a digital scale is ± 0.5 of the last resolvable digit, i.e. if the mass balance reads to the nearest 0.01 g the reading uncertainty is ± 0.005 g. However, the uncertainty when the scale reads 0.00 g is also ± 0.005 g, so the total reading uncertainty would be given by (0.005 g + 0.005 g) = ± 0.01 g.[7] Errors in the mass of solvent filled into the dilutor cell are estimated to be around ± 0.01 g. This results in a very small insignificant error in the limiting activity coefficients. The sensitivity analysis was performed for an error 10 times that as shown in Table 8-11. The result shows that errors in mass do not affect limiting activity coefficients substantially. The error is well below the error tolerance of 1 % even for an exaggerated error in the mass reading.

Experimental Data			Error in Mass	Corrected	Deviation
T (°C)	Solvent Mass (g)	γ^{∞}	(g)	γ^{∞}	(%)
35.35	114.83	6.282	0.1	6.287	0.08
45.18	114.83	5.971	0.1	5.977	0.10
55.04	114.83	5.685	0.1	5.690	0.09
64.82	114.83	5.414	0.1	5.417	0.06
35.35	114.83	6.282	-0.1	6.276	-0.10
45.18	114.83	5.971	-0.1	5.966	-0.08
55.04	114.83	5.685	-0.1	5.680	-0.09
64.82	114.83	5.414	-0.1	5.408	-0.11

Table 8-11: Deviation of limiting activity coefficients due to errors in mass readings for the solvent NMP.

[7] www.hyperion.cc.uregina.ca/bergbusp/~uglabs/p109/Experiments/EXPT02Meas&Error007.pdf

8.1.15.3 Uncertainty in Flow Rate Readings

There are definitely errors when obtaining flow rate from the soap bubble flow meter due to reaction time when timing the rising ring and errors of parallax when looking at the increments on the burette like tube. The rule of thumb for estimating uncertainty in direct reading devices (things that don't have digital displays) is to use ± 0.25 the smallest scale division in a single reading. But, since in this case it takes two readings to make a measurement, one at each end of the burette like tube (start timing at 0 ml and stop at 10 ml), the total reading uncertainty is actually ± 0.5 the smallest scale division. The smallest scale division on the soap bubble flow meter is 1 ml, therefore the maximum error in reading is ± 0.5 ml.[8]

There is also an error due to reaction time. A small study was conducted on the effect of human reaction time on stopwatch and timer calibration uncertainties by Gust et al. (2004). They have concluded that the average reaction time is usually ± 230 ms. The effect of reaction time and error of parallax needs to be accounted for simultaneously in the sensitivity analysis. The effect of this on the limiting activity coefficient is shown in Tables 8-12 to 8-13.

Experimental Data			Error in t	Corrected	Deviation
T (°C)	D (ml/min)	γ^{∞}	(s)	γ^{∞}	(%)
35.35	10.126	6.282	0.23	6.33	0.76
45.18	10.122	5.971	0.23	6.017	0.77
55.04	10.014	5.685	0.23	5.728	0.76
64.82	10.004	5.414	0.23	5.454	0.74
35.35	10.126	6.282	-0.23	6.233	-0.78
45.18	10.122	5.971	-0.23	5.924	-0.79
55.04	10.014	5.685	-0.23	5.641	-0.77
64.82	10.004	5.414	-0.23	5.371	-0.79

Table 8-12: Deviations in the limiting activity coefficient due to a reaction time of ± 230 ms when using the stopwatch to measure the flow rate of the inert gas

[8] www.leiderdorpinstruments.nl/International%20web/Temperatuursensoren

Experimental Data			Error in volume (v)	Corrected	Deviation
T (°C)	D (ml/min)	γ^{∞}	(ml)	γ^{∞}	(%)
35.35	**10.126**	**6.282**	**0.5**	**5.711**	**-9.09**
45.18	10.122	5.971	0.5	5.428	-9.09
55.04	10.014	5.685	0.5	5.168	-9.09
64.82	10.004	5.414	0.5	4.921	-9.11
35.35	10.126	6.282	-0.5	6.979	11.10
45.18	10.122	5.971	-0.5	6.633	11.09
55.04	10.014	5.685	-0.5	6.315	11.08
64.82	10.004	5.414	-0.5	6.013	11.06

Figure 8-13: Deviation in limiting activity coefficients due to an error of parallax of 0.5 ml when reading the soap bubble flow meter.

The deviation in limiting activity coefficient due to reaction time is not as significant as that for the error of parallax. The sensitivity analysis shows that the limiting activity coefficient is extremely sensitive to the inert gas flow rate. Due to financial constraints it was not possible to purchase an electronic gas flow meter. The gas flow rate was measured several times during the experiment and the average value taken as the flow rate for the run. The effect of a simultaneous combination of all errors (Tables 8-10 to 8-13) on the limiting activity coefficient is shown in Table 8-14. The first row in the table has the actual measured values obtained from the experiment. Rows 2-3 show only the maximum possible errors in the limiting activity coefficient calculated from Equation 6.55. This is the result of the combination that would give the maximum possible error.

T	Solvent Mass	D	Experimental	Corrected	Deviation
(°C)	(g)	(ml/min)	γ^{∞}	γ^{∞}	(%)
35.35 (+0.22)	114.83 (-0.1)	10.126 (t=-0.23 v=+0.5)	6.282	5.666	-9.81
35.35 (-0.22)	114.83 (+0.1)	10.126 (t=+0.23 v=-0.5)	6.282	7.034	11.97
45.18 (+0.24)	114.83 (-0.1)	10.122 (t=-0.23 v=+0.5)	5.971	5.395	-9.65
45.18 (-0.24)	114.83 (+0.1)	10.122 (t=+0.23 v=-0.5)	5.971	6.685	11.96
55.04 (+0.26)	114.83 (-0.1)	10.01 (t=-0.23 v=+0.5)	5.685	5.128	-9.80
55.04 (-0.26)	114.83 (+0.1)	10.01 (t=+0.23 v=-0.5)	5.685	6.364	11.94
64.82 (+0.28)	114.83 (-0.1)	10.004 (t=-0.23 v=+0.5)	5.414	4.883	-9.81
64.82 (-0.28)	114.83 (+0.1)	10.004 (t=+0.23 v=-0.5)	5.414	6.059	11.91

Table 8-14: Maximum deviations in the limiting activity coefficient determined from Equation 6.55 as a result of a combination of errors in the experimentally measured variables.

A maximum positive error of 11.9 % and a maximum negative error of -9.8 % were observed with all the reported limiting activity coefficients obtained from Equation 6.55. This means that if

there is an error in the measured variables the actual limiting activity coefficient for T = 35 °C lies between 5.66 and 7.03. For peace of mind the entire equipment was very well insulated and the Class A Pt-100 is a very high precision devise for measuring temperature and when calibrated correctly will give extremely accurate temperatures. The calibration curve for the dilutor cell Pt-100 can be found in Chapter 4 (Figure 4-5). This was done for all the other equations as well and the maximum errors for each equation as a result of possible errors in the experimentally measured values are reported in Table 8-15.

Equation	Maximum Positive Deviation (%)	Maximum Negative Deviation (%)
6.55	11.97	-9.81
6.23	8.34	-13.46
6.24	7.95	-13.87
6.29	7.92	-13.84
6.33	8.17	-13.63
6.65	11.48	-10.01

Table 8-15: Percentage deviation range for calculated limiting activity coefficients for each equation as determined via sensitivity analysis for the system n-hexene (1) + NMP (2).

The range of error percentages for the limiting activity coefficient is different for all equations used to determine it. All the limiting activity coefficients in Chapter 7 calculated from their respective equations share similar deviations in the actual reported values given in Table 8-14. It is not exactly the same, as the different solutes have their own volatilities affecting the system differently. However it can only be speculated that there is an uncertainty in the reported limiting activity coefficients, as it is uncertain as to whether there may be errors or not when measuring temperature, pressure and flow rate. The calculated limiting activity coefficient values themselves do not show any significant indication as to whether their values may be compromised by errors in the experimentally determined variables. For any given experimental condition the graphs show smooth trends with very little differences in the limiting activity coefficients measured at different inert gas flow rates.

8.1.16 Sources of Error

There are some imperfections in the design of the equipment used for the inert gas stripping technique. Some of the difficulties experienced and the errors as a result off, are outlined below. Some recommendations have also been provided in order to prevent these errors.

8.1.16.1 Experimental Difficulties

- Due to the pressure build-up in the cell, it became necessary to clamp the Teflon plug.
- The heated lines gave rise to power trips each time the variac was turned on. The problem was rectified by removing the existing insulation and re-insulating those lines. This involved insulating the line first, then wrapping the insulated nichrome wire around the line.
- When using the bubble flow meter, it was observed that there was an inconsistency in the flow measurement. The flow rate varied by ±0.5 ml min^{-1}. This was due to the coalescence of smaller bubbles into one large bubble when the upward movement of the smaller bubbles was hampered by the ceramic-based glue surrounding the branch point of the capillaries.
- The GC was unable to produce a perfect component split with some systems such as acetone (1) + heptane (2). Despite all attempts it was not possible to determine limiting activity coefficients for that system without the use of another GC or column.

8.1.16.2 Experimental Errors

- Leaks around the Teflon plug and through fittings attached to the plug at high inert gas flow rates. Detection of leaks found using Snoop™, which does not leave any residue when dried. Attempts were made to stop leaks using Loctite™ adhesion but this does not adhere to Teflon but it did manage to minimize the leaks especially at low inert gas flow rates and at low temperatures.
- The sample loop was not a single complete loop, but rather made up of three smaller parts joined together. As a result the sample loop was too large for sample injection into the GC. Attempts were made to reduce the length of the loop, but due to the diameter and stiffness of the material making up the loop, this was not possible and a relatively large sample was still injected in to the GC. It was observed that a very small sample of gas injected into the GC gave better separation of the components.
- Inaccurate flow measurement using the bubble flow meter. Due to the gas flow meter not functioning properly, the bubble flow meter had to be used for flow measurement. Due to reaction times when using the stopwatch the flow rates could not be accurately determined as desired. It was very difficult to control the

gas flow rate using the gas flow meter as it took a long time for the gas to pass through the system to the bubble flow meter for measurement.

- Error in flow measurement due to coalescence of small bubbles into larger bubbles. Large bubbles caused flow variations.

Chapter IX – Conclusion

The research presented in this work represents a detailed look at the intricate determination of limiting activity coefficients at infinite dilution. The calculation of limiting activity coefficients in the region of infinite dilution is known to be especially tedious, but of special importance for problems which are common in various industrial processes. Therein lies the dedication, motivation and perseverance for pursuing this work. Of all the methods to determine limiting activity coefficients the IGS technique has most appeal and will be growing in potential as a technique in the years to come.

The IGS method requires neither calibration of the chromatographic detector nor any tedious preparation of the experimental device. It was shown that it is quiet simple to obtain values for limiting activity coefficients in different solvents and solvent mixtures with high reliability using the dilutor technique. A comparison with published limiting activity coefficients, where possible, shows good agreement. The dilutor technique is particularly suited for the measurement of limiting activity coefficients in solvent mixtures because the use of the saturator cell guarantees a constant solvent composition in the measurement cell. Other techniques for example Gas Liquid Chromatography (GLC) are not suited for the measurement of limiting activity coefficients in solvent mixtures.

Furthermore it has the advantage that it is possible to study the limiting activity coefficient of any solute dissolved in any multi-component mixture and even with volatile solvents the only condition being the separation of the peaks of the solutes. By use of the inert gas stripping method, infinite dilution activity coefficients for different types of systems, especially for those containing multi-component solvents have been determined directly with high reproducibility (standard deviations less than 1 % for all systems investigated). Thus, application of limiting activity coefficients would be more efficient than before.

The inert gas stripping technique is a very attractive method for the determination of limiting activity coefficients and with proper cell design can be extended to the determination of Henry's constants. The technique is quiet simple and does not require tedious preparations. The accuracy of the measurements is good and this method is generally more reliable as it is a direct method. This technique, being a direct method, will have more preference by industries for experimental and theoretical investigation of their complex chemical systems in the future. There

is scope for further investigations into this technique as the types of systems that can be analysed are endless.

The inert gas stripping method is well suited for the determination of limiting activity coefficients for all types of systems. The reliability of the newly built apparatus for the determination of limiting activity coefficients using binary and ternary systems has been demonstrated by the highly accurate and reproducible results obtained. There is still room for exploring more complex higher order systems which other techniques find difficult to analyse. Also with detector calibration it is possible to study the variation of the solute activity coefficient with its concentration in the liquid mixture with the same equipment. For these reasons it may be expected that this method could be used in theoretical investigations as well as future industrial problems of solvent screening for separation processes.

Chapter X – Recommendations

A number of changes and improvements can be made to the existing equipment in order to minimize errors. However the equipment was suitable for the types of systems studied. Below are some of the recommended changes that can be made and some of the protocols that need to be followed in order to obtain accurate results.

- In the case of pressure build-up at the higher flow rates, the Teflon plug should be clamped in order to avoid leaks.
- A 200 - 500 µl sample loop should be used in order to have a sample size that is not too big or small for a perfect split of the injected components.
- The use of a thermo-statted soap bubble flow meter or thermo-statted electronic flow meter to monitor any temperature changes in the gas leaving it.
- Every equipment or material that comes in contact with the inert gas and absorbed vapours need to be thermo-regulated to avoid condensation and temperature variations after entering the system.
- The use of a more efficient stirrer would aid in creating smaller bubbles and provide better dispersion of the bubbles in the gas phase (the one used in this experiment was too small; a larger stirrer could not be used due to the small size of the cell and the length of the capillaries).
- The use of a more appropriate GC (different type of column, packing, etc.) would result in better separation for multi-component systems.
- If an appropriate GC is not available, then low carrier gas flow rates and column temperatures should be used for effective component separation.
- A sample septum should be included in the cell in order to take liquid samples. These samples can be analysed using the Gas Chromatography method, which can serve as a consistency check for computed activity coefficients at infinite dilution values.
- Electronic flow measurement devices should be used to measure the flow rate of the inert gas.
- The entire equipment should be built in an oven so that everything can be at system temperature and as a result there won't be any condensation taking place in the any of the lines.

- A cold finger should be immersed in the cold trap to keep the acetone as cold as possible throughout the experiment so that the correct nitrogen gas flow rate can be measured.
- The "O' -rings should not come in contact with the liquid in the cell as this could cause it to swell and must then be replaced.
- Do not leave chemicals in the cells once the experiment has been completed as this will result in longer start-up times i.e. the time required to flush the equipment from unwanted vapours is longer.
- The chemicals in the cell will move up the capillaries when the gas is shut off and this then becomes difficult to clean. It is preferable that the capillaries are removed from the equilibrium cells or the solution is removed before stopping the flow of inert gas to the system.

References

Journal References

1. ABRAHAM M. H., (1993), *"Scales of solute hydrogen-bonding: their construction and application to physicochemical and biochemical processes"*, **Chem. Soc. Rev.**, Vol. 22, Pg. 73-83

2. ANAND S. C., GROLIER J-P. E., KIYOHARA O., HALPIN C. J. & BENSON G.C., (1975), *"Thermodynamic Properties of some Cylcoalkane-Cycloalkanol Systems at 298.15 K. III."*, **Journal of Chemical and Engineering Data**, Vol. 20, Pg. 184-189

3. ASPRION N., HASSE H. & MAURER G., (1998), *"Limiting Activity Coefficients in Alcohol-Containing Organic Solutions from Headspace Gas Chromatography"*, **J. Chem. Eng. Data**, Vol. 43, Pg. 74-80

4. ATIK Z., GRUBER D., KRUMMEN M. & GMEHLING J., (2004), *"Measurement of Activity Coefficients at Infinite Dilution of Benzene, Toluene, Ethanol, Esters, Ketones and Ethers at Various Temperatures in Water Using the Dilutor Technique"*, **Journal of Chemical Engineering Data**, Vol. 49, Pg. 1429-1432

5. BAO J. B. & HAN S-J., (1992), *"Two developments of gas stripping method for determination of infinite dilution activity coefficients"*, **Natural Gas Chem. Ind.**, Vol. 17, Pg. 53-56

6. BAO J. B. & HAN S-J., (1995), *"Infinite Dilution Activity Coefficients for Various Types of Systems"*, **Fluid Phase Equilibria**, Vol. 112, Pg. 307-316

7. BAO J. B., HANG L. L. & HAN S-J., (1994), *"Infinite Dilution Activity Coefficients of (propanone + an n-alkane) by Gas Stripping"*, **J. Chem. Thermodynamics**, Vol. 26, Pg. 673-680

8. BAO J. B., HANG L. L., LING Y-P., CHEN G-H. & HAN S-J., (1993a), *"Studies on the determination of infinite dilution activity coefficients of acetone-cycloalkane systems by gas stripping method"*, **Chem. J. Chin. Univ.**, Vol. 14, Pg. 1280-1283

9. BOA J. B., HUANG Q., CHEN G-H & HAN S-T. (1993b), *"Determination of large value activity coefficients at infinite dilution"*, **Acta Phys. Chem.**, Vol. 9, Pg. 724-727

10. BOA J. B., LIU W-P. & HAN S-J., (1990), *"The measurement of infinite dilution activity coefficients for alcohol-n-alkane systems by gas stripping method"*, **J. Zhejiang Univ.**, Vol. 24, Pg. 374-382

11. BURNETT M. G., (1963), *"Determination of partition coefficients at infinite dilution by the gas chromatographic analysis of the vapor above dilute solutions"*, **Analytical Chemistry**, Vol. 35, Pg. 1567-1570

12. CORI L. & DELOGU P., (1986), *"Infinite dilution activity coefficients of ethanol-n-alkanes mixtures"*, **Fluid Phase Equilibria**, Vol. 27, Pg. 103-118

13. DALLINGA L., SCHILLER M. & GMEHLING J., (1993), *"Measurement of Activity Coefficients at Infinite Dilution Using Differential Ebulliometry and Non-Steady State Gas Liquid Chromatography"*, **Journal of Chemical Engineering Data**, Vol. 38, Pg. 147-155

14. DOHNAL V. & HORAKOVA I., (1991), *"A New Variant of the Rayleigh Distillation Method for the Determination of Limiting Activity Coefficients"*, **Fluid Phase Equilibria**, Vol. 68, Pg. 173-185

15. DOHNAL V. & HOVORKA S., (1999), *"Exponential Saturator: A Novel Gas-Liquid Partitioning Technique for Measurements of Large Limiting Activity Coefficients"*, **Ind. Eng. Chem. Res.**, Vol. 38, Pg. 2036-2043

16. DOLEZAL B. & HOLUB R., (1985), *"Approximation relations for determining the activity coefficient at very low concentration by the method of variation of solute concentration"*, **Collect. Czech. Chem. Comm.**, Vol. 50, Pg. 704-711

17. DOLEZAL B., POPL M. & HOLUB R., (1981), *"Determination of activity coefficients at very low concentrations by the inert gas stripping method"*, **Journal of Chromatography**, Vol. 207, Pg. 193-201

18. DUHEM P. & VIDAL J., (1978), *"Extension of the Dilutor Method to Measurement of High Activity Coefficients at Infinite Dilution"*, **Fluid Phase Equilibria**, Vol. 2, Pg. 231-235

19. ECKERT C. A. & SHERMAN S. R., (1996), *"Measurement And Predictions Of Limiting Activity Coefficients"*, **Fluid Phase Equilibria**, Vol. 116, Pg. 333-342

20. FOWLIS I. A. & SCOTT. R. P. W., (1963), *"A vapour dilution system for detector calibration"*, **Journal of Chromatography**, Vol. 11, Pg. 1-10

21. GAUTREAUX M. F. & COATES J., (1955), *"Activity coefficients at infinite dilution"*, **AIChE Journal**, Vol. 1, Pg. 496-500

22. GMEHLING J. & KOLBE B., (1992), **Thermodynamik**, VCH-Verlag: Weinheim, Germany

23. GRUBBER D., KRUMMEN M. & GMEHLING J., (1999), *"The Determination of Activity Coefficients at Infinite Dilution with the Help of the Dilutor Technique (Inert Gas Stripping)"*, **Chemical Engineering and Technology**, Vol. 22, Pg. 827-831

24. HAIMI P., UUSI-KYYNY P., POKKI J-P., AITTAMAA J. & KESKINEN K. I., (2006), *"Infinite dilution activity coefficient measurements by inert gas stripping"*, **Fluid Phase Equilibria**, Vol. 243, Pg. 126-132

25. HOVORKA S. H. & DOHNAL V., (1997), *"Determination of Air-Water Partitioning of Volatile Halogenated Hydrocarbons by the Inert Gas Stripping Method"*, **J. Chem. Eng. Data**, Vol. 42, Pg. 924-933

26. HOVORKA S. H., DOHNAL V., ROUX A. H. & ROUX-DESGRANGES G., (2002), *"Determination of temperature dependence of limiting activity coefficients for a group of moderately hydrophobic organic solutes in water"*, **Fluid Phase Equilibria**, Vol. 201, Pg. 135-164

27. HOWELL W. J., KARACHEWSKI A. M., STEPHENSON K. M., ECKERT C. A., PARK J. H., CARR P. W. & RUTAN S. C., (1989), *"An improved MOSCED equation for the prediction and application of infinite dilution activity coefficients"*, **Fluid Phase Equilibria**, Vol. 52, Pg. 151-160

28. HRADETZKY G., WOBST M., VOPEL H. & BITTRICH H-J., (1990), *"Measurement of activity coefficients in highly dilute solutions part 1"*, **Fluid Phase Equilibria**, Vol. 54, Pg. 133-145

29. KORLIE M. S., (2000), *"3-D Particle Modeling of Gas Bubbles in a Liquid"*, **Computers and Mathematics with Applications**, Vol. 39, Pg. 235-246

30. KREPPER E., LUCAS D. & PRASSER H-M., (2005), *"On the modeling of bubbly flow in vertical pipes"*, **Nuclear Engineering and Design**, Vol. 235, Pg. 597-611

31. KRUMMEN M. & GMEHLING J., (2004), *"Measurements of Activity Coefficients at Infinite Dilution In N-methyl-2-pyrrolidone and N-formylmorpholine and their Mixtures with Water using the Dilutor Technique"*, **Fluid Phase Equilibria**, Vol. 215, Pg. 283-294

32. KRUMMEN M., GRUBER D. & GMEHLING J., (2000), *"Measurement of Activity Coefficients At Infinite Dilution in Solvent Mixtures using the Dilutor Technique"*, **Ind. Eng. Chem. Res.**, Vol. 39, Pg. 2114-2123

33. KRUMMEN M., WASSERSCHEID P. & GMEHLING J., (2002), *"Measurement of Activity Coefficients at Infinite Dilution in Ionic Liquids using the Dilutor Technique"*, **J. Chem. Eng. Data.**, Vol. 47, Pg. 1411-1417

34. LEBERT A. & RICHON D., (1984), *"Infinite dilution activity coefficients of n-alcohols as function of dextrin concentration in water dextrin-systems"*, **Journal of Agricultural and Food Chemistry**, Vol. 32, Pg. 1156-1191

35. LEGRET D., DESTEVE J., RICHON D. & RENON H., (1983), *"Vapor-liquid equilibrium constants at infinite dilution determined by a gas stripping method: Ethane, propane, n-butane, n-pentane in the methane-n-decane system"*, **AIChE Journal**, Vol. 29, Pg. 137-144

36. LEROI J. C., MASSON J. C., RENON H., FABRIES J. F. & SANNIER H., (1977), *"Accurate Measurement of Activity Coefficients at Infinite Dilution by Inert Gas Stripping and Gas Chromatography"*, **Ind. Eng. Chem. Process Des. Dev**, Vol. 16, Pg. 139-144

37. LI J., DALLAS A. J., EIKENES D. I., CARR P. W., BERGMANN D. L., HAIT M. J. & ECKERT C. A., (1993), *"Measurement of a Large Infinite Dilution Activity Coefficients of Nonelectrolytes in Water by Inert Gas Stripping and Gas Chromatography"*, **Analytical Chemistry**, Pg. 3212-3218

38. LI J. J. & CARR P. W., (1994), *"Gas chromatographic study of salvation enthalpy by solvatochromically based linear salvation energy relationships"*, **Journal of Chromatography**, Vol. 659, Pg. 367-380

39. LIN S-T. & SANDLER S. I., (1999), *"Infinite Dilution Activity Coefficients from Ab Anitio Solvation Calculations"*, **AIChE Journal**, Vol. 45, No. 12, Pg. 2606-2618

40. MITCHELL B. E. & JURS P. C., (1998), *"Prediction of Infinite Dilution Activity Coefficients of Organic Compounds in Aqueous Solution from Molecular Structure"*, **J. Chem. Inf. Comput. Sci.**, Vol. 38, Pg. 200-209

41. MIYANO Y, (2004a), *"Hendry's constants and infinite dilution activity coefficients of propane, propene, butane, isobutene, 1-butene, isobutene, trans-2-butene and 1,3-butadiene in 1-propanol at T = 260 to 340 K"*, **Journal of Chemical Thermodynamics**, Vol. 36, Pg. 101-106

42. MIYANO Y., (2004b), *"Hendry's constants and infinite dilution activity coefficients of propane, propene, butane, isobutene, 1-butene, isobutene, trans-2-butene and 1,3-butadiene in isobutanol and tert-butanol"*, **Fluid Phase Equilibria**, Vol. 36, Pg. 865-869

43. MIYANO Y., (2005), *"Hendry's law constants and infinite dilution activity coefficients of propane, propene, butane, isobutene, 1-butene, isobutene, trans-2-butene and 1,3-butadiene in 1-pentanol, 2-pentanol and 3-pentanol"*, **Journal of Chemical Thermodynamics**, Vol. 37, Pg. 463-469

44. MIYANO Y. & FUKUCHI K., (2004), *"Hendry's constants of propane, propene, trans-2-butene and 1,3-butadiene in methanol at 255-320K"*, **Fluid Phase Equilibria**, Vol. 226, **2004**, Pg 183-187

45. MIYANO Y., NAKANISHI K. & KUKUCHI K., (2003), *"Hendry's constants of butane, isobutene, 1-butene and isobutene in methanol at 255-320K"*, **Fluid Phase Equilibria**, Vol. 208, Pg. 223-238

46. NANNOOLAL Y., RAREY J. & RAMJUGERNATH D., (in preparation), *"Estimation of Pure Component Properties, Part 3. Estimation of the Vapour Pressure of Non-Electrolyte Organic Compounds via Group Contributions and Group Interactions"*

47. OVECKOVA J., SUROVY J. & GRACZOVA E., (1991), *"A modified method for vapour-liquid equilibria measurement by inert gas stripping"*, **Fluid Phase Equilibria**, Vol. 68, Pg. 163-172

48. PIVIDAL K. A., BIRTIGH A. & SANDLER S. I., (1992), *"Infinite dilution activity coefficients for oxygenated systems determined using a differential static cell"*, **Journal of Chemical Engineering Data**, Vol. 37, Pg. 484-487

49. PUTNAM R., TAYLER R., KLAMT A., ECKERT F. & SCHILLER M., (2003), *"Prediction of Infinite Dilution Activity Coefficients Using COSMO-RS"*, **Ind. Eng. Chem. Res.**, Vol. 42, Pg. 3635-3641

50. RICHON D., ANTOINE P. & RENON H., (1980), *"Infinite Dilution Activity Coefficients of Linear and Branched Alkanes from C_1 to C_9 in n-Hexadecane by Inert Gas Stripping"*, **Ind. Eng. Chem. Process Des. Dev.**, Vol. 19, Pg. 144-147

51. RICHON D. & RENON H., (1980), *"Infinite Dilution Hendry's Constants of Light Hydrocarbons in n-Hexadecane, n-Octadecane and 2,2,4,4,6,8,8-Heptamethylnonane by Inert Gas Stripping"*, **J. Chem. Eng. Data.**, Vol. 25, Pg. 59-60

52. RICHON D., SORRENTINO F. & VOILLEY A., (1985), *"Infinite Dilution Activity Coefficients by Inert Gas Stripping Method: Extension to the Study of Viscous and Foaming Mixtures"*, **Ind. Eng. Chem. Process Des. Dev.**, Vol. 24, Pg. 1160-1165

53. RITTER J. J. & ADAMS N. K., (1976), *"Exponential Dilution as a Calibration Technique"*, **Analytical Chemistry**, Vol. 48, Pg. 612-619

54. SHERMAN S. R., TRAMPE D. B., BUSH D. M., SCHILLER M., ECKERT C. A., DALLAS A. J., LI J. & CARR P. W., (1996), *"Compilation and Correlation of Limiting Activity Coefficients of Nonelectrolytes in Water"*, **Ind. Eng. Chem. Res.**, Vol. 35, Pg. 1044-1058

55. SLATTERY J. C. & BIRD R. B., (1958), *"Calculation of the diffusion coefficient of dilute gases and of the self-diffusion coefficient of dense gases"*, **AIChE Journal**, Vol. 4, Pg. 137-142

56. SOAVE G., (1972), *"Equilibrium constants from a modified Redlich-Kwong equation of state"*, **Chemical Engineering Science**, Vol. 27, Pg. 1197-1203

57. THOMAS E. R. & ECKERT C. A., (1984), *Prediction of limiting activity coefficients by a modified separation of cohesive energy density model and UNIFAC*", **Ind. Eng. Chem. Proc. Des. Dev.**, Vol. 23, Pg. 194-209

58. VRBKA P. & DOHNAL V., (2004), *"Limiting Activity Coefficients by Comparative Tensimetry: 1-Propanol and 1-Butanol in Heptane and in Octane"*, **Journal of Chemical Engineering Data**, Vol. 49, Pg. 867-871

59. VRBKA P., FENCLOVA D., LASTOVKA V. & DOHNAL V., (2005), *"Measurement of infinite dilution activity coefficients of 1-alkanols (C_1-C_5) in water as a function of temperature (273-373 K)"*, **Fluid Phase Equilibria**, Vol. 237, Pg. 123-129

60. VRBKA P., HAUGE B., FRYDENDAL L. & DOHNAL V., (2002), *"Limiting Activity Coefficients of Lower 1-Alkanols in n-Alkanes: Variation with Chain Length of Solvent Alkane and Temperature"*, **J. Chem. Eng. Data**, Vol. 47, Pg. 1521-1525

61. WILKE C. R. & CHANG P., (1955), *"Correlation of diffusion in dilute solutions"*, **AIChE Journal**, Vol. 1, Pg. 264-270

62. WOBST M., HRADETZKY G. & BITTRICH H. J., (1992), *"Measurement of Activity Coefficients in Highly Dilute Solution Part II"*, **Fluid Phase Equilibria**, Vol. 77, Pg. 297-312

Book References

1. CRANK J., *"The Mathematics of Diffusion"*, Oxford University Press, London, **1956**
2. GUST J. C., GRAHAM R. M., LOMBARDI M. A., *"Stopwatch and Timer Calibrations"*, US Government Printing Office, **2004**, Pg 37-39
3. PERRY R. H., GREEN D. W., *"Perry's Chemical Engineers' Handbook", Seventh Edition*, McGraw-Hill, **1997**
4. REID R. C., PRAUSNITZ J. M., POLING B. E., *"The Properties of Gases and Liquids"*, Second Edition, McGraw-Hill Companies, **1966**
5. SMITH J. M., VAN NESS H. C., ABBOTT M. M., *"Introduction to Chemical Engineering Thermodynamics"*, Fifth Edition, McGraw-Hill, **1996**
6. SONI M., *"Vapour-liquid Equilibria and Infinite Dilution Activity Coefficient Measurements of Systems involving Diketones"*, MSc. Eng. Thesis, University Of Natal, **2004**

Websites

1. www.chromatography-online.org/GC-Detectors/Flame-Ionization/rs36
2. www.elderdorpinstruments.nl/International%20web/Temperatuursensoren
3. www.hyperion.cc.uregina.ca/~bergbusp/uglabs/p109/Experiments/EXPT02Meas&Error07.pdf
4. www.vici.com/support/app/app11j.php
5. www.wag.caltech.edu/home/stlin/research.html

Other

1. Jourdain F., (2000), *"Inert Gas Stripping Technique for the Determination of Activity Coefficients at Infinite Dilution"*, University of Natal, School of Chemical Engineering Internal Report, Pg. 1-9

Appendix A

The fugacity coefficient was calculated using the Soave/Redlich/Kwong (SRK) equation of state and compared to the Peng/Robinson (PR) equation just to check if there is consistency between the calculated fugacity coefficients under all experimental conditions. This was done in MATLAB as it was difficult to solve some of the equations otherwise. All the equations concerned are shown below.

The liquid and vapour roots of the generic cubic equation of state are required for the determination of fugacity coefficients. For pure species i as a vapour,

$$Z_i = 1 + \beta_i - q_i\beta_i\left[\frac{Z_i - \beta_i}{(Z_i + \varepsilon\beta i)(Z_i + \sigma\beta_i)}\right] \qquad \text{A1}$$

For pure species i as a liquid,

$$Z_i = \beta_i + (Z_i + \varepsilon\beta_i)(Z_i + \sigma\beta_i)\left[\frac{1 + \beta_i - Z_i}{q_i\beta_i}\right] \qquad \text{A2}$$

The fugacity coefficient is given by the following equation:

$$ln\,\varphi_i^x = Z_i - 1 - ln(Z_i - \beta_i) - q_i I, \qquad \text{A3}$$

$ln\,\varphi_i^{sat} = Z_i - 1 - ln(Z_i - \beta_i) - q_i I$

For saturated-liquid and saturated-vapour states at temperature (T), $ln\,\varphi_i^l = ln\,\varphi_i^v$ and $P = P_i^{sat}$ so one can use either A1 or A2. It's better to evaluate both just as a check to see whether the program calculates the correct value for the compressibility factor. The other equations required are:

$$\beta_i = \frac{b_i P_i^{sat}}{RT} \qquad \text{A4}$$

$$b_i = \Omega\frac{RT_{Ci}}{P_{Ci}} \qquad \text{A5}$$

$$q_i = \frac{a_i(T_C)}{b_i RT} \qquad \text{A6}$$

$$a_i(T_C) = \psi \frac{\alpha(T_{ri}) R^2 T_{Ci}^2}{P_{Ci}} \qquad \text{A7}$$

$$I_i = \frac{1}{\sigma - \varepsilon} ln\left(\frac{Z_i + \sigma\beta_i}{Z_i + \varepsilon\beta_i}\right) \qquad \text{A8}$$

The values to the constants and unknown variables are given in Table A1. These values are for use with all the equations above.

E.O.S	$\alpha(T_{ri})$	σ	ε	Ω	ψ	Z_C
SRK	$\alpha_{SRK}(T_{ri}, \omega_i)$	1	0	0.08664	0.42748	1/3
PR	$\alpha_{PR}(T_{ri}, \omega_i)$	$1+\sqrt{2}$	$1-\sqrt{2}$	0.07779	0.45724	0.3074

Table A1: Parameter assignments for the SRK and PR equations of state

Lastly

$$\alpha_{SRK}(T_{ri}, \omega_i) = \left[1 + \left(0.480 + 1.574\omega_i - 0.176\omega_i^2\right)\left(1 - T_{ri}^{0.5}\right)\right]^2 \qquad \text{A9}$$

$$\alpha_{PR}(T_{ri}, \omega_i) = \left[1 + \left(0.37464 + 1.54226\omega - 0.26992\omega^2\right)\left(1 - T_{ri}^{0.5}\right)\right]^2 \qquad \text{A10}$$

The pure component vapour pressures were estimated using an equation proposed by Nannoolal et al. (in preparation) and checked using the well known Antoine equation. The equation proposed by Nannoolal et al. (in preparation) is shown below:

$$log\, P^{sat} = (4.1012 + dB)\left(\frac{T_{rb} - 1}{T_{rb} - \frac{1}{8}}\right) \qquad \text{A11}$$

Where $T_{rb} = \frac{T}{T_b}$

T is the system temperature and T_b is the pure component boiling point temperature.

The Antoine equation is shown below (Perry and Green (1997)):

$$\ln P^{sat} = A - \frac{B}{T + C} \qquad \text{A12}$$

Appendix B

Sample Calculation

The sample calculation procedure was done for the results obtained from the Krummen et al. (2000) equation (Equation 6.55).

Experimental Data		$\gamma^{\infty}_{experiment}$
D (ml/min)	T (°C)	
10.13	35.02	6.28
10.12	45.01	5.97
10.01	55.03	5.68
10.00	64.98	5.41
20.07	35.01	6.27
20.16	45.00	5.99
20.22	55.00	5.71
20.06	65.00	5.44
29.99	34.99	6.30
29.82	45.01	6.01
29.48	55.03	5.70
29.90	64.98	5.42

Table B1: Section of Table 7-16 that was used for the calculation

For each flow rate (10, 20 and 30 ml) a plot of liming activity coefficient against temperature was made (see Figure B1). The equation of the curve from the three plots was used to determine limiting activity coefficients for the new temperatures 25.00, 35.00, 45.00, 55.00, 65.00 and 75.00 °C (see Columns 2 to 4 in Table B2) for the each flow rate. In the case of n-hexene + o-cresol system plots of $\ln(\gamma^{\infty})$ against $100/T$ were made. This was the only system that gave a straight line for interpolation and extrapolation in this manner (see Figure 8-2). The average limiting activity coefficient for each temperature was then calculated (Column 5 of Table B2). A similar calculation was done for the limiting activity coefficients calculated from the equation proposed by Hovorka and Dohnal (1997) (Equation 6.65).

For the Equations proposed by Leroi et al. (1977) (Equations 6.23 and 6.24), Duhem and Vidal (1978) (Equation 6.29) and Boa and Han (1997) (Equation 6.33) the average was first taken and

then a plot of the average was made for interpolation and extrapolation. For each temperature there would be one limiting activity coefficient instead of four. The calculation procedure then follows as above

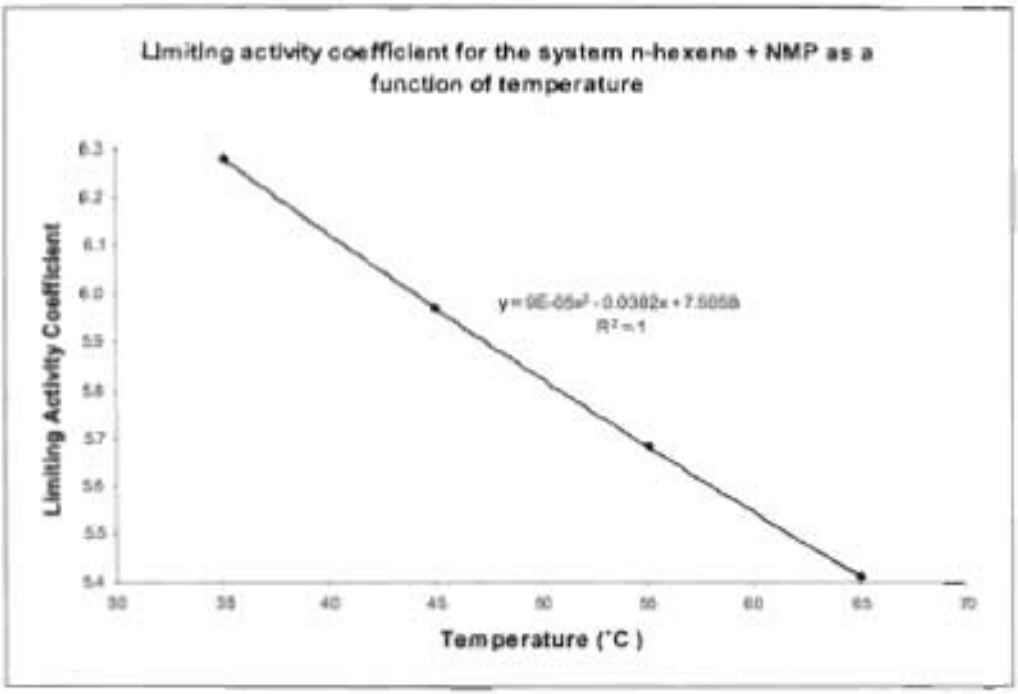

Figure B1: Plot of limiting activity coefficient versus temperature to obtain the second order polynomial equation for the 10 ml/min flow rate

T (°C)	Limiting Activity Coefficients			
	D = 10 ml/min	D = 20 ml/min	D = 30 ml/min	Average
25.00	6.61	6.57	6.61	6.59
35.00	6.28	6.28	6.31	6.29
45.00	5.97	6.00	6.01	5.99
55.00	5.68	5.72	5.72	5.70
65.00	5.40	5.45	5.43	5.43
75.00	5.15	5.19	5.14	5.16

Table B2: New limiting activity coefficients for the three flow rates at different temperatures

Notes